Westinghouse
Electric Corporation

Energy Systems

Nuclear Technology Division

Box 355
Pittsburgh Pennsylvania 15230-0355

July 28, 1994
CAW-94-699

Document Control Desk
US Nuclear Regulatory Commission
Washington, DC 20555

Attention: Mr. William T. Russell, Director

APPLICATION FOR WITHHOLDING PROPRIETARY
INFORMATION FROM PUBLIC DISCLOSURE

Subject: "Braidwood Unit 1 Technical Support for Cycle 5 Steam Generator Interim Plugging Criteria" (WCAP-14046)

50-456

Dear Mr. Russell:

The proprietary information for which withholding is being requested is further identified in Affidavit CAW-94-699 signed by the owner of the proprietary information, Westinghouse Electric Corporation. The affidavit, which accompanies this letter, sets forth the basis on which the information may be withheld from public disclosure by the Commission and addresses with specificity the considerations listed in paragraph (b)(4) of 10 CFR Section 2.790 of the Commission's regulations.

Accordingly, this letter authorizes the utilization of the accompanying Affidavit by Commonwealth Edison Company.

Correspondence with respect to the proprietary aspects of the application for withholding or the Westinghouse affidavit should reference this letter, CAW-94-699, and should be addressed to the undersigned.

Very truly yours,

N. J. Liparulo, Manager
Nuclear Safety Regulatory and Licensing Activities

Enclosures

cc: Kevin Bohrer/NRC (12H5)

CIN481:RJM/072894

CAW-94-699

AFFIDAVIT

COMMONWEALTH OF PENNSYLVANIA:

ss

COUNTY OF ALLEGHENY:

Before me, the undersigned authority, personally appeared Henry A. Sepp, who, being by me duly sworn according to law, deposes and says that he is authorized to execute this Affidavit on behalf of Westinghouse Electric Corporation ("Westinghouse") and that the averments of fact set forth in this Affidavit are true and correct to the best of his knowledge, information, and belief:

Henry A. Sepp, Manager
Regulatory and Licensing Initiatives

Sworn to and subscribed
before me this 28th day
of July, 1994

Notarial Seal
Denise K. Henderson, Notary Public
Monroeville Boro, Allegheny County
My Commission Expires Oct. 28, 1996
Member, Pennsylvania Association of Notaries

Denise K. Henderson
Notary Public

1325C-RJM-1:072894

(1) I am Manager, Regulatory and Licensing Initiatives, in the Nuclear Technology Division, of the Westinghouse Electric Corporation and as such, I have been specifically delegated the function of reviewing the proprietary information sought to be withheld from public disclosure in connection with nuclear power plant licensing and rulemaking proceedings, and am authorized to apply for its withholding on behalf of the Westinghouse Energy Systems Business Unit.

(2) I am making this Affidavit in conformance with the provisions of 10CFR Section 2.790 of the Commission's regulations and in conjunction with the Westinghouse application for withholding accompanying this Affidavit.

(3) I have personal knowledge of the criteria and procedures utilized by the Westinghouse Energy Systems Business Unit in designating information as a trade secret, privileged or as confidential commercial or financial information.

(4) Pursuant to the provisions of paragraph (b)(4) of Section 2.790 of the Commission's regulations, the following is furnished for consideration by the Commission in determining whether the information sought to be withheld from public disclosure should be withheld.

(i) The information sought to be withheld from public disclosure is owned and has been held in confidence by Westinghouse.

(ii) The information is of a type customarily held in confidence by Westinghouse and not customarily disclosed to the public. Westinghouse has a rational basis for determining the types of information customarily held in confidence by it and, in that connection, utilizes a system to determine when and whether to hold certain types of information in confidence. The application of that system and the substance of that system constitutes Westinghouse policy and provides the rational basis required.

Under that system, information is held in confidence if it falls in one or more of several types, the release of which might result in the loss of an existing or potential competitive advantage, as follows:

(a) The information reveals the distinguishing aspects of a process (or component, structure, tool, method, etc.) where prevention of its use by any of Westinghouse's competitors without license from Westinghouse constitutes a competitive economic advantage over other companies.

(b) It consists of supporting data, including test data, relative to a process (or component, structure, tool, method, etc.), the application of which data secures a competitive economic advantage, e.g., by optimization or improved marketability.

(c) Its use by a competitor would reduce his expenditure of resources or improve his competitive position in the design, manufacture, shipment, installation, assurance of quality, or licensing a similar product.

(d) It reveals cost or price information, production capacities, budget levels, or commercial strategies of Westinghouse, its customers or suppliers.

(e) It reveals aspects of past, present, or future Westinghouse or customer funded development plans and programs of potential commercial value to Westinghouse.

(f) It contains patentable ideas, for which patent protection may be desirable.

There are sound policy reasons behind the Westinghouse system which include the following:

(a) The use of such information by Westinghouse gives Westinghouse a competitive advantage over its competitors. It is, therefore, withheld from disclosure to protect the Westinghouse competitive position.

(b) It is information which is marketable in many ways. The extent to which such information is available to competitors diminishes the Westinghouse ability to sell products and services involving the use of the information.

(c) Use by our competitor would put Westinghouse at a competitive disadvantage by reducing his expenditure of resources at our expense.

(d) Each component of proprietary information pertinent to a particular competitive advantage is potentially as valuable as the total competitive advantage. If competitors acquire components of proprietary information, any one component may be the key to the entire puzzle, thereby depriving Westinghouse of a competitive advantage.

(e) Unrestricted disclosure would jeopardize the position of prominence of Westinghouse in the world market, and thereby give a market advantage to the competition of those countries.

(f) The Westinghouse capacity to invest corporate assets in research and development depends upon the success in obtaining and maintaining a competitive advantage.

(iii) The information is being transmitted to the Commission in confidence and, under the provisions of 10CFR Section 2.790, it is to be received in confidence by the Commission.

(iv) The information sought to be protected is not available in public sources or available information has not been previously employed in the same original manner or method to the best of our knowledge and belief.

(v) The proprietary information sought to be withheld in this submittal is that which is appropriately marked in "Braidwood Unit 1 Technical Support for Cycle 5 Steam Generator Interim Plugging Criteria", WCAP-14046 (Proprietary), May, 1994 for Byron Unit 1, being transmitted by Commonwealth Edison Company letter and Application for Withholding Proprietary Information from Public Disclosure, to Document Control Desk, Attention William T. Russell. The proprietary information as submitted for use by Commonwealth Edison Company for Byron Unit 1 is expected to be applicable in other licensee submittals in response to certain NRC requirements for justification of steam generator tube interim plugging criteria.

This information is part of that which will enable Westinghouse to:

(a) Provide documentation for steam generator tube interim plugging criterion.

(b) Provide a basis for the form of the steamline break (SLB) leak rate correlation.

(c) Provide SLB leak rate analyses.

(d) Assist the customer in obtaining NRC approval.

Further this information has substantial commercial value as follows:

(a) Westinghouse plans to sell the use of similar information to its customers for purposes of meeting requirements for licensing documentation.

(b) Westinghouse can sell support and defense of the technology to its customers in the licensing process.

Public disclosure of this proprietary information is likely to cause substantial harm to the competitive position of Westinghouse because it would enhance the ability of competitors to provide similar methodologies and licensing defense services for commercial power reactors without commensurate expenses. Also, public disclosure of the information would enable others to use the information to meet NRC requirements for licensing documentation without purchasing the right to use the information.

The development of the technology described in part by the information is the result of applying the results of many years of experience in an intensive Westinghouse effort and the expenditure of a considerable sum of money.

In order for competitors of Westinghouse to duplicate this information, similar technical programs would have to be performed and a significant manpower effort,

having the requisite talent and experience, would have to be expended for developing testing and analytical methods and performing testing.

Further the deponent sayeth not.

Proprietary Information Notice

Transmitted herewith are proprietary and/or non-proprietary versions of documents furnished to the NRC in connection with requests for generic and/or plant-specific review and approval.

In order to conform to the requirements of 10 CFR 2.790 of the Commission's regulations concerning the protection of proprietary information so submitted to the NRC, the information which is proprietary in the proprietary versions is contained within brackets, and where the proprietary information has been deleted in the non-proprietary versions, only the brackets remain (the information that was contained within the brackets in the proprietary versions having been deleted). The justification for claiming the information so designated as proprietary is indicated in both versions by means of lower case letters (a) through (f) contained within parentheses located as a superscript immediately following the brackets enclosing each item of information being identified as proprietary or in the margin opposite such information. These lower case letters refer to the types of information Westinghouse customarily holds in confidence identified in Sections (4)(ii)(a) through (4)(ii)(f) of the affidavit accompanying this transmittal pursuant to 10 CFR 2.790(b)(1).

Copyright Notice

The reports transmitted herewith each bear a Westinghouse copyright notice. The NRC is permitted to make the number of copies of the information contained in these reports which are necessary for its internal use in connection with generic and plant-specific reviews and approvals as well as the issuance, denial, amendment, transfer, renewal, modification, suspension, revocation, or violation of a license, permit, order, or regulation subject to the requirements of 10 CFR 2.790 regarding restrictions on public disclosure to the extent such information has been identified as proprietary by Westinghouse, copyright protection notwithstanding. With respect to the non-proprietary versions of these reports, the NRC is permitted to make the number of copies beyond those necessary for its internal use which are necessary in order to have one copy available for public viewing in the appropriate docket files in the public document room in Washington, DC and in local public document rooms as may be required by NRC regulations if the number of copies submitted is insufficient for this purpose. Copies made by the NRC must include the copyright notice in all instances and the proprietary notice if the original was identified as proprietary.

WESTINGHOUSE CLASS 3

WCAP-14047 SG-94-06-002

BRAIDWOOD UNIT 1
TECHNICAL SUPPORT FOR CYCLE 5
STEAM GENERATOR
INTERIM PLUGGING CRITERIA

MAY 1994

Approved by: _____
J. N. Esposito, Manager
Steam Generator Technology & Engineering

WESTINGHOUSE ELECTRIC CORPORATION
NUCLEAR SERVICES DIVISION
P. O. BOX 158
MADISON, PENNSYLVANIA 15663-0158

9405050364 27pp

BRAIDWOOD UNIT 1: TECHNICAL SUPPORT FOR CYCLE 5
STEAM GENERATOR INTERIM PLUGGING CRITERIA

TABLE OF CONTENTS

BRAIDWOOD UNIT 1: TECHNICAL SUPPORT FOR CYCLE 5
STEAM GENERATOR INTERIM PLUGGING CRITERIA

TABLE OF CONTENTS (Continued)

BRAIDWOOD UNIT 1: TECHNICAL SUPPORT FOR CYCLE 5 STEAM GENERATOR INTERIM PLUGGING CRITERIA

1.0 INTRODUCTION

Following the completion of Cycle 4 operation, eddy current inspections of the tube support plate (TSP) intersections of the steam generator (S/G) tubes have identified 2733 bobbin coil indications of which 1566 were confirmed as being axial crack-like ODSCC indications using RPC inspection techniques. The size and number of indications could result in significant tube repairs with current plugging criteria and repairs that are not required to meet NRC Regulatory Guide 1.121 guidelines for tube repair. Braidwood Station has therefore requested a Technical Specification change to implement an interim plugging criteria (IPC) for ODSCC at TSP intersections. The requested IPC repair limits and inspection requirements have been based on the Catawba-1 NRC SER which approved a 1.0 volt repair limit. The methodology to support the Braidwood-1 IPC differs from previously approved IPCs in that it applies the EPRI data outlier evaluation methodology and SLB leak rate versus voltage correlation based on the NRC guidance of the February 8, 1993 NRC/industry meeting on resolution of comments on draft NUREG-1477. In addition, Braidwood-1 IPC analyses demonstrate limited TSP displacement relative to the tube in a SLB event, and show structural integrity with respect to tube burst considerations.

The evaluations supporting the Braidwood-1 IPC are based upon bobbin coil voltage amplitude which is correlated with tube burst capability and leakage potential. Detailed analyses provided in this report (Section 4) have demonstrated limited relative tube support plate to tube movement which minimizes the potential for significant leakage or tube burst during both normal and accident conditions. For SLB leakage analyses, the tube support plate crevices are assumed to be free span or open crevices, which lead to more conservative leak rates compared to the expected packed crevices under normal and accident conditions. The analyses for demonstrating limited TSP displacement utilize thermal-hydraulic loads for a postulated SLB at normal operating conditions and for a SLB at hot standby conditions. The loads utilize existing analyses and the hot standby loads are very conservative as the initial conditions include low water level combined with an excess feedwater transient, both of which tend to increase the loads. The dynamic structural analyses yield TSP displacements as a function of tube location. Tube burst analyses performed for the crack length exposed by the TSP displacements have been conservatively performed by assuming that the exposed crack length is throughwall. Even with these conservative assumptions, it is demonstrated that Braidwood-1 has adequate tube burst margin.

In accordance with draft NUREG-1477, SLB leak rates were calculated for a total of six probability of leak (POL) correlations including the EPRI reference l.g logistic correlation.

The six correlations (Section 6) evaluated included linear and log voltage formulations for logistic, normal and Cauchy cumulative distribution functions. The reference leak rate with the log logistic correlation and five additional leak rates for assessing the sensitivity to the POL correlation are given in this report (Section 8). The SLB leak rate analyses utilize voltage distributions consistent with the draft NUREG-1477 guidance including adjustments for probability of detection.

The plugging criteria were developed from testing of tube specimens with laboratory-induced ODSCC, extensive examination of pulled tubes from operating S/Gs and field experience for leakage due to indications at TSPs. The recommended criteria represent conservative criteria, based upon Electric Power Research Institute (EPRI) and industry-supported development programs that are continuing to further refine the plugging criteria. At the end of Cycle 4, four tubes with 13 intersections and 6 RPC confirmed indications were pulled at Braidwood-1 for future enhancement of the EPRI database and validate the industry developed EPRI leak and burst correlations applied in this report.

Implementation of the tube plugging criteria was supplemented by 100% bobbin coil inspection requirements at TSP elevations having ODSCC indications, reduced operating leakage requirements, inspection guidelines to provide consistency in the voltage normalization, and rotating pancake coil (RPC) inspection requirements to establish repair requirements for indications above the 1.0 volt repair limit and to characterize the principal degradation mechanism as ODSCC. In addition, potential SLB leakage was calculated for tubes with indications left in service at TSPs to demonstrate that the cumulative EOC-5 leakage is less than the allowable limits.

2.0 SUMMARY AND CONCLUSIONS

This report documents the technical support for a Braidwood Unit 1, Cycle 5 Interim Plugging Criteria (IPC) of 1.0 volt for ODSCC indications at TSPs.

2.1 Overall Conclusions

An IPC with a 1.0 bobbin voltage repair limit has been developed for Braidwood-1, Cycle 5 operation. Inspection requirements typical of IPC practice, such as the guidelines of the Catawba-1 NRC SER, were applied at the Cycle 4 refueling outage to support implementation of the IPC. These requirements include eddy current analysis guidelines, training of analysts, cross calibration of ASME standards to a reference standard, use of probe wear standards, 100% bobbin probe inspection and RPC inspection of bobbin indications above 1.0 volt together with a sample of dented TSP intersections.

R.G. 1.121 guidelines for tube integrity are conservatively satisfied at end-of-cycle five (EOC-5) conditions for the 1.0 volt IPC. The results of the Braidwood-1 assessment can be summarized as follows:

- The projected EOC-5 SLB leakage is 3.1 gpm for the limiting SG, which is less than the allowable limit of 9.1 gpm for Braidwood-1. The SLB leak rate was evaluated for the six alternate formulations of the probability of leak versus voltage correlation identified in draft NUREG-1477 and found to be essentially (within 0.1 gpm) independent of the correlation applied in the analysis. The SLB leak rates were obtained by applying the leak rate versus voltage correlation based on the EPRI database and outlier evaluation consistent with the NRC guidance of the February 8, 1994, NRC/industry meeting on resolution of draft NUREG-1477 comments.

- The tube burst probabilities estimated at EOC-5 are 5×10^{-5} for a SLB at normal operating conditions and 8×10^{-4} for a SLB at hot standby conditions. Weighting these probabilities by the relative operating times leads to a combined burst probability of 3.1×10^{-5}. These burst probabilities are significantly lower than the IPC acceptance guideline of 2.5×10^{-2} shown to be acceptable in NUREG-0844. When combined with the corresponding SLB event frequencies, the frequency of a postulated SLB event with a subsequent tube rupture is very low at 5.5×10^{-8} per year. The tube burst probabilities are developed based on limited TSP displacements calculated during a SLB event for the Braidwood-1 S/Gs, even when applying very conservative load conditions for the hot standby SLB. Deterministic tube burst analyses show that the projected EOC-5 voltage obtained with voltage growth rates up to 99% cumulative probability on the Cycle 4 measured growth distribution, is less than the R.G. 1.121 structural limit of 4.54 volts for a $1.43 \times \Delta P_{SLB}$

accident condition burst margin. The R.G. 1.121 structural limit guideline of three times normal operating pressure differential is inherently satisfied by the tube constraint provided by the tube support plates at normal operating conditions.

The modest SLB leakage, acceptable tube burst margins and low tube burst probabilities presented in this report support full cycle operation for Cycle 5 at Braidwood-1 following implementation of the 1.0 volt IPC.

2.2 Summary

Braidwood-1 Interim Plugging Criteria

The implementation of the IPC at Braidwood-1 for ODSCC at TSPs can be summarized as follows:

- Tube Plugging Criteria
  Tubes with bobbin flaw indications exceeding the 1.0 volt IPC voltage repair limit and ≤2.7 volts are plugged or repaired if confirmed as flaw indications by RPC inspection. Bobbin flaw indications >2.7 volts attributable to ODSCC are repaired independent of RPC confirmation.

- Inspection Requirements
  A 100% bobbin coil inspection was performed for all TSP intersections. All bobbin flaw indications greater than the 1.0 volt repair limit were RPC inspected and the RPC inspection included a sample of dented TSP intersections.

- Operating Leakage Limits
  Plant shutdown will be implemented if normal operating leakage exceeds 150 gpd per SG.

- SLB Leakage Criterion
  Predicted end of cycle SLB leak rates from tubes left in service, including a POD = 0.6 adjustment and allowances for NDE uncertainties and ODSCC growth rates, must be less than 9.1 gpm for the S/G in the faulted loop.

- Exclusions from Tube Plugging Criteria
  Certain tube locations, as identified in Section 4 of this report, are excluded from application of the IPC repair limits. The analyses indicate that these tubes may potentially deform or collapse following a postulated LOCA + SSE event.

EOC-4 Inspection Results

Eddy current inspection at EOC-4 resulted in the identification of 2733 bobbin indications at the TSP intersections and 1566 or 57% of the bobbin indications were confirmed by RPC inspection. The indications ranged from 272 in S/G B to 1061 in S/G C. To evaluate Cycle 4 voltage growth, all indications of ODSCC at TSP intersections at EOC-4 had the EOC-3 bobbin data reevaluated to obtain Cycle 4 growth rates. In addition, Braidwood-1 had a 100% inspection of S/G C during October, 1993 as the result of a primary to secondary tube leak unrelated to ODSCC at the TSPs. This allowed a growth evaluation for S/G C from October 1992 to October 1993, a S/G C evaluation from November 1993 to March 1994 and a growth evaluation on S/Gs A, B and D for the entire Cycle 4. The results of this growth rate analysis were conservatively applied to the BOC-5 indications left in service to project the EOC-5 voltage distributions for tube integrity analyses. The average growth for all 4 S/Gs over Cycle 4 was 0.23 volts per EFPY or 48% of the BOC-4 average voltage amplitudes. The average growth for S/G C over the first part of Cycle 4 was 0.19 volts per EFPY (48%) and was 0.11 volts per EFPY (16%) over the second part of Cycle 4. A few indications (~1%) showed larger than typical growth with the largest growth rate being 9.76 volts.

The Braidwood-1, RPC confirmed TSP bobbin indications show axially oriented indications that are typical of those of other plants which have been confirmed as having ODSCC; i.e., the Braidwood-1 results are consistent with axial ODSCC as the degradation mechanism and the associated EPRI database is applicable for the Braidwood-1 IPC. Four tubes including 13 TSP intersections and six RPC confirmed bobbin indications ranging from 1.0 to 10.4 volts were pulled during the outage for subsequent laboratory testing and destructive examination. The results from these pulled tube examinations will be used to enhance the EPRI database and leakage/burst correlations. The effect of these data on the correlations and results of this report will be assessed upon completion of the destructive examinations.

Correlations of bobbin voltage to burst pressure and to SLB leakage and a correlation for the probability of SLB leakage are provided which are consistent with NUREG-1477 and the Catawba-1 SER. These correlations form the basis for determining repair limits and the corresponding margins for burst and leakage as summarized below.

Structural Integrity Assessment

To support the Cycle 5 tube integrity assessment under the conservative assumptions of the larger Cycle 4 growth rates reoccurring in Cycle 5 and a probability of detection of 0.6 (draft NUREG-1477 guidance), additional analyses were performed to demonstrate limited TSP displacement in a postulated SLB event. With limited displacement, the part of the overall

ODSCC crack length covered by the TSP is constrained against burst and the burst capability of the indication is that associated with the exposed crack length. Thus, limited relative displacement of the tubes and TSPs results in increased tube burst margins and an associated low probability of tube burst.

The two sets of Model D4 S/G thermal-hydraulic loads available for this report are (a) those for a SLB at normal full power operating conditions and (b) those for a very conservative SLB at hot standby conditions with low water level combined with an excess feedwater transient. The initial conditions for the latter hot standby SLB event are excessively conservative as shown by comparison with a Model D3 S/G, hot standby SLB event with normal water levels and no feedwater transient. TSP displacements for each TSP and each tube location were obtained by dynamic, finite element analyses for each of the aforementioned SLB loading conditions.

The results of the Model D4 S/G SLB analyses at normal operating conditions and for the Model D3 S/G at hot standby conditions show maximum TSP displacements at tube locations of <0.44 inch. These displacements expose a crack length less than the 0.51 inch throughwall crack length that satisfies R.G 1.121 criteria for the structural limit of $1.43 \times \Delta P_{SLB}$. The estimated tube burst probability for the SLB at normal operating conditions, very conservatively assuming a throughwall crack equal to the exposed crack length, is 5×10^{-7} which is negligible for tube integrity considerations. Thus structural integrity is maintained throughout Cycle 5 for a SLB at normal operating conditions. Since the time at power operation is typically 96% of the operating cycle for Braidwood-1, large structural margins exist for the dominant part of the operating cycle.

Even for the very conservative Model D4 hot standby loads, TSP displacements are limited to less than 0.35 inch for all TSPs having bobbin indications at Braidwood-1 except for plates 3 and 7. At plate 3, the maximum TSP displacement at a tube location is 0.57 inch which is well less than the 0.75 inch length for burst at the SLB pressure differential of 2560 psi for tubes with LTL material properties. The probability of tube burst for an assumed 0.57 inch throughwall crack is about 6×10^{-4} which is negligible compared to allowables since only 12 (.26% of TSP intersections) tube locations on plate 3 have TSP displacements greater than the 0.51 inch structural limit. At the EOC-4 inspection, only 1 indication was found on plate 3 at a location with displacements >0.5 inch. This indication had a small 0.59 volt amplitude at a tube location with 0.51 inch TSP displacement. Thus the number and voltage amplitudes of indications found at plate 3 locations with significant TSP displacements is negligible for tube integrity considerations. Since maximum TSP displacements maintain adequate tube burst margins even if throughwall cracks are assumed and since the larger tube displacements involve only a few tubes, it is concluded that adequate structural margins are maintained for Cycle 5 operation for all potential indications at plate 3.

Only plate 7 has significant tube-to-TSP displacements which provide potential concerns for exceeding EOC-5 structural integrity considerations. At plate 7, 124 tubes (2.6% of TSP intersections) have TSP displacements exceeding 0.5 inch corresponding to the R.G. 1.121 structural margin for throughwall cracks and the maximum TSP displacement at any tube location is 0.87 inch. Based on the EOC-4 inspection results of plate 7 locations, only 8 indications in any one S/G, and a total of 20 indications in all 4 S/Gs (0.7% of all indications) have SLB displacements exceeding 0.5 inch. The maximum bobbin voltage at any tube location with SLB displacements exceeding 0.35 inch was 1.24 volts and the maximum voltage indication found in any S/G at plate 7 was 2.74 volts. This is well below the 4.54 volts corresponding to R.G. 1.121 margins against burst for free span indications. Thus it is concluded that only a few, relatively low voltage indications are likely to occur at the plate 7 locations with significant SLB displacements at hot standby conditions. A statistical assessment is necessary to assess the potential for a structurally significant indication to occur at a plate 7 location with relatively large TSP displacements. A tube burst probability assessment was performed for SLB hot standby conditions (conservative Model D4 loads) and the resulting probability of a tube burst at EOC-5 conditions was only 8×10^{-4}; this is negligible compared to IPC acceptance guidelines of 2.5×10^{-2}. The burst probability for an SLB during power operation at EOC-5 is 5×10^{-5}. Since only about 3.8% of the Braidwood-1 operating time is at hot standby (Mode 3) conditions, the combined burst probability is only about 3×10^{-5}.

The Braidwood-1 SLB event frequencies and conditional tube rupture probabilities described above have been combined to obtain a frequency of 5.5×10^{-8} per year for a SLB event with a subsequent tube rupture. This very low frequency has negligible influence on the core damage frequency and supports full cycle operation at Braidwood-1 for Cycle 5.

Leakage Integrity

Based on sensitivity analyses for SLB leakage, it was concluded that S/G D is the most limiting S/G and was analyzed for potential SLB leak rates at EOC-5. The analysis utilized the EPRI IPC database, probability of leakage correlation and SLB leak rate versus voltage correlation following the NRC guidance at the February 8, 1994, meeting on resolution of draft NUREG-1477 comments. Projected EOC-5 bobbin voltage distributions were obtained including a POD adjustment of 0.6, an allowance for NDE uncertainties, and an allowance for voltage growth based on the S/G D voltage growth distribution obtained for Cycle 4. The resulting SLB leak rate for the limiting SG at EOC-5 was 3.1 gpm, which is significantly less than the allowable leak rate of 9.1 gpm obtained for Braidwood-1.

Based on draft NUREG-1477 guidance, the SLB leak rate was assessed for six alternate formulations of the probability of leakage correlation including linear and log voltage forms

for logistic, normal and Cauchy distributions. A negligible leak rate dependence on the probability of leakage form was found, with a variation of only 0.1 gpm between the six distributions.

3.0 CRACK MORPHOLOGY

3.1 General Discussion

Four tubes were pulled from Braidwood-1 including 13 TSP intersections with 6 reported bobbin and RPC indications. The resulting tube examinations will confirm the crack morphology for indications at the tube support intersections. The schedule for the tube exams will be based on obtaining the appropriate technical results and the results will be available for review after the tests are completed. In the interim period, comparisons of RPC data from the current Braidwood-1 inspection are compared in Section 3.2 below with RPC results for pulled tubes with known morphology of dominantly axial ODSCC typical of the EPRI database.

With the performance of the tube metallography on the pulled tube specimens from Braidwood-1, the 3/4" database will be expanded by 6 TSP intersections with clearly identifiable degradation and 7 other intersections for which EC interpretation guidelines, as practiced in the field, did not find a basis for reporting as possible flaws; these NDD specimens will help to define the extent of ODSCC which may be present at such locations. The Braidwood-1 pulled tubes can be expected to demonstrate a crack morphology of dominantly axial ODSCC typical of the EPRI database. Together with leak and burst testing, the ground truth provided from these samples is expected to support the detection probability concerning the adequacy of bobbin EC testing of non-dented TSPs as the appropriate NDE technique for TSP interim plugging criteria. The bobbin results from the 5H level of R37C34 in particular are suggestive of possible flaw conditions, but both the bobbin and the RPC field analyses were reported as NDD; the metallography results could confirm the sensitivity of the bobbin probes' integration of many small cracks, producing a detectable signal, while the RPC probe response is too small to distinguish a signal produced from only a fraction of the total cracks present in its helical path at any instant. In either case, the voltage range of 1.0 to 10.4 volts for the Braidwood-1 pulled tubes will enhance the EPRI database and resulting correlations while the 7 NDD intersections will supplement the bobbin and RPC detectability data.

3.2 Crack Morphology Inferred from Inspection Data

Comparison of typical MRPC pseudo-isometric graphics (C-scans) for some of TSP indications which were confirmed shows that the Braidwood-1 TSP degradation is enveloped by examples from other plants and that the condition represented by the C-scans is quite consistent with ODSCC. Figures 7-1 to 7-6 in Section 7 illustrate the distributions of axial indications, all confined within the edges of the support plates; the distributions of bobbin indications with elevation and voltage are similar to that found in plants with axial indications verified by previous investigations to be ODSCC by metallographic studies of pulled tubes.

The intersections pulled during the EOC-4 inspection which exhibited EC indications were R37C34-3H and 5H and R16C42-3H from SG D, followed by R27C43-3H and R42C44-3H and 5H, both from SG A; these MRPC indications are shown in Figures 7-42 to 7-47 and are typical of the variety of TSP ODSCC in Braidwood-1 confirmed bobbin indications from 1.04 volts to 10.4 volts. Comparable C-scan results from Plant R and Plant S, both with SG's of similar design to the Braidwood-1 SGs, shown in Figures 3-1 to 3-5, confirm the appropriateness of the judgment that all of these indications represent TSP ODSCC within the definition relevant to the IPC.

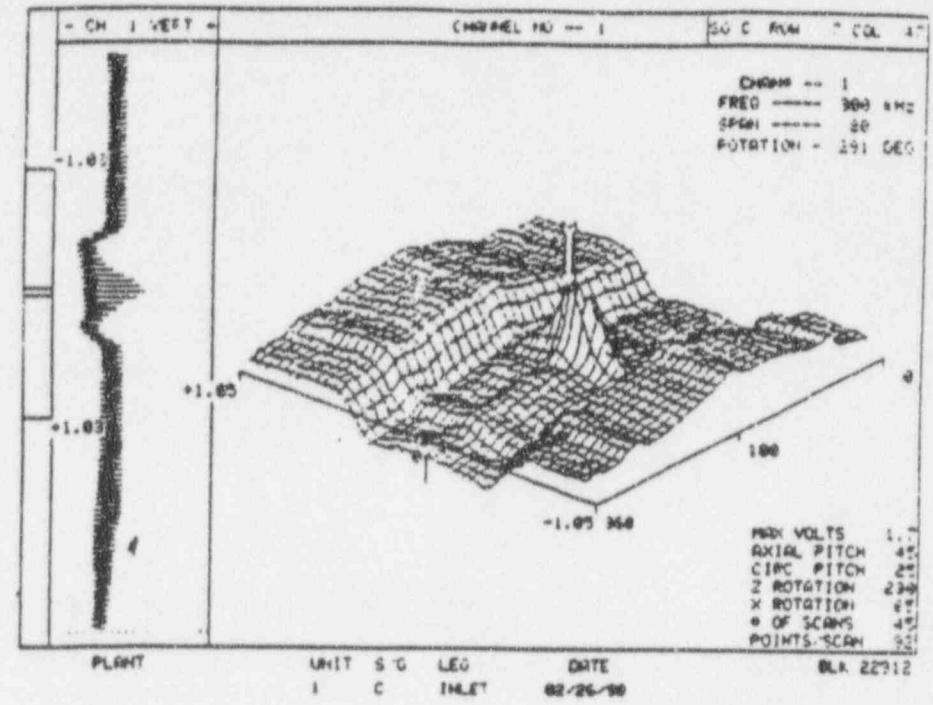

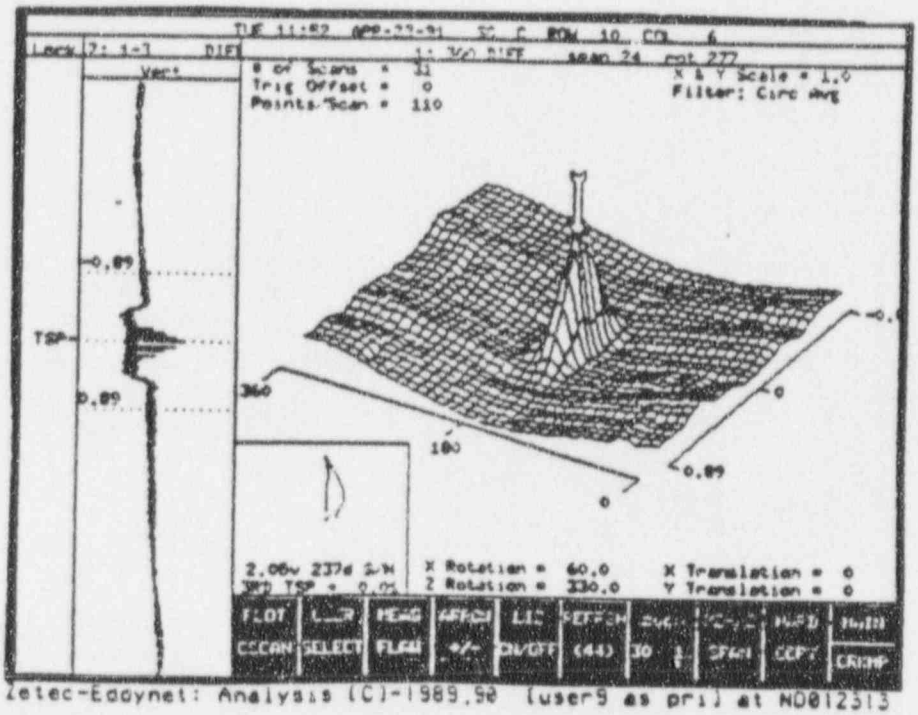

Figure 3-1. Plant R Example RPC Traces for Support Plate Locations

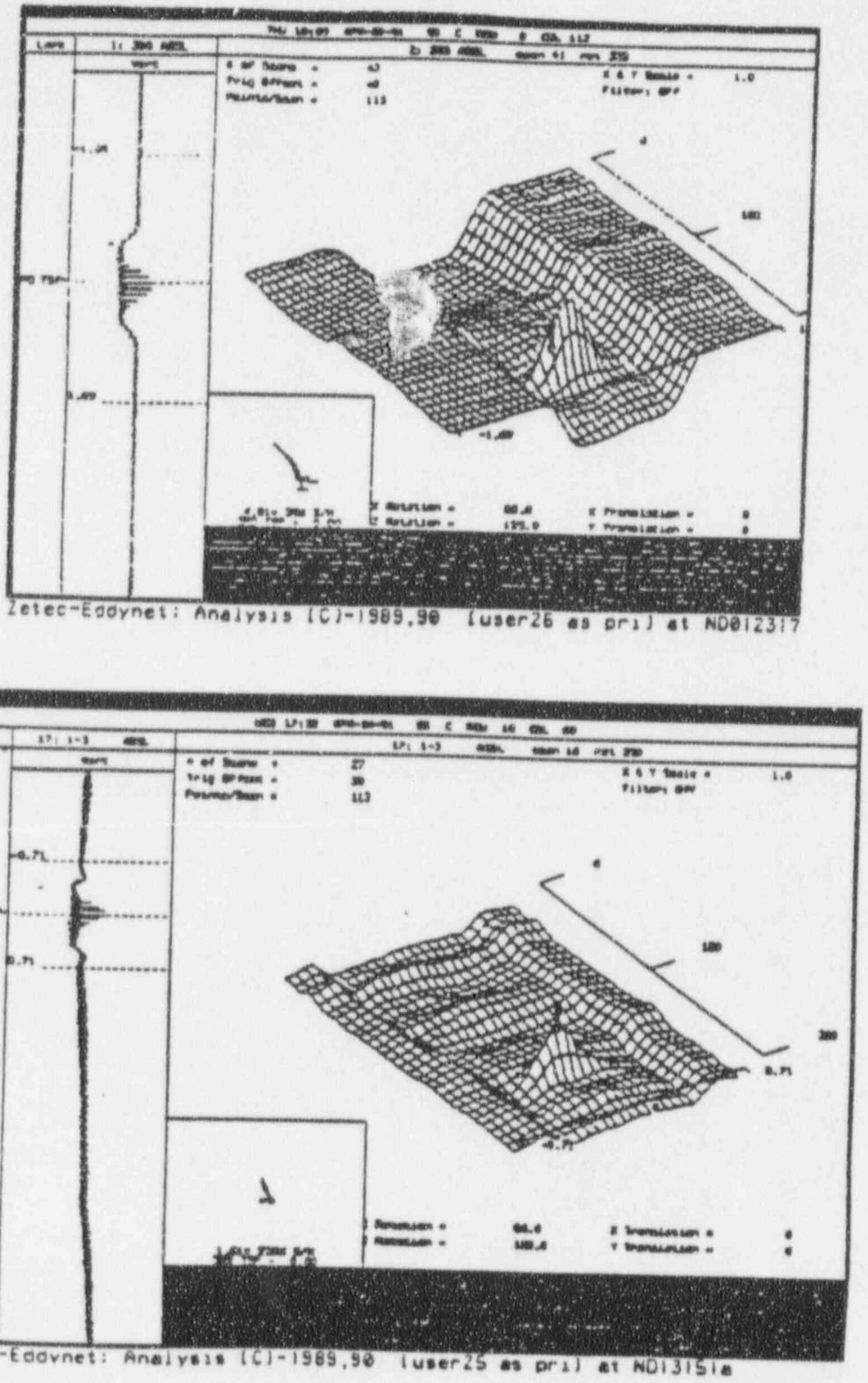

Figure 3-2. Plant R Example RPC Traces from Hot Leg Support Plate Locations

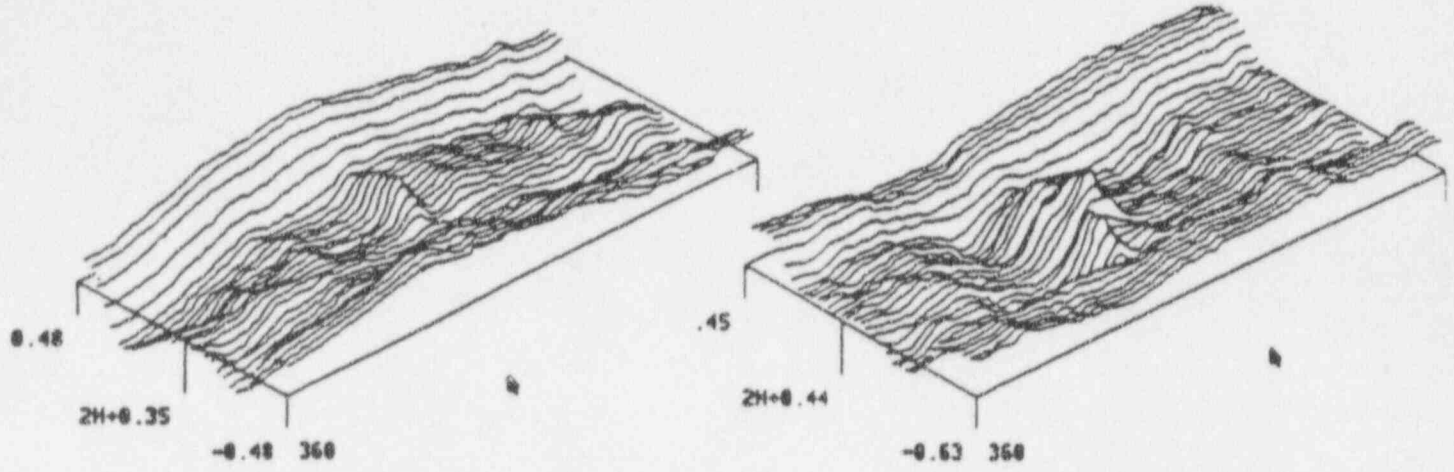

a) R4 C67, Location 2H

b) R42 C48, Location 2H

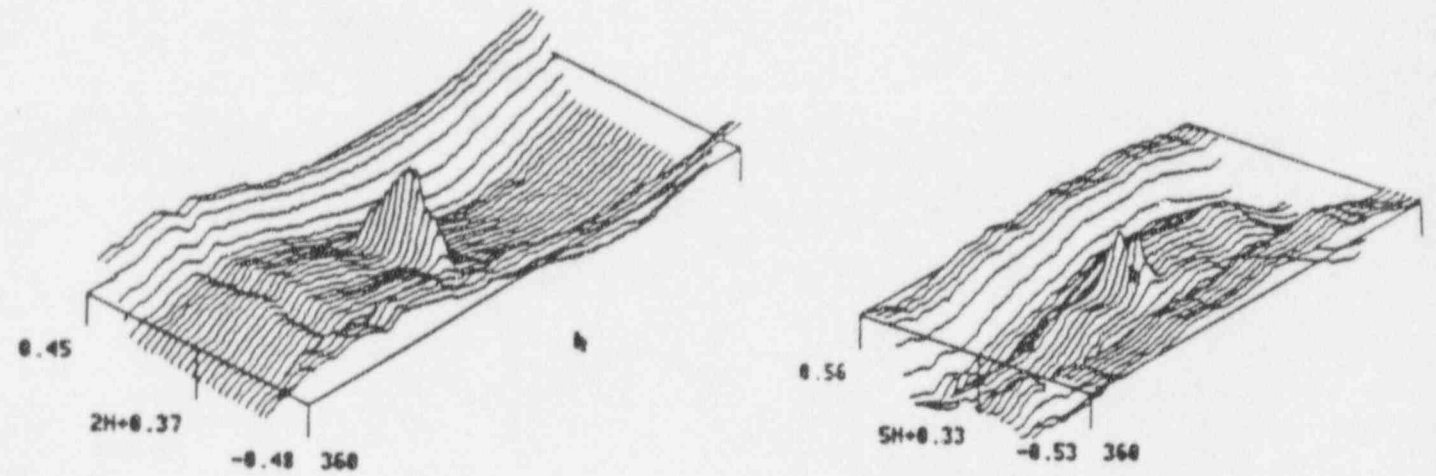

c) R27C99, Location 2H

d) R14 C56, Location 5H

Figure 3-3. Plant S Example RPC Traces from Hot Leg Support Plate Locations in SG A

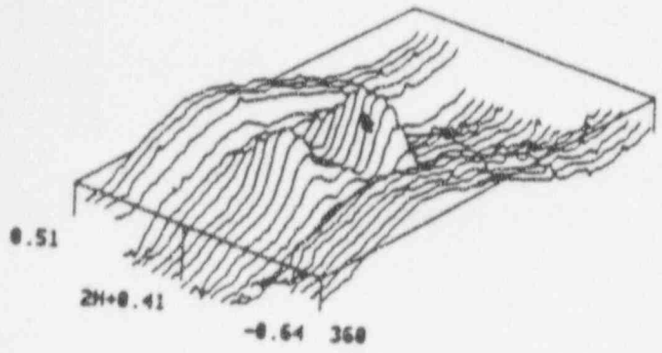

a) R810C44, Location 2H

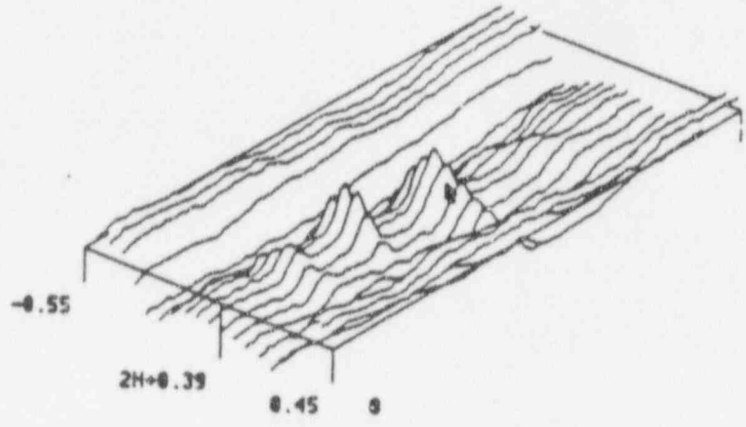

b) R10 C94, Location 2H

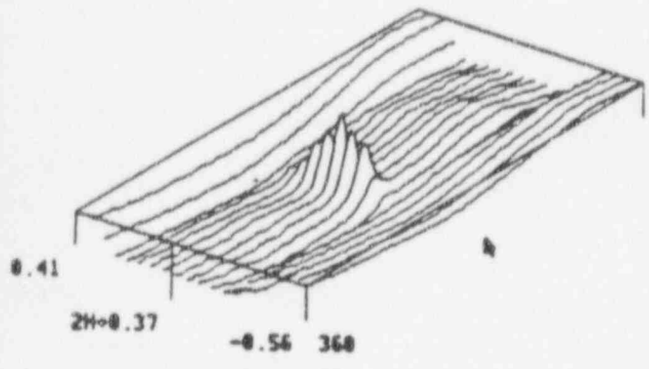

c) R9 C103, Location 2H

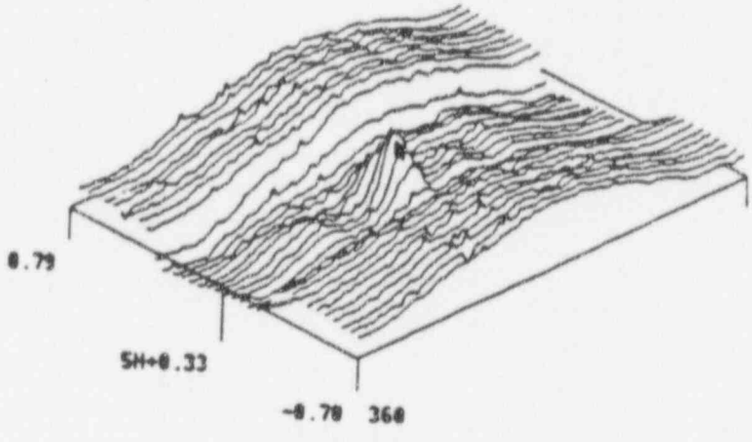

d) R46 C71, Location 5H

Figure 3-4. Plant S Example RPC Traces from Hot Leg Support Plate Locations in SG B

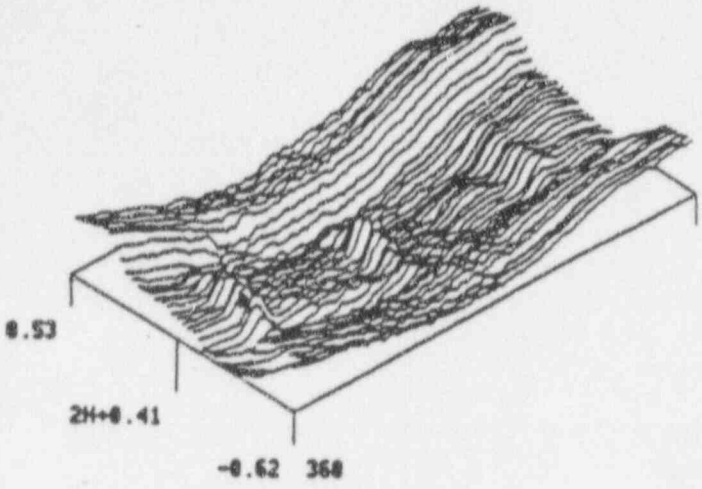

a) R39 C91, Location 2H

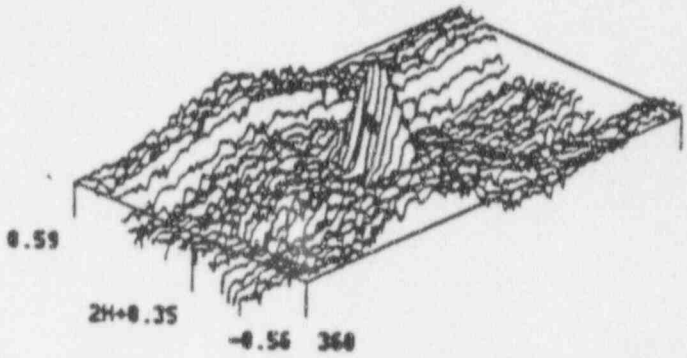

b) R8 C27, Location 2H

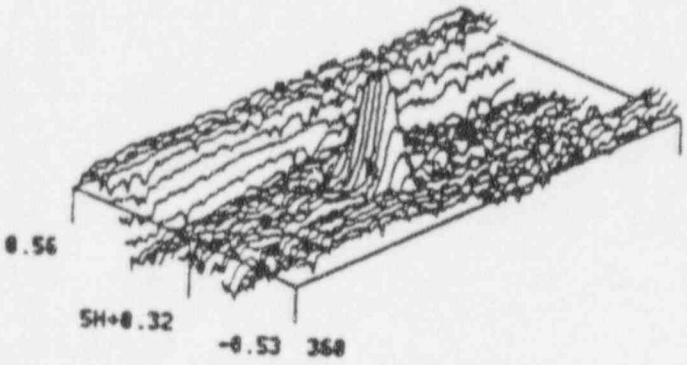

c) R37 C40, Location 5H

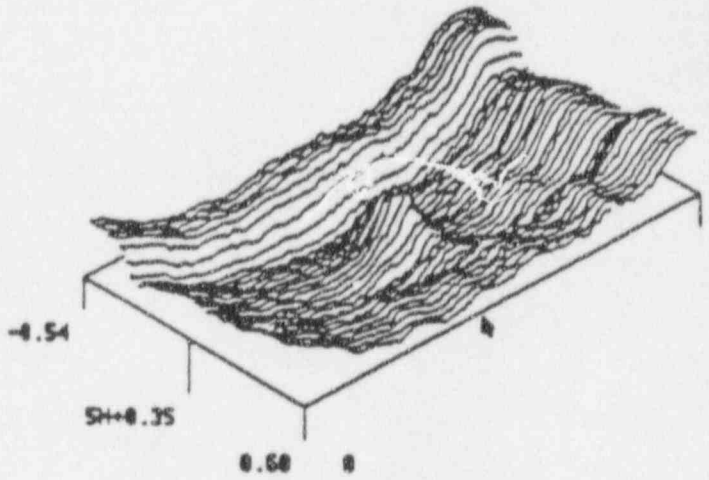

d) R21 C84, Location 5H

Figure 3-5. Plant S Example RPC Traces from Hot Leg Support Plate Locations in SG C

4.0 ACCIDENT CONSIDERATIONS

4.1 General Considerations for Accident Condition Analyses

The approach being applied to demonstrate tube integrity at Braidwood-1 is based on applying SLB analyses demonstrating limited TSP displacement to reduce the likelihood of a tube burst in a SLB event to negligible levels. In addition, it is demonstrated that the SLB leak rate, even under the conservative assumption of leak rates for free span indications, is within acceptable limits. The allowable limit on the SLB leak rate is developed in Section 4.8.

Section 4.2 develops the SLB thermal hydraulic loads on the TSPs which are used in the structural analyses of Sections 4.3 to 4.5 to obtain TSP displacements. At this time, Model D4 S/G loads are available for an SLB at normal operating conditions and for a very conservative SLB at hot standby conditions. The hot standby loads include conservatisms based on low water levels (at level of the top TSP) and include a simultaneous feedwater transient. The potential level of conservatism in the Model D4 hot standby loads is demonstrated by comparing the loads with those obtained from a Model D3 S/G analysis with normal water level and no feedwater transient. Both SLB analyses, at normal operating conditions and at conservative hot standby conditions, for TSP displacements developed in this section are applied in Section 8 to develop tube burst margins. The TSP displacements are calculated relative to the tube location at the start of the transient, as discussed in Section 4.5. Section 4.4 includes an assessment of the structural integrity of the TSPs and their supports (bar, wedge welds). Section 4.6 develops the frequencies of occurrence for an SLB at Braidwood-1 at both normal operating and hot standby (Mode 3) conditions. It is shown that the frequency of an SLB at hot standby conditions, for which the TSP displacements are higher, is significantly lower than that for an SLB at normal operating conditions.

For a postulated accident condition combining a LOCA simultaneously with a SSE, it is possible to have some tubes near TSP wedges deformed by the resulting loading condition. Due to the potential for secondary to primary leakage in the combined LOCA plus SSE, the tubes subject to significant tube deformation near the wedges are excluded from application of the IPC repair limits. The analyses describing this consideration are described in Section 4.7.

Some of the analyses described in this section use the Westinghouse labeling system for numbering TSPs which differs from that applied at Braidwood-1. The following relates the Westinghouse and Braidwood-1 nomenclatures for hot leg TSP identification:

Westinghouse TSP	Braidwood-1 TSP
A	1
C	3
F	5
J	7
L	8
M	9
N	10
P	11

TSP 1 is the Flow Distribution Baffle (FDB). The FDB has large tube to plate clearances (nominal [ ]" diameter) in the central region of the plate and radialized holes (nominal [ ]" width) in the outer region. No indications have been found at the FDB in the Braidwood-1 SGs. For comparison, the Model D3 SG, for which indications have been found at the FDB, has a nominal hole diameter of [ ]".

4.2 Thermal Hydraulic Loads on TSP in a SLB Event

4.2.1 Introduction

A postulated steam line break (SLB) event results in blowdown of steam and water. The fluid blowdown leads to depressurization of the secondary side fluid. Pressure drop develops and exerts hydraulic loads on the tube support plate (TSP) or flow baffle. These hydraulic loads were determined for the Model D4 and D3 steam generator using the TRANFLO Code. This code is a network flow based code that can model the thermal and hydraulic characteristics of fluid through the steam generator internals. TRANFLO code predicts the transient flow rate, pressures and pressure drops.

The hydraulic loads vary with initial conditions and boundary conditions of the SLB event. The significant initial conditions are mode of operation and water level. The important boundary conditions are those associated with feedwater nozzle and steam nozzle; these include the size and location of break, and flow rate through the feedwater nozzle during the event. The most likely initial conditions are of full power operation with a normal water level.

When fluid moves in the tube bundle, water will exert a higher pressure drop across the TSP when compared to steam. Hot standby at zero power provides a solid water pool in the tube bundle while power operation generates a steam and water mixture. Thus, hot standby would be conservative in estimating the hydraulic loads on the TSPs, although the most likely mode of operation is power operation if a SLB event occurred. Previous studies confirmed that the

hot standby yields the largest hydraulic loads when compared to full or partial power operation.

Once a SLB event begins, it triggers a rapid depressurization, which leads to water flashing across the water level. The rapid water flashing generates water motion, and the closer the TSP to the water level the higher the flow rate, and thus the larger the pressure drop. Previous parametric evaluations indicate that a lower water level tends to yield higher hydraulic loads on the tube support plates or baffles.

It would be ideal to calculate the hydraulic loads on the TSPs of the Model D4 steam generator under the no load, hot standby conditions. Although there are currently no such calculations, there are other calculations of Model D3 and D4 for developing conservative, bounding loads for the Model D4. This section presents such a task. These bounding loads for the Model D4 and the more applicable Model D3 loads at hot standby with normal water level.

4.2.2 Hydraulic Loads of Model D3 under No Load, Hot Standby with Normal Water Level

In 1993, a TRANFLO calculation of hydraulic loads on the TSP under a SLB event was made for a Model D3 steam generator. The calculation considers the initial conditions of zero load, hot standby and a water level at about normal setting. The following describes the calculation model.

The Model D3 steam generator maintains a normal water level of [ ]* above the top of the tubesheet during no load, hot standby. The computational model considers a water level of [ ]* above the top of the tubesheet. Use of the no load, hot standby and a water level of [ ]* is thus conservative in estimating the pressure loads to tube support plates. Water and steam temperature is initially at 557°F, and primary coolant pressure is at 2350 psia. and secondary side steam pressure is at 1106 psia, and feedwater temperature at 75°F.

A network of nodes and connectors was created to represent the secondary side fluid, tube metal heat transfer and primary coolant. Figures 4-1 and 4-2 show the nodal layout of the secondary side of the Model D3 steam generator. Figures 4-3 and 4-4 present the nodal network of the secondary fluid, primary fluid and tube metal. In the tube bundle area, the space between support plates or baffles forms a fluid node, and a flow connector links the adjacent nodes. Pressure drops through support plates or baffles are calculated by the code for each flow connector, which represent a plate or baffle.

Blowdown flow induces fluid flow in the secondary side, and thus pressure loads to various TSPs and baffle plates. Figures 4-5 through 4-7 show pressure loads through TSPs and baffle

plates outside the preheater. The peak of pressure loads across TSP or baffle plates develops within one second, and it then drops to a small value or becomes a quasi-steady state.

The flow splits take place in the lower tube bundle; it occurs at about TSP L (see Figure 4-1). Plates A, C and G experience downward flow because the fluid leaves in a downward direction from the tube bundle up into the downcomer. Plates above TSP L experiences upward flow as the fluid leaves in the upward direction through the tube bundle. Maximum loads occur at TSPs A, B and T; about [ ]* at the peak for TSP B on the cold leg, [ ]* for TSP A on the hot leg, and [ ]* for TSP T (i.e., the uppermost TSP).

4.2.3 Hydraulic Loads of Model D4 under Full Power with Normal Water Level

Although there are differences in the preheater design between the Model D3 and D4 steam generator, it is judged that there would be no significant differences in the hydraulic loads on the TSPs outside the preheater. It would be ideal to have a TRANFLO calculation for the Model D4 steam generator with initial conditions and boundary conditions like Case 1 for the Model D3. However, no such run is currently available. Calculations are available for hydraulic loads on the TSPs for the Model D4 steam generator under full power operation with a normal water level when a SLB begins.

Figure 4-8 illustrates the nodal layout of the secondary side of the Model D4 steam generator, which is similar to Figure 4-1 for the Model D3. The calculation was made for design analyses in the 1970's. Table 4-1 lists the initial and boundary conditions for three cases for which SLB loads are available; Case 3 will be discussed later.

Results of Case 2 are presented in Figures 4-9 through 4-11. As discussed earlier, hydraulic loads for a steam and water mixture in the tube bundle are less than a solid water pool. Therefore, hydraulic loads of Case 2 for the Model D4 is less than those of Case 1 for the Model D3. When a SLB event initiates from a power operation, the blowdown flow path is essentially in the upward direction from the tubesheet towards the riser barrels. Therefore, hydraulic loads tend to be higher at the upper TSPs, as shown in the above figures. Since the event begins from full power operation, the steam content increases with the bundle height. The uppermost TSP is thus lower in water content, and the resulting hydraulic load is less than the N plate below it. In addition, the highest loads occurs at the TSP L on the hot leg because the flow area is half of a whole TSP and the majority of flow is passing through the hot leg side.

Compared to Case 1 for the Model D3, which experiences flow splits, loads of Case 2 for Model D4 are less even under the situation of no flow splits. The reason for this is because of its relatively mild initial conditions.

4.2.4 Hydraulic Loads of Model D4 under No Load, Hot Standby with a Water Level at the Uppermost TSP and an Excessive Feedwater Flow Transient

The TRANFLO computational model for this case is identical to Case 2 except for its initial and boundary conditions. This calculation of Case 3 uses extremes of both initial and boundary conditions. No load at hot standby is already conservative compared to a most likely mode of full power operation; it considers a water level at the uppermost TSP, which is by itself a very rare transient. In addition, it imposes an excessive feedwater flow transient. As discussed already, a water level at the uppermost TSP generates higher hydraulic loads than a normal water level. An excessive feedwater flow introduces more solid water into the tube bundle, which provides additional source of water for flashing action to trigger more water motion.

Figures 4-12 through 4-14 presents hydraulic loads on various TSPs. Like Case 1, flow splits take place for Case 3 since both cases initiate from a no load, hot standby condition. However, Case 3 yields much higher loads than case 1 because of severe initial and boundary conditions discussed above.

4.2.5 Summary

Table 4-2 summarizes the key parameters regarding the loads. As far as the maximum peak load is concerned Case 2 for Model D4 yields slightly higher loads than Case 1 for Model D3. This is because the flow area for the plate with maximum load is half of the whole plate only, and there is no flow split. The lower TSPs of Case 2 experience hydraulic loads much less than those of Case 1, because there is almost no downward flow split for Case 2.

Peak loads of Case 3 are more than twice those of Case 2. Use of loads of Case 3 is conservative. It is believed that loads for Model D4 would be about the same as those of Case 1 for Model D3, if the same initial and boundary conditions are used in the computational model.

4.3 Structural Modeling for SLB TSP Displacement Analyses

This section summarizes the structural modeling of the Model D4 tube bundle region. A finite element model of the hot leg region of the tube bundle is prepared, and corresponding mass and stiffness matrices are generated. The mass and stiffness matrices are then used in a subsequent dynamic analysis to determine TSP displacements under SLB loads. Structural

members included in the model include all TSPs, the tierods and spacers.[1] Since the present analysis considers only the response of the hot leg to the SLB loading, the finite element model includes 90° of the tube bundle.

4.3.1 Material Properties

A summary of component materials is contained in Table 4-3, with the corresponding material properties summarized in Tables 4-4 through 4-6. The properties are taken from the 1971 edition (through summer 1972 addenda) of the ASME Code, which is the applicable code edition for Braidwood Unit 1. Since temperature dependent properties cannot be used in substructures, properties for the finite element model correspond to the values at 550°F. The material properties for the tube support plates are modified to account for the tube penetrations and flow holes. The density of the TSPs is also modified to account for the added mass of the secondary side fluid.

4.3.2 TSP Support System

The support system for the TSPs is a combination of several support mechanisms. A schematic of the tube bundle region is shown in Figure 4-15, with each of the plates identified. [

]^{a}

---

[1] For the analysis of the Model D3 steam generators under SLB loads, the finite element model also included the shell, wrapper, partition plate, and channel head. Except for the tubesheet, these structures were included to account for support locations for the TSPs and baffle plates. However, compared to the stiffness of the TSPs, baffle plates, and tierods, these structures are essentially infinitely stiff and have insignificant displacements (<0.010) under SLB loads. Therefore, it is acceptable to treat these structures as points of rigid support for the plates, and not include them explicitly in the model.

Regarding the tubesheet, although not considered explicitly in the finite element model, tubesheet displacements are considered in the analysis. Due to similarities in geometry of the tubesheet, shell, and channel head, displacements are scaled from the Model D3 analysis. The tubesheet displacements are quite small relative to the TSP displacements, and scaling of Model D3 displacements is an acceptable approximation. Further discussion of the tubesheet displacements is provided in Section 4.4.

The Model D3 analysis also considered the non-linear interaction between tubes and TSP due to TSP rotation. The present analysis has not incorporated this effect, primarily due to the limited time available to develop the system model. This effect may be considered in subsequent evaluations to limit plate displacements.

[

]*

The lack of a rigid link between the spacers and TSPs for the outer tierods / spacers results in a non-linear dynamic system. However, the nature of the SLB transient results in an essentially linear system response. During installation a small positive preload is introduced into the tierod/spacer system. As shown in Section 4.2, the plates are subject either to an upward or downward pressure loading, with the exception being Plate J, which sees a both a significant upward and downward loading. Thus, the response is essentially linear either upward or downward. The tierods/spacers have a different stiffness characteristic for upward and downward loads. These differences have been incorporated into the model. For Plate J, the weaker of the two stiffnesses has been incorporated to provide a conservative response.

---

[2] [

]*

[3] [

]*

The various support locations for the plates are shown in Figures 4-16 through 4-24. Figure 4-16 shows the locations of the tierods and spacers. Plate / wrapper support locations are shown in Figures 4-17 through 4-24. The finite element model representation of the plates and tierods/spacers is shown in Figure 4-25.

4.3.3 Revised Material Properties

As noted earlier, the material properties for the tubesheet and tube support plates are modified to account for the tube penetrations, flow holes, and various cutouts. The properties that must be modified are Young's modulus, Poisson's ratio, and the material density. The density must be additionally modified to account for the added mass of the secondary side fluid.

In calculating revised values for Young's modulus and Poisson's ratio, separate formulations are used for plates with and without flow holes. Due to square penetration patterns, different properties exist in the pitch and diagonal directions. The first step is to establish equivalent parameters for Young's modulus and Poisson's ratio in the pitch and diagonal directions (E_p^*/E, E_d^*/E, ν_d^*, ν_p^*), respectively. The equivalent Young's modulus for the overall plate is taken as the average of the pitch and diagonal directions. The next step in the process is to determine an equivalent value for the shear modulus, G^*/G, for the plate. This is done in a similar manner as for Young's modulus, starting with values in the pitch and diagonal directions, and then taking an average of the two values. The final equivalent value for Poisson's ratio is determined from the relationship between Young's modulus and the shear modulus. A summary of the revised values for Young's modulus and Poisson's ratio is provided in Table 4-7.

There are two aspects to revising the plate density. The first is based on a ratio of solid area to the modeled area. The second aspect corresponds to the plate moving through the secondary side fluid, displacing that fluid, and creating an "added mass" effect. The added hydrodynamic mass is a direct function of the fluid density. Because the dynamic analysis cannot account for the change in fluid density with time, the analysis uses the average density value for the duration of the transient. Results of the calculations to determine effective plate densities are summarized in Table 4-8. This table provides a summary of the actual (structural) and modeled plate areas, the metal and added fluid masses, and the final effective plate densities. The fluid densities correspond to SLB events initiating from hot shutdown conditions (as opposed to full power operation). Calculations were also performed for densities corresponding to full power operation. The change in effective plate densities did not have a significant effect on the dynamic response of the plates.

4.3.4 Dynamic Degrees of Freedom

In setting up the dynamic substructures, it is necessary to define the dynamic degrees of freedom. In order to define dynamic degrees of freedom for the TSPs, two sets of modal calculations are performed for each of the plates. The first set of calculations determine plate mode shapes and frequencies using a large number of degrees of freedom (approximately 120 per plate). The second set of calculations involves repeating the modal analysis, using a significantly reduced set of degrees of freedom (DOF). The reduced DOF are selected to predict all frequencies for a given plate below 50 hertz to within 10% of the frequencies for the large set of DOF. A frequency of 50 hertz was selected as a cutoff, as it is judged that higher frequencies will have a small energy content compared to the lower frequencies. This can be confirmed by noting that the highest frequency content in the first one and a half seconds of the pressure drop time-history input loadings is typically less than 10 hertz. For each of the modal runs, in addition to symmetry boundary conditions along the "Y-axis", and vertical restraint at vertical bar locations, all the plates are assumed to be constrained vertically at tierod/spacer locations.

A sample set of mode shape plots is provided for Plate A. Mode shape plots for the full set of DOF are shown in Figures 4-26 through 4-28, while mode shapes for the reduced set of DOF are shown in Figures 4-29 through 4-31. A comparison of the natural frequencies for the full and reduced sets of DOF for the plates is provided in Table 4-9. Based on the tabular summary, the reduced set of DOF are concluded to provide a good approximation of the plate response. Note that for Plate P, the frequency for Modes 3 and 5 for the reduced set of DOF slightly exceeds the 10% objective for matching frequencies. These variations are not considered to be significant, and the selected DOF are judged to give an acceptable representation of the Plate P response. The reduced set of DOF consists of 8 - 10 DOF for each of the plates.

4.3.5 Displacement Boundary Conditions

The displacement boundary conditions for the substructure generation consist primarily of prescribing symmetry conditions along the "Y" axis for each of the components. Vertical constraint is provided where the plates are constrained by the vertical bars welded to the partition plate and wrapper, and to the tierods at there bottom end. For the TSPs, rotations normal to the plate surface are also constrained, as required by the stiffness representation for the plate elements.

4.3.6 Application of Pressure Loading

The SLB pressure loads act on each of the TSPs. To accommodate this, load vectors are prescribed for each of the plates using a reference load of 1 psi. The reference loads are scaled during the dynamic analysis to the actual time-history (transient) loading conditions, as defined in Section 4.2.

The transient pressures summarized in Section 4.2 are relative to the control volume for the thermal hydraulic analysis. The area over which the hydraulic pressure acts corresponds to the area inside the wrapper minus the tube area. These pressures must be scaled based on a ratio of the plate area in the structural model to the control volume area in the hydraulic model. A summary of the transient pressure drops is given in Section 4.2. These pressure drops were modified as discussed above and applied to the structural model for the dynamic analysis.

4.4 Results of SLB TSP Displacement Analyses

As discussed in Section 4.2, several sets of SLB loads were considered in performing this analysis. In addition to the system analysis, some preliminary single-plate evaluations were performed to estimate the plate response to the applied loadings. Calculations were also performed using the single plate models to estimate the effects of expanding tubes at various locations in the tube bundle to limit plate motions. The results for each set of calculations is summarized within this section of the report.

An overall summary of the limiting displacements for each of the plates for the various cases considered is provided in Table 4-10. The displacements in this table are relative to the initial starting plate positions. The magnitude of the tubesheet displacements and there affect on these results is discussed below.

The first two sets of results in Table 4-10 are for the most limiting SLB loading (SLB with a simultaneous Feedwater Transient) using the single plate models, with and without tube expansion. These results show that tube expansion significantly reduces plate displacement for all of the plates. The third set of results is again for the limiting SLB transient for the full system model. Comparing these results to the single plate models shows that the single plate models provide a good indication of the relative plate motions, but that plate interaction does result in an increase in the plate responses, more for some plates than others.

Comparing the results for the three SLB sets of loads using the system model shows that for the limiting SLB loads, Plates A (1H), C (3H), and J (7H) experience displacements greater

than 0.350 inch. For a transient initiating from normal operation that only Plate J (7H) sees any significant motions, and for the Model D3 SLB loads case, only Plates A (1H) and C (3H) show any significant response. Based on the single plate response to the limiting load with expanded tubes, it is concluded that expansion of a limited number of tubes would be effective in reducing the response of each of these plates to very low levels.

The limiting plate displacements in all cases are limited to a small region of the plate at their outer edge near the tube lane, where the distance between vertical supports is greatest. Displaced geometry plots for Plates A (1H), C (3H), and J (7H) for the limiting set of SLB loads are shown in Figures 4-32 through 4-35. The consistent displacement pattern is apparent for the three plates. Displacement time histories for each of the plates for the limiting transient loads are provided in Figures 4-36 and 4-37. The bottom four plates are shown in Figure 4-36 and the upper four plates in Figure 4-37.

As discussed previously, tubesheet displacements are not significant and were scaled from the Model D3 analysis. The geometry of the tubesheet and supporting structures for the two designs is nearly identical. A summary of key dimensions for the two models of steam generators is provided in Table 4-11. Displacement results for the tubesheet from the Model D3 analysis as a function of distance from plate center for several transient times are summarized in Table 4-12. At the bottom of this table a summary of the tubesheet displacements relative to time zero are presented. The relative displacements are shown to be quite small relative to the plate displacements. This is especially true at the outer edge of the tubesheet where the plate displacements are a maximum.

Since the dynamic analysis is based on elastic response, calculations were performed to assure that the tierods, a significant support element for the plates remain elastic throughout the transient. The dynamics analysis results establish that the stayrods do, in fact, remain elastic throughout the transient. [

]* In both instances, these elongations are well below the yield point for the stayrods.

Also relevant in assessing the appropriateness of the elastic solution, are the stresses in the plates. Thus, in conjunction with the displacement results from the dynamic analysis, stresses are calculated for the hot leg plates at the times corresponding to the maximum plate displacements. The stresses are calculated by extracting displacements from the dynamic analysis for each plate degree of freedom, and then applying those displacements to the finite element model. The finite element code then back-calculates the displacements and stresses for the overall plate model.

In order to extract the appropriate displacements from the tape created by the dynamic analysis, a special purpose computer program is used. This program extracts the displacements for a given plate at specific transient times and writes the resulting nodal displacements to output in a form that can be input directly to the WECAN program as displacement boundary conditions. Using this program, displacement boundary conditions are extracted at the times of maximum relative displacement for Places A (1H), C (3H), and J (7H) at the critical times for the SLB + Excess Feedwater transient and for Plates A (1H) and C (3H) for the Model D3 transient. Note that for Plate J for the SLB + Excess Feedwater transient, stresses are calculated for the times corresponding to both the maximum upward displacement and also for the maximum downward displacement. These are the transients and plates that are judged to be limiting based on the plate displacement results.

Additional boundary conditions corresponding to lines of symmetry and appropriate rotational constraints are also applied to the model. The finite element results give a set of displacement and stress results for the overall plate. The resulting plate stresses, however, correspond to the effective Young's modulus, and must be multiplied by the inverse ratio of effective-to-actual Young's modulus to get the correct plate stresses. The stress multiplication is performed by another special purpose computer program, SRATIO.

In order to interpret the stress results, stress contour plots for the maximum and minimum stress intensities have been made for each plate. The limiting stresses for each of the plates occur for the SLB + Excess Feedwater transient. Plots showing the maximum and minimum stress intensities for Plates A(1H), C(3H), and J(7H) are shown in Figures 4-38 to 4-45, respectively. These plots show the distribution of stress throughout the plate. As expected, the maximum stresses occur near the locations of vertical support, the tierod / spacers and vertical bars. The ASME Code minimum yield strength for the TSP material is 23.4 ksi. Except for one very local area for Plate J corresponding to the upward loading on the plate (Figure 4-42), the stresses are elastic throughout the plate. Recalling that the present analysis does not account for either the wedge support for Plate J at the 10° location, or the potential for tube/plate interaction due to plate rotation, the stresses in Figures 4-42 and 4-43 for Plate J are judged to be conservative. Thus, it is judged that the effective plate stresses will be judged to be elastic for all transient cases.

The plate stresses cannot be compared directly to the material yield strength, as these stresses correspond to an equivalent solid plate. In order to arrive at the plate ligament stresses, additional detailed stress analysis of the plates is required. Such an analysis is outside the scope of this program. The equivalent plate stresses do provide a general guideline as to those areas of the plate that are most limiting from a stress viewpoint. The plate stresses are meaningful in that they indicate that the stresses are generally low throughout the plate, and that the elastic analysis is a good approximation of the transient plate response.

Calculations have also been performed to determine the stresses in the welds between the vertical bars and the partition plate and wrapper. The loads at the various support points are extracted from the static WECAN runs in the form of reaction forces at the times of maximum plate deflection. Loads have been extracted for the limiting plates (based on plate motions) for each of the SLB load cases, and for Plate P, which experiences the highest pressure loads, for the SLB + Excess Feedwater transient.

[

]* The corresponding stress intensity is twice the shear stress.

A summary of the reaction forces and corresponding stresses for each of the bar locations for the locations considered is provided in Table 4-13. The results show all of the stresses to be low (<2 ksi) for a faulted event. The allowable stress for the welds is based on $2.4S_m$ x 1.5 x 0.35 (for fillet welds with visual examination) for carbon steel. S_m at 550°F is 15.5 ksi. The resulting allowable stress intensity is 19.53 ksi, and the weld stresses are acceptable.

Overall, it is concluded that the elastic analysis provides a good approximation of the dynamic response of the TSPs to the applied loading.

4.5 SLB Displacements By Tube Location

In order to establish probabilities for tube burst as a result of relative plate / tube movement, calculations are performed to determine how many tubes are associated with a given displacement magnitude for a given plate. The plate displacements are categorized into groups, starting at 0.35 inch, and increasing in 0.05 inch increments to a maximum displacement > 0.80 inch. It is the relative plate / tube displacement that is of interest, with the tube and plate positions at the start of the SLB transient defined as the reference position. At hot standby, the TSP positions relative to cracks inside the TSP are essentially the same as at cold shutdown. Every known S/G cold condition inspection shows ODSCC cracks within the non-dented TSP with a trend towards being centered within the TSP. Therefore, the cold condition TSP location relative to the tubes is essentially the same as for the full power condition where the cracks formed, which is also the position during hot shutdown. These inspections indicate that there is little relative movement between the tubes and plates throughout the operating cycle. Thus, this analysis calculates relative tube / TSP motions based on the tube / plate positions at the initiation of the SLB transient.

The algorithm for calculating the relative displacements is as follows:

$$\Delta D = (D_{t=T} - D_{t=0})_{Plate} - (D_{t=T} - D_{t=0})_{Tubesheet}, \text{ where}$$

D_{Plate} = Plate Displacement

$D_{Tubesheet}$ = Tubesheet Displacement

T = Time of maximum displacement from dynamic analysis

In order to calculate the relative displacements across the full plate, displacement (stress) solutions are performed for the limiting plates at the times of maximum displacement. Calculations were performed for each set of transient loads for those plates where the maximum absolute displacement exceeded 0.350 inch.

The displacement solutions are performed using the finite element representations for the plates. Displacements for the dynamic degrees of freedom for the limiting plates are extracted at the times of interest from a file containing the DOF displacements for the full transient. These displacements are applied to the finite element model as boundary conditions (along with any other appropriate boundary conditions representing symmetry or ground locations), and displacements for the entire plate are then calculated. These results are then combined with the scaled tubesheet displacements, to arrive at a combined relative displacement between the tubes and plates. The combined relative displacements are then superimposed on a tube bundle map, and the results interpolated to arrive at a displacement value for each tube location.

A summary of the number of tubes falling into each of the displacement groupings for the limiting plates is provided in Table 4-14. Note that the numbers of tubes in Table 4-14 correspond to the full plate. The number of tubes in each plate quadrant is one-half of the values listed. A summary of the total number of tubes having displacements > 0.35 inch for each of the SLB loads is provided in Table 4-15. Note that at the top of Table 4-14, the limiting displacements as reported in Table 4-10 are repeated, while the number of tubes where the relative plate/tube displacements exceed 0.350 inch are summarized at the bottom of the table.

Summarized in Table 4-16 is a comparison of the maximum plate displacement to the plate displacement at the limiting tube location (the tube having the highest displacement), R1C1. As can be observed in the displaced geometry plots in Figures 4-32 - 4-35, the displacement gradients at the corner of the plate are high, so the maximum differential displacement at R1C1 is less than the maximum plate displacement reported in Table 4-15.

4.6 SLB Frequency at Hot Standby and Full Power Conditions

In order to identify the frequency of main steamline break in both the hot standby and full power conditions to support the steamline break tube support plate displacement analysis for Braidwood Unit 1, a review of References 4-1 and 4-2 for the Byron Nuclear Power Station Units 1 and 2 was completed.

4.6.1 Secondary Side Breaks

Two main feedline pipe breaks have occurred on Westinghouse designed PWRs. The feedline breaks were downstream of the main feedwater isolation valves (MFWIVs), outside containment. The number of years at criticality calculated for all Westinghouse designed PWRs is 1370 years (Reference 4-1).

Using the Bayes theorem, the mean frequency of occurrence may be determined (Reference 4-2) by:

$$mean = \frac{2r+1}{2t}$$

where r is the number of failures and t is the time interval. Substituting r = 2 and t = 1370,

$$mean = \frac{2(2)+1}{2(1370)} = \frac{2.5}{1370} = 1.8E\text{-}03/year$$

Since no secondary side breaks have occurred, other than these two main feedline breaks, the mean of the frequency for this event is 1.8E-03/year (Reference 4-1).

Based on the plant response to steamline/feedline breaks, this event is split into two initiators: (1) secondary side breaks downstream of the main steam isolation valves (MSIVs) or upstream of the MFWIVs and (2) secondary side breaks upstream of the MSIVs or downstream of the MFWIVs. The same frequency is used for both types of steamline/feedline breaks. That is,

Secondary side breaks upstream of MSIVs or downstream of MFWIVs = 1.8E-03/year
Secondary side breaks downstream of MSIVs or upstream of MFWIVs = 1.8E-03/year

4.6.2 Hot Standby and Full Power Conditions Evaluations

A review of the operating histories for Braidwood Unit 1 Cycle 3 and 4 was completed to determine the amount of time spent in Mode 3 versus full power operation. The result of this evaluation is shown in Table 4-17. The frequency of Mode 3 operation is defined as:

$$Frequency\ of\ Mode\ 3 = \frac{Days\ in\ Mode\ 3}{Days\ in\ Cycles\ 3\ \&\ 4} = \frac{36.1}{959} = 0.038$$

$$Frequency\ of\ Mode\ 1 = 1 - Mode\ 3 = 0.962$$

The results of these calculations show a frequency in Mode 3 of 0.038 and frequency of Mode 1 of 0.962. Combining these frequencies with the IPE frequency of secondary side break upstream of the MSIVs gives a frequency of secondary side break upstream of the MSIVs in the Mode 3 condition and in the Mode 1 condition of:

$$Mode\ 3\ Secondary\ Side\ Break = (1.8E\text{-}03/year) \times 0.038 = 6.8E\text{-}05/yr.$$

$$Mode\ 1\ Secondary\ Side\ Break = (1.8E\text{-}03/year) \times 0.962 = 1.7E\text{-}03/yr.$$

4.7 Tubes Subject to Deformation in a SSE + LOCA Event

This section deals with accident condition loadings in terms of their effects on tube deformation. The most limiting accident conditions relative to these concerns are seismic (SSE) plus loss of coolant accident (LOCA). For the combined SSE + LOCA loading condition, the potential exists for yielding of the tube support plate in the vicinity of the wedge groups, accompanied by deformation of tubes and subsequent loss of flow area and a postulated in-leakage. Tube deformation alone, although it impacts the steam generator cooling capability following a LOCA, is small and the increase in PCT is acceptable. Consequent in-leakage, however, may occur if axial cracks are present and propagate throughwall as tube deformation occurs. This deformation may also lead to opening of pre-existing tight through wall cracks, resulting in primary to secondary leakage during the SSE + LOCA event, with consequent in-leakage following the event. In-leakage is a potential concern, as a small amount of leakage may cause an unacceptable increase in the core PCT. Thus, any tubes that are defined to be potentially susceptible to deformation under SSE + LOCA loads are excluded from consideration under the IPC.

In the absence of plant specific LOCA and SSE loads for Braidwood Unit 1, a conservative upper bound estimate was made of the maximum number of tubes that would be affected at each wedge location. Using the results of an analysis for another plant having the same model steam generators, a conservative upper bound of [ ]* per wedge group was established for the Braidwood Unit 1 steam generators. A summary of the applicable tubes for each of the wedge locations is provided in accompanying tables and figures.

Braidwood Unit 1 is a four-loop plant. As such, there are two loops with "left-hand" steam generators and two loops with "right-hand" steam generators. These designations refer to the orientation of the nozzles and manways on the channel head. For the purpose of this analysis, "left-hand" units are defined to be those loops where the primary fluid flows from the reactor to the steam generator to the pump and back to the reactor vessel in a counter-clockwise direction. Conversely, for the "right-hand" units, the flow is in the clockwise direction. The left- versus right-hand designation affects the location of the nozzles and manways, and the manner in which the columns are numbered for tube identification purposes. Reference configurations used in identifying wedge locations are shown in Figures 4-46 and 4-47 for the left-hand and right-hand units, respectively. As shown in the figures, for left-hand units, the nozzle and tube column 1 are located at 0°, while for right-hand units they are located at 180°.

Tabular summaries of the tubes that are potentially susceptible to collapse and subsequent in-leakage are summarized in Tables 4-18 to 4-23 for the left-hand units, and in Tables 4-24 to 4-29 for the right-hand units. For the Braidwood Unit 1 steam generators there is a flow distribution baffle, seven tube support plates, and three baffle plates. The plate configuration is shown in Figure 4-15. Plate A corresponds to the flow distribution baffle, Plates B, E, and H are the flow baffles, and Plates C D, F/G, J/K, and L, M, N, and P are the tube support plates.

Prior analysis for steam generators of similar design show the flow distribution baffle to not impact the wrapper/shell under seismic loads. Thus, it is judged that there will not be any tubes at the flow distribution baffle location that are potentially susceptible to collapse under combined LOCA+SSE. It will be noted that separate summary tables are provided for the lower TSPs, B-K (except E and H where a table common to both is used), and a single table for the upper TSPs L-P. This is due to the orientation of wedge groups for each of the TSP. For the lower TSPs, the wedge groups are rotated in some instances relative to the other TSPs, while for the upper TSPs, the wedge groups have the same angular orientation.

Maps showing the location of the potentially susceptible tubes are provided in Figures 4-48 to 4-57. The maps provide row and column designations relative to the left-hand units. Column numbers for the right-hand units are shown in brackets. Identification of the potentially susceptible tubes is based on crush test results for both Model D and Series 51 steam

generators. For both sets of tests, however, wedge / tube configurations identical to those for the Braidwood Unit 1 steam generators were not tested. As such, it was not possible to identify exactly the [ ]* that might be limiting at each wedge group. Thus, due to the uncertainties involved, there are generally [ ]* identified at each wedge group as being limiting.

Finally, Table 4-30 provides an index of the applicable tables and figures identifying the potentially susceptible tubes for each TSP.

4.8 Allowable SLB Leakage Limit

An evaluation has been performed to determine the maximum permissible steam generator primary to secondary leak rate during a steam line break for the Braidwood Nuclear Plant Unit 1. The evaluation considered both pre-accident and accident initiated iodine spikes. The results of the evaluation show that the accident initiated spike yields the limiting leak rate. This case was based on a 30 rem thyroid dose at the site boundary and initial primary and secondary coolant iodine activity levels of 1 μCi/gm and 0.1 μCi/gm I-131, respectively. A leak rate of 9.1 gpm was determined to be the upper limit for allowable primary to secondary leakage in the SG in the faulted loop. The SG in each of the three intact loops was assumed to leak at a rate of 150 gpd (approximately 0.1 gpm), the proposed Technical Specification LCO for implementation of IPC. The allowable leak rate will increase in inverse proportion to a reduction in the primary and secondary equilibrium coolant activity.

Thirty rem was selected as the thyroid dose acceptance criteria for a steam line break with an assumed accident initiated iodine spike based on the guidance of the Standard Review Plan (NUREG-0800) Section 15.1.5, Appendix A. Only the release of iodine and the resulting thyroid dose was considered in the leak rate determination. Whole-body doses due to noble gas immersion have been determined, in other evaluations, to be less limiting than the corresponding thyroid doses.

The salient assumptions follow.

- Initial primary coolant iodine activity - 1 μCi/gm DE I-131

  The calculation of primary coolant DE I-131 is based on a mixture of 5 iodine nuclides (I-131 through I-135) and the dose conversion factors of TID-14844, consistent with the Braidwood Technical Specification definition of DE I-131.

- Initial secondary coolant iodine activity - 0.1 μCi/gm I-131

  The calculation of secondary coolant iodine activity is based on actual I-131 activity rather than DE I-131. Although, this is somewhat more conservative than the Technical Specification LCO which is based on DE I-131, secondary coolant activity still accounts for less than 6% (1.75 rem) of the allowable offsite dose.

- Steam released to the environment (0 to 2 hours)

  - from 3 SGs in the intact loops, 416,573 lb
  - from the affected SG, 96,000 lb (the entire initial SG water mass)

- Iodine partition coefficients for primary-secondary leakage

  - SGs in intact loops, 1.0 (leakage is assumed to be above the mixture level)
  - SG in faulted loop, 1.0 (SG is assumed to steam dry)

- Iodine partition coefficients for activity release due to steaming of SG water

  - SGs in intact loops, 0.1
  - SG in faulted loop, 1.0 (SG is assumed to steam dry)

- Atmospheric dispersion factor (SB 0 to 2 hours), 7.70E-4 sec/m^3

- Thyroid dose conversion factors (I-131 through I-135) utilized in offsite dose calculation, ICRP-30

The activity released to the environment due to a main steam line break can be separated into two distinct releases: the release of the iodine activity that has been established in the secondary coolant prior to the accident and the release of the primary coolant iodine activity that is transferred by tube leakage during the accident. Based on the assumptions stated previously, the release of the activity initially contained in the secondary coolant (4 SGs) results in a site boundary thyroid dose of approximately 1.75 rem. The dose contribution from 1 gpm of primary-to-secondary leakage (4 SGs) is approximately 3 rem. With the thyroid dose limit of 30 rem and with 1.75 rem from the initial activity contained in the secondary coolant, the total allowable primary-to-secondary leak rate is (30 rem - 1.75)/3 rem per gpm, or 9.4 gpm. Allowing 0.1 gpm per each of the 3 intact SGs leaves (9.4 - 0.3) or 9.1 gpm for the SG on the faulted loop.

4.9 Acceptability of the Use of TRANFLO Code

4.9.1 Background

In the early 1970's, there was a need to accurately predict the steam generator behavior under transient conditions, such as a steam line break (SLB) event; a transient can develop thermal hydraulic loads on the internal components and shell of the steam generator. Structural analyses are required to analyze the adequacy of the individual components and the whole steam generator under various thermal and hydraulic loads. With the assistance of MPR Associates, Westinghouse developed and verified the TRANFLO computer code to conservatively model the thermal and hydraulic conditions within the steam generator under transient conditions.

The secondary side of the steam generator involves water boiling under high pressure during normal operating conditions. During a transient such as a SLB event, it may be subject to vapor generation due to rapid depressurization. Therefore, analysis methods have to recognize this characteristic of two-phase fluid behavior. In the early stage of the computer code development and technology of two phase flow, a homogeneous model was used. For current analyses, a more accurate slip flow model is used which takes into consideration the relative velocity between the liquid and vapor phases. Development of the TRANFLO code reflects this general trend of the two-phase flow modeling. The first version of TRANFLO was a homogeneous model, and it was later updated to a drift flux model to simulate the effect of two-phase slip. Since the original issue of the code, Westinghouse has made several enhancements to the code and has performed the appropriate verification and validation of these changes. These changes do not significantly affect the calculated pressure drops across the steam generator tube support plates.

4.9.2 Acceptability of Application of TRANFLO

The original version of the TRANFLO code (Reference 4-3) was reviewed and approved by the NRC in Reference 4-4. TRANFLO was used as part of the Westinghouse mass and energy release/containment analysis methodology. Specifically, the code was used to predict steam generator (SG) secondary side behavior following a spectrum of steam line breaks. Its output was the prediction of the quality of the steam at the break as a function of time. The quality is calculated as a function of power level, as well as break size. In order to assure that the TRANFLO code evaluates a conservatively high exit quality, Reference 4-4 states that the calculational sequences were reviewed for the determination of "conditions prior to entering into the separation stages. The calculated rate, quality and energy content of the two-phase mixture entering the separation stages must be evaluated conservatively". This review was completed and found to be acceptable, as the NRC staff concludes in

Reference 4-4 that the TRANFLO code is an acceptable code for calculating mass and energy release data following a postulated MSLB. Therefore, it is concluded that the TRANFLO model is appropriate for predicting SG behavior (including tube bundle region) under the range of SLB conditions.

For the current application, TRANFLO is used in conjunction with a structural analysis code to predict TSP movement following the same SLB event. The key data transferred between the transient code and the structural code is the pressure drop across the TSP as a function of time. This pressure drop calculation depends on the fluid conditions in the steam generator and on the adequacy of the loss coefficients along the flow paths. The conditions in the tube bundle as calculated by TRANFLO have been previously reviewed. Further justification of the adequacy of the pressure drop calculation is discussed in Section 4.9.4.

4.9.3 Different Versions of TRANFLO

The original version of the TRANFLO code has been reviewed and approved by the NRC. Westinghouse has continued to update the code with new models that more accurately predict steam generator behavior. Four versions of TRANFLO have been used in calculation. The following are descriptions of each of them.

The Original Version (April 1974)

This is the original homogeneous model, which MPR Associates developed in April 1974. The code predicts mass flow rate, pressure, pressure drop, fluid temperature, steam quality and void fraction. The code document includes results of TRANFLO calculations for a 51 Series steam generator subject to water and steam blowdown due to an SLB event. The document also presents code verification using blowdown test data from pressurized vessels.

Westinghouse documented this version in detail in September 1976, including code verification using vessel blowdown data. Sensitivity analyses were also performed and documented to show that the modelling was conservative. This included sensitivities to loss coefficient.

The TRANFLO code uses an elemental control volume approach to calculate the thermal-hydraulics of a steam and water system undergoing rapid changes. Fluid conditions may be subcooled, two-phase or superheated. The code considers fluid flows being one-dimensional.

Control volumes simulate the geometrical model, and flow connectors allow mass and energy exchange between control volumes. Each nodal volume has mass and energy that are homogeneous throughout the volume. Flow connectors account for flow and pressure drops. The system model allows flow entering or leaving any control volume. This then allows that

feedwater flows into a steam generator and steam flows out of it. The system models also permit a heat source, which then can simulate the tube bundle with hot water flow.

TRANFLO solves for system conditions by satisfying mass, momentum and energy equations for all control volumes. It models the effects of two-phase flows on pressure losses. The code allows a variety of heat transfer correlations for the tube bundle. It covers all regimes from forced convection to subcooled liquid through boiling and forced convection to steam.

The Drift-Flux Version (November 1980)

This version implements a drift-flux model to better simulate relative flow velocity between water and steam. For example, it allows a realistic simulation of counter-current flow of steam and water. It required modification of the mass, momentum and energy equations of the two-phase flow. A capability is provided for monitoring calculated variables for convenient examination of results.

TRANFLO Version 1.0 (November 1991)

This version accepts transient data of parameters as direct inputs, rather than supplying input subroutines, as used in the drift-flux version. It also improves printouts and plots. This version maintains the drift-flux model, and includes the addition of thermal conductivity of Alloy 690 tubing.

TRANFLO Version 2.0 (January 1993)

This version provides an option for two inlets of feedwater flow into the steam generator. It involves minor changes to a subroutine for specifying feedwater flow. This version is used for separate inlets of simultaneous feedwater flow from main and auxiliary feedwater nozzle.

4.9.4 Verification of Loop Pressure Drop Correlations

As discussed earlier, an accurate prediction of mass and energy release from the vessel means that the TRANFLO code properly calculates local thermal-hydraulics in various nodes (i.e., elemental control volume and flow connector). It is critical to accurately simulate the pressure drop inside a steam generator that consists of various components, such as the tube bundle with tube support plates, moisture separators, and downcomer. Hydraulic loads on various components depend on accurate pressure drop calculations. Thus, it is important to verify the pressure drop calculations through the circulation loop.

The TRANFLO code uses the same pressure drop correlations as the Westinghouse GENF code, which is a performance program. The GENF code predicts one-dimensional steady

state conditions, which include pressure drops along the circulation flow loop. Both laboratory tests and field data validate the accuracy of the GENF code. The GENF code is used extensively for steam generator performance analysis and has been shown to accurately predict operating steam generator conditions.

When provided with all geometrical input and operating conditions, GENF calculates the steam pressure, steam flow rate, circulation ratio, pressure drops, and other thermal-hydraulic data. The circulation ratio is a ratio of total flow through the tube bundle to feedwater flow. For a dry and saturated steam generator, there exists a hydrostatic head difference between the downcomer and the tube bundle. This head difference serves as the driving head to circulate flow between them (see Figure 4-58). The driving head is constant for given operating specifications, such as power level and water level. The total pressure drop through the circulation loop is equal to the driving head.

Pressure drops depend on loss coefficient and flow rate (i.e., velocity). Loss coefficient consists of friction loss and form loss; the majority of the loss is due to the form loss in the steam generator. Since the driving head is constant, a higher loss coefficient means a lower circulation flow rate and a lower circulation ratio. A lower loss coefficient yields a higher circulation ratio. Therefore, an accurate prediction of the circulation ratio depends on an accurate loss coefficient.

Model boiler and field tests are used in qualifying the loss coefficients in the flow loop of the steam generator. For example, the major contributors of the pressure drop are the primary separator and tube support plates. The loss coefficient of the primary separator has been verified using model boilers and field steam generators (Reference 4-5). Similarly, loss coefficients of tube support plates have been developed using test data; Figure 4-59 presents the correlation of the loss coefficient and test data.

Figure 4-60 shows a typical comparison between predicted and actual measured circulation ratio. There is good agreement in circulation ratio between the prediction and measurement.

The TRANFLO model uses the same loss coefficient correlations as GENF code. This provides assurance in properly calculating the pressure drops throughout the steam generator.

4.9.5 Summary

This section presents a summary of the adequacy of the TRANFLO code for its current applications. Blowdown test data of simulated reactor vessels validate the adequacy of the code in predicting the steam and water blowdown transient. The NRC has accepted the TRANFLO code in calculating mass and energy release to the containment during a steam generator blowdown due to feed or steam line break.

As part of its review, the NRC accepted the code's ability to accurately predict local thermal-hydraulics in the vessel. The calculated pressure agrees well with the measured vessel pressure. Flow through the internals of the steam generator depends on accurate prediction of pressure drops, which relies on the accuracy of the loss coefficients along the flow paths. Test data of pressure drops from model boiler and field steam generators have been applied to verify the correlations for the loss coefficients.

Westinghouse has made modifications to the code to better predict steam generator behavior following a SLB event. Westinghouse has performed the verification and validation consistent with the methods approved by the NRC staff for the original version.

In conclusion, the TRANFLO code is a verified program for adequately predicting thermal-hydraulic conditions during the blowdown transient of a steam generator due to a feed or steam line break.

4.10 References

4-1. "Quantification of Byron IPE Steamline/Feedline Break Frequency", CN-COA-92-537-R1, Appendix R1-B, April 1993.

4-2. "Byron IPE Initiating Event Calculations and Notebook - Draft", CN-COA-92-537-R0, December 1993.

4-3. R. E. Land, "TRANFLO Steam Generator Code Description", Westinghouse Nuclear Energy System, WCAP-8821, September 1976.

4-4. Memo from C. O. Thomas to E. P. Rahe, "Proprietary Content Review of SER on WCAP-8821 and WCAP-8822", October 14, 1982.

4-5. P. W. Bird and P. J. Prabhu, "Review of Primary Separator Loss Coefficient", WTD-TH-80-010, July 1980.

Table 4-1

Initial and Boundary Conditions of the TRANFLO Calculation Models for Model D3 and D4 Steam Generator

		Initial Conditions		Boundary Conditions	
Case	SG Model	Mode of Operation	Water Level	Steam Nozzle Flow Limiter	FeedwaterFlow
1	D3	Hot Standby	@ ~ Normal Setting	Yes	Small
2	D4	Full Power	@ Normal Setting	Yes	Full Flow
3	D4	Hot Standby	@ Uppermost TSP	Yes	Excessive

Table 4-2

Peak Pressure Drop at Different Tube Support Plates
(Hot Leg Only for Half Plate)

Parameter	SG & Case D3 - 1	SG & Case D4 - 2	SG & Case D4 - 3
Flow splits within tube bundle	Yes	No	Yes
TSP with max peak Dp	[		] a
Peak Dp @ uppermost TSP			
Max peak Dp, psi			
Peak max Dp @ bottom Plate			
Dp @ Hot Leg Top TSP	]		

Table 4-3

Summary of Component Materials

Component	Material
Tube Support Plate	SA-285 Grade C
Stayrod	SA-106 Grade B
Spacer	SA-106 Grade B
Tube	Inconel 600

Table 4-4

Summary of Material Properties
SA-285, Gr. C

PROPERTY	CODE ED.	TEMPERATURE						
		70	200	300	400	500	600	700
Young's Modulus	71	27.90	27.70	27.40	27.00	26.40	25.70	24.80
Coefficient of Thermal Expansion	71	6.07	6.38	6.60	6.82	7.02	7.23	7.44
Density	---	0.284 7.35	0.283 7.33	0.283 7.32	0.282 7.30	0.281 7.28	0.281 7.26	0.280 7.25

PROPERTY	UNITS
Young's Modulus	psi x 1.0E06
Coefficient of Thermal Expansion	in/in/deg. F x 1.0E-06
Density	lb/in^3 lb-sec^2/in^4 x 1.0E-4

Table 4-5

Summary of Material Properties
SA-106, Gr. B

		TEMPERATURE						
PROPERTY	CODE ED.	70	200	300	400	500	600	700
Young's Modulus	71	27.90	27.70	27.40	27.00	26.40	25.70	24.80
Coefficient of Thermal Expansion	71	6.07	6.38	6.60	6.82	7.02	7.23	7.44
Density	---	0.284 7.35	0.283 7.33	0.283 7.32	0.282 7.30	0.281 7.28	0.281 7.26	0.280 7.25

PROPERTY	UNITS
Young's Modulus	psi x 1.0E06
Coefficient of Thermal Expansion	in/in/deg F x 1.0E-06
Density	lb/in^3 lb-sec^2/in^4 x 1.0E-4

Table 4-6

Summary of Material Properties
SB-166

PROPERTY	CODE ED.	TEMPERATURE						
		70	200	300	400	500	600	700
Young's Modulus	71	31.70	30.90	30.50	30.00	29.60	29.20	28.60
Coefficient of Thermal Expansion	71	7.13	7.40	7.56	7.70	7.80	7.90	8.00
Density	---	---	0.306	0.305	0.305	0.304	0.303	0.302
		---	7.923	7.905	7.886	7.867	7.847	7.828

PROPERTY	UNITS
Young's Modulus	psi x 1.0E06
Coefficient of Thermal Expansion	in/in/deg. F x 1.0E-06
Density	lb/in^3 lb-sec^2/in^4 x 1.0E-4

Table 4-7

Summary of Equivalent Plate Properties

Plate	Reference Young's Modulus	Effective Young's Modulus	Effective Poisson's Ratio
A - Inside 32" Radius	2.605E+07	4.810E+06	0.2466
A - Outside 32" Radius	2.605E+07	5.850E+06	0.2654
C, F, J, L, M, N, P*	2.605E+07	2.470E+06	0.6445

* - These plates have flow holes, resulting in a significantly reduced value for Young's Modulus

Table 4-8

Summary of Effective Plate Densities

[ ]a

DISK 215 - BRDWD\TBL436 - 04/18/94

Table 4-9

Comparison of Natural Frequencies
Full Versus Reduced DOF

[[a]

Table 4-10

Summary of TSP Displacements for
Postulated SLB Events for Model D3 and D4 Steam Generators*

[ ]a

DISK 215 - BRDWD\TBL441 - 04/18/94

Table 4-11

Comparison of Component Dimensions
Model D3 versus Model D4 Steam Generators

Dimension	Model D3	Model D4
Shell ID	[	] a
Shell Thickness		
Channel Head Bowl Radius		
Channel Head Thickness		
Tubesheet Thickness		
Hole Diameter		
Number Holes		
Tube Pitch		

Table 4-12

Summary of Tubesheet Displacements
Model D3 SLB Analysis

a

Table 4-13

Summary of Vertical Bar Stresses
Model D4 Steam Generators

[a

] a

Table 4-14

Summary of Number of Tubes Having Different Displacement Magnitudes
Model D4 Steam Generator
Steam Line Break Load Cases

[ ]a

DISK 215 - BRDWD\TBL451 - 04/19/94

Table 4-15

Summary of Tubes Having Relative Tube / Plate Displacements
That Exceed 0.400 inch

[redacted]

Table 4-16

Comparison of Maximum Displacement at Plate Edge and at Limiting Tube Location

[ ] [ ]a

Table 4-17

Braidwood Unit 1 Mode 3 Durations

Event	Offline Date	Hours in Mode 3	Online Date	Online Days
Cycle 3				
A1R02	N/A	360 *	5/18/91	
A1F19	7/16/91	0	7/27/91	60
A1F20	10/9/91	0	10/14/91	74
A1F21	11/6/91	54	11/11/91	24
A1F22	2/5/92	62	2/7/92	86
A1F23	3/21/9	8	3/21/92	43
A1R03	9/1/92	26*	N/A	165
	Hours in Mode 3 = 510 Days in Mode 3 = 21.2		Online Days = 452 Days in Cycle = 472	
Cycle 4				
A1R03	N/A	56*	11/3/92	
A1M03	11/20/92	124	11/25/92	18
A1F24	1/7/93	38	1/14/93	44
A1M04	5/29/93	35	5/30/93	136
A1F25	6/2/93	65	6/7/93	4
A1F26	10/24/93	21	11/11/93	140
A1R04	3/4/94	18*	N/A	114
	Hours in Mode 3 = 357 Days in Mode 3 = 14.9		Online Days = 456 Days in Cycle = 487	

* Mode 3 times associated with planned refueling outages

Cycle 3 percent of time spent in Mode 3 = 4.50%.
Cycle 3 percent of time spent in Mode 3 minus Refuelling Mode 3 hours = 1.09%.

Cycle 4 percent of time spent in Mode 3 = 3.05%.
Cycle 4 percent of time spent in Mode 3 minus Refuelling Mode 3 hours = 2.42%.

Table 4-18

Tubes Potentially Susceptible to Collapse and In-Leakage
TSP C, D
Left-Hand Unit

[redacted]

Table 4-19

Tubes Potentially Susceptible to Collapse and In-Leakage
TSP F, G
Left-Hand Unit

[ ] a

Table 4-20

Tubes Potentially Susceptible to Collapse and In-Leakage
TSP J, K
Left-Hand Unit

[ ] a

Table 4-21

Tubes Potentially Susceptible to Collapse and In-Leakage
TSP L-P
Left-Hand Unit

[redacted]

a

Table 4-22
Tubes Potentially Susceptible to Collapse and In-Leakage
TSP B
Left-Hand Unit

[a]

Table 4-23

Tubes Potentially Susceptible to Collapse and In-Leakage
TSP E, H
Left-Hand Unit

[redacted]

a

Table 4-24

Tubes Potentially Susceptible to Collapse and In-Leakage
TSP C, D
Right-Hand Unit

[ ]a

Table 4-25

Tubes Potentially Susceptible to Collapse and In-Leakage
TSP F, G
Right-Hand Unit

[ ] a

Table 4-26

Tubes Potentially Susceptible to Collapse and In-Leakage
TSP J, K
Right-Hand Unit

[ ]a

Table 4-27

Tubes Potentially Susceptible to Collapse and In-Leakage
TSP L-P
Right-Hand Unit

[ ] a

Table 4-28

Tubes Potentially Susceptible to Collapse and In-Leakage
TSP B
Right-Hand Unit

[ ] a

Table 4-29

Tubes Potentially Susceptible to Collapse and In-Leakage
TSP E, H
Right-Hand Unit

[redacted]

a

DISK 215 - BRDWD\TBL42 - 04/19/94

Table 4-30

Table and Figure Index for TSP Row/Column Identification

TSP	Summary Tables		Tube Map Figures
	Left-Hand SG	Right-Hand SG	
B	4-22	4-28	4-48, 4-49
C	4-18	4-24	4-48, 4-49
D	4-18	4-24	4-50, 4-51
E	4-23	4-29	4-52, 4-53
F	4-19	4-25	4-54, 4-55
G	4-19	4-25	4-50, 4-51
H	4-23	4-29	4-52, 4-53
J	4-20	4-26	4-48, 4-49
K	4-20	4-26	4-48, 4-49
L	4-21	4-27	4-56, 4-57
M	4-21	4-27	4-56, 4-57
N	4-21	4-27	4-56, 4-57
P	4-21	4-27	4-56, 4-57

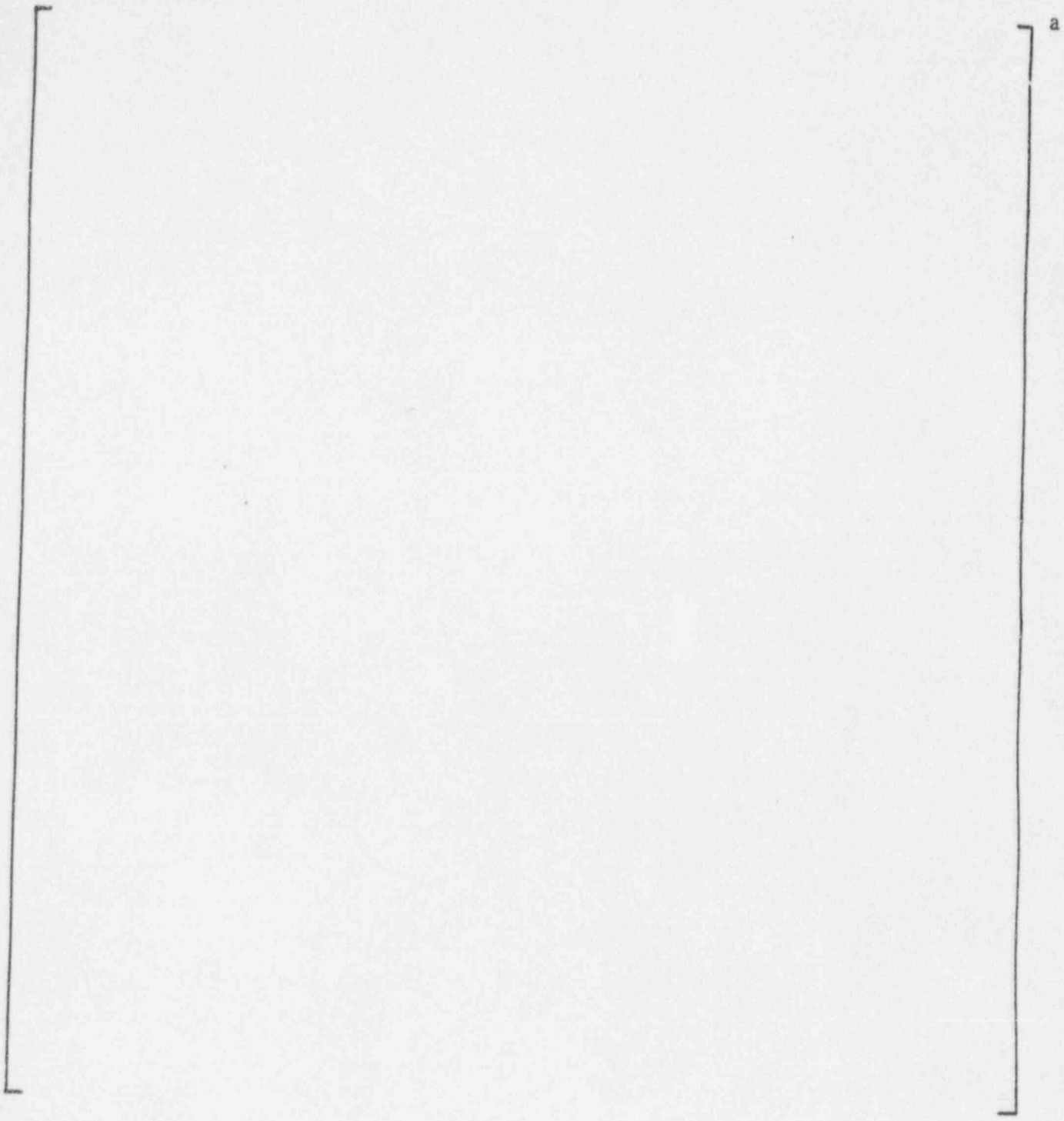

Figure 4-1. Secondary Side Nodes, and Tube Support Plate Identification (See Figure 4-2 for Preheater Detail)

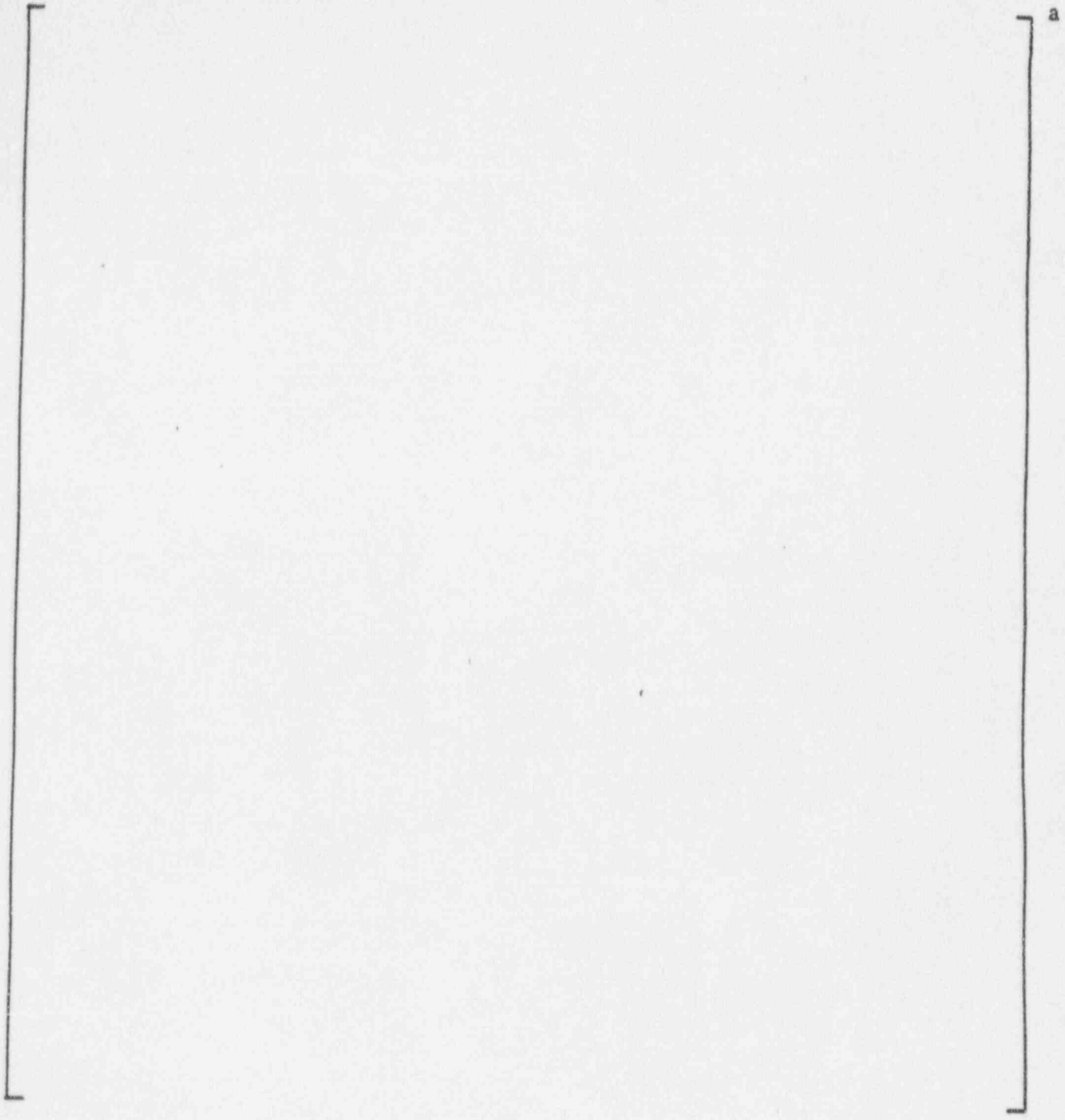

Figure 4-2. Preheater Nodes, and Baffle Identification of Model D3 Steam Generator

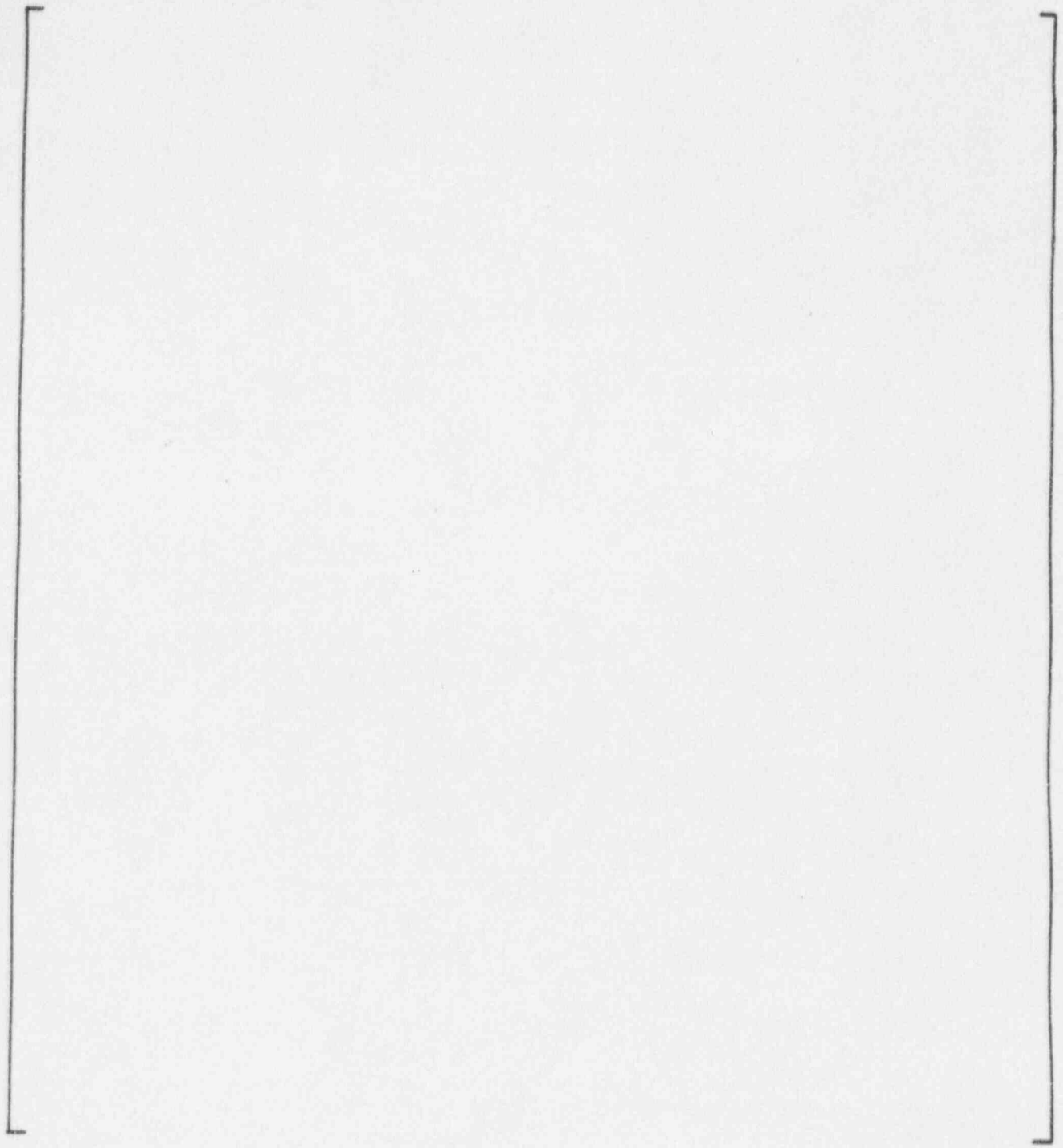

Figure 4-3. Secondary Side Fluid Nodes and Flow Connectors for Model D3 Steam Generator

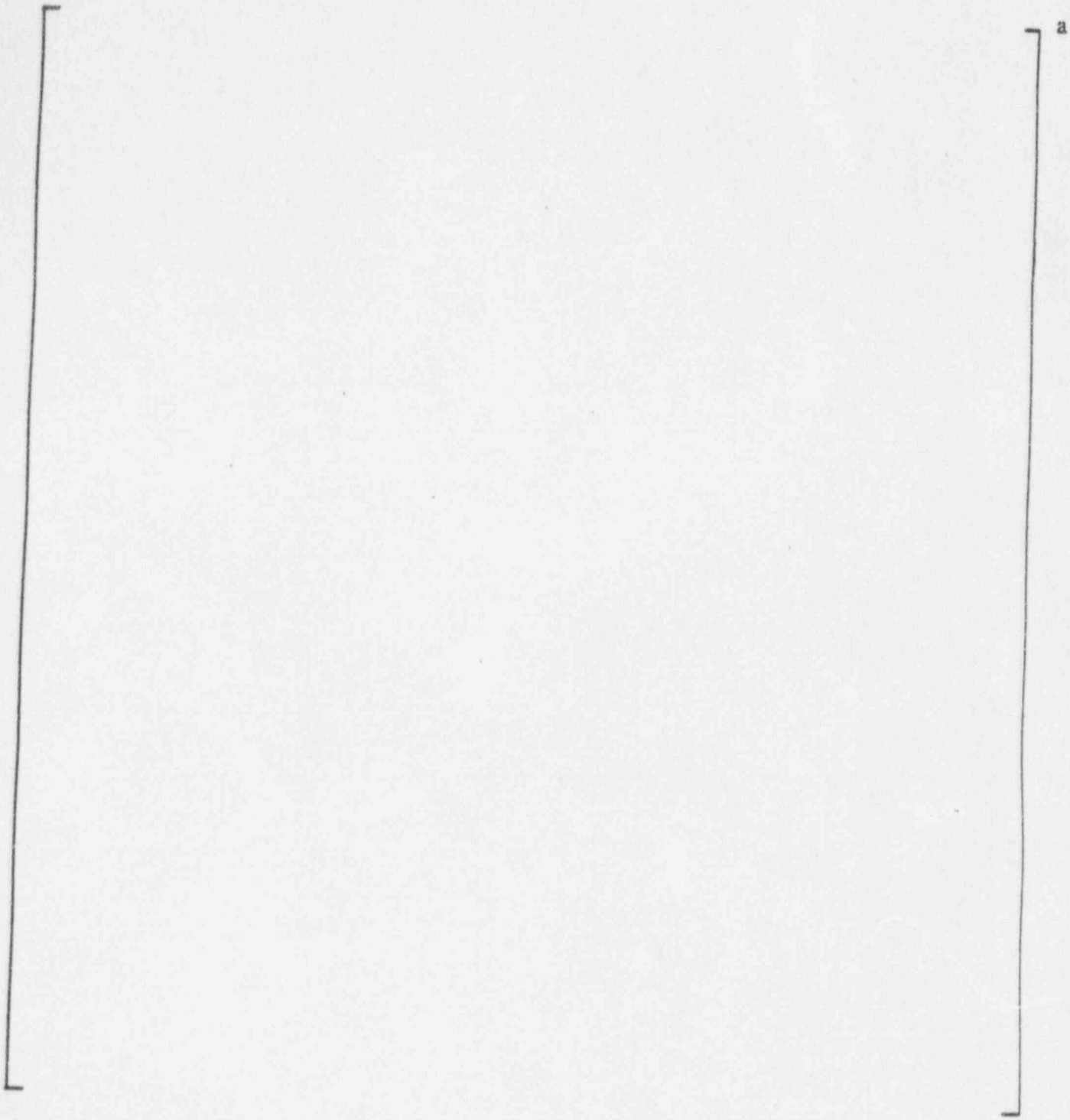

Figure 4-4. Primary Fluid Nodes and Its Flow Connectors, Metal Heat Nodes and Its Heat Transfer Connectors, and Secondary Fluid Modes Within Tube Bundle

Figure 4-5 Pressure drop through tube support plates T, S and R during steam line break of a Model D3 (Case 1; ■ - TSP T, ❑ - TSP S, ◆ - TSP R)

Figure 4-6 Pressure drop through tube support plates Qhot, L and G during steam line break of a Model D3 (Case 1; ■ - TSP Qhot, ❑- TSP L, ◆ - TSP G)

Figure 4-7. Pressure drop through tube support plates Qhot, L and G during steam line break of a Model D3 (Case 1; ■ - TSP C, ❑- TSP A)

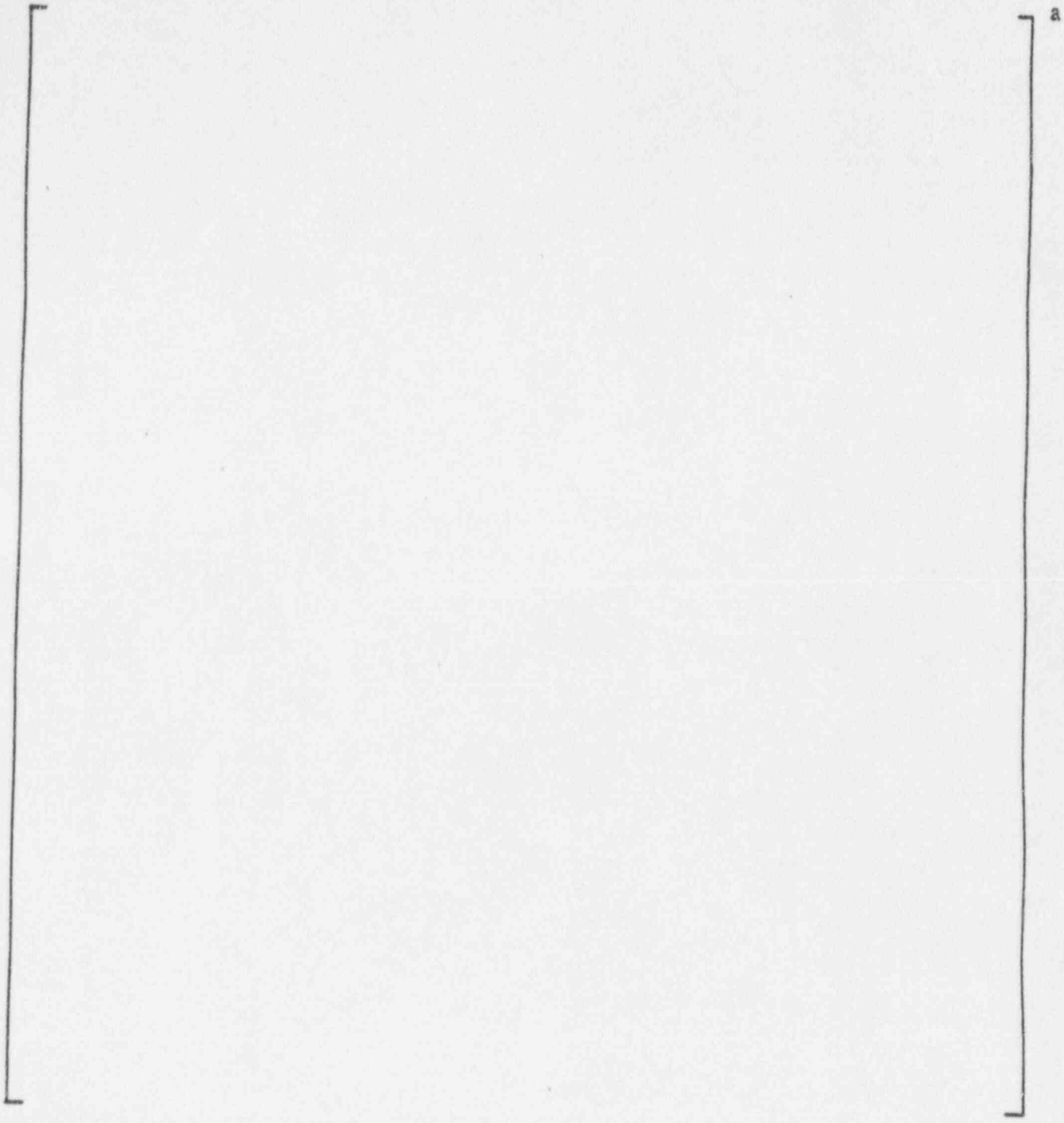

Figure 4-8. Secondary Side Nodes and Tube Support Plates Identification of TRANFLO Model for Model D4 Steam Generator

Figure 4-9 Pressure drop through tube support plates M, N and P during steam line break of a Model D4 (case 2; ❑ - TSP N, ■ - TSP P, ◆ - TSP M)

Figure 4-10 Pressure drop through tube support plates L, J and F during steam line break of a Model D4 (Case 2; ❑ - TSP J, ■ - TSP L, ◆ - TSP F)

Figure 4-11 Pressure drop through tube support plates A and C during steam line break of a Model D4 (Case 2; ❑- TSP A, ■ - TSP C)

Figure 4-12 Pressure drop through tube support plates M, N and P during steam line break of a Model D4 (Case 3; ■ - TSP P, - TSP N, ◆ - TSP M)

Figure 4-13 Pressure drop through tube support plates M, N and P during steam line break of a Model D4 (Case 3; ■ - TSP L, ❑ - TSP J, ◆ - TSP F)

Figure 4-14 Pressure drop through tube support plates M, N and P during steam line break of a Model D4 (Case 3; ■ - TSP C, ❑ - TSP A)

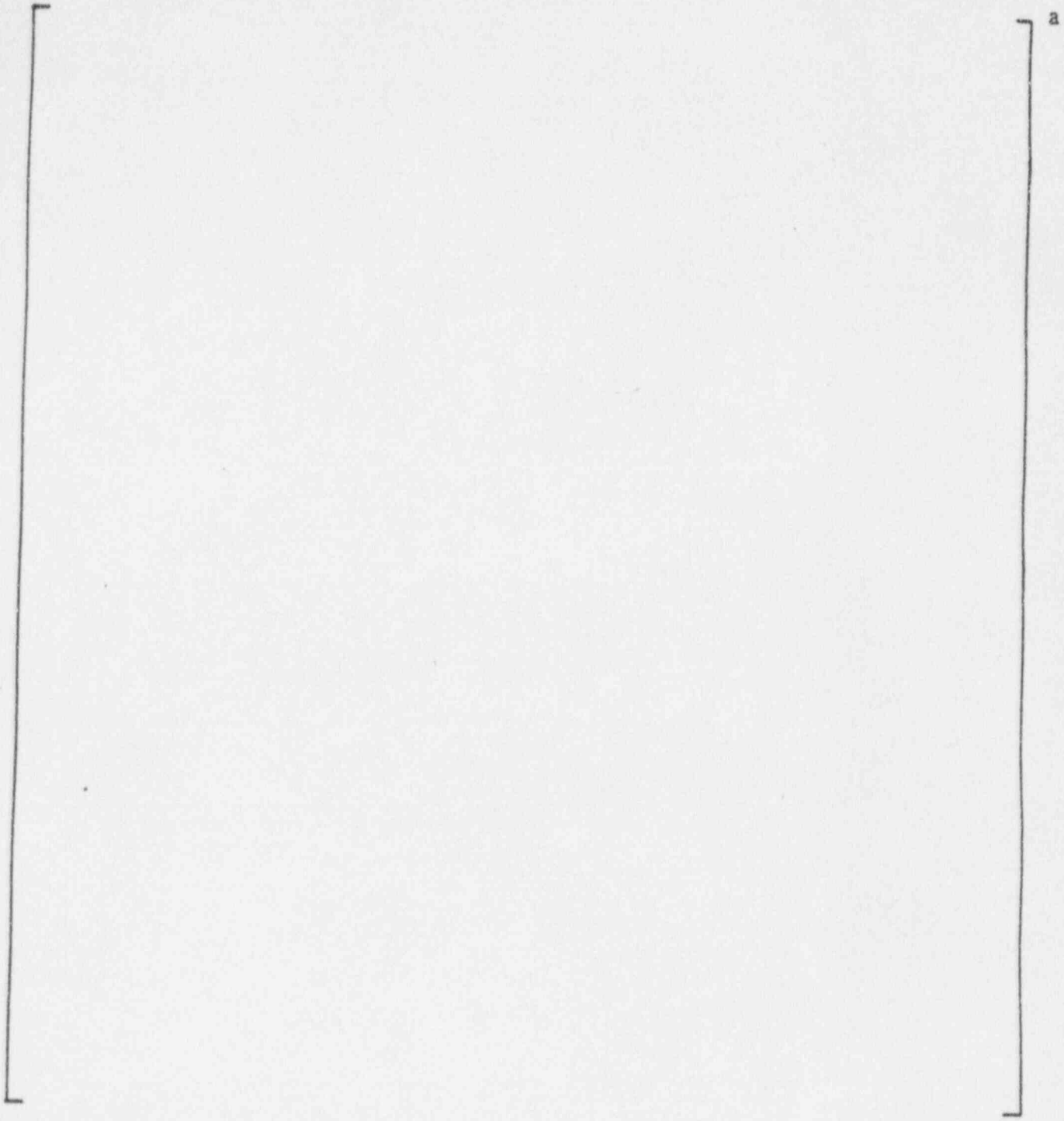

Figure 4-15. Tube Bundle Geometry

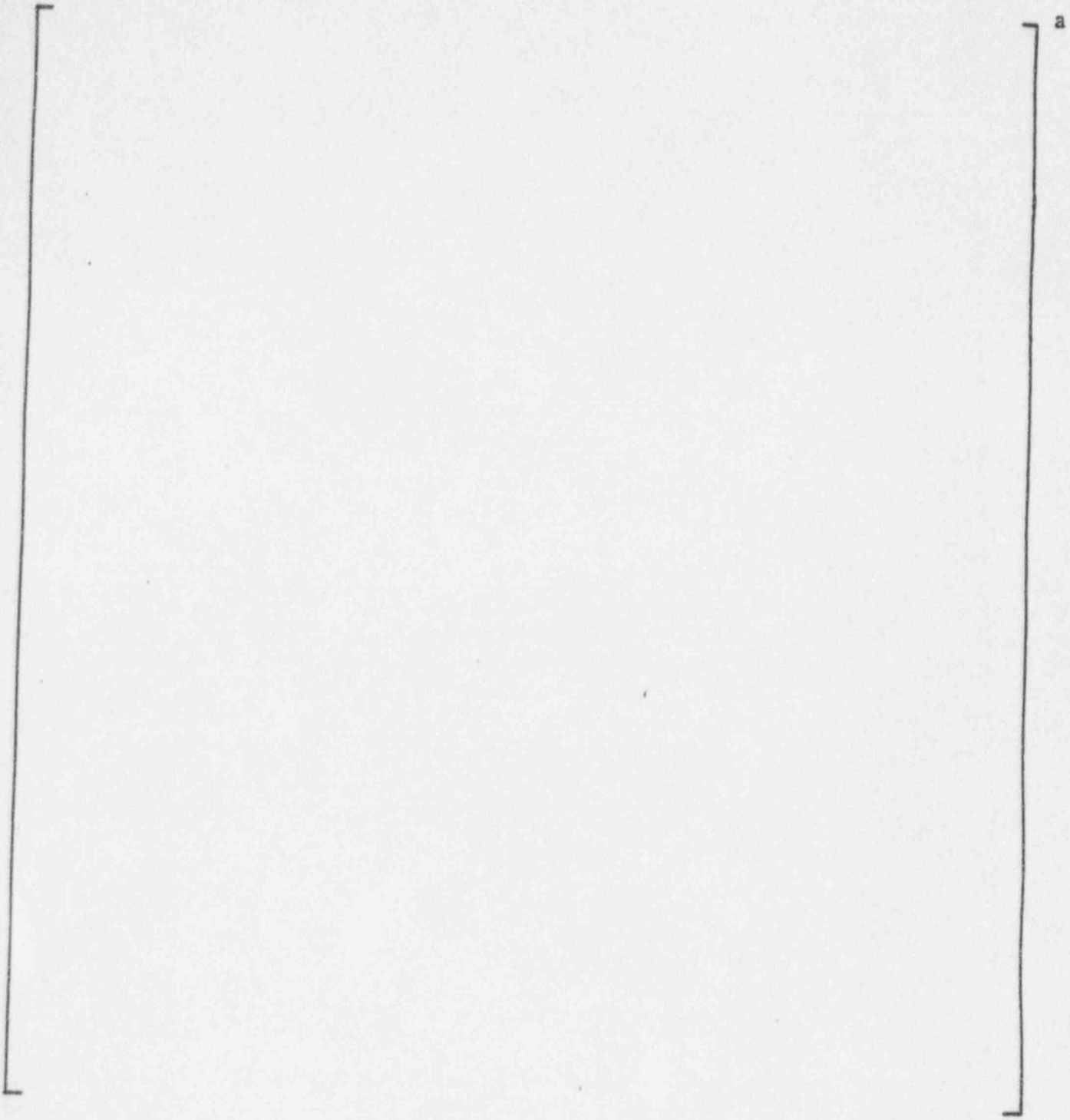

Figure 4-16. Tierod / Spacer Locations

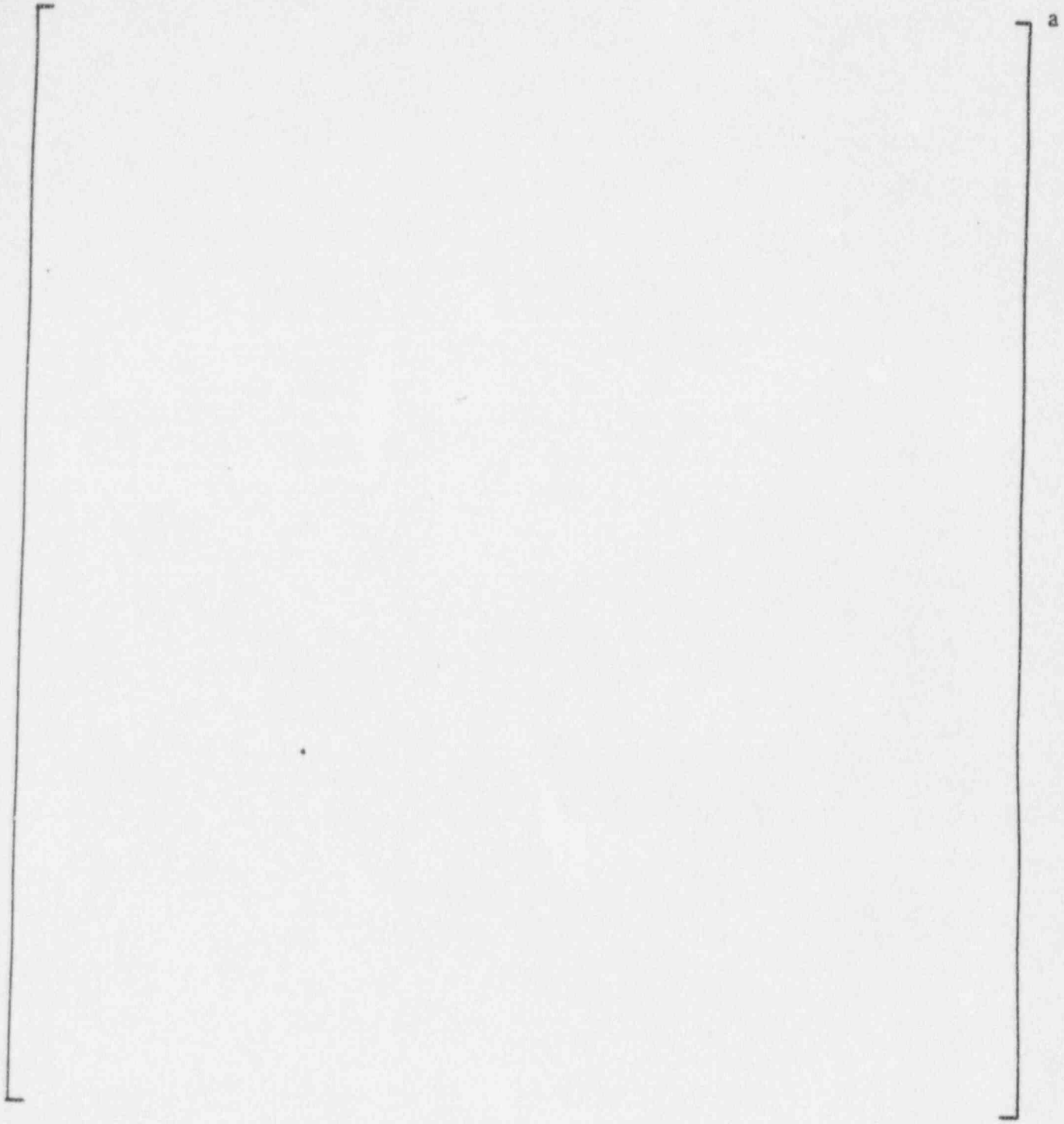

Figure 4-17. Plate A (1H) Support Locations

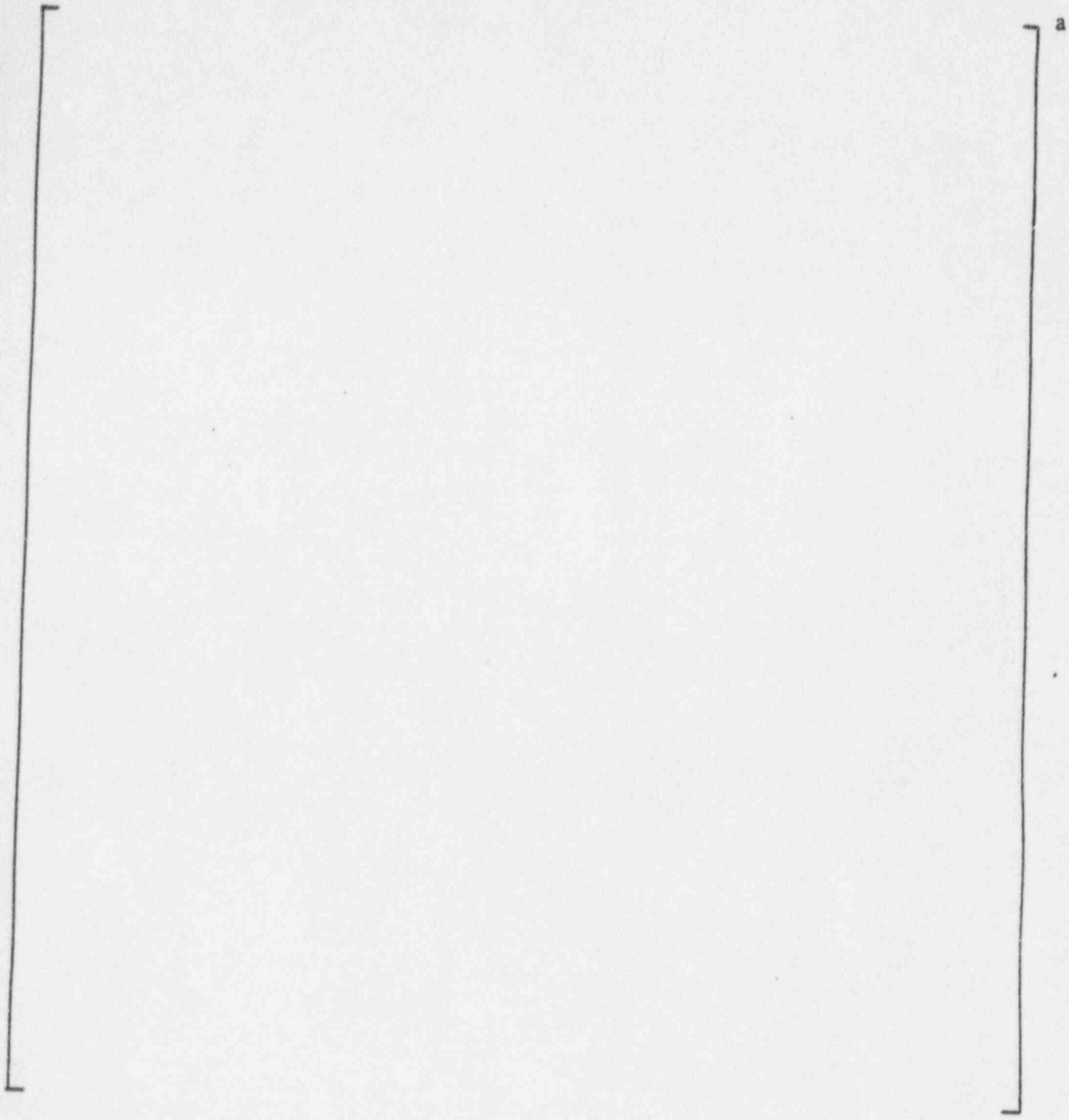

Figure 4-18. Plate C (3H) Support Locations

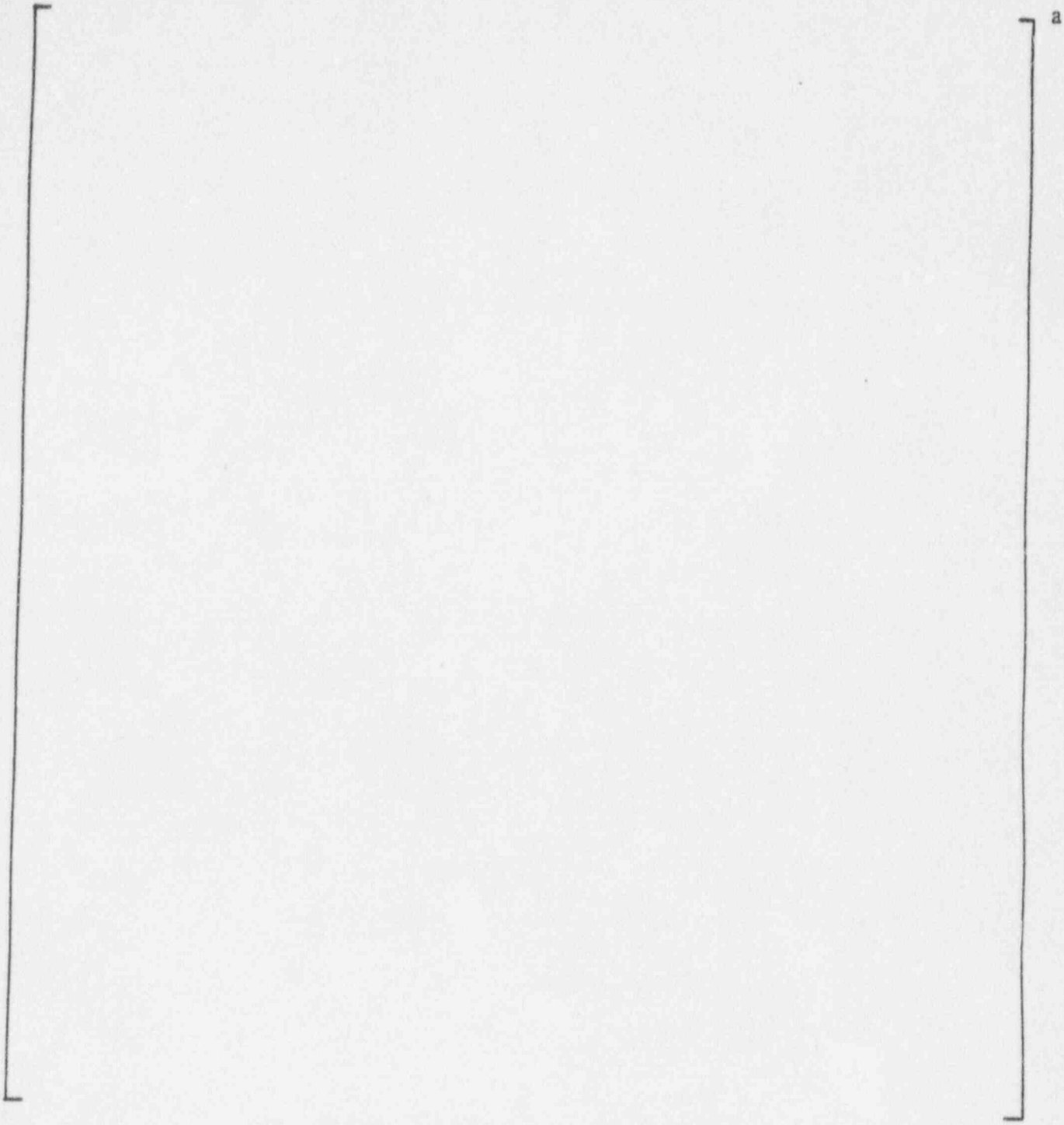

Figure 4-19. Plate F (5H) Support Locations

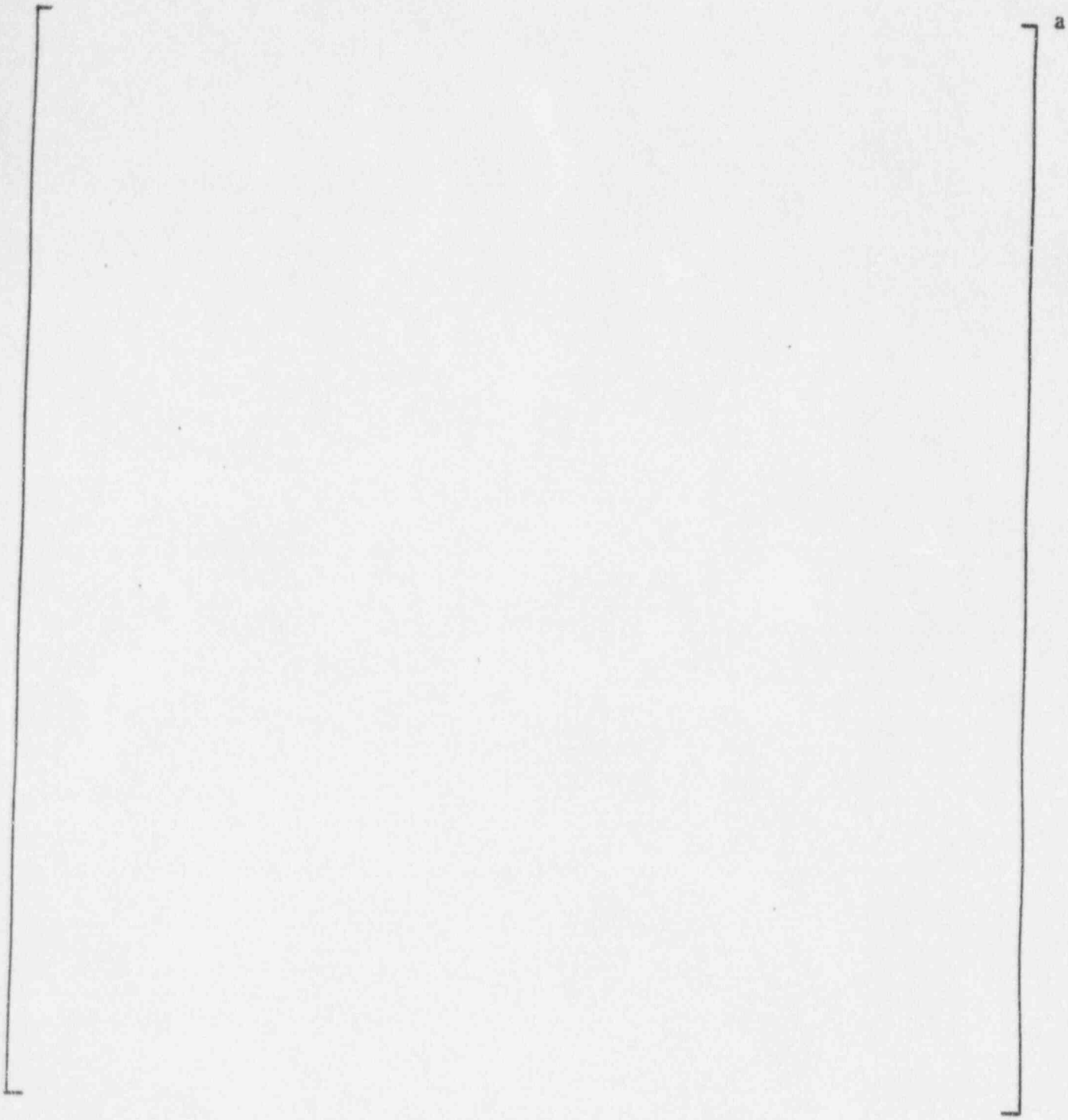

Figure 4-20. Plate J (7H) Support Locations

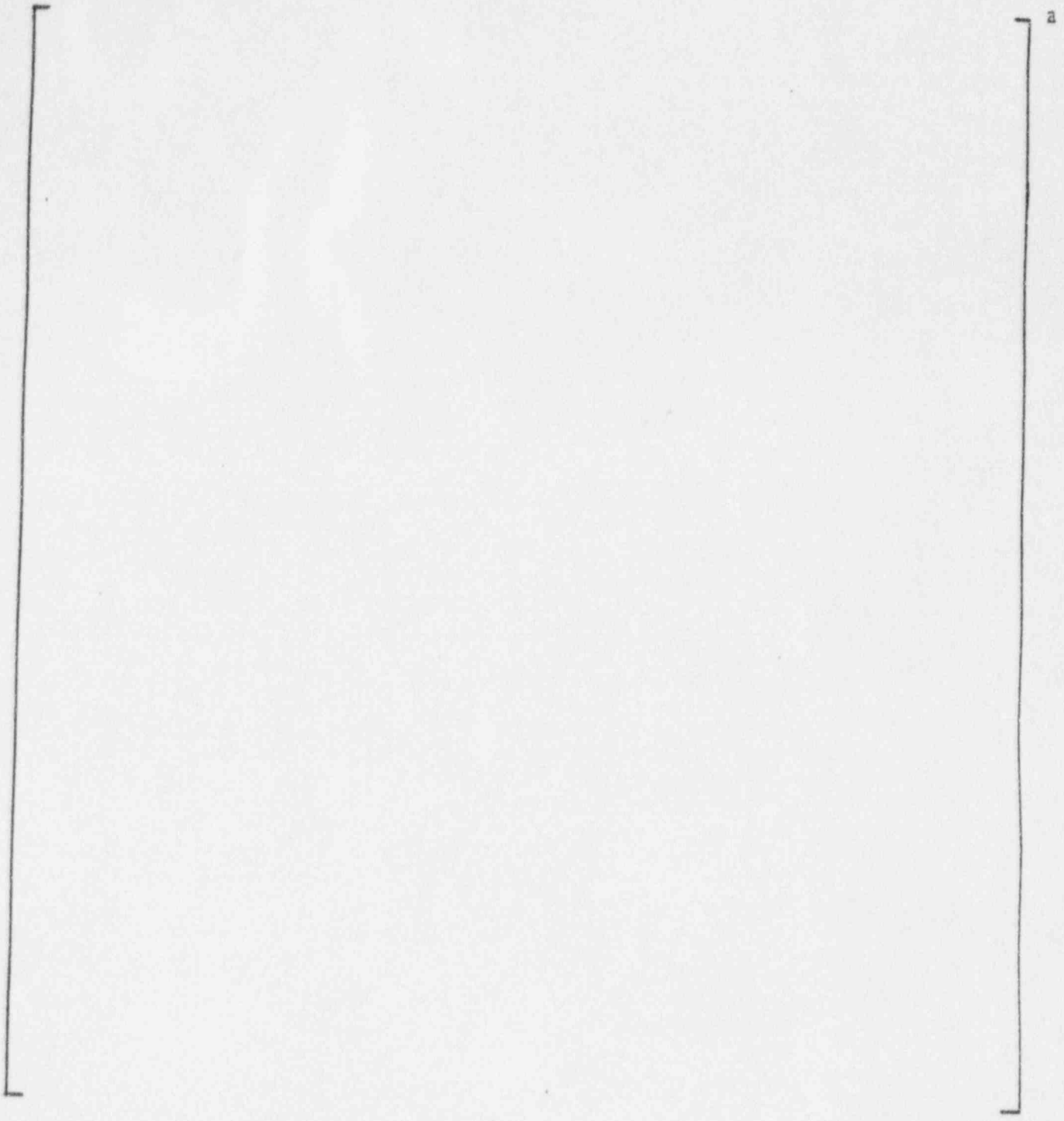

Figure 4-21. Plate L (8H) Support Locations

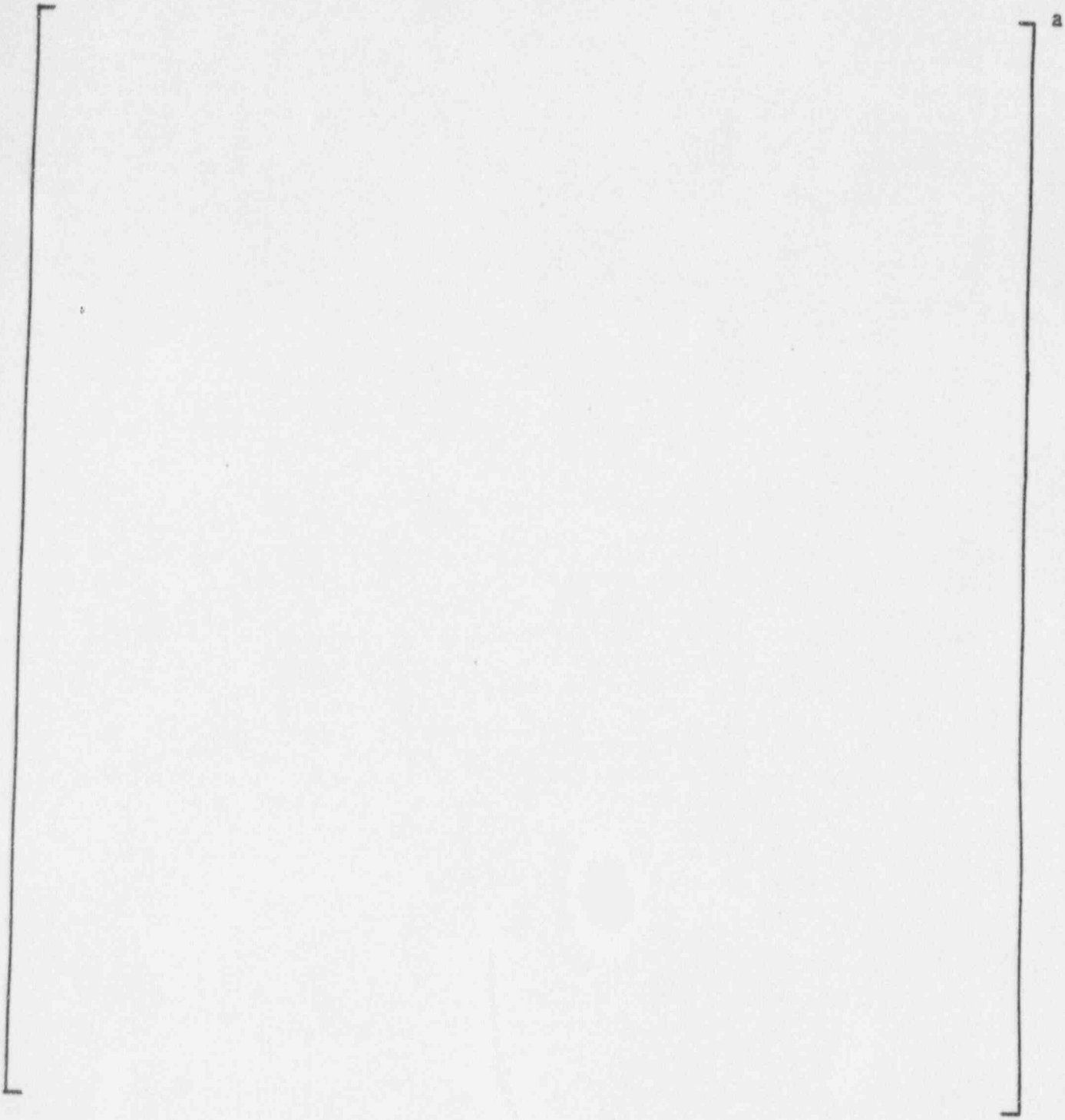

Figure 4-22. Plate M (9H) Support Locations

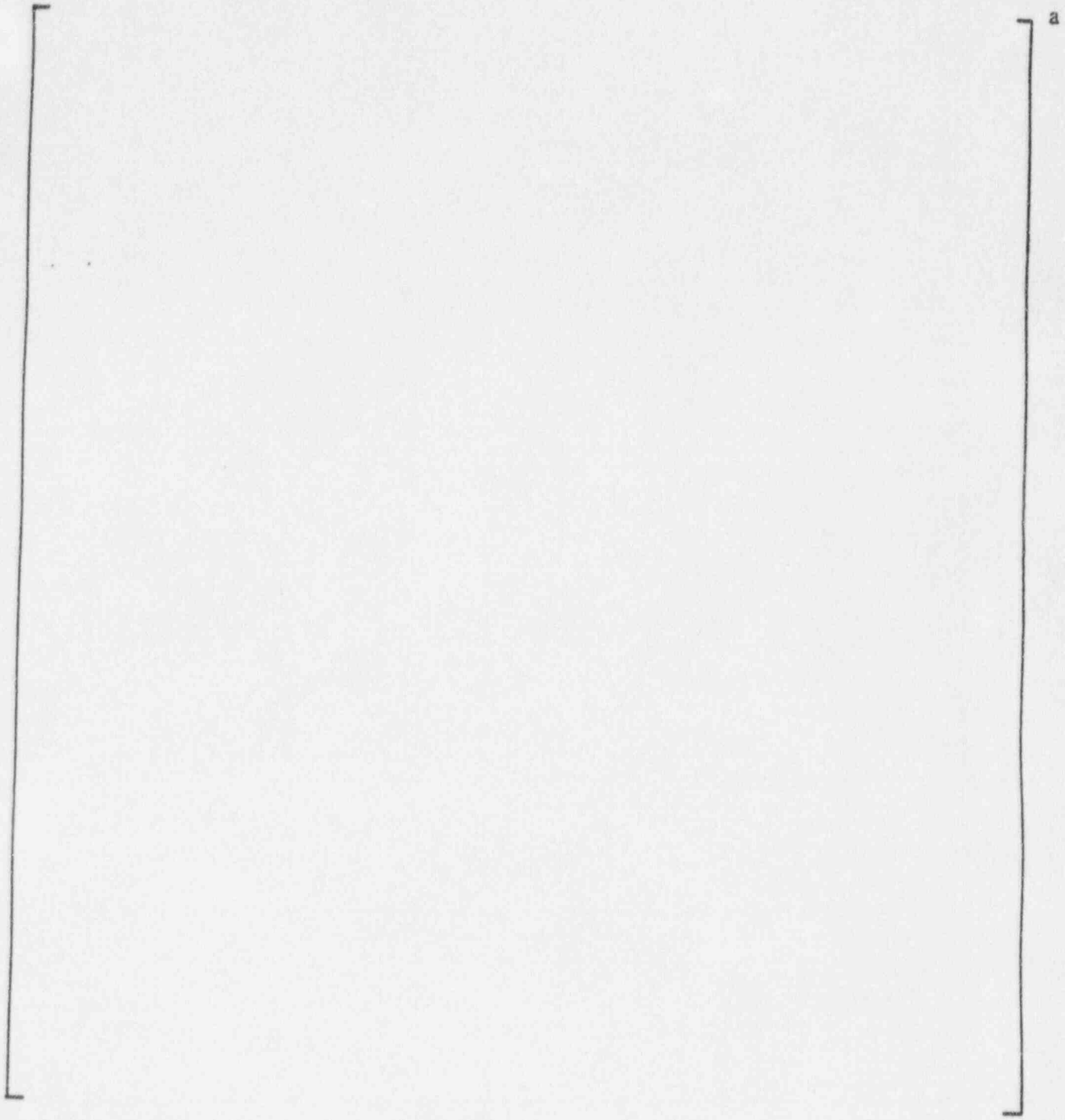

Figure 4-23. Plate N (10H) Support Locations

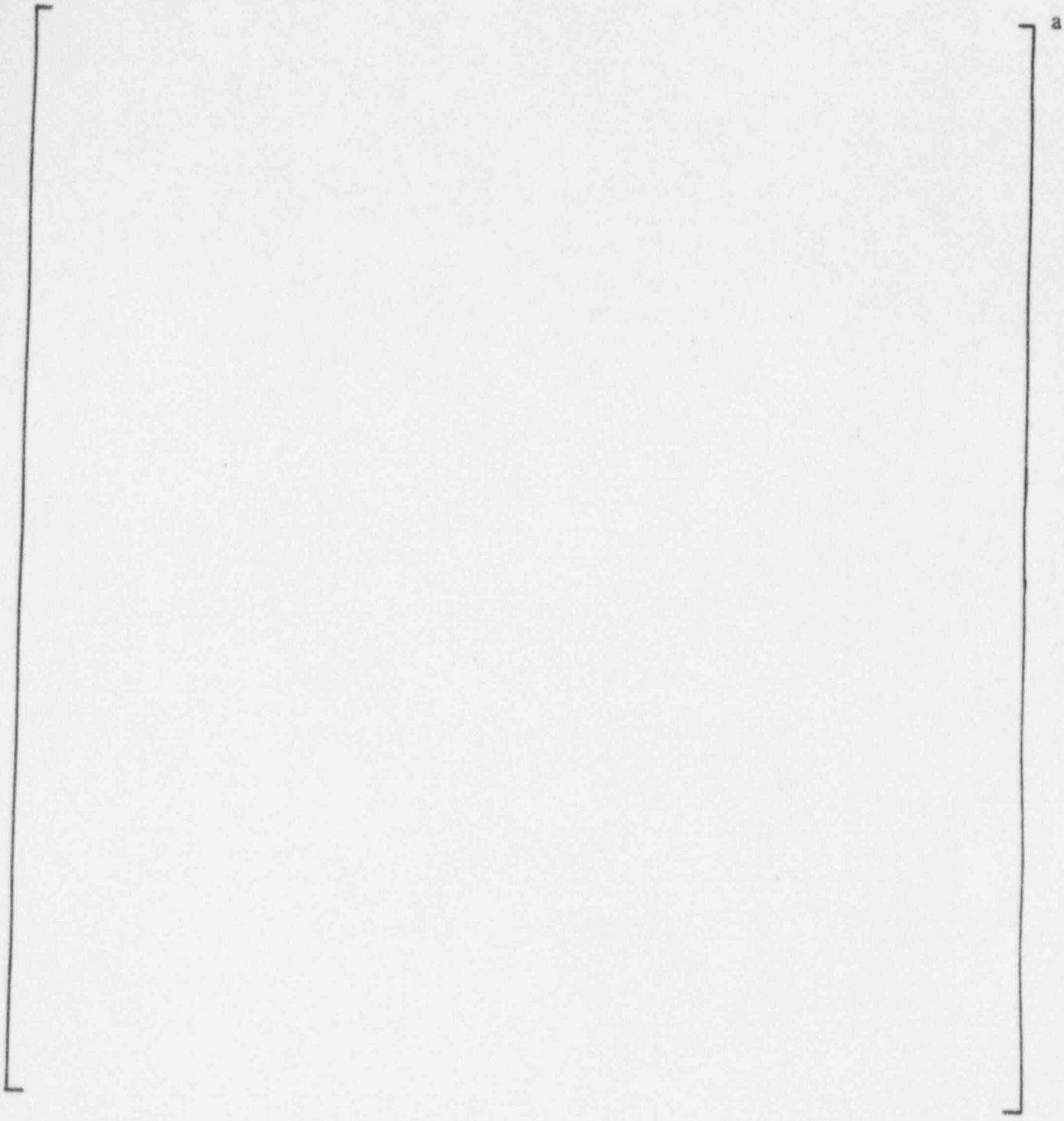

Figure 4-24. Plate P (11H) Support Locations

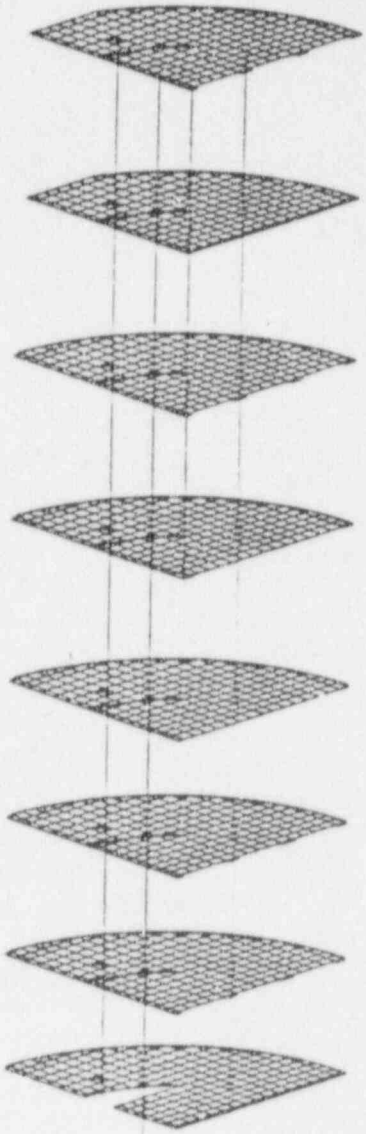

Figure 4-25. Overall Finite Element Model Geometry

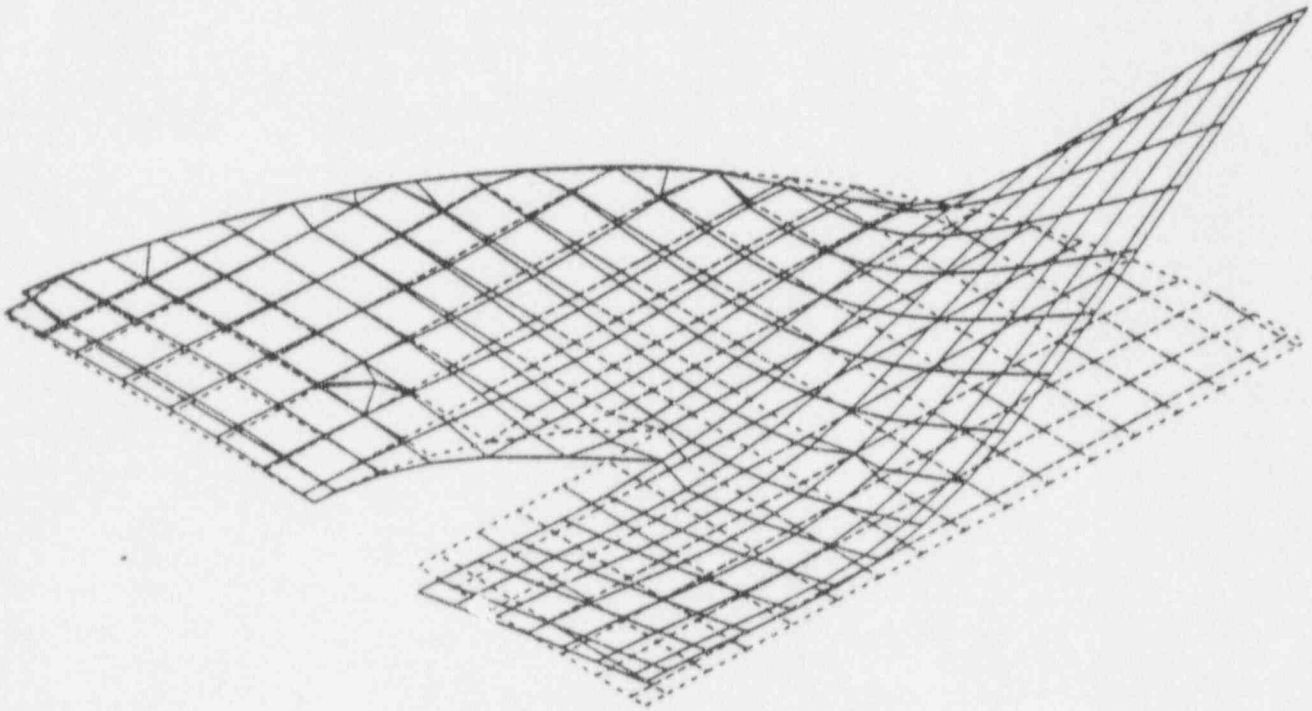

Figure 4-26. Mode Shape Plot - Plate A
Full Set of DOF
Mode 1

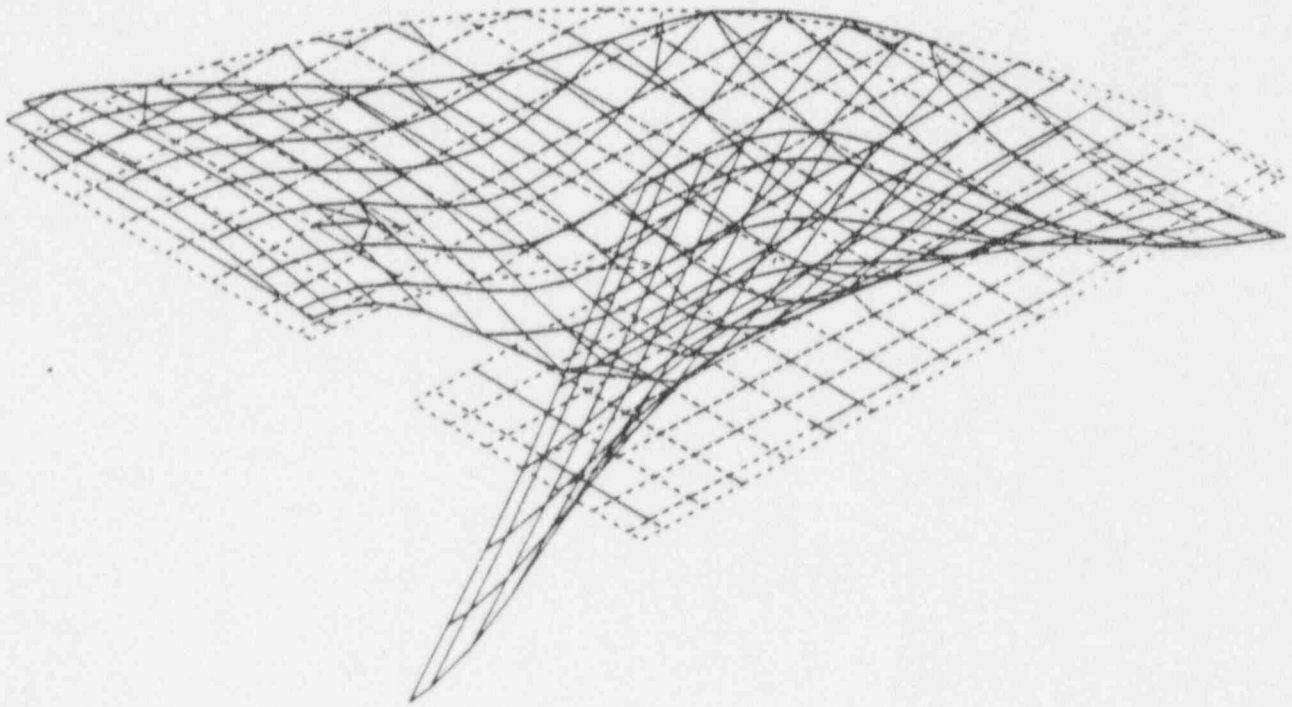

Figure 4-27. Mode Shape Plot - Plate A
Full Set of DOF
Mode 2

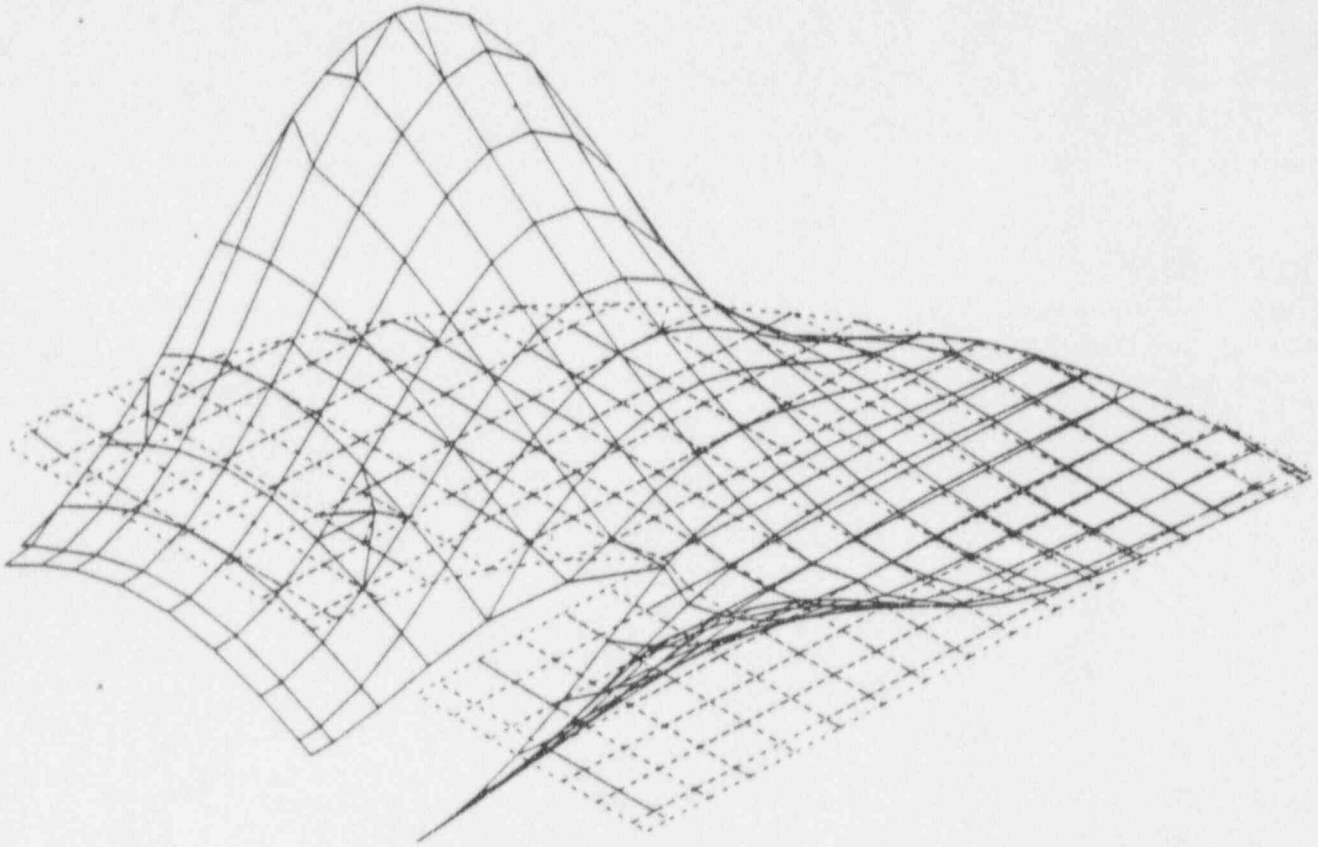

Figure 4-28. Mode Shape Plot - Plate A
Full Set of DOF
Mode 3

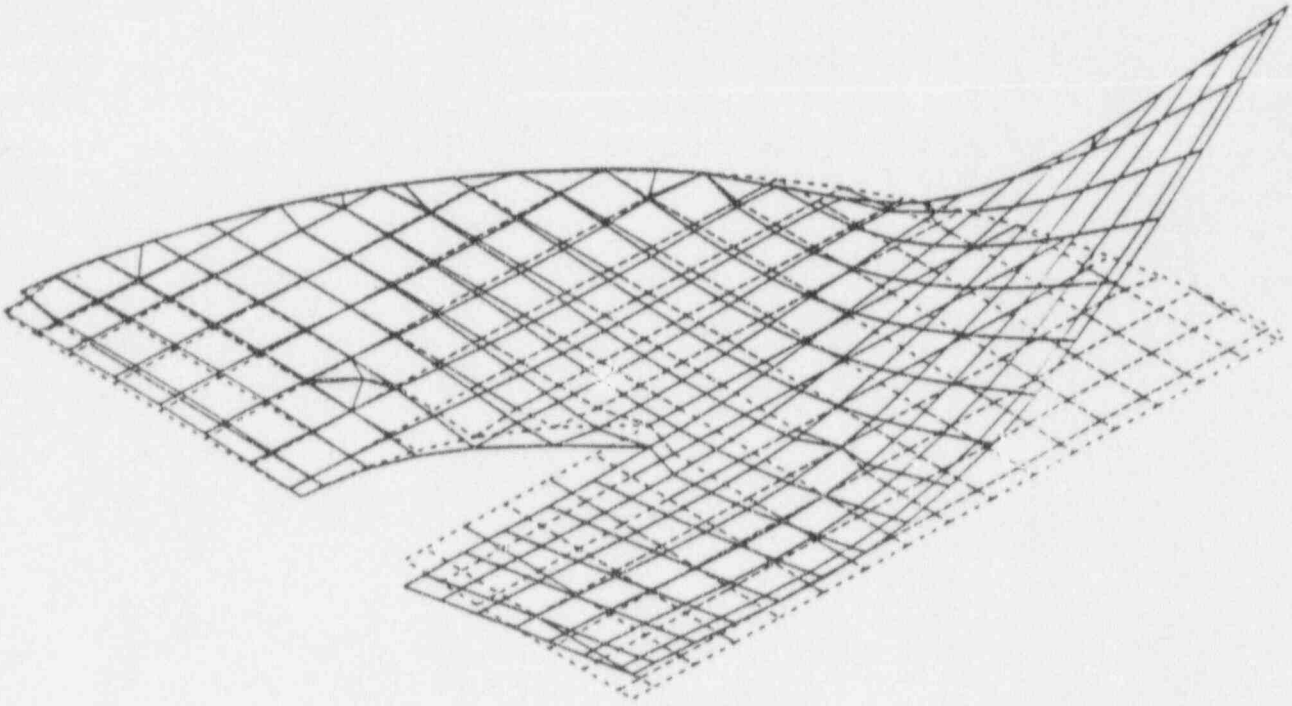

Figure 4-29. Mode Shape Plot - Plate A
Reduced Set of DOF
Mode 1

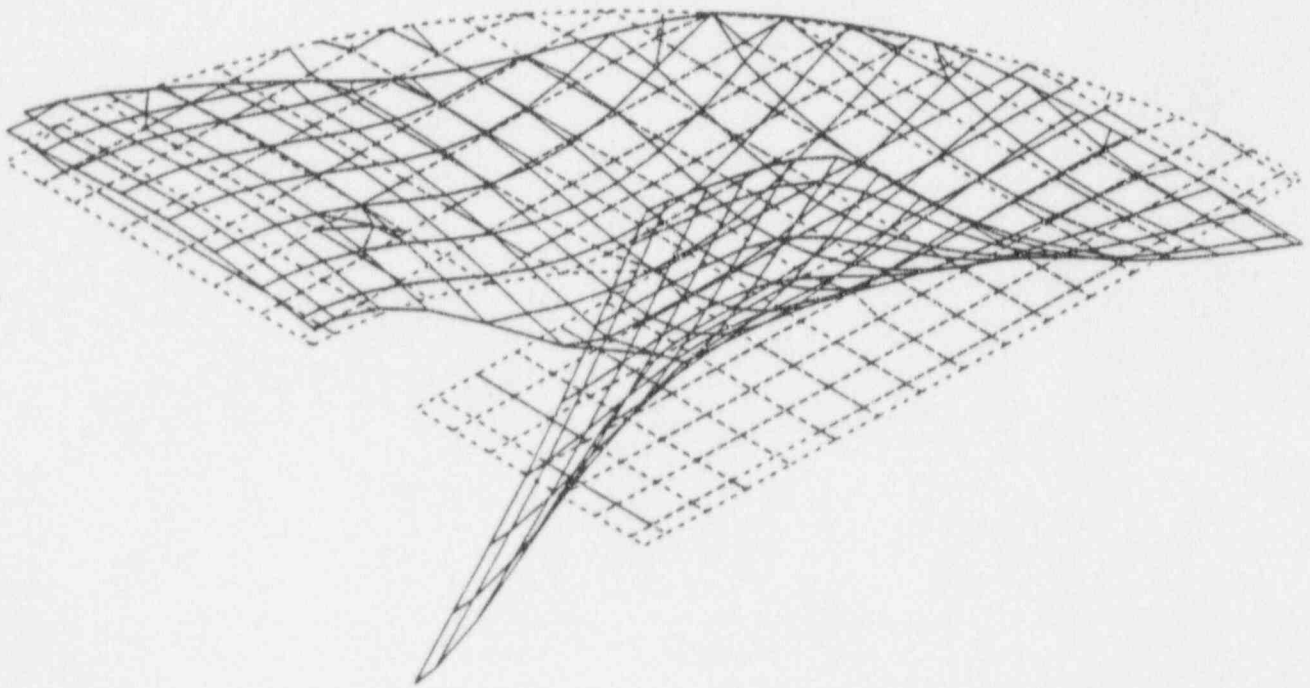

Figure 4-30. Mode Shape Plot - Plate A
Reduced Set of DOF
Mode 2

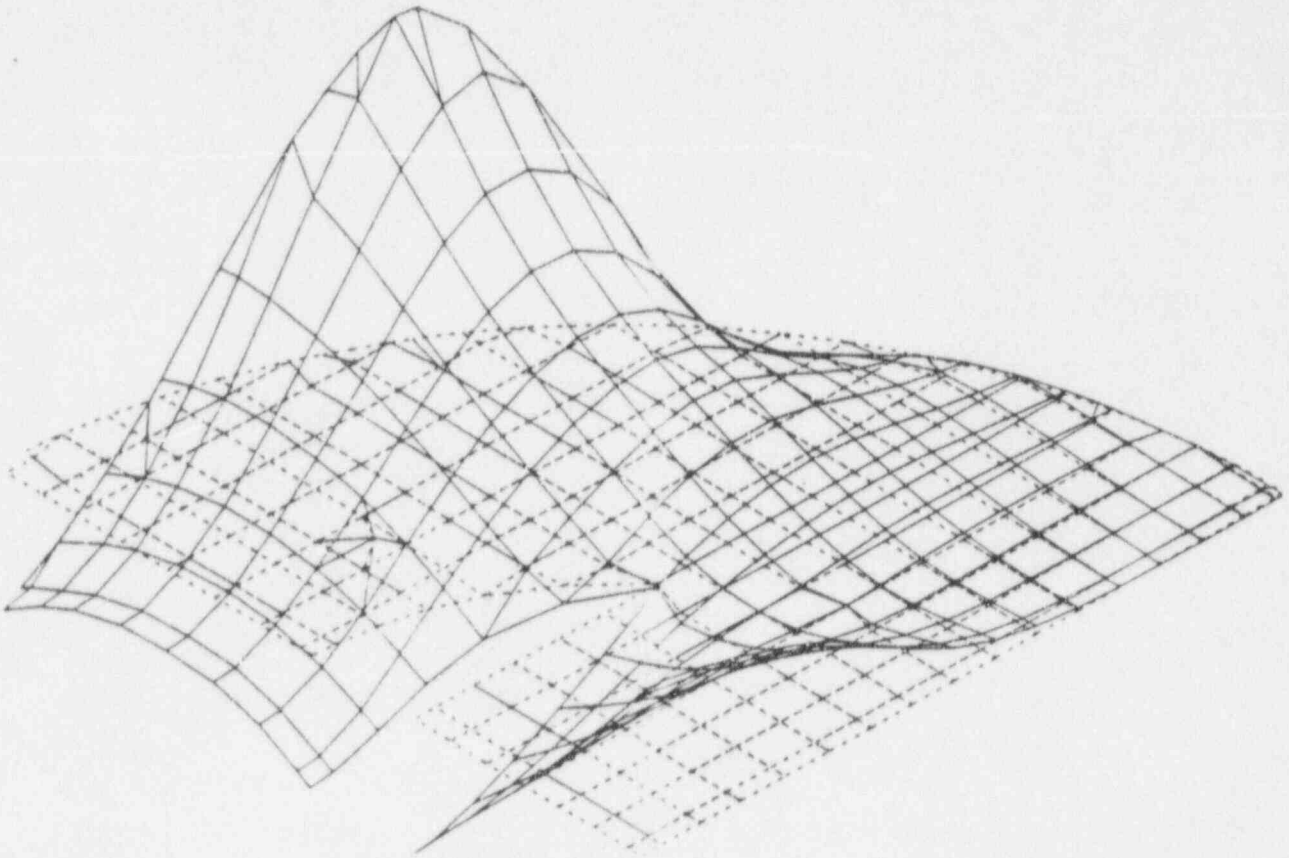

Figure 4-31. Mode Shape Plot - Plate A
Reduced Set of DOF
Mode 3

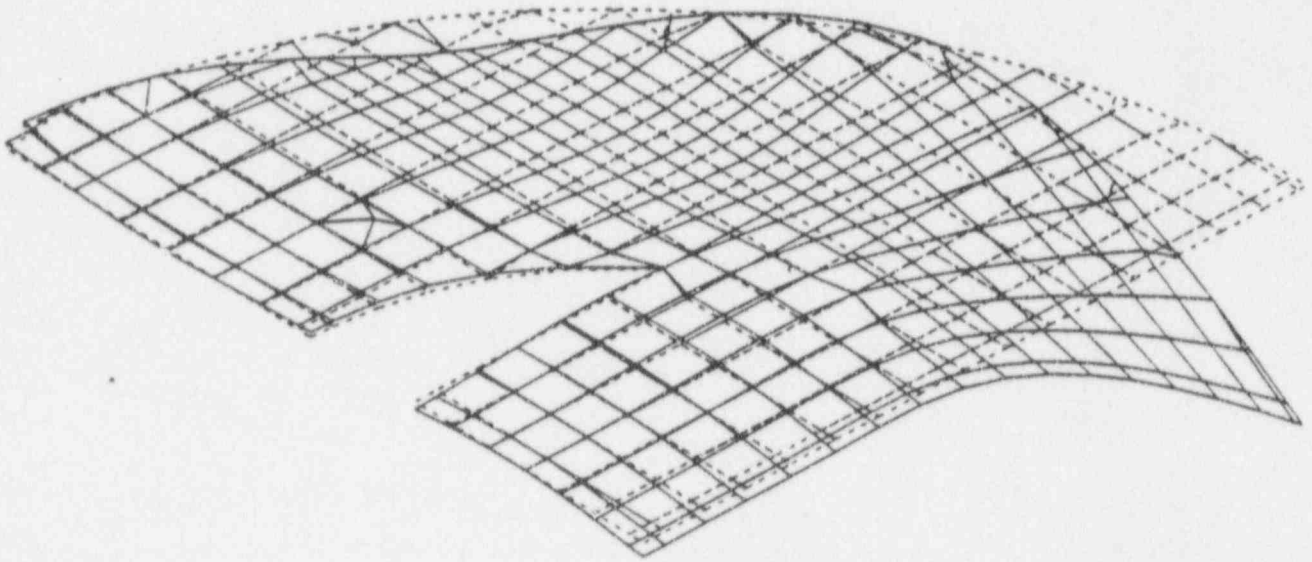

Figure 4-32. Displaced Geometry
Plate A(1H) : Time = 0.902 sec
SLB + Excess Feedwater Transient

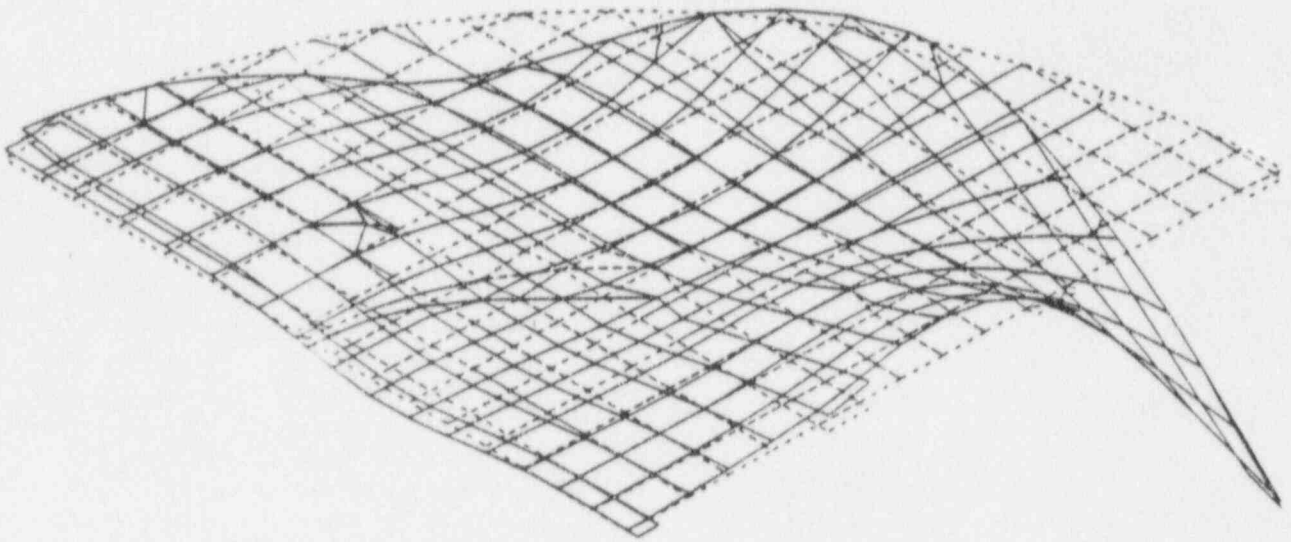

Figure 4-33. Displaced Geometry
Plate C(3H) : Time = 1.886 sec
SLB + Excess Feedwater Transient

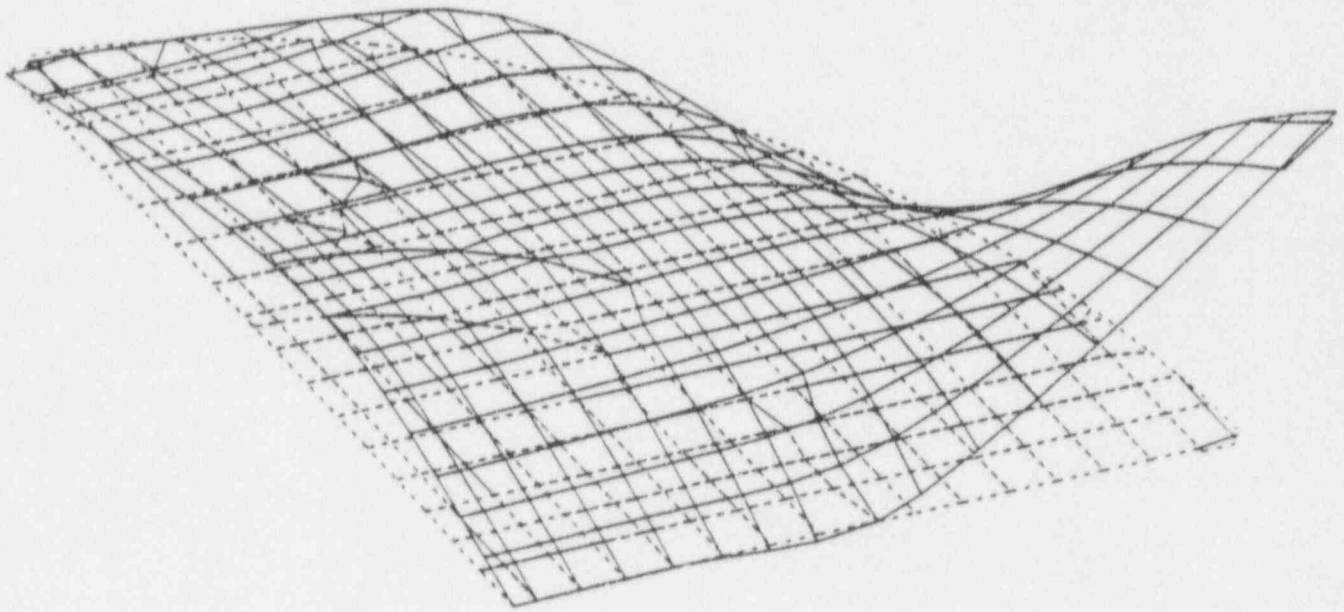

Figure 4-34. Displaced Geometry
Plate J(7H) : Time = 0.264 sec
SLB + Excess Feedwater Transient

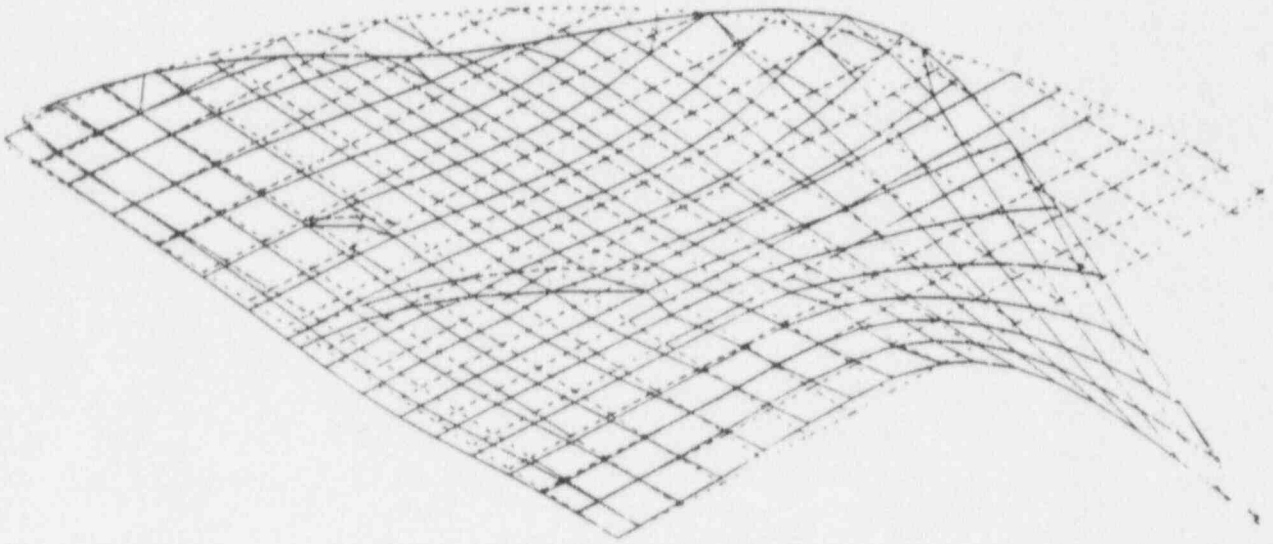

Figure 4-35. Displaced Geometry
Plate J(7H) : Time = 1.926 sec
SLB + Excess Feedwater Transient

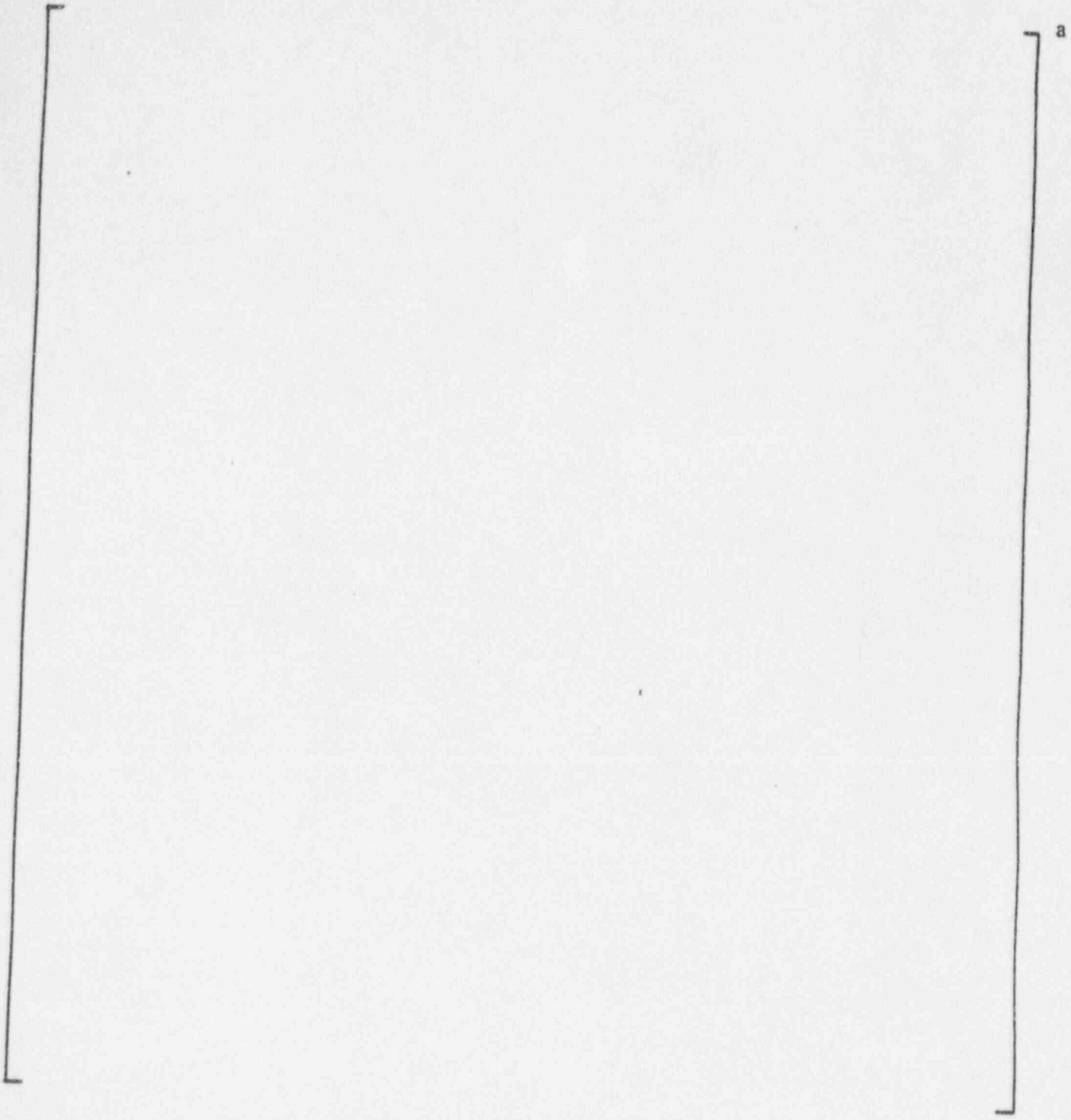

Figure 4-36. Displacement Time History Response
SLB + Excess Feedwater Transient
Plates A(1H), C(3H), F(5H), J(7H)

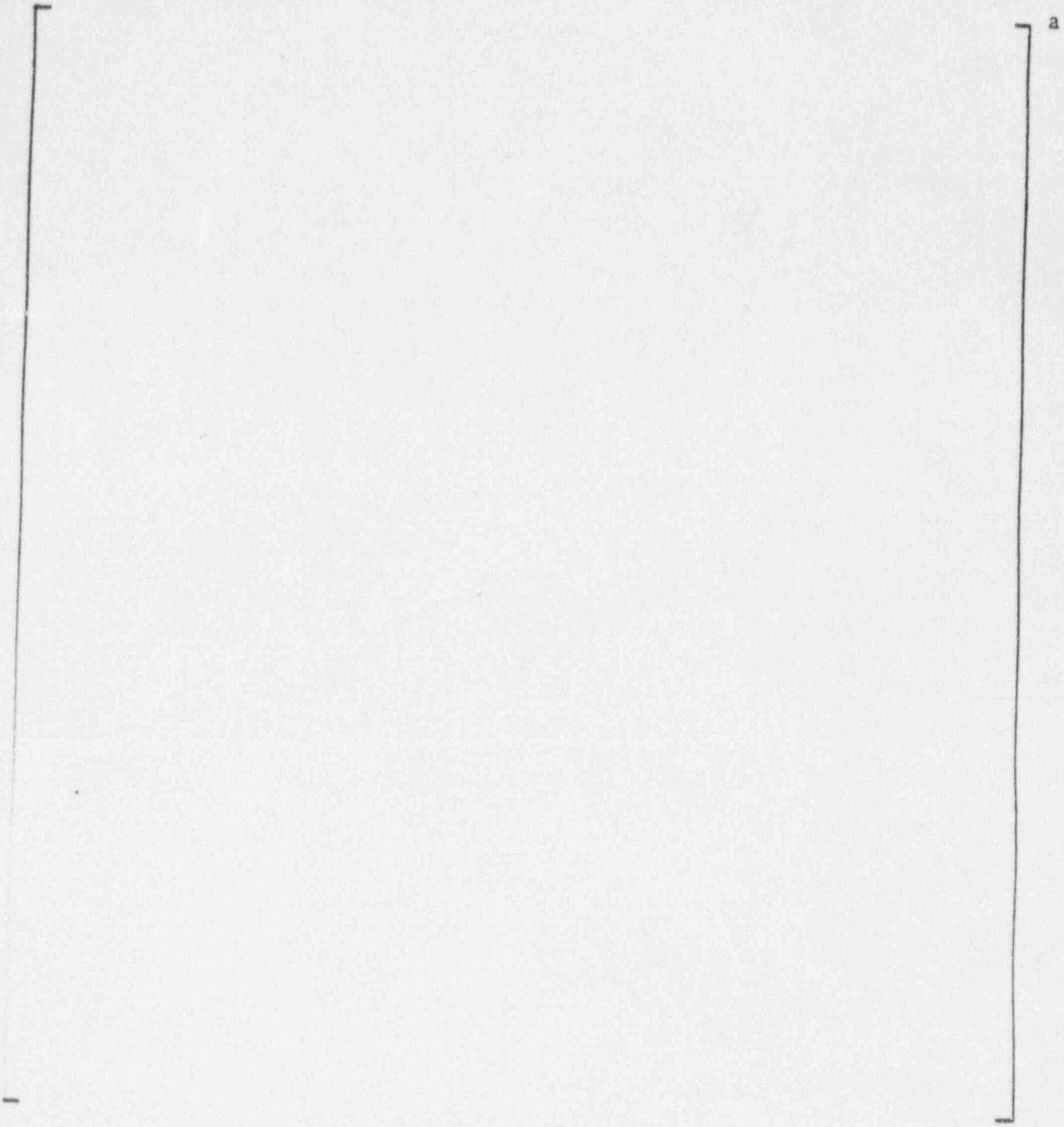

Figure 4-37. Displacement Time History Response
SLB + Excess Feedwater Transient
Plates L(8H), M(9H), N(10H), P(11H)

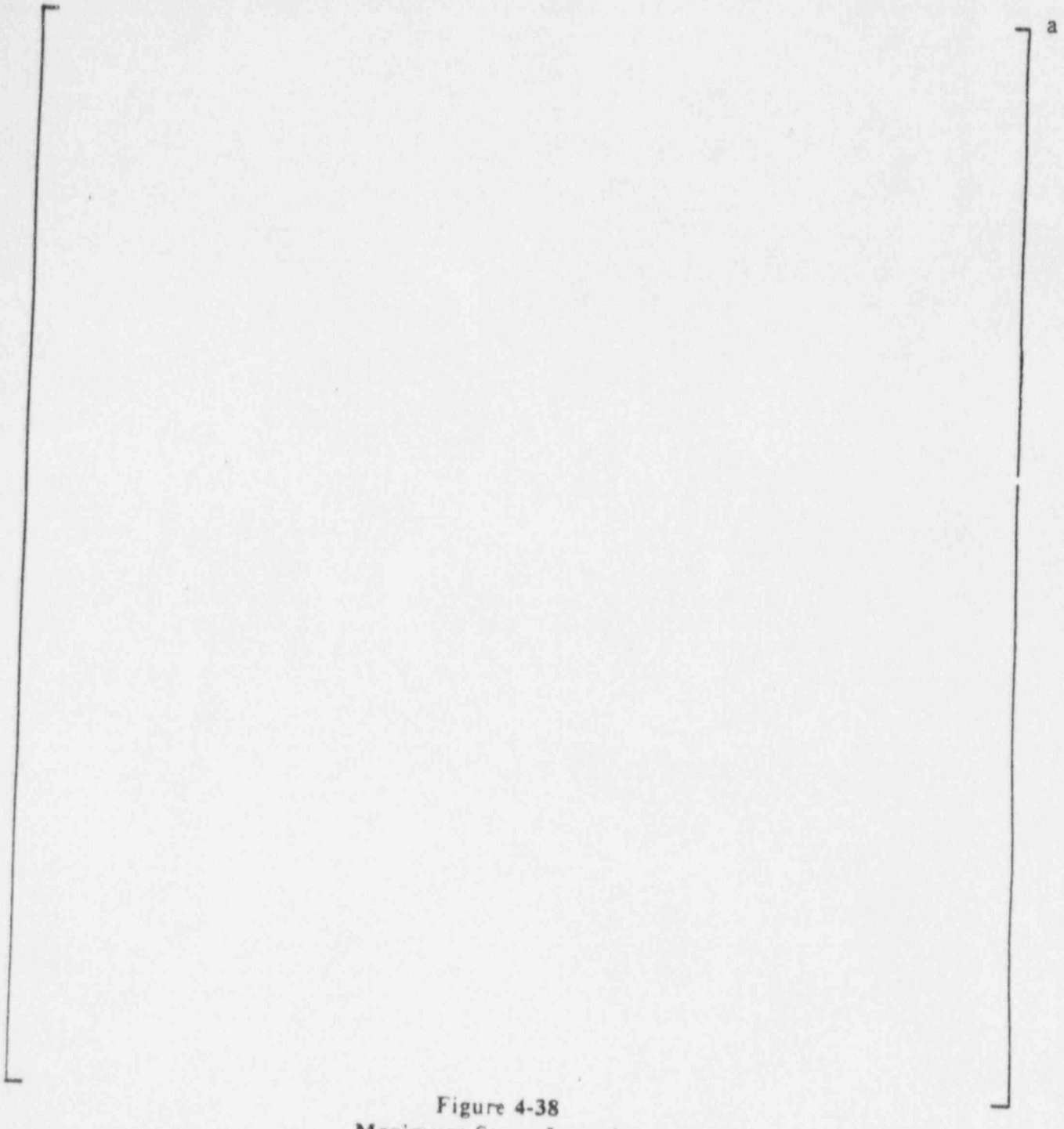

Figure 4-38
Maximum Stress Intensity
SLB + Excess Feedwater Transient
Plate A (1H)

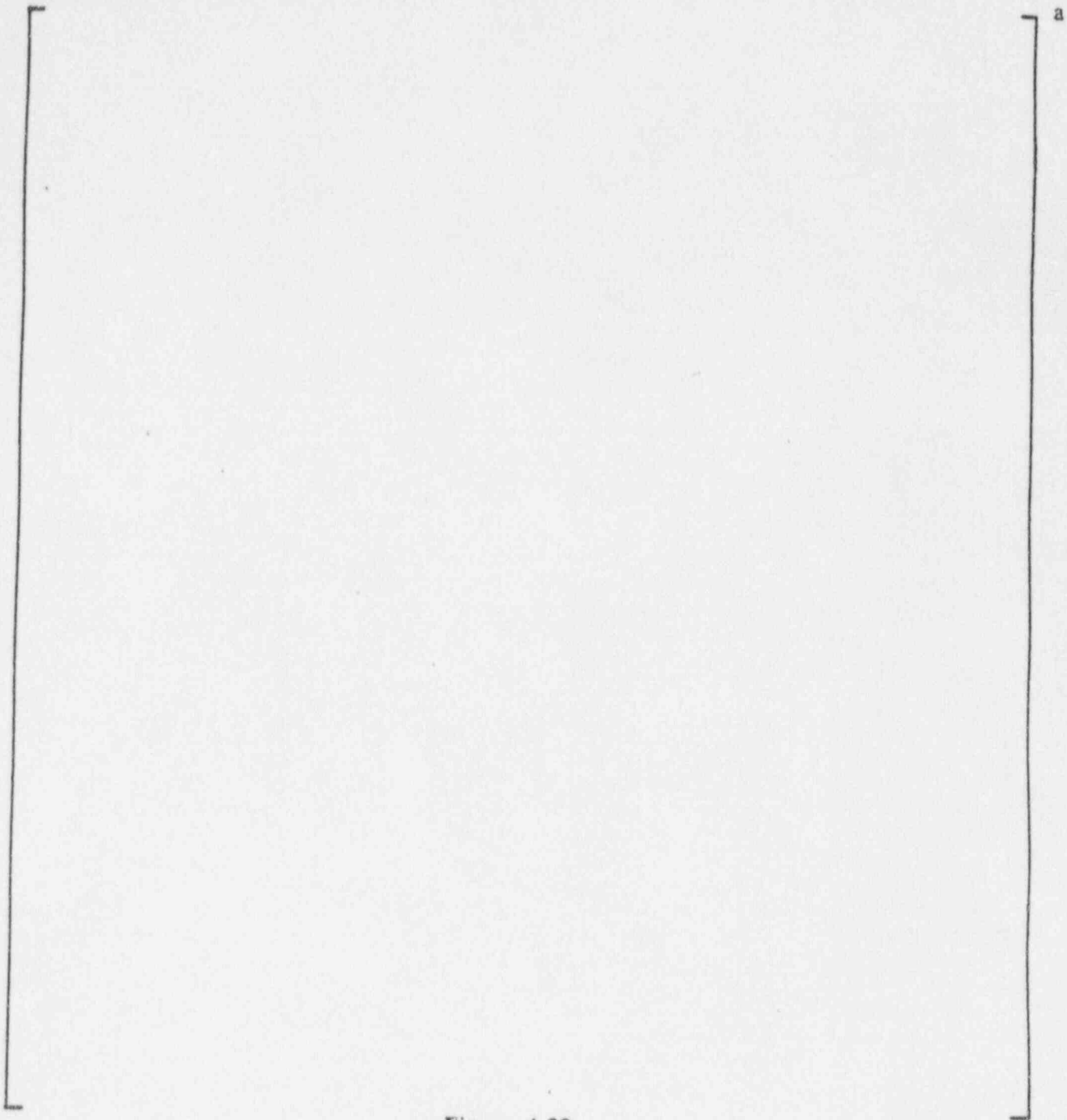

Figure 4-39
Minimum Stress Intensity
SLB + Excess Feedwater Transient
Plate A (1H)

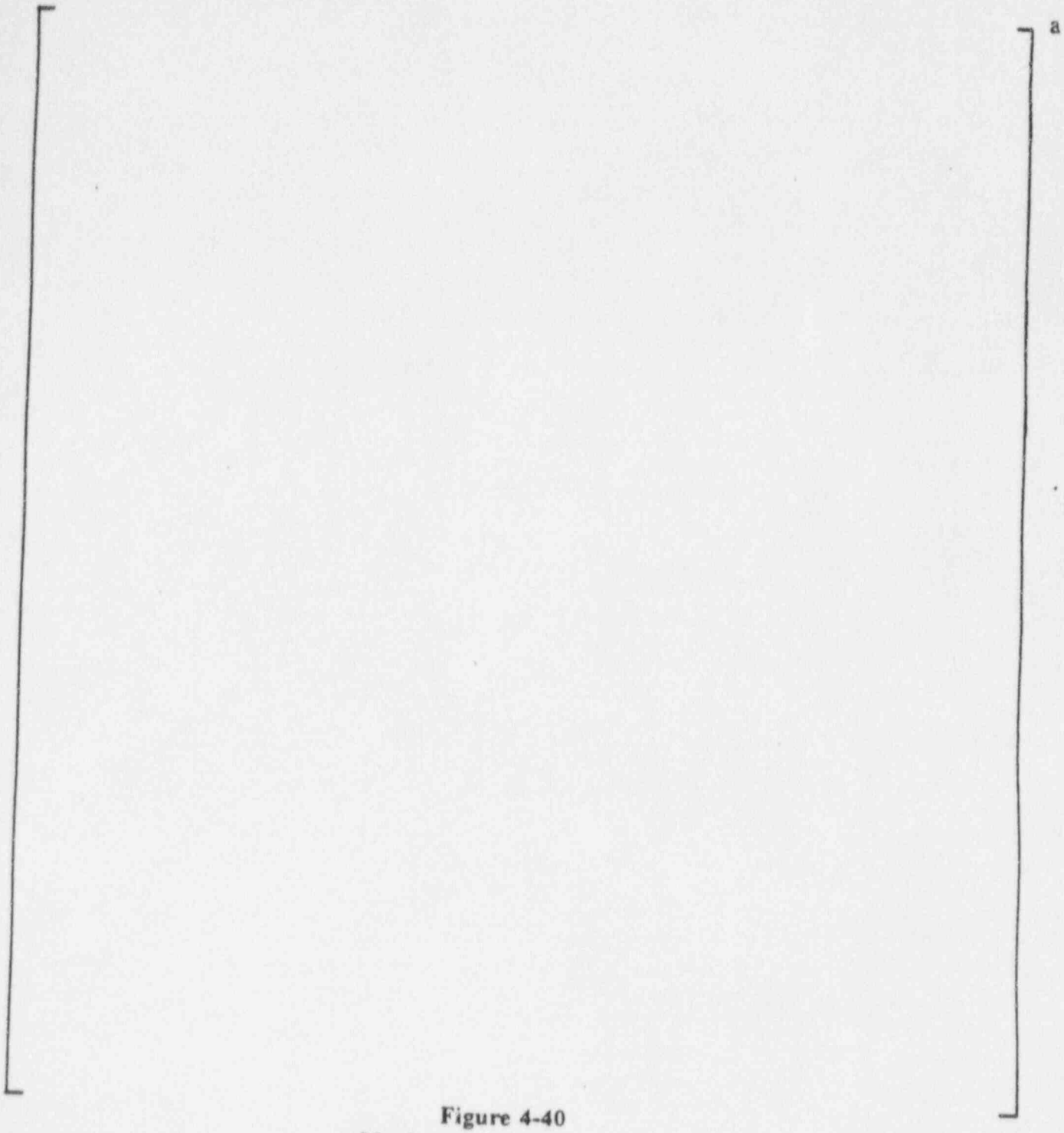

Figure 4-40
Maximum Stress Intensity
SLB + Excess Feedwater Transient
Plate C (3H)

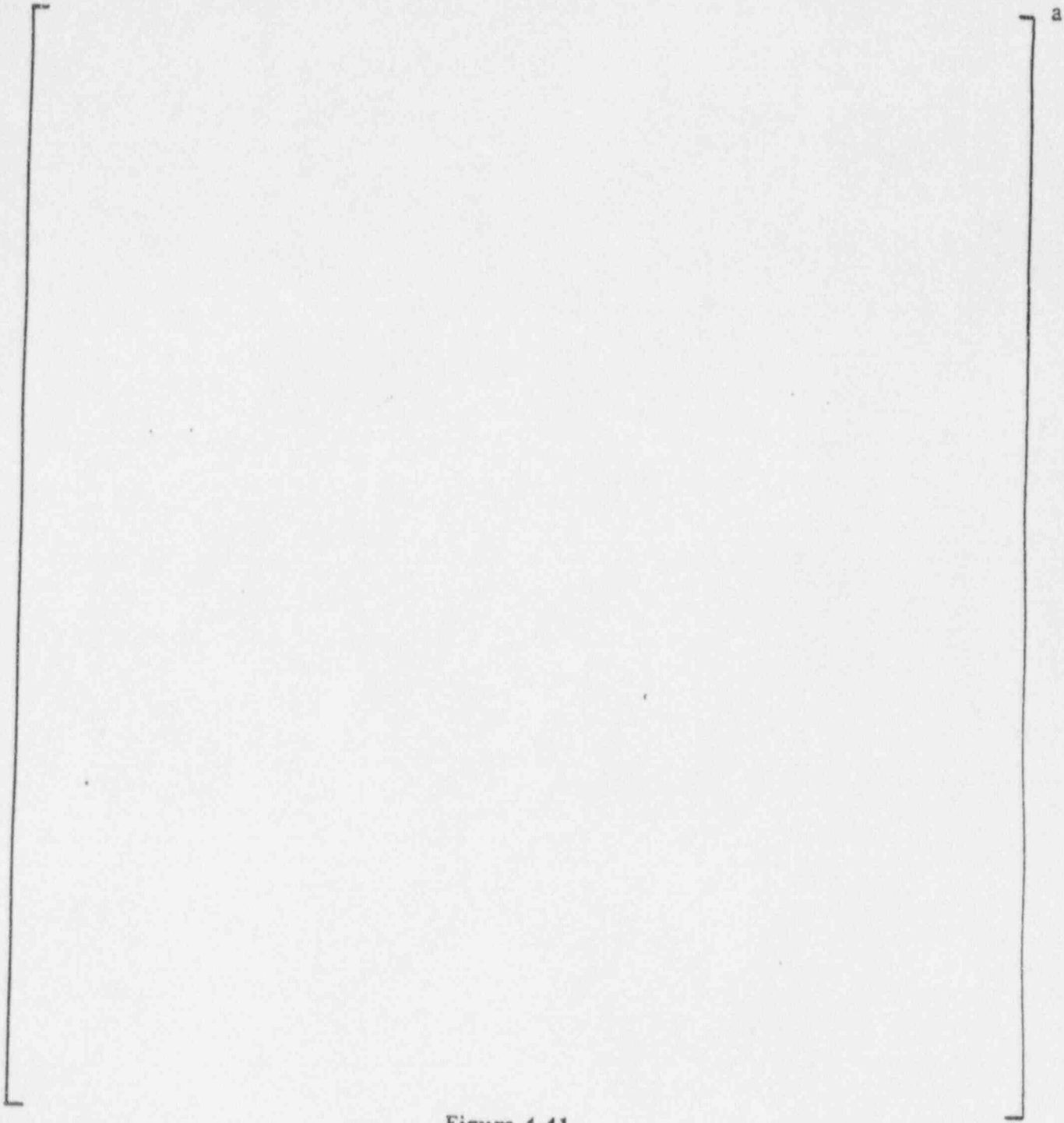

Figure 4-41
Minimum Stress Intensity
SLB + Excess Feedwater Transient
Plate C (3H)

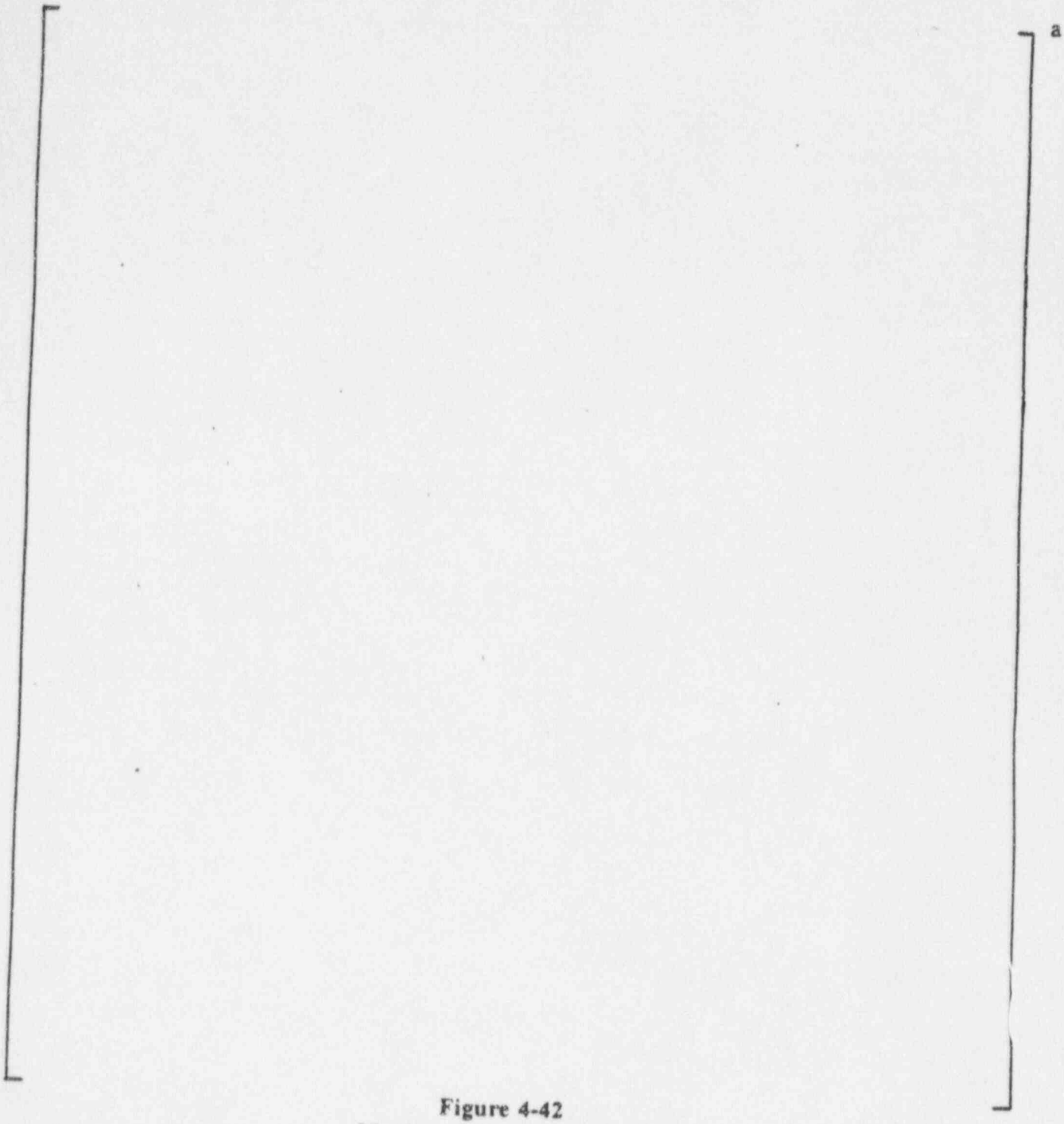

Figure 4-42
Maximum Stress Intensity
SLB + Excess Feedwater Transient
Plate J (7H) (Maximum Upward Response)

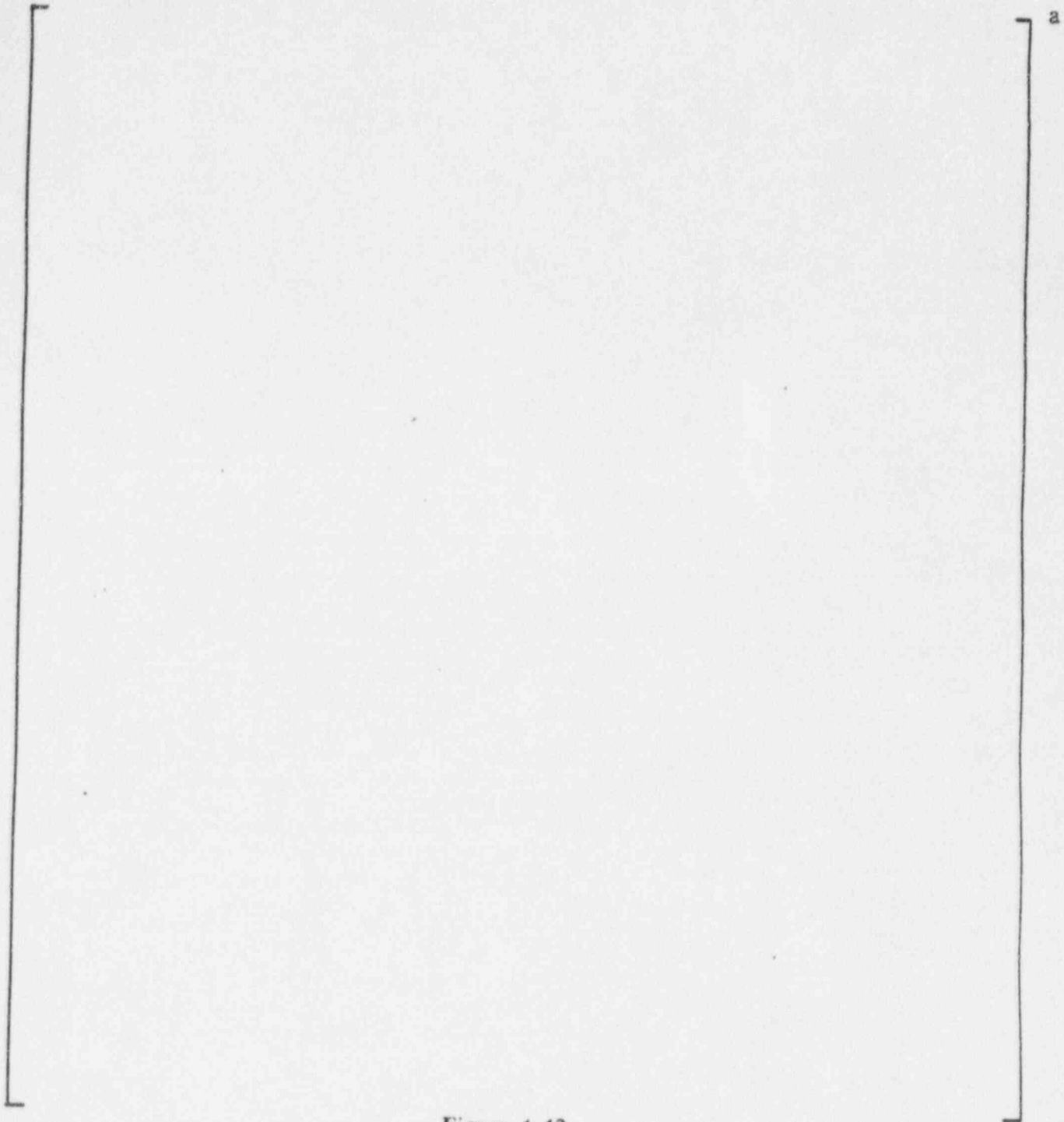

Figure 4-43
Minimum Stress Intensity
SLB + Excess Feedwater Transient
Plate J (7H) (Maximum Upward Response)

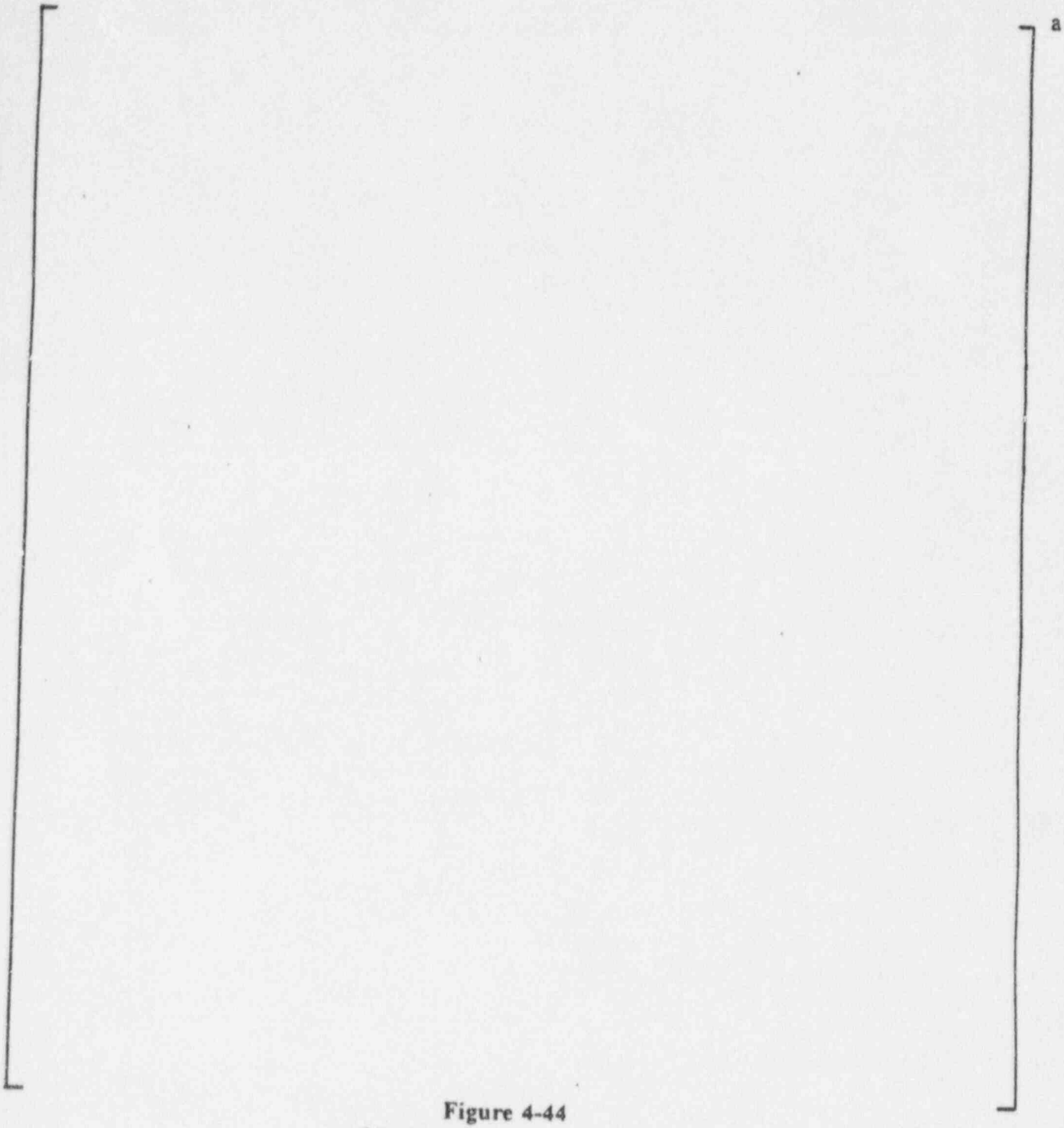

Figure 4-44
Maximum Stress Intensity
SLB + Excess Feedwater Transient
Plate J (7H) (Maximum Downward Response)

[ ]a

Figure 4-45
Minimum Stress Intensity
SLB + Excess Feedwater Transient
Plate J (7H) (Maximum Downward Response)

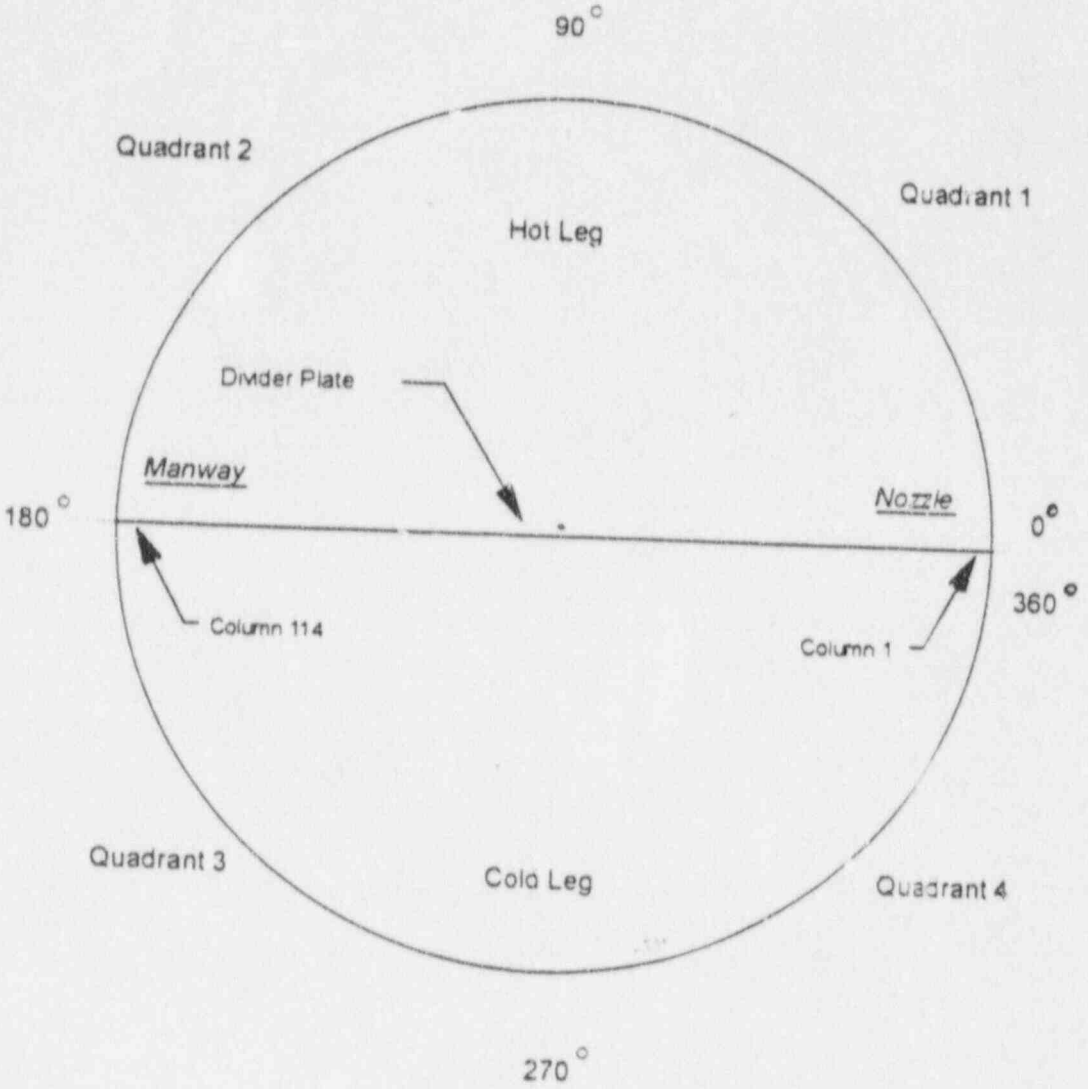

Figure 4-46. Reference Configuration Looking Down on Steam Generator Left-Hand Unit

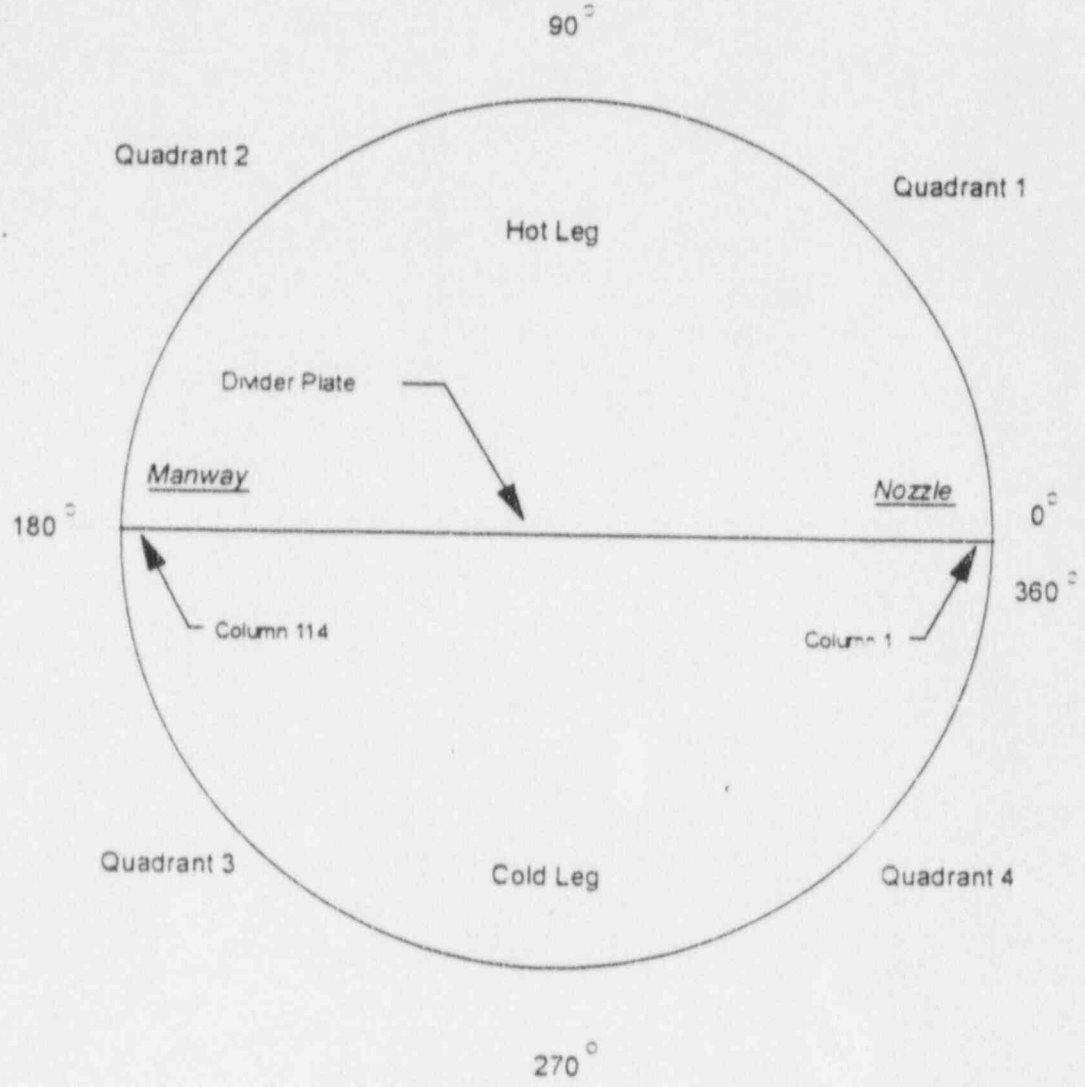

Figure 4-47. Reference Configuration Looking Down on Steam Generator Right-Hand Unit

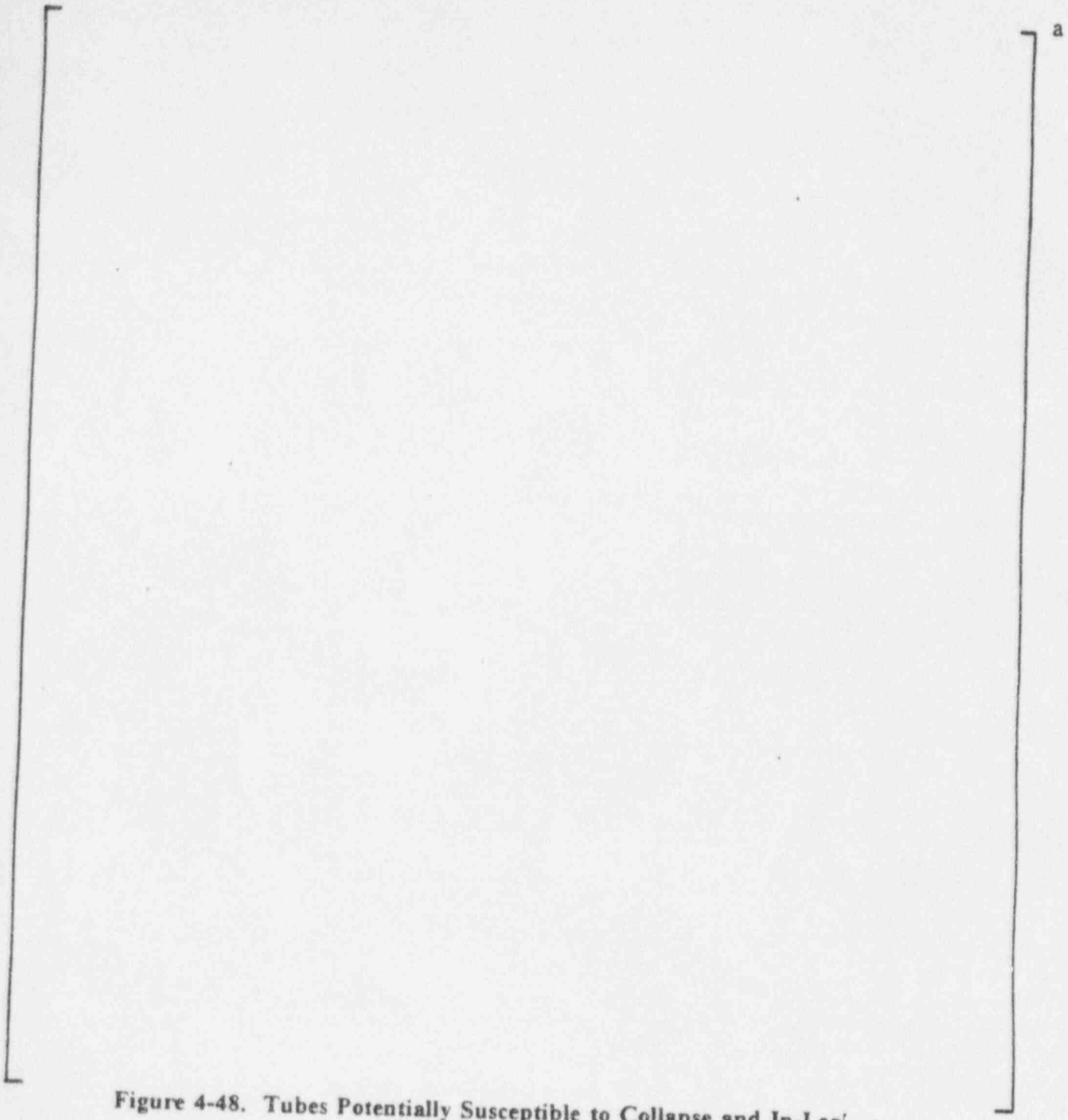

Figure 4-48. Tubes Potentially Susceptible to Collapse and In-Leal...
Braidwood Unit 1
TSP C, J
Quadrant 1

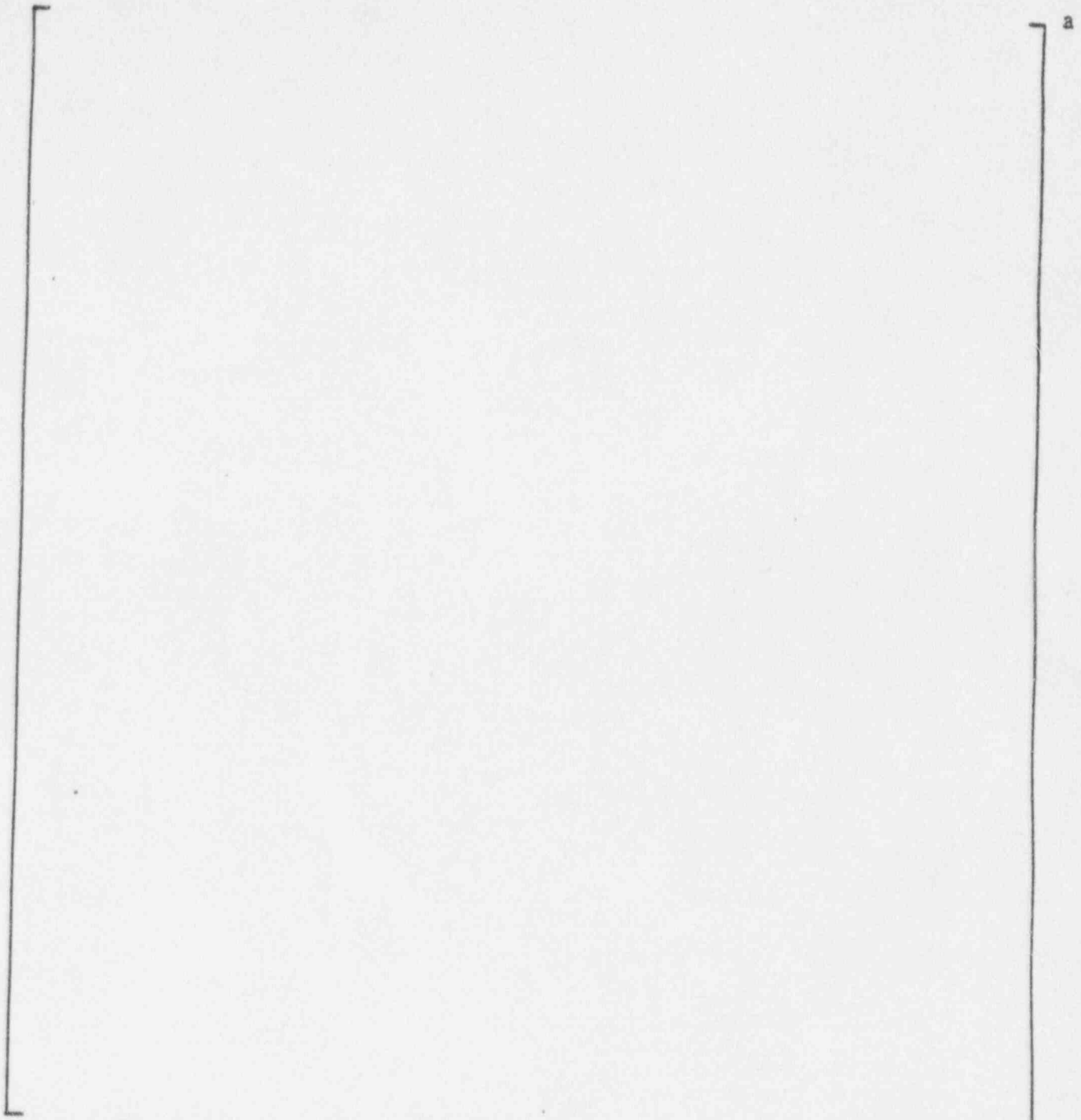

Figure 4-49. Tubes Potentially Susceptible to Collapse and In-Leakage
Braidwood Unit 1
TSP C, J
Quadrant 2

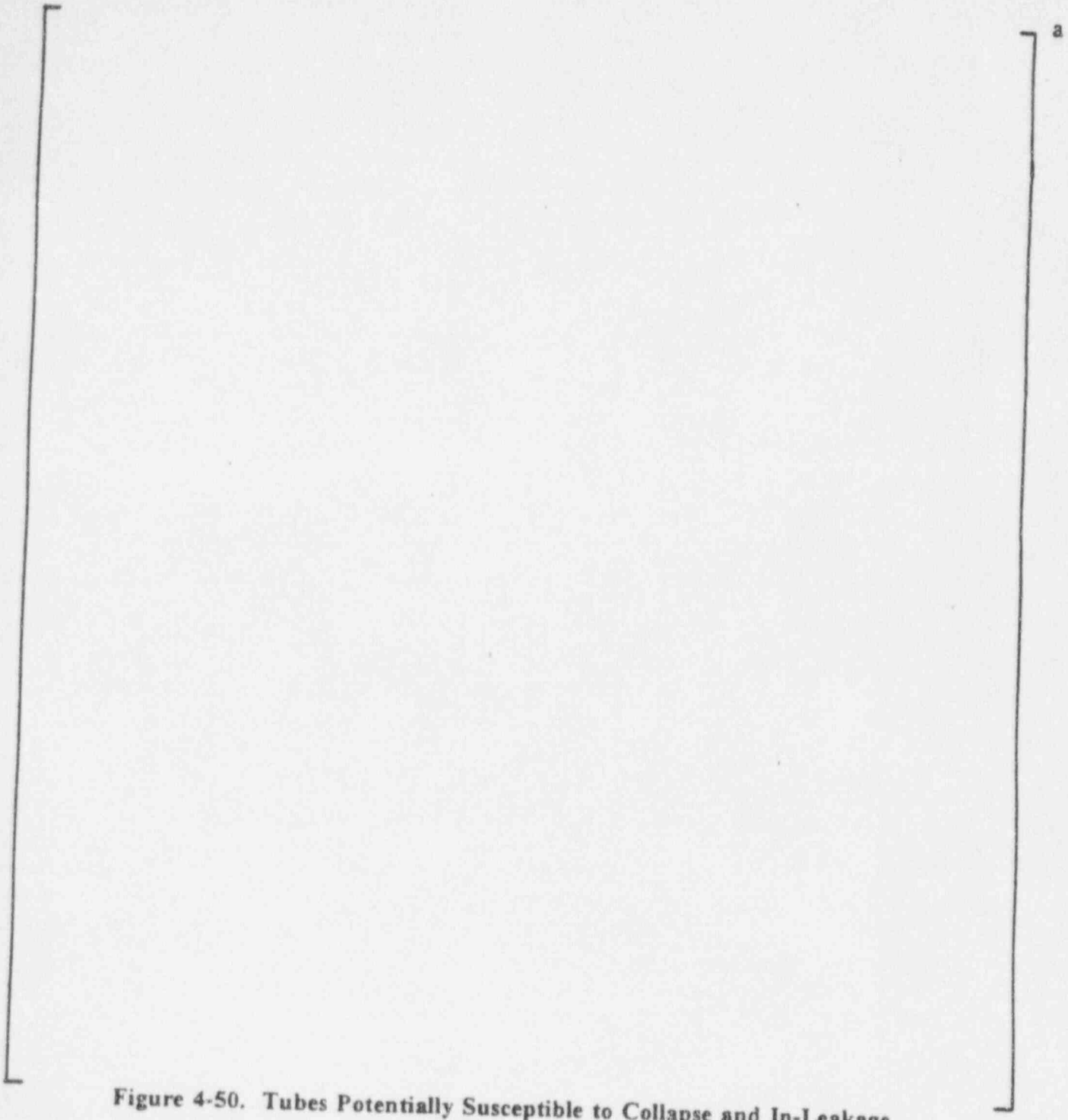

Figure 4-50. Tubes Potentially Susceptible to Collapse and In-Leakage
Braidwood Unit 1
TSP D, G
Quadrant 3

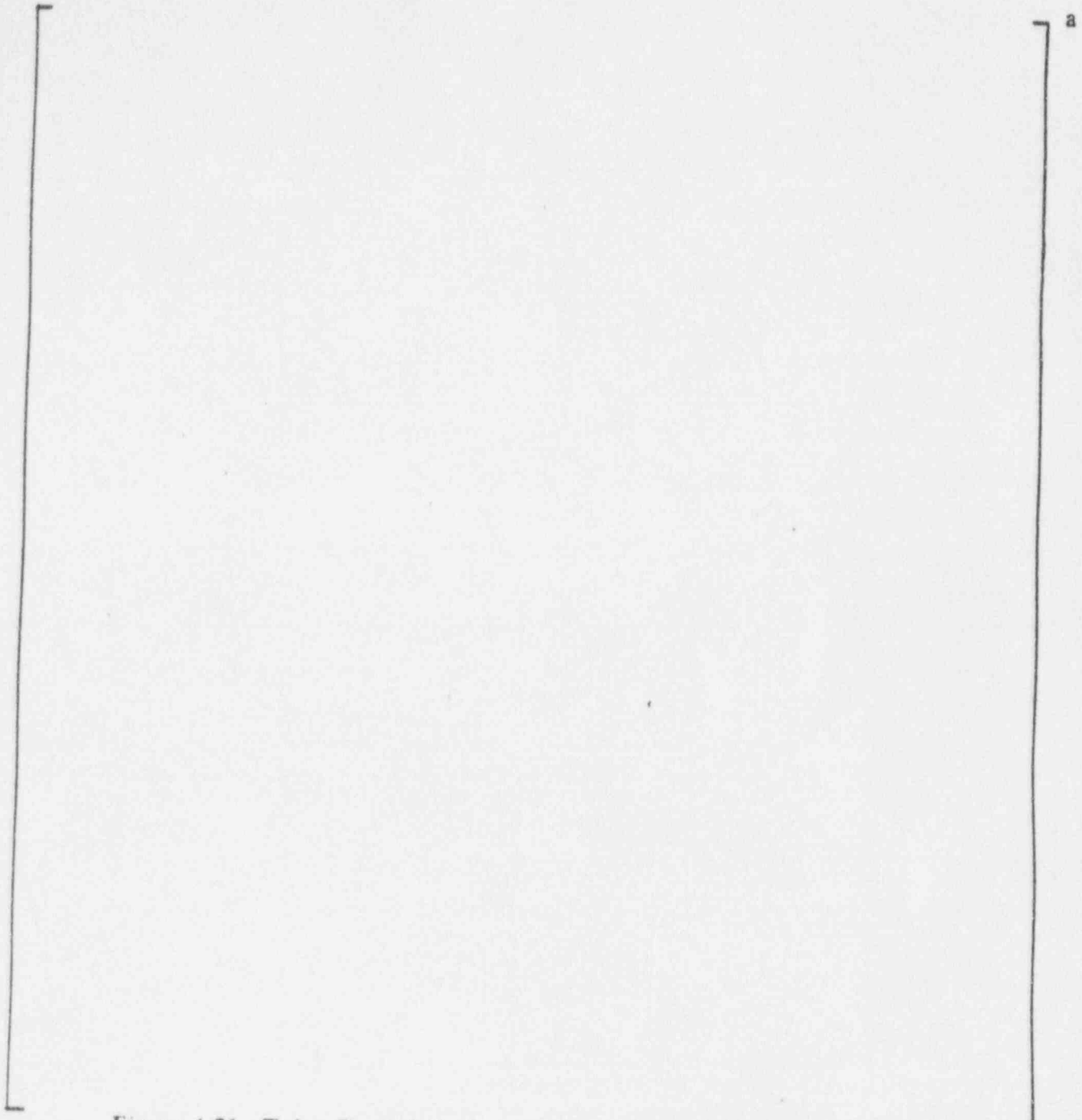

Figure 4-51. Tubes Potentially Susceptible to Collapse and In-Leakage
Braidwood Unit 1
TSP D, G
Quadrant 4

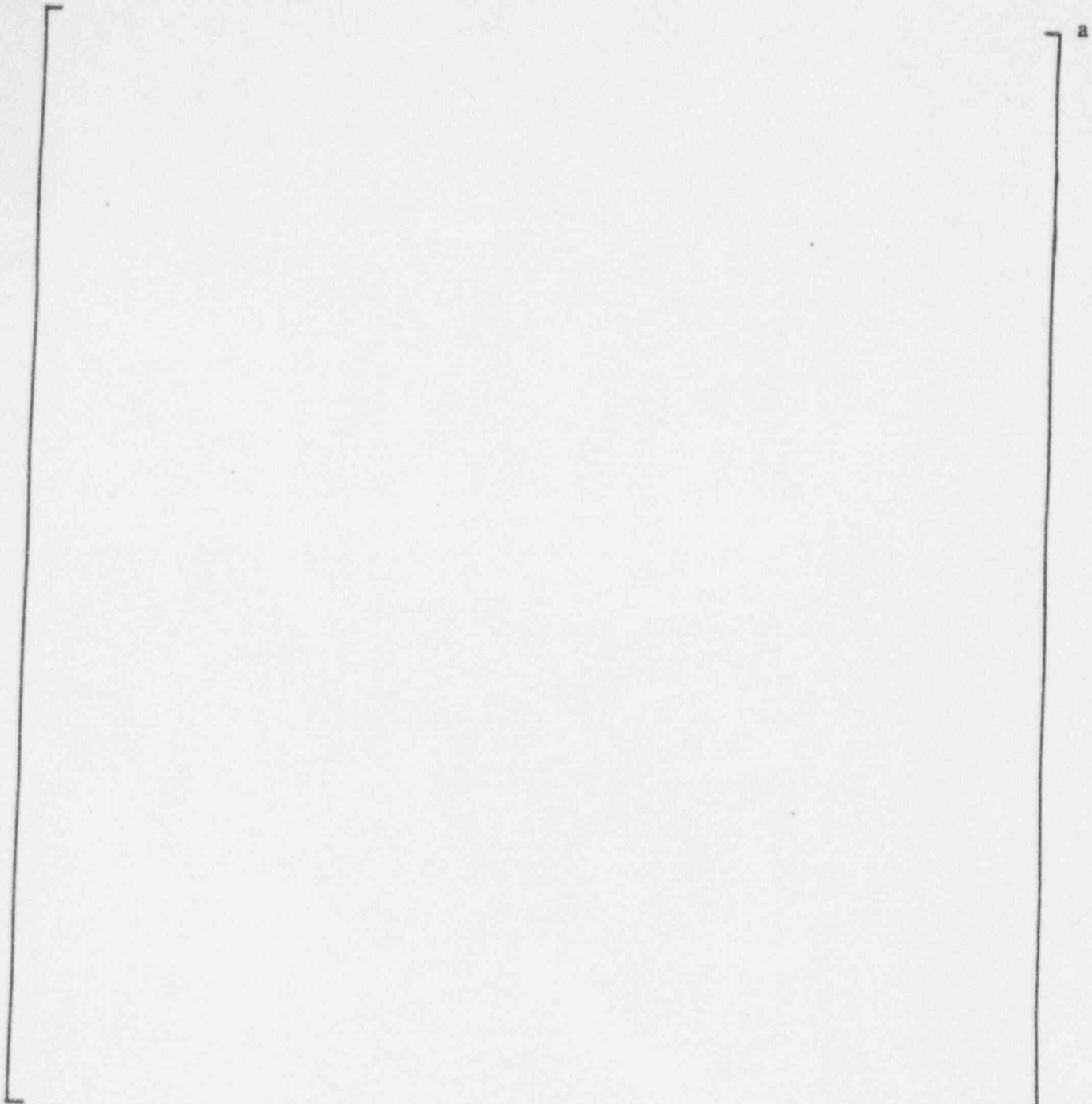

Figure 4-52. Tubes Potentially Susceptible to Collapse and In-Leakage
Braidwood Unit 1
TSP E, H
Quadrant 3

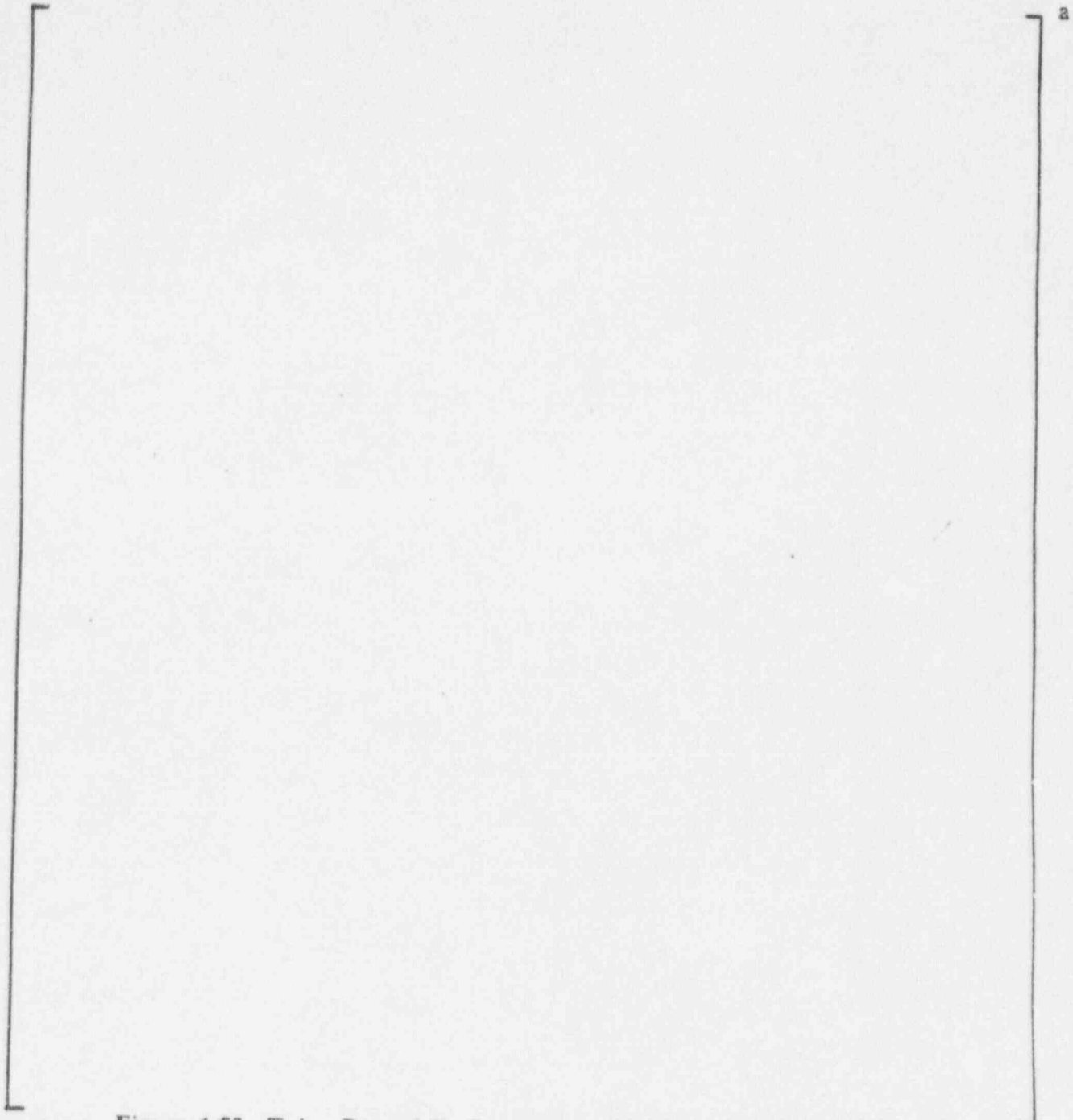

Figure 4-53. Tubes Potentially Susceptible to Collapse and In-Leakage
Braidwood Unit 1
TSP E, H
Quadrant 4

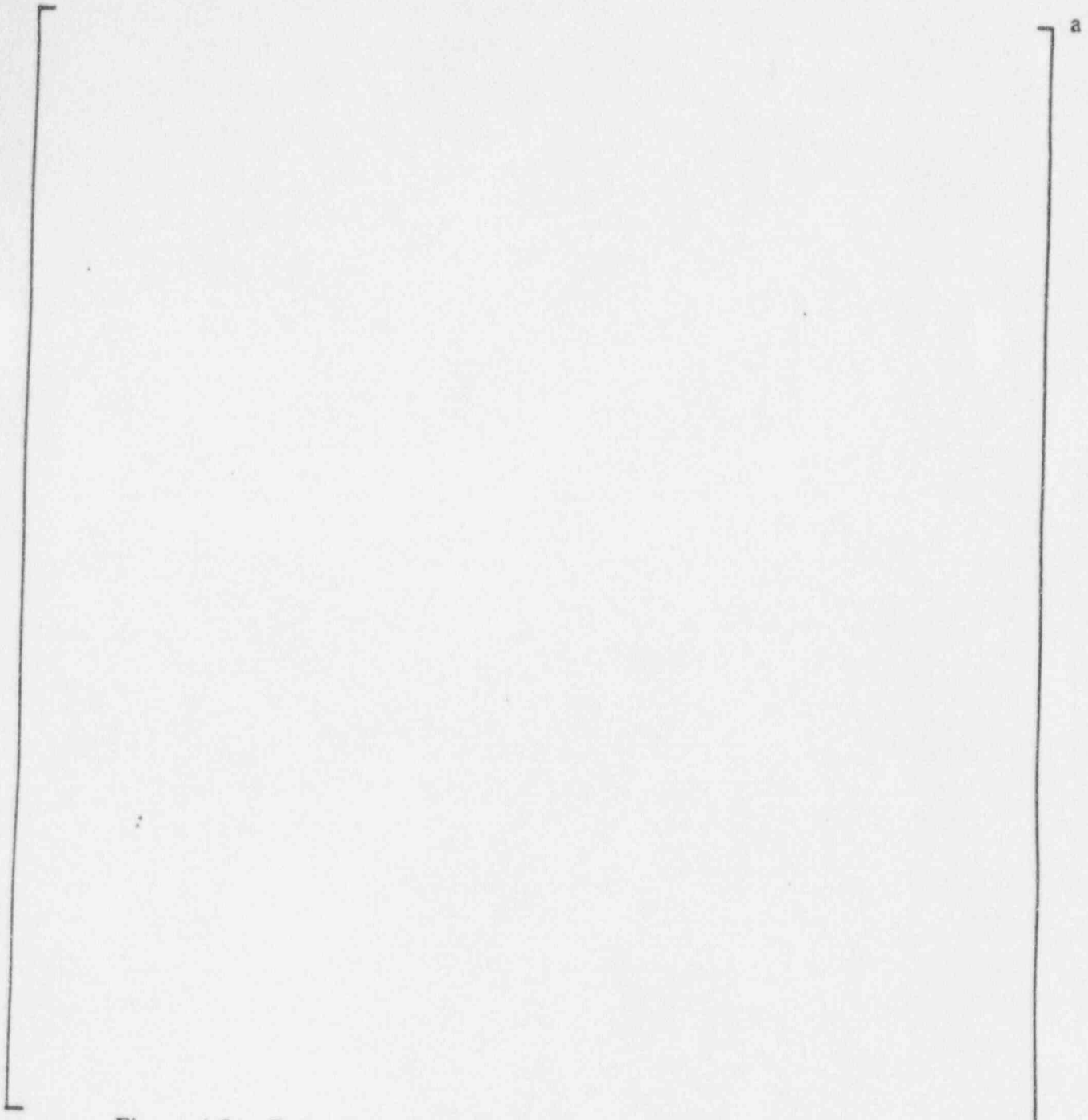

Figure 4-54. Tubes Potentially Susceptible to Collapse and In-Leakage
Braidwood Unit 1
TSP F
Quadrant 1

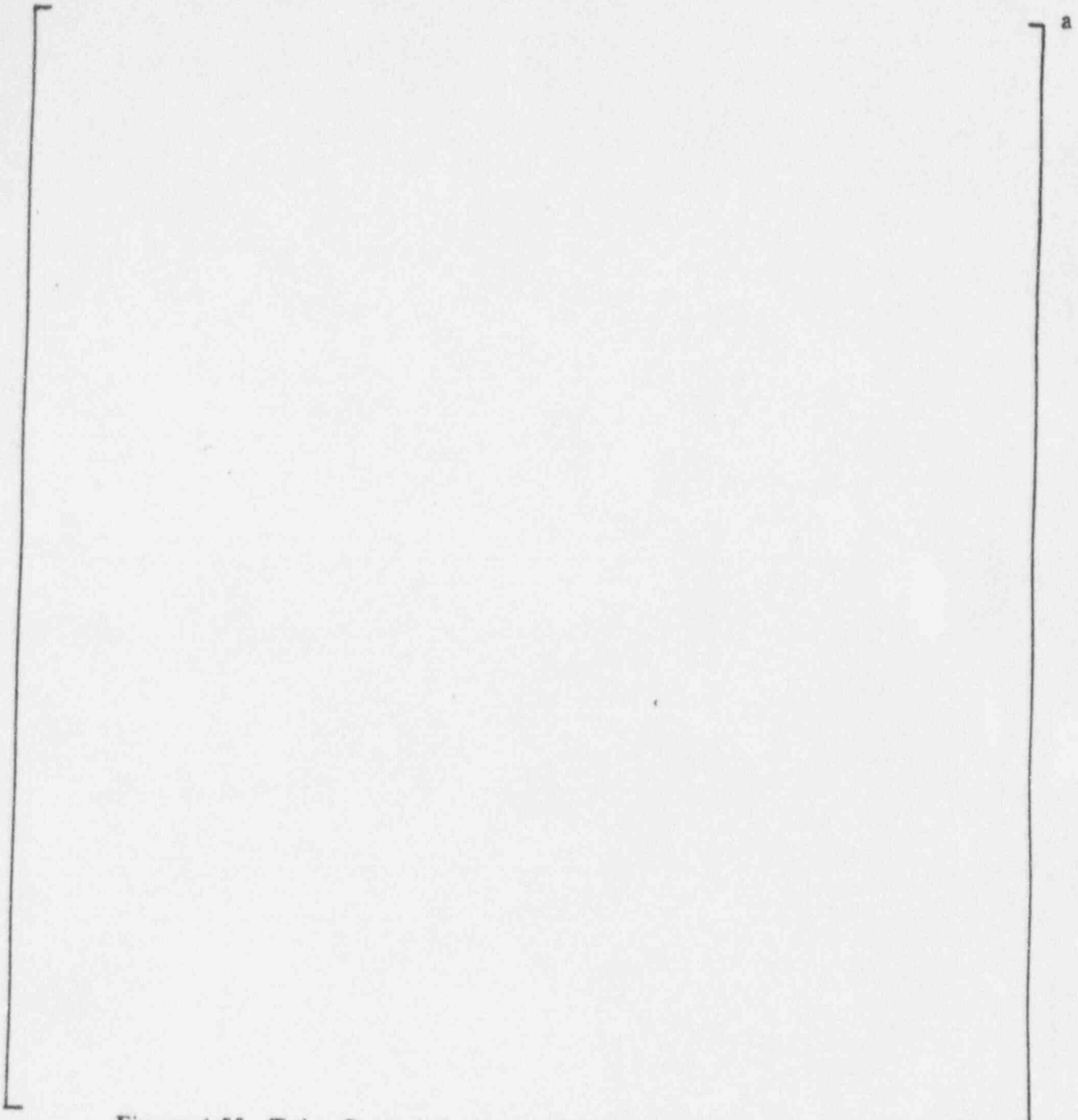

Figure 4-55. Tubes Potentially Susceptible to Collapse and In-Leakage
Braidwood Unit 1
TSP F
Quadrant 2

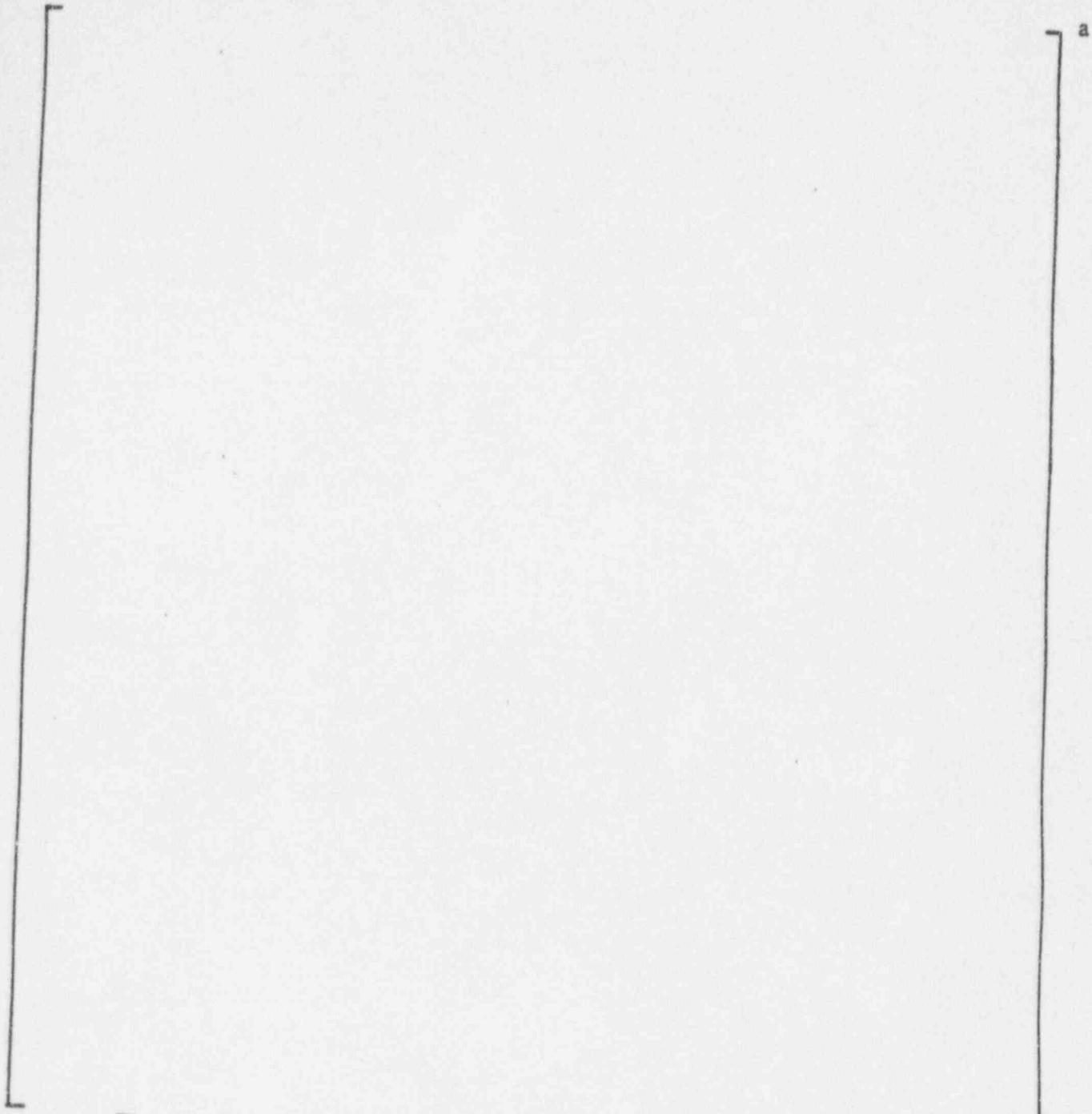

Figure 4-56. Tubes Potentially Susceptible to Collapse and In-Leakage
Braidwood Unit 1
TSP L, M, N, P
Quadrant 1

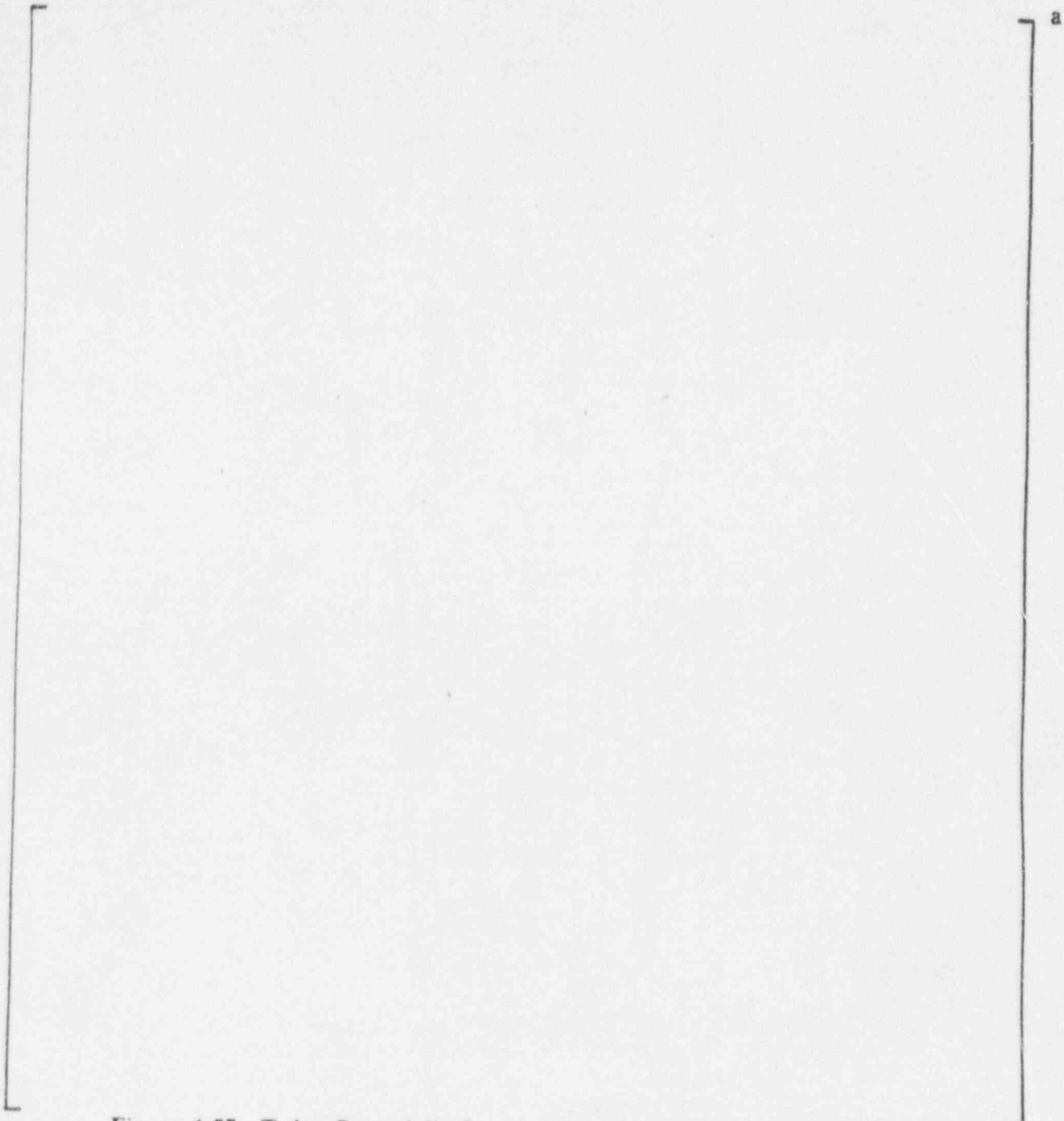

Figure 4-57. Tubes Potentially Susceptible to Collapse and In-Leakage
Braidwood Unit 1
TSP L, M, N, P
Quadrant 2

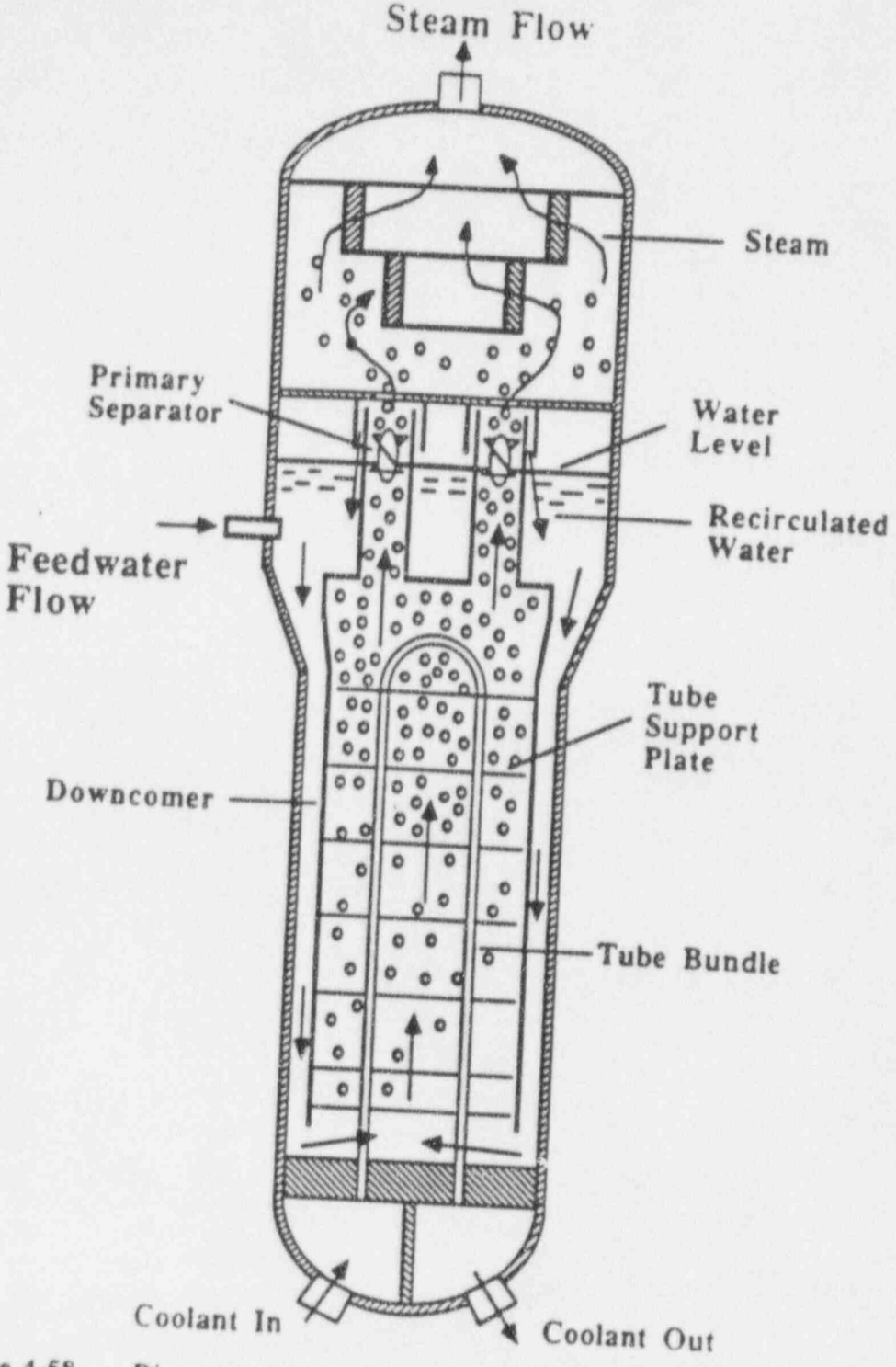

Figure 4-58. Diagram of Flow Circulation During Power Operation

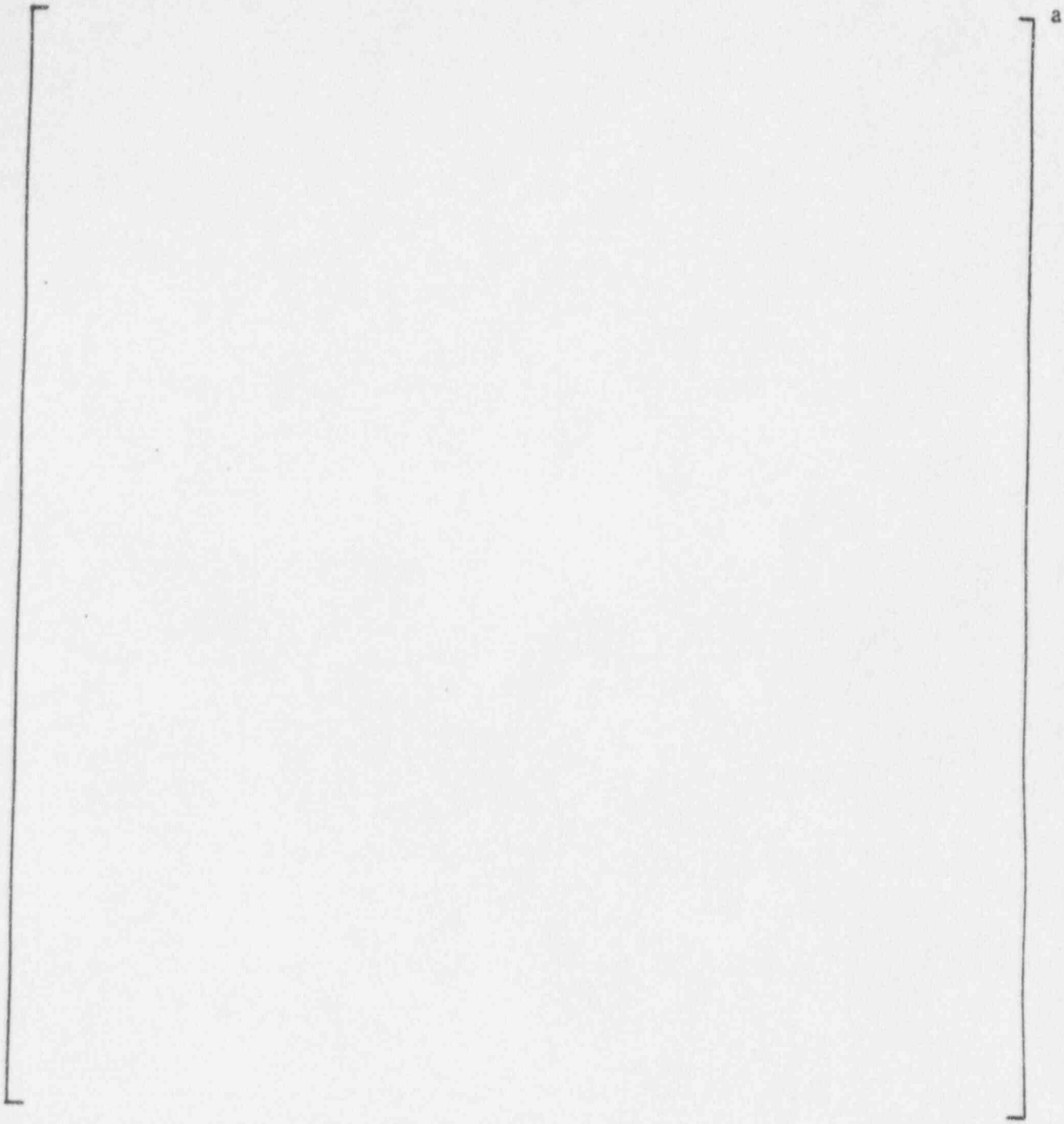

Figure 4-59. Counterbored Structural Quatrefoil Loss Coefficients

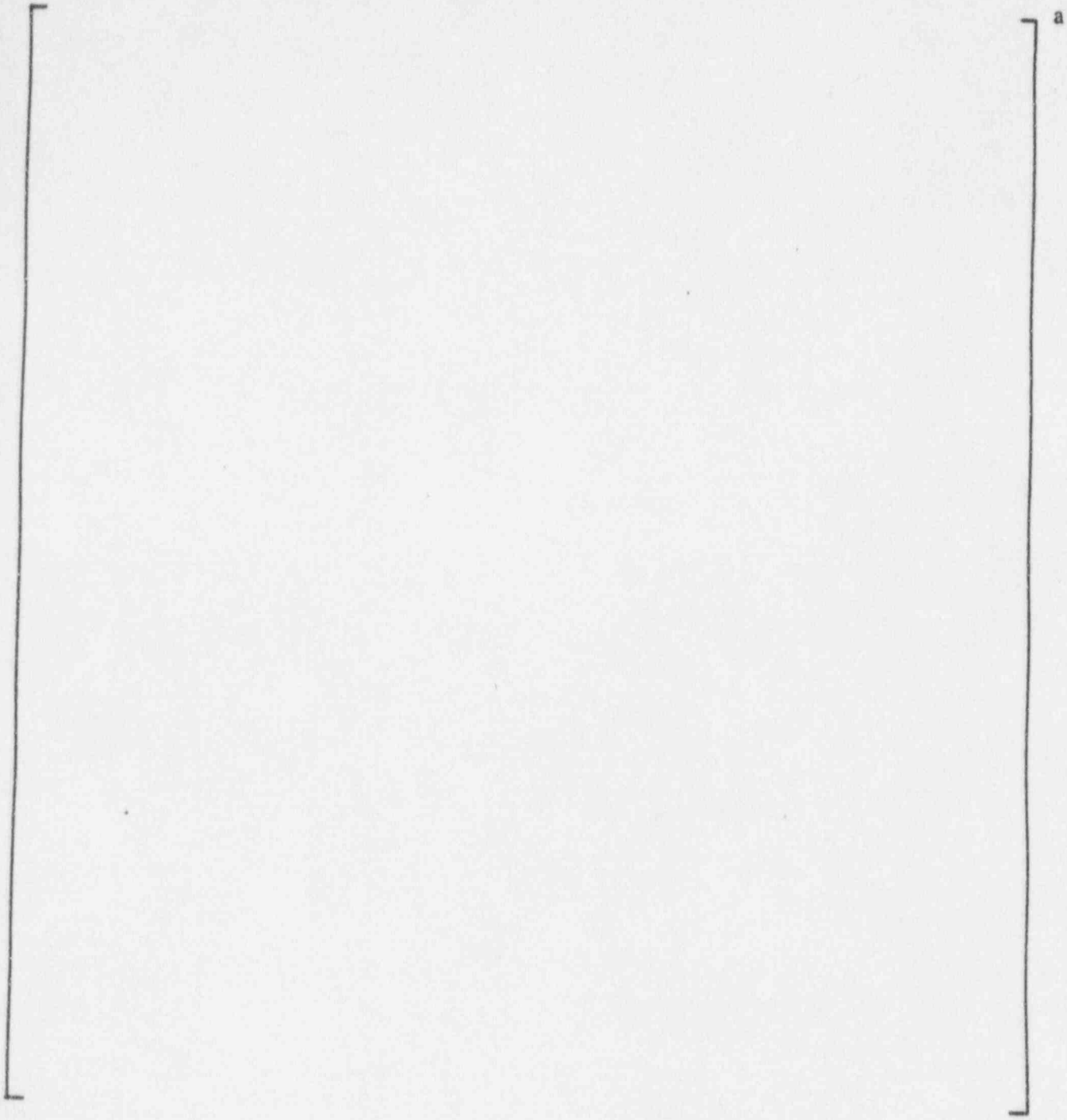

Figure 4-60. GENF Verification, Circulation Ratio Versus Load

5.0 DATABASE SUPPORTING ALTERNATE REPAIR CRITERIA

This section describes the database supporting the alternate repair criteria (ARC) burst and leak rate correlations. The database for 3/4 inch diameter tubing is described in EPRI Report NP-7480-L, Volume 2 (Reference 5-1). However, at the February 8, 1994 NRC/Industry meeting, the NRC presented resolution of industry comments on draft NUREG-1477. The NRC identified guidelines for application of leak rate versus voltage correlations and for removal of data outliers in the burst and leak rate correlations. This section applies the NRC guidance on removal of outliers to update the database for the 3/4 inch tubing correlations.

5.1 Data Outlier Evaluation

At the February 8 meeting, the NRC provided the following guidance for removal of data outliers:

- Data can be deleted in case of an invalid test.
- Any morphology criteria for deleting outliers must be rigorously defined and applied to all the data.
- Criteria for deleting outliers must be able to be unambiguously applied by an independent observer.
- It is acceptable to modify data or a model in a conservative manner.

Based on the above NRC guidance, the outlier evaluation of Reference 5-1 is updated in this section. Consistent with the NRC guidance, criteria for removal of outliers are defined in this section and applied to the database. These criteria were developed and approved by the EPRI Adhoc Alternate Repair Criteria (ARC) Committee. Consistent with Reference 5-1, only conservative outliers which are high on the burst correlation or low on the leak rate correlation are evaluated for removal from the database. Although the outliers are conservative in this manner, their retention in the database can increase the uncertainties from the regression analyses such that their removal from the database can lead to non-conservatisms in analyses applying uncertainties at upper or lower tolerances.

Criterion 1 for outlier removal applies to invalid data including unacceptable specimens, invalid measurements, etc. To describe the invalid test condition, Criteria 1a to 1e are defined as described in Table 5-1. Table 5-1 provides examples of invalid data that are applicable to the EPRI database.

Criterion 2 for outlier removal applies to specimens with atypical or non-prototypic crack morphology. Criterion 2a applies to specimens with atypical ligament morphology while Criterion 2b applies to severe degradation significantly exceeding the EPRI database. The specific criteria for deleting outliers based on morphology considerations are given in Table 5-2. Table 5-2 also includes the indications excluded from the correlations based on Criterion 2b. No 3/4" indications were removed from the database based on Criterion 2a. Specimen 598-1 is excluded by Criterion 2b. This data point's voltage is more than 40 volts higher than the next largest specimen. There is insufficient data at the high voltage (64.9 volts) to assess the protypicality of the specimen or applicability to the database. This singular point may unduly influence the correlations without comparable voltage data to define the appropriate trend in the data at these high voltages. Based on destructive examination results providing identification of remaining uncorroded ligaments, the criteria of Table 5-2 can be unambiguously applied by an independent observer and thus satisfies the NRC guidance for removal of data outliers.

Criterion 3 for outlier removal applies to specimens with abnormal leakage behavior due to a suspected test problem. In the performance of leak tests, the crack can become plugged by deposits resulting in abnormally low leak rates or a measurement error could occur. For these cases, the cause for the measurement error is not as apparent as for Category 1 and the test results must be evaluated for apparent errors. It is not appropriate to include the spread in leak rates resulting from plugging of cracks in leak tests in the leak rate correlation and each leak rate measurement should be evaluated against the criteria of this section before including the data in the database. Table 5-3 defines Criterion 3 provides for either SLB leak rates insignificantly greater than normal operating leak rates or for leak rates much lower than expected for the throughwall crack length found by destructive examination as a basis for excluding data from the correlations. Also included in Table 5-3 are the 3/4" tubing specimens excluded from the database by this criterion and the basis for exclusion.

Criterion 3 applies to extreme cases of low leak rate outliers, such as more than a factor of 50 lower than predicted by verified analytical models. In addition, the factor of 50 criterion applies only to specimens which have no remaining uncorroded ligaments within the throughwall length of the crack. The principal effects causing lower than expected variation in leak rates are remaining ligaments in the crack face, tortuosity (oblique steps in the crack, surface irregularities) and presence of deposits. These effects tend to lower leakage for modest throughwall crack lengths. All three effects become smaller as crack length increases and crack opening increases. Longer throughwall cracks tend to have lost the ligaments by corrosion, the wider crack openings reduce the influence of surface irregularities and reduce the potential for deposits plugging the crack. From the database, "long" cracks appear to be about > 0.3" throughwall as above this length, the variability from predicted leak rates as a function of length appears to be smaller (see Figure 5-1). For 0.3" throughwall cracks, the

crack width is about 1 mil at 2560 psid and increases to about 10 mils for a 0.5" long crack. Thus, crack lengths < 0.3" are more susceptable to plugging from deposits.

From Figure 5-1, it is seen that model boiler specimens 598-3 and 604-2 have very low leak rates for their respective throughwall crack lengths. The remaining data are reasonably clustered with trends similar to that expected as shown for the CRACKFLO analyses in Figure 5-1. There is no indication through spread in the data that other specimens are significantly influenced by probable deposits in the crack face. Criterion 3 has been applied to specimen 598-3 to eliminate this indication from the leak rate correlation, as this specimen is more than a factor of 100 lower than the mean of the other data at about the 0.27" crack length of this specimen. Criterion 3 has not been applied to specimen 604-2, as this specimen is not clearly a factor of 50 less than the mean of the data, although the leak rate is apparently affected by deposits.

Criterion 3 can be unambiguously applied by an independent observer to all measured leak rates given the results from leak rate measurements and/or destructive examinations and thus satisfies the NRC guidance for removal of outliers. This criterion is applied only to low leak rate measurements. For conservatism, high leak rate measurements are not considered for removal from the database.

Based on Criteria 1 to 3 as described in Tables 5-1 to 5-3, the EPRI database of Reference 5-1 was reviewed for identification of data outliers to be removed from the database. Tables 5-4 to 5-6 summarize the data points removed from the database applied to the burst, leak rate and probability of leak correlations, respectively.

Data were removed from the EPRI database in Reference 5-1 based on the same technical considerations, although less formal, as the criteria of Tables 5-1 to 5-3. However, the updated criteria lead to no changes from Reference 5-1. Plant S pulled tube R28C41 was deleted from the database of Reference 5-1 and would also be deleted by the more explicit criteria of this section. However, special considerations have been applied to this indication as described below.

Special Consideration for Plant S Pulled Tube R28C41

Plant S pulled tube R28C41 had leak rates exceeding the initial hot cell leak rate facility capacity at pressure differentials near SLB conditions. Test results are given in Table 5-7. Measured leak rates of 43.4 and 95.1 l/hr at 2335 and 2650 psid, respectively, exceeded facility capacity and are not valid measurements. At 1500 psid, a measured leak rate of 12.3 l/hr was within the facility capability (~ 25 l/hr) and represents a valid measurement. The facility capacity was increased and attempts to reach 2650 psid for a valid leak rate measurement (i.e., without hysteresis effects) were not successful as the leakage exceeded the

new facility capacity. At the first 2650 psi unsuccessful leak test, the cracks were plastically deformed such that succeeding tests below 2650 psi are not directly applicable due to the crack opening or hysteresis effect. As a consequence of not having an acceptable SLB leak rate measurement, this data point was not included in the EPRI leak rate database of Ref. 5-1.

This indication is given special consideration, per NRC request, because of the crack morphology for this indication. The crack face had a 5% ID ligament about 0.31" long separating throughwall cracks in an overall, near throughwall crack length of 0.67" and a total crack length of 0.80". Destructive examination results for the crack length versus depth are given in Table 5-8. The uncorroded ligaments where the crack depth is 95% (Ligaments 1 and 2) include the widest (0.013") ligament and tend to reinforce the remaining 5% wall thickness against tearing. Based on the increase in voltage after the tube pull, it is known that some ligaments were torn as a result of the tube pull. The initial leak rate was measured at 1500 psid. A pressurization to 2650 psi followed, but leak rates were too high to be measured in that facility. Leak rate tests performed in a facility with larger flow capacity can be used to estimate the effective through wall crack length and the leak rate at steam line break conditions. The method applied herein was developed by Paul Hernalsteen of Laborelec. The general methodology is based on the fact that the initial pressurization to 2650 results in a crack opening that has a significant plastic opening component. Subsequent measured leak rates, performed at lower pressure differentials, are affected by the plastic deformation which resulted from the pressurization to 2650 psid.

The evaluations described below are based on crack opening areas calculated by the CRACKFLO Code. SLB leak rates calculated for R28C41 by CRACKFLO are in very good agreement with results obtained by Hernalsteen using the LABOLEAK Code. Differences in crack openings calculated by the two codes are small.

The process used for the evaluation of the test results on the pulled tube included the following steps. These steps are summarized in Table 5-9 and use the test results from Table 5-7. For each step, the plastic and elastic crack opening widths are presented in Table 5-9 along with the crack lengths and leak rate.

1. Figure 5-2 shows CRACKFLO leak rates at the conditions of Test 1. Based on the measured leak rate for this test, 12.3 l/hr, a crack length of 0.38 inches is inferred. This length is greater than the 0.26 inch length of 100% depth (Table 5-8) determined assuming that ligaments 3 and 4 were torn during the tube pull. Thus, tearing of ligaments with modest throughwall crack extension was probable from the tube pulling operations.

2. The pressurization to 2650 psid (Test 3) is assumed to have introduced an irreversible minimum plastic opening in the existing crack. Using CRACKFLO, the plastic opening

area was calculated as a function of crack length. These results are presented in Figure 5-3, along with a curve fit ( ) the calculations. The curve fit was used to develop a modified version of CRACKFI) which maintains the minimum plastic opening resulting from the pressurization to 2650 psid and combines it with an additional elastic opening due to the pressure differential of subsequent tests.

3. Using the modified CRACKFLO code with plastic crack opening at 2650 psid, the leak rate as a function of crack length was determined for the conditions of Test 4, Table 5-7. The results are presented in Figure 5-4. The figure shows that a crack length of 0.42 inch is inferred from the measured leak rate of 79.8 l/hr. Some additional tearing of the ligaments and throughwall crack extension from the 2650 psid pressurization is suggested by the throughwall crack length increase from 0.38 to 0.42 inch between Tests 1 to 3 and Test 4.

4. The modified code, a 0.42 inch crack length and the conditions for Test 6 give a leak rate of 114 l/hr at 1615 psid. This is substantially less than the 448 l/hr measured for this test, suggesting significant tearing of the crack has occurred from thermal cycling and pressurization between Tests 4 and 6.

5. Destructive examination of the tube after a tube burst test indicated a crack length up to 0.67 inches was possible. Using this crack length, a leak rate of 375 l/hr is obtained for the conditions of Test 6. This value is reasonably close to the measured leak rate of 448 l/hr. For this calculation CRACKFLO was used since the plastic opening area, 2.0×10^{-3} inch, was greater than the 1.5×10^{-3} inch calculated to be present after the pressurization to 2650 psid. Thus it is expected that complete tearing of all ligaments and the 5% wall thickness occurred between Tests 4 and 6.

6. Using the desired steam line break conditions (2560 psid and 616 °F primary temperature) for the EPRI database, the as-pulled crack length of 0.38 inch (Step 1) is expected to have torn to 0.42 inch and a leak rate of 111 l/hr is calculated.

The estimated leak rate for Plant S tube R28C41 at SLB conditions (2560 psid) is therefore 111 l/hr. This result is reasonably consistent with Plant S tube R33C20, which was measured in the large capacity facility. Tube R33C20 had a throughwall corrosion length of 0.33", compared to the 0.26" continuous length for R28C41. Both indications likely had ligament tearing and crack extension from tube pulling and pressurization to 2560 psid. The measured leak rate for R33C20 at 2560 psid was 137 l/hr, compared to the estimate of 111 l/hr for R28C41.

Based on similar analyses using a few runs with the LABOLEAK code and analytical ratios of crack areas between 2650 and 1200 psid, Paul Hernalsteen of Laborelec estimated a

R28C41 throughwall crack length of 0.475 inch at 2650 psid and predicted a leak rate of 123 l/hr at 2560 psid. This result is in very good agreement with the CRACKFLO estimate of 111 l/hr.

To bound the CRACKFLO and LABOLEAK analyses, a SLB leak rate of 125 l/hr at 2560 psid is assigned to R28C41 for the EPRI database.

5.2 Database for ARC Correlations

No new data for 3/4 inch diameter tubing has been obtained since the preparation of Reference 5-1. The data of Reference 5-1 are updated for the present application based on the outlier evaluation of Section 5.1 above. Table 5-10 summarizes the data having burst pressure and leak rate tests. Table 5-11 summarizes the data for use in the probability of leak correlation.

5.3 NDE Uncertainties

For IPC applications, NDE uncertainties are required to support projections of EOC voltage distributions, SLB leak rates and SLB tube burst probabilities as discussed in Section 8.0. The database supporting NDE uncertainties is described in Reference 5-1, and NDE uncertainties for IPC/APC applications are given in the EPRI repair criteria report (Reference 5-2). From Reference 5-2, the NDE uncertainties are comprised of uncertainties due to the data acquisition technique, which is based on use of the probe wear standard, and due to analyst interpretation, which is sometimes called the analyst variability uncertainty.

The data acquisition (probe wear) uncertainty has a standard deviation of 7.0% about a mean of zero and has a cutoff at 15%, with implementation of the probe wear standard requiring probe replacement at 15% differences between new and worn probes. ASME standards cross-calibrated against the reference laboratory standard and the probe wear standard were implemented in the Braidwood-1 EOC-4 inspection.

The analyst interpretation (analyst variability) uncertainty has a standard deviation of 10.3% about a mean of zero. Typically, this uncertainty has a cutoff at 20% based on requiring resolution of analyst voltage calls differing by more than 20%. However, as of the February 8, 1994 meeting, the NRC has not accepted the 20% cutoff on the analyst interpretation uncertainty. Pending a further resolution of this issue with the NRC, the analyst interpretation uncertainty was applied for Braidwood-1 without a cutoff. For EOC voltage projections, separate distributions are applied for probe wear with a cutoff at 15% and the analyst interpretation with no cutoff.

5.4 References

5-1. "Steam Generator Tubing Outside Diameter Stress Corrosion Cracking at Tube Support Plates - Database for Alternate Repair Criteria, Volume 2: 3/4-Inch Diameter Tubing", NP-7480-L, Volume 2, October 1993.

5-2. "PWR Steam Generator Tube Repair Limits - Technical Support Document for Outside Diameter Stress Corrosion Cracking at Tube Support Plates", TR-100407, Revision 1, Draft Report, August 1993.

Table 5-1

Criteria 1a to 1e for Excluding Data from Correlations

Criterion 1a: Unacceptable Bobbin Voltage Measurement

- Excludes specimen from all applications
- Examples: Welded specimen extension influences voltage measurement, specimen damage prior to test completion

Criterion 1b: Unacceptable Burst Test

- Excludes specimen only from burst correlation
- Examples: Incomplete burst test (e.g. leak but not burst), test malfunction, burst inside TSP

Criterion 1c: Unacceptable Leak Test

- Excludes specimen from leak rate correlation and requires prob. of leak evaluation
- Examples: Leak rate exceeded facility capacity, test malfunction

Criterion 1d: Unacceptable Leak Data Due to Tube Pull Damage

- Excludes specimen from leak rate correlation and requires prob. of leak evaluation
- Requires analyses to demonstrate uncorroded ligament would not have torn at accident conditions
- Example ID ligament torn during tube pull as demonstrated by post-pull voltage and higher than expected leak rates at or below normal operating conditions. Structural analysis shows uncorroded ligament would not be expected to tear at accident conditions.

Criterion 1e: Unacceptable Data for Estimating Probability of Leak

- Prob. of leak (yes/no) cannot be confidently estimated from destructive exam crack morphology and leak test not performed
- Examples: Short TW corrosion cracks such as < 0.1" which normally do not leak at SLB conditions. No destructive exam data available for estimating prob. of leak

Table 5-2

Criteria 2a and 2b for Excluding Data from Correlations

Criterion 2a: Atypical Ligament Morphology

- Cracks having ≤ 2 uncorroded ligaments in shallow cracks < 60% maximum depth should be excluded from the database as having bobbin voltages significantly higher than the dominant database which shows more uncorroded ligaments in shallow cracks
  - Results in atypical voltages and associated specimens are excluded from all corr.
  - No 3/4" specimens are excluded from the database due to this criterion

Criterion 2b: Severe Degradation

- Exclude data points having bobbin voltages > 20 volts larger than next data point from correlations, as singular data points at the tail of distributions can have undue influence on regression correlation. In this case, there is insufficient data at comparable voltages to assess the prototypicality of the crack morphology and applicability to the database.
  - Results in atypical voltages and associated specimens are excluded from all corr.
  - Excludes 3/4" model boiler specimen 598-1 (64.9 volts) which is > 40 volts larger than the next highest voltage point (22 volts)

Table 5-3

Criterion 3 for Excluding Data from Correlations

Criterion 3: Suspected Test Error

- Data are excluded from only the SLB leak rate versus voltage correlation if either or both of the following criteria are satisfied

- Leak rates at SLB pressure differentials should be at least 10% higher than that measured at normal operating pressure differentials for free span leak tests

  - No 3/4" specimens are excluded from the database for this criterion

- For throughwall cracks with no ligaments, the measured leak rate should be within a factor of less than about 50 of the mean measured leak rate at the associated throughwall crack length

  - For 3/4" tubing, this criterion excludes model boiler specimen 598-3 (0.27" TW, 0.02 l/hr leak rate). The measured leak rate for this specimen with no remaining ligaments is more than a factor of 100 less than the mean measured leak rate for a 0.27" crack length

  - The most limiting specimen compared to this criteria retained in the database is model boiler specimen 604-2 (0.19"TW, 0.05 l/hr), for which the mean measured leak rate is about 0.2 to 0.3 l/hr

Table 5-4

Basis for Excluding Data from the 3/4" Burst Correlation

Tube	TSP	Basis for Excluding Indications from Tube Burst Correlation	Exclusion Category	EPRI* Report Section
Plant E-4				
R19C35	2	Burst inside TSP. Yields much higher burst pressure than free span burst tests of ARC data base.	1b	4.4
R45C54	2	Burst inside TSP	1b	
R47C66	2	Burst inside TSP	1b	
Plant S				
R28C41	1	Incomplete burst test - burst opening length less than macrocrack length (no tearing)	1b	2.5, 4.5
Plant R-1				
R7C71	3	Test recorder malfunction	1b	2.2, 4.3
R5C112	2,3	Incomplete burst test	1b	
R10C6	2,3	Incomplete burst test	1b	
R10C69	2,3	Incomplete burst test	1b	
R20C46	2,3	Incomplete burst test	1b	
R7C47	3	Incomplete burst test	1b	
Model Boiler Specimens				
591-3.		Unacceptable specimen preparation due to bobbin voltage influenced by cracks in model boiler Teflon spacer below TSP as well as cracking within TSP. This results in two bands of cracks.	1a	5.6
598-1		Bobbin voltage (64.93 volts) and three large throughwall indications not prototypic of field indications and single data point >20 volts unduly influences burst correlation	2b	5.6
593-4,595-4, 596-1, 597-4, 603-4, 604-4		These bobbin NDD specimens all burst at a welded joint made to extend the specimen length for burst testing and are not valid tests. These data have been excluded from the 3/4 inch data base discussed in the EPRI report.	1b	

* EPRI Report NP-7480-L, Vol. 2 (Reference 5-1)

Table 5-5

Basis for Excluding Data from the 3/4" Leak Rate Correlation

Tube	TSP	Basis for Excluding Indications from Leak Rate Correlation	Exclusion Category	EPRI* Report Section
Plant R-1				
R5C112	3	Max. corrosion depth of 97%. Remaining TW ligament torn during tube pull as indicated by post-pull voltage and leak at 500 psi. Analyses indicate ligament would not have torn at accident conditions.	1d	2.2, 4.3
Plant B-1				
R4C61	5	No leakage identifiable during pressure test above SLB conditions. Test accuracy not sufficient to conclude no leakage.	1e	2.2, 4.3
Model Boiler Specimens				
591-3		Unacceptable specimen preparation due to bobbin voltage influenced by cracks in model boiler Teflon spacer below TSP as well as cracking within TSP. This results in two bands of cracks.	1a	5.6
598-1		Bobbin voltage (64.93 volts) and three large throughwall indications not prototypic of field indications and single data point >20 volts unduly influences correlation.	2b	5.6
598-3		Specimen had no operating leakage and 0.02 l/hr at SLB conditions. Crack was found to be 0.27" TW with no ligaments for which leak rate of 5 to 20 l/hr would be expected, based on the mean of the measured data. It is concluded that crack became plugged by deposits or a measurement error was made.	3	

* EPRI Report NP-7480-L, Vol. 2 (Reference 5-1)

Table 5-6

Basis for Excluding Data from the 3/4" Prob. of Leak Correlation

Tube	TSP	Basis for Excluding Indications from Prob. of Leak Correlation	Exclusion Category	EPRI* Report Section
Plant R-1				
R7C47	2	No destructive exam data or burst test to estimate probability of leakage.	1e	4.3
R5C112	3	Max. corrosion depth of 97%. Remaining TW ligament torn during tube pull as indicated by post-pull voltage and leak at 500 psi. Analyses indicate ligament would not have torn at accident conditions.	1d	2.2, 4.3
Plant B-1				
R4C61	5	No leakage identifiable during pressure test above SLB conditions. Test accuracy not sufficient to conclude no leakage.	1e	2.2, 4.3
Model Boiler Specimens				
591-3		Unacceptable specimen preparation due to bobbin voltage influenced by cracks in model boiler Teflon spacer below TSP as well as cracking within TSP. This results in two bands of cracks.	1a	5.6
598-1		Bobbin voltage (64.93 volts) and three large throughwall indications not prototypic of field indications and single data point >20 volts unduly influences correlation	2b	5.6
* EPRI Report NP-7480-L, Vol. 2 (Reference 5-1)				

Table 5-7

Plant S R28C41 Leak Rate Tests

Test	Primary Conditions Temperature (°F)	Primary Conditions Pressure (psia)	Differential Pressure (psid)	Secondary Pressure (psia)	Leak Rate (l/hr)
Initial Series					
1	612	2000	1500	500	12.3
2		2650	2335	315	> 43 *
3		2850	2650	200	> 96 *
Second Series					
4	550	1930	1200	730	78.9
5	560	2375	1535	840	321
6	580	2550	1615	935	448
7	550	2500	1375	1125	478 **

* Leak rate exceeded facility capacity.

** Note increase in leak rate at low pressure differential which indiates additional deformation of crack opening.

Table 5-8

Plant S SG Tube Macrocrack Profile for R28C41

Tube, Location	Length vs. Depth (inch/% throughwall)	Ductile Ligament Location
R28C41, FDB	0.00 / 0	
	0.07 / 100	
	0.13 / 100	
	0.19 / 95 ←	Ligament 1, 0.013" wide
	0.25 / 95	
	0.32 / 95 ←	Ligament 2, 0.004" wide
	0.38 / 95	
	0.44 / 100	
	0.52 / 100 ←	Ligament 3, 0.007" wide
	0.60 / 100	
	0.70 / 100 ←	Ligament 4, 0.008" wide
	0.75 / 70	
	0.80 / 0	

Table 5-9

Evaluation Summary, R28C41 Tube Leak Rate Tests

Case	Crack Opening Plastic (x 10^{-3} in)	Crack Opening Elastic (x 10^{-3} in)	Crack Length (in.)	Leak Rate (l/hr)
Before Pressurizing to 2650 psi ΔP				
Step 1 Crack Length inferred from measured leak rate at ΔP=1502 psi	0.12	0.65	0.38	12.3*
After Pressurizing to 2650 psi ΔP				
Step 3 Crack Length inferred from measured leak rate at ΔP=1200 psi and 550 °F	1.5	0.65	0.42	79.8*
Step 4 Leak rate for a crack length of 0.42" at ΔP=1615 psi & 580 °F	1.5	0.86	0.42	114
		Measured leak rate		448*
Step 5 Crack Length = 0.67 in. at ΔP=1615 psi & 580°F assumed	2.0	2.6	0.67	375
Calculated Leak Rate at 2560 psi ΔP (Step 3 length of 0.42")				
Step 6 Leak rate for a crack length of 0.42" at ΔP=2560 psi & 616 °F	1.4	1.4	0.42	111

* Measured leak rates - see Table 5-7

Table 5-10

Burst Pressure and Leak Rate Data Base for 3/4 Inch Tubing

Plant	Row/Col or Specimen No.	TSP	Bobbin Volts	Bobbin Depth	RPC Volts	Destructive Exam Max. Depth	Destructive Exam Length (1)	SLB Leak (2) Rate (l/hr) 2560 psid	Adjusted Burst (3) Pressure (ksi)	Correlation (4) Application Leak Rate	Correlation (4) Application Burst
[redacted]											

e

Table 5-10
(continued)
Burst Pressure and Leak Rate Data Base for 3/4 inch Tubing

Plant	Row/Col or Specimen No.	TSP	Bobbin Volts	Bobbin Depth	RPC Volts	Destructive Exam Max. Depth	Destructive Exam Length (1)	SLB Leak (2) Rate (l/hr) 2560 psid	Adjusted Burst (3) Pressure (ksi)	Correlation (4) Application Leak Rate	Correlation (4) Application Burst
[redacted]											

Table 5-10
(continued)
Burst Pressure and Leak Rate Data Base for 3/4 Inch Tubing

Plant	Row/Col or Specimen No.	TSP	Bobbin Volts	Bobbin Depth	RPC Volts	Destructive Exam Max. Depth	Destructive Exam Length (1)	SLB Leak (2) Rate (l/hr) 2560 psid	Adjusted Burst (3) Pressure (ksi)	Correlation (4) Application Leak Rate	Correlation (4) Application Burst
[											] e

Table 5-11: Database for Probability of Leak for 3/4" Diameter Tubes					
Plant or Model Boiler Sample Number	Bobbin Amplitude (V)	Probability of Leak	Plant or Model Boiler Sample Number	Bobbin Amplitude (V)	Probability of Leak

e

Figure 5-1
Comparison of 3/4" Leak Test Data with CRACKFLO Predictions

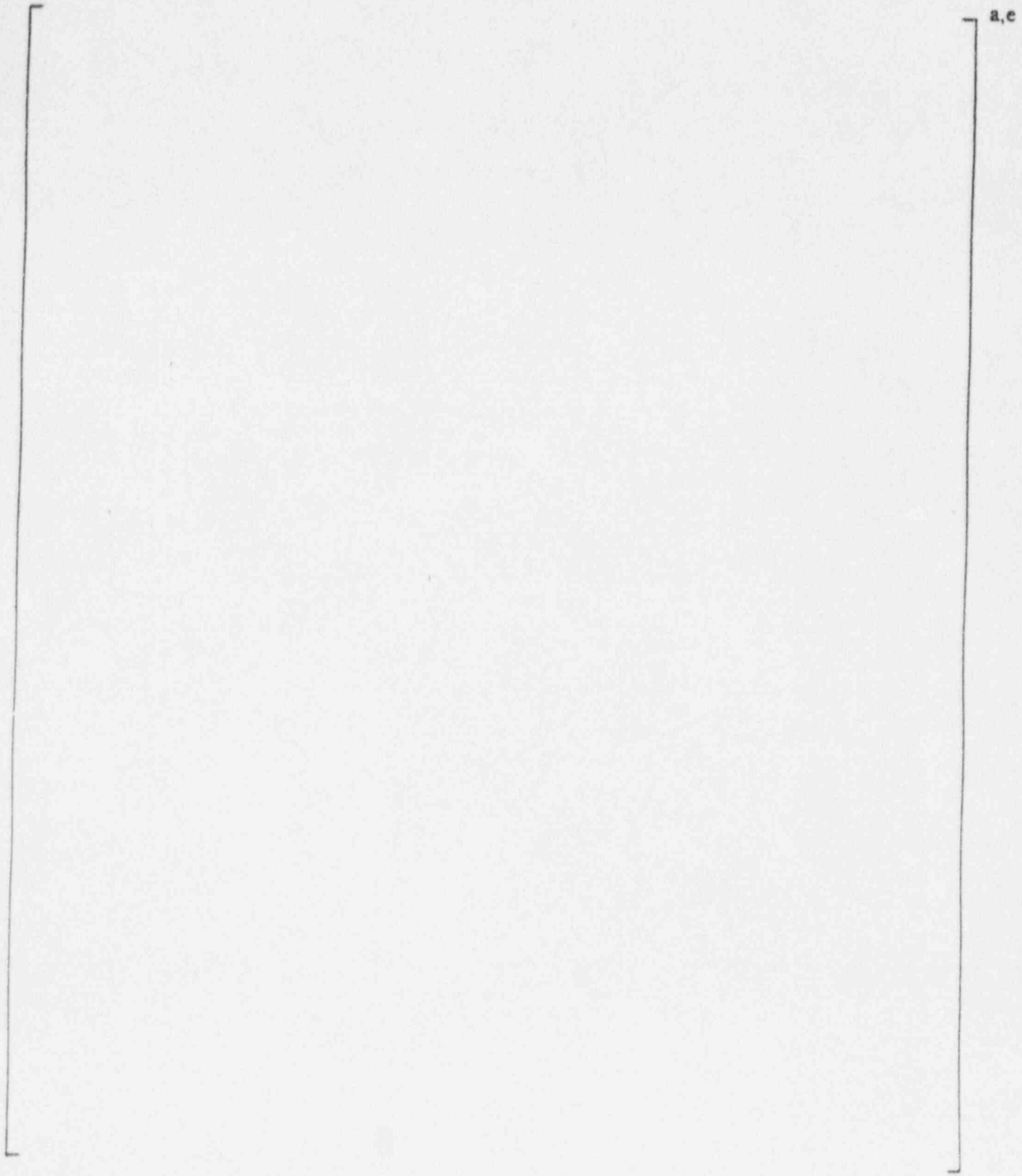

Figure 5-2

As Pulled Tube Leak Rate
1500 psi Pressure Drop

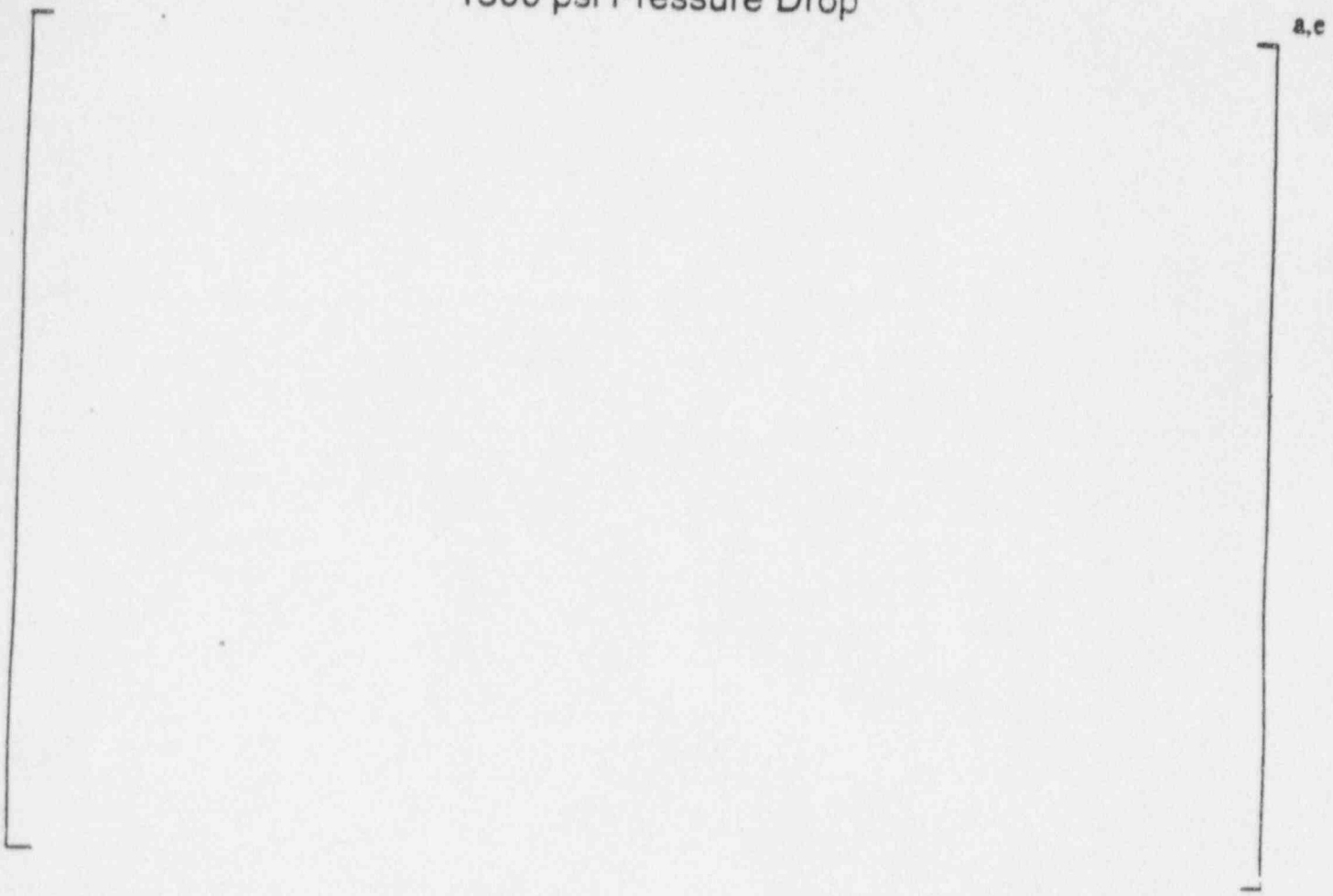

Figure 5-3

Plastic Correction Area
2650 psi Pressure Difference

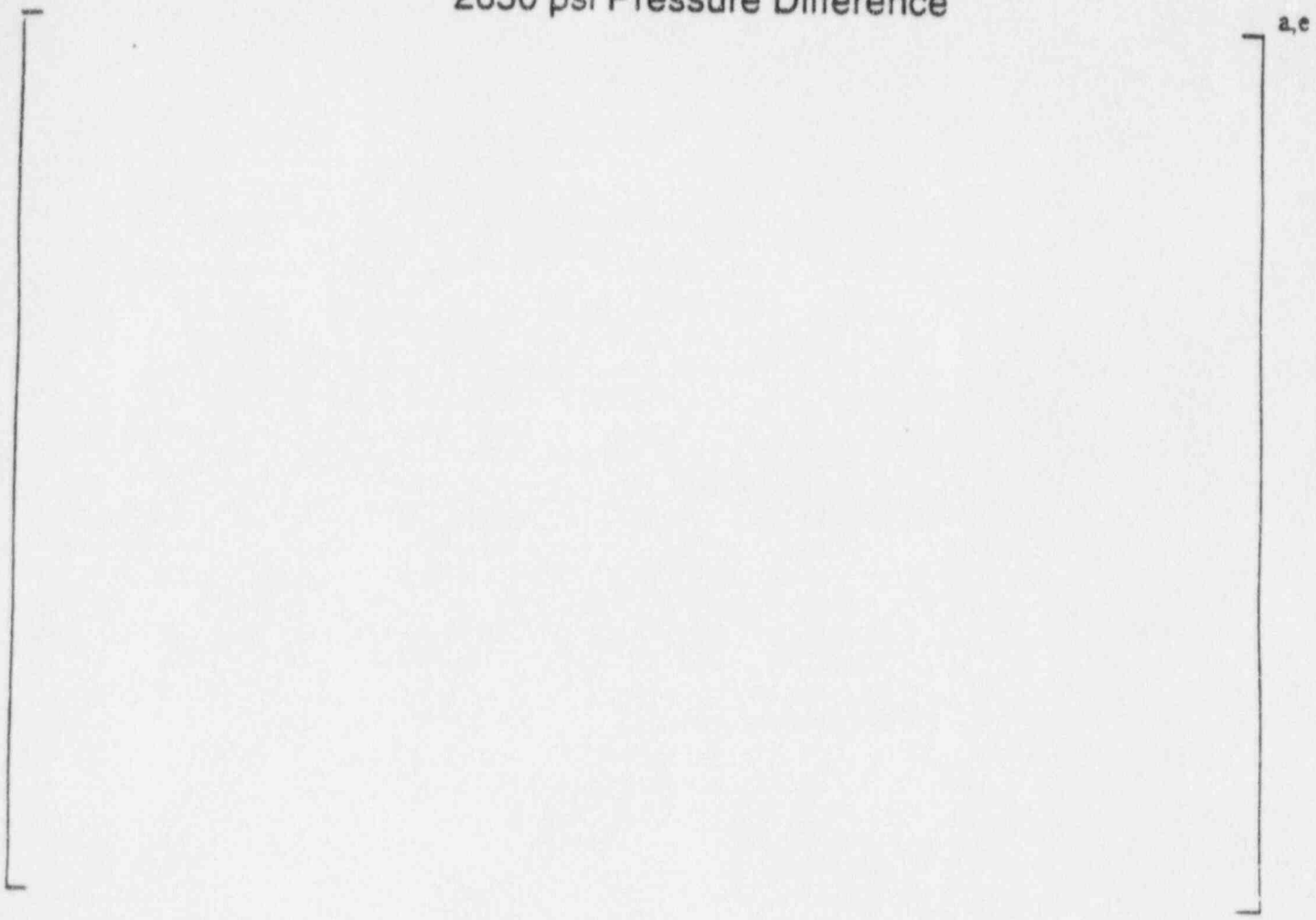

Figure 5-4

Modified Code Leak Rate
1200 psi Pressure Drop

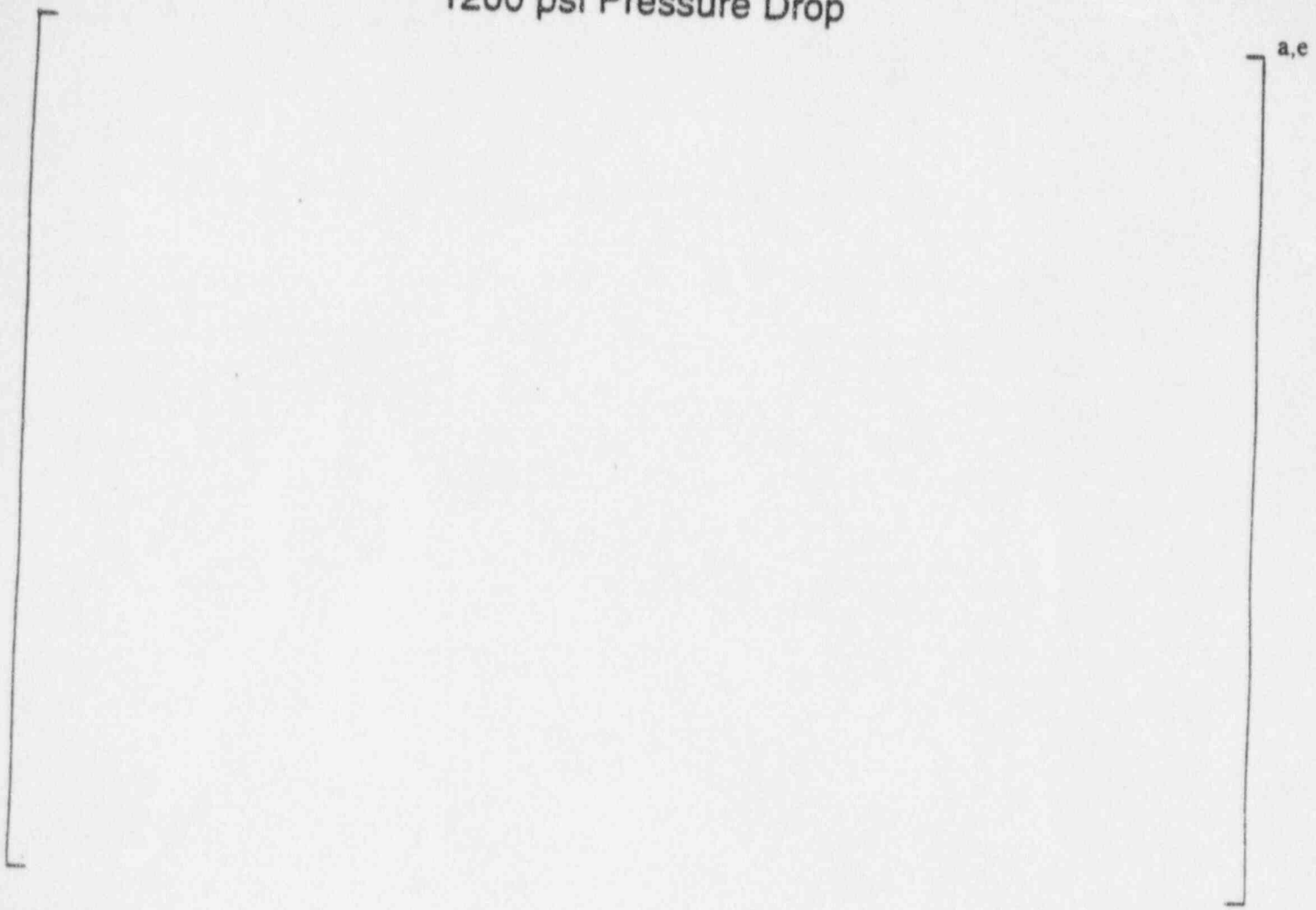

a,e

6.0 BURST AND SLB LEAK RATE CORRELATIONS

6.1 EPRI ARC Correlations

As part of the development of alternate repair criteria (ARC), correlations have been developed for tubes containing ODSCC indications at TSP locations between the bobbin amplitude, expressed in volts, of those indications and the free-span burst pressure, the probability of leak, and the free-span leak rate for indications that leak, References 6.1 and 6.2. The database used for the development of the correlations is presented and discussed in Reference 6.2. Guidelines for the identification and exclusion of inappropriate data, termed *outliers*, are provided in Reference 6.3. In addition to the aforementioned, an empirical correlation curve for the burst pressure as a function of crack length has been developed for tubes with free-span, through-wall, axial cracks. In 1993, the NRC issued draft NUREG-1477, Reference 6.4, for public comment. The draft NUREG delineated a set of guidelines for criteria to be met for the application of Interim Plugging Criteria (IPC) for ODSCC indications. The criteria guidelines permitted the use of, with adequate justification, a burst pressure to bobbin amplitude correlation and a probability of leak to bobbin amplitude correlation. The criteria guidelines did not permit the use of a leak rate to bobbin amplitude correlation for the estimation of end of cycle (EOC) total leak rates. In essence, References 6.1 and 6.2 provided comments on the Reference 6.4 guidelines. Reference 6.5 provided an NRC response and position relative to resolving the differences between References 6.1 & 6.2 and Reference 6.4, along with responses to other public comments. Of significance to this report, is that Reference 6.5 indicated that a correlation between leak rate and bobbin amplitude could be employed if the correlation could be statistically justified at a 95% confidence level, and provided direction for the development of guidelines, e.g., Reference 6.3, that could then be employed for the identification and exclusion of outlying experimental data. Subsequent discussions with NRC personnel have revealed potential issues associated with the manner in which the leak rate to bobbin amplitude correlation is used, thus, the potential leak rate during a postulated steam line break (SLB) is herein estimated by alternate Monte Carlo and deterministic methods to demonstrate that either method yields acceptable results.

The purpose of this section is to provide information and justification for all of the correlations developed in support of the application of an IPC for the Braidwood 1 nuclear power plant. Information is first presented relative to the correlation of burst pressure to bobbin amplitude and to through-wall crack length, followed by a discussion of the correlation between the probability of leak and the bobbin amplitude, and lastly a discussion of the correlation of leak rate to bobbin amplitude. The use of each of the correlations is also documented.

6.2 Burst Pressure versus Bobbin Voltage Correlation

The bobbin coil voltage amplitude and burst pressure data presented in the EPRI database report for 3/4" tubes, Reference 6.2, were used to estimate the degree of correlation between the burst pressure and bobbin voltage amplitude. The details of performing the correlation analysis, and subsequent regression analysis to estimate the parameters of a log-linear relationship between the burst pressure and the bobbin amplitude, are provided in the EPRI database report. The evaluations examined the scale factors for the coordinate system to be employed, the detection and treatment of outliers, the order of the regression equation, the potential for measurement errors in the variables, and the evaluation of the residuals following the development of a relation by least squares regression analysis. The results of the analyses indicated that an optimum linear, first order relation could be obtained from the regression of the burst pressure on the common logarithm (base 10) of the bobbin amplitude voltage.

A linear, first order equation relating the burst pressure to the logarithm of the bobbin amplitude was developed. Examination of the residuals from the regression analysis indicated that they are normally distributed, thus verifying the assumption of normality inherent in the use of least squares regression. The regression curve (line) is given by

$$\begin{aligned} P_{B_i} &= a_0 + a_1 \log(V_i) \\ &= 7.822 - 3.077 \log(V_i), \end{aligned} \tag{6.1}$$

where the burst pressure is measured in *ksi* and the bobbin amplitude is in *volts*. The *index of determination* for the regression was 80.7%, thus the correlation coefficient is 0.90, which is significant at a >99.999% level. This means that the *p-value* for the slope of the line is < 0.001%. The estimated standard deviation of the residuals, i.e., the error of the estimate, s_P, of the burst pressure was 0.95 ksi. A summary of the results from the regression analysis is provided in Table 6-1.

The data base and the regression curve are illustrated on Figure 6-1. Using the regression relationship, a lower 95% prediction bound for the burst pressure as a function of bobbin amplitude was developed. These values were further reduced to account for the lower 95%/95% tolerance bound for the Westinghouse data base of tubing material properties at 650°F. Both of these are also depicted on Figure 6-1. Using this reduced lower prediction bound, the bobbin amplitude corresponding to a *free-span* burst pressure of 3657 psi was found to be 4.54 V. The value of 3657 psi results from considering a SLB differential pressure of 2560 psi divided by 0.7 in accord with the guidelines of RG 1.121, Reference 6.6.

6.3 Burst Pressure versus Through-Wall Crack Length Correlation

For a tube with a mean radius of r_m and a thickness t, the normalized burst pressure as a function of the actual burst pressure, P_B, is given by

$$P_{bar} = \frac{P_B r_m}{(S_T + S_U)\, t} . \tag{6.2}$$

Thus, P_{bar} is the ratio of the maximum Tresca stress intensity, taking the average compressive stress in the tube to be $P_B/2$, to twice the flow strength of the material. The normalizing parameter for crack length, a, is given by

$$\lambda = \frac{a}{\sqrt{r_m t}} , \tag{6.3}$$

a form which arises in the theoretical solutions. The burst pressure as a function of axial crack length for a specific tube size is then easily obtained from the non-dimensionalized relationship.

Examination of the normalized burst pressure data indicated that a variety of functional forms would result in similar fit characteristics. An exponential function, i.e.,

$$P_{bar} = b_0 + b_1 e^{-\frac{\lambda}{b_2}} , \tag{6.4}$$

was finally selected based on the combination of maximizing the goodness of fit, and minimizing the number of coefficients in the function. Equation (6.4) was also found to be advantageous in that it can easily be inverted to yield λ as a function of P_{bar}. For the data analyzed, the coefficients of equation (6.4) were found to be

$$P_{bar} = 0.065 + 0.534\, e^{-\frac{\lambda}{3.611}} . \tag{6.5}$$

The index of determination for the fit was 99.3%, with a standard error of the estimate of 0.015. The F distribution statistic for the regression, the ratio of the mean square due to the regression to the mean square due to the residuals, was 4625. Thus, the fit of the equation to the data is excellent. Note that this does not mean that equation (6.4) is the true form of a

functional relationship between the two variables, only that it provides an excellent description of the relationship. Equation (6.4) was then rearranged to yield the inverse relation

$$\lambda = -3.611 \ln\left(\frac{P_{bar} - 0.0615}{0.534} \right), \tag{6.6}$$

for the normalized crack length as a function of normalized burst pressure.

In order to present the results in a form directly applicable to the Braidwood 1 tubes, the normalized relationships were converted for 0.750" diameter by 0.043" thick tubes having a flow stress of 71.6 ksi, the average of the Westinghouse database. The converted data base, the regression curve, and the regression curve adjusted for lower 95%/95% tolerance limit material properties are shown on Figure 6-2.

Using the regression results, the probability of burst during SLB was estimated as a function of crack length. The mean estimate of the burst pressure is given by the regression equation as

$$P_B = \frac{P_{bar}\, t}{R_m} \left(S_Y + S_U \right). \tag{6.7}$$

An unbiased estimate of the variance of P_B which accounts for the variation in P_{bar} about the regression curve and the variation in S_Y+S_U can be calculated as

$$\mathbf{V}(P_B) = \left(\frac{2\,t}{R_m} \right) \left[P_{bar}^2\, \mathbf{V}(S_f) + \bar{S}_f^2\, \mathbf{V}(P_{bar}) - \mathbf{V}(P_{bar})\, \mathbf{V}(S_f) \right], \tag{6.8}$$

where $\mathbf{V}$ is used to represent an unbiased estimate of the variance of the respective term in parentheses, and S_f, the flow stress for Alloy 600 material, is one-half of the sum of the yield and ultimate strengths. Taking the standard deviation of the burst pressure as the square root of the estimated variance allows for the estimation of the probability of burst using a Student's t-distribution. Specifically, the difference between the estimated burst pressure for a given crack length, a, and the SLB pressure is divided by the estimated standard deviation of the burst pressure to obtain a t-deviate. The probability of occurrence of the value of t is then an estimate of the probability of burst for that crack length during a SLB. The number of degrees of freedom used in estimating the probability of occurrence of a t-deviate greater than t is conservatively taken as the lesser of the number of degrees of freedom of P_{bar} or S_f. An alternate estimate of the probability of burst can be obtained by simulating P_{bar} and S_f independently. In this case, a large number of values of P_{bar} and S_f are independently

calculated using randomly generated independent t-variates and the respective estimated standard deviations of P_{bar} about the regression curve and S_f about the mean of the database. These are then combined using equation (6.7) to obtain a burst pressure for a single simulation. The number of occurrences of the calculated burst pressure being less than the SLB pressure is then an estimate of the probability of burst. Based on the specific simulation results, an upper bound for the estimate of the probability of burst may then be made using non-parametric methods. The results of the calculational and the Monte Carlo simulation determinations are depicted on Figure 6-3. Also shown are the 99% upper confidence bounds for the Monte Carlo estimated values. The calculational procedure is seen to lead to a conservative estimate of the probability of burst for a given crack length. An examination of the distribution of the burst pressures from the Monte Carlo simulations reveals that is skewed right. Thus, the tail of the distribution is shorter for the lower burst pressures, hence the lower probabilities of burst.

6.4 NRC Draft NUREG-1477 SLB Leak Rate POD and Uncertainty Methodology

The NRC methodology of draft NUREG-1477 obtains the number of indications that are to be considered as being returned to service, N, as:

$$N = N_d + N_{nd} - N_r = N_d + \frac{1 - \text{POD}}{\text{POD}} N_d - N_r = \frac{N_d}{\text{POD}} - N_r, \qquad (6.9)$$

where, N_d = number of detected bobbin indications
N_r = number of repaired indications
N_{nd} = number of indications not detected by the bobbin inspection
POD = probability of detection (0.6 for NRC methodology)

The above adjustments for POD have been incorporated in the BOC and EOC voltage distributions so that no further adjustments are required for the leakage calculation. Section 3.3 of draft NUREG-1477 states that the total leak rate, T, should be determined as:

$$T = \mu P + Z \sqrt{\sigma^2 P + \mu^2 P - \sum_i (N_i P_i^2)}, \qquad (6.10)$$

where, μ = mean of the leak rate data independent of voltage
σ = standard deviation of the leak rate data independent of voltage
P_i = probability that a tube leaks for the i^{th} voltage bin
N_i = number of indications (after POD adjustment) in the i^{th} voltage bin
P = $\Sigma(N_i P_i)$ = expected number of indications that leak summed over all voltage bins
Z = standard normal distribution deviate (establishes level of confidence on leakage)

For the total leakage, the first term of the above equation represents a mean expected leak rate while the square root term is an effective standard deviation for the total leakage based on the variance of the product of the probability of leak and the predicted leak rate. Draft NUREG-1477 recommends that Z be applied as 2, which corresponds to a level of confidence of 98%, while Reference 6.5 indicates that Z may be taken as 1.645, corresponding to a confidence level of 95%.

6.5 Probability of Leakage Correlations

Historically, the probability of leakage has been evaluated by segregating the model boiler and field data into two categories, i.e., specimens that would not leak during a SLB and those that would leak during a SLB. These data were analyzed to fit a sigmoid type equation to establish an algebraic relationship between the bobbin amplitude and the probability of leak. The specific algebraic form used to date has been the logistic function with the common logarithm of the bobbin amplitude employed as the regressor variable, i.e., letting P be the probability of leak, and considering a logarithmic scale for volts, V, the logistic expression is:

$$P(leak \mid V) = \frac{1}{1 + e^{-[\beta_1 + \beta_2 \log(V)]}} \tag{6.11}$$

This is then rearranged as:

$$\ln\left(\frac{P}{1-P}\right) = \beta_1 + \beta_2 \log(V), \tag{6.12}$$

to permit an iterative, linear, least squares regression to be performed to find the maximum likelihood estimators, b_1 and b_2, of the coefficients, β_1 and β_2.

Reviews of those evaluations, e.g., NUREG-1477, have resulted in the NRC requesting that alternate sigmoid function forms be investigated, and that the evaluations also consider the potential dependence to be on the bobbin amplitude instead of the logarithm of the bobbin amplitude. NUREG-1477 specifically mentions that the cumulative normal, or Gaussian, distribution function and the Cauchy distribution function be investigated. Discussions with NRC personnel led to the stipulation that these functions be analyzed and used in predicting the end-of-cycle leak rate for the Braidwood 1 plant steam generator tube indications. Reference 6.7 has acknowledged that any non-conservatism associated with the exclusive use of the log-logistic function would be expected to be small in comparison to the conservatism inherent in the methodology used to estimate the radiological consequences of leakage associated with a postulated SLB. On this basis, the evaluation and results presented herein for alternative function forms is considered to be for information only.

The use of the logistic function for the analysis of dichotomous data is standard in many fields. The differential form assumes that the rate of change of the probability of leak is proportional to the product of the probability of leak and the probability of no leak. As noted, the function is sigmoidal in shape, and is similar to the cumulative normal function, and likewise similar to using a probit model (which is a normal function with the deviate axis shifted to avoid dealing with negative values). In principle, any distribution function that has a cumulative area of unity could be fit as the distribution function, a limitless number of possibilities. Trying to identify a latent, or physically based, distribution for the probability of leak would be considered to be unrealistic and unnecessary. For most purposes the logistic and normal functions will agree closely over the mid-range of the data being fitted. The tails of the distributions do not agree as well, with the normal function approaching the limiting probabilities of 0 and 1 more rapidly than the logistic function. Thus, relative to the use of the normal distribution, the use of the logistic function is conservative. Given its wide acceptance in multiple fields it was judged that the logistic function would be suitable for use in determining a probability of leak as a function of voltage.

In addition, consideration was given as to whether the bobbin amplitude or the logarithm of the bobbin amplitude should be used. Since the logistic, normal and Cauchy distribution functions are unbounded, the use of volts would result in a finite probability of leak from non-degraded tubes, and would be zero only for $V=-\infty$. By contrast, the use of the logarithm of the voltage results in a probability of leak for non-degraded tubes of zero. Clearly, the second situation is more realistic than the first, especially in light of the fact that a voltage threshold is a likely possibility. To comply with the NRC request, however, each distribution function was fitted to the data using the logarithm of the bobbin amplitude and the bobbin amplitude as the regressor.

The three functions to be evaluated fall into a category of models referred to as *Generalized Linear Models* (GLMs). This simply means that the models can be transformed into a linear form, e.g., equation (6.12). The left side of equation (6.12) is referred to as the link function for the logistic model. For the normal or cumulative Gaussian distribution function, the model to be fitted is:

$$P(leak) = \frac{1}{\sqrt{2\pi}} \int_{-\infty}^{\beta_1 + \beta_2 \log(V)} e^{-\frac{z^2}{2}} dz, \tag{6.13}$$

and the model to be fitted for the Cauchy distribution function is:

$$P(leak) = \frac{1}{2} + \frac{1}{\pi} \tan^{-1}\left[\beta_1 + \beta_2 \log(V)\right]. \tag{6.14}$$

The link function for the Gaussian function is:

$$\eta = \Phi^{-1}(P) = \beta_1 + \beta_2 \log(V), \tag{6.15}$$

while the link function for the Cauchy function is:

$$\eta = \tan\left[\pi\left(P - \frac{1}{2}\right)\right] = \beta_1 + \beta_2 \log(V). \tag{6.16}$$

To fit the equation forms to the bobbin amplitude rather than log of the amplitude, V is substituted for $\log(V)$. Each equation was fitted to the data using an iterative least squares technique, which results in the maximum likelihood estimates of the parameters.

The results of all of the regression analyses are summarized in Table 6-2. The coefficients of the equations are provided along with the elements of the variance-covariance matrix for the coefficients. In addition, the deviance for each solution is also given. One accepted measure of the goodness of the solution or fit for GLMs is the deviance, given by,

$$D = 2\sum_{i=1}^{n}\left\{P_i \ln\left[\frac{P_i}{P(V_i)}\right] + (1 - P_i)\ln\left[\frac{1 - P_i}{1 - P(V_i)}\right]\right\}. \tag{6.17}$$

where P_i is the probability associated with data pair i and $P(V_i)$ is the calculated probability from V_i. The deviance is used similar to the residual sum of squares in linear regression analysis and is equal to the error, or residual, sum of squares (SSE) for linear regression. For the probability of leak evaluation P_i is either zero or one, so Equation (6.17) may be written

$$D = -2\sum_{i=1}^{n}\left\{P_i \ln[P(v_i)] + (1 - P_i)\ln[1 - P(v_i)]\right\}. \tag{6.18}$$

Since the deviance is similar to the SSE, lower values indicate a better fit, i.e., the lower the residual sum of squares the more of the variation of the data is considered to be explained by the regression equation. The smallest deviances, 28.9, were obtained from the logistic and normal function fits. The deviances for the remaining four functions ranged from 32.5 to 33.8, about 12% to 17% higher than for the first two functions. For similar calculations performed using 7/8" tube data, the deviances obtained using either of the Cauchy forms were about 15% to 20% higher than for the other four functions. These differences are not considered to be numerically significant in themselves relative to selecting the best form of a fitting function.

The results of fitting each of the equations are depicted on Figures 6-4 and 6-5. A comparison of the results shown on Figure 6-4 with those shown on Figure 6-5 indicates that the use of the logarithm of the volts results in a spreading of the functions with the probability of leak at, say, 3 volts being higher for the logarithmic forms. In the very low voltage range, less than 1 volt, the probability of leak is lower for the logarithmic forms. This is because the tails must extend to $-\infty$. In general, the Cauchy cumulative distribution function has longer tails than either the logistic or normal functions. It also rises much more sharply in the middle of the data range. The regression results on Figure 6-2 illustrate the non-realistic nature of the Cauchy fit for the non-logarithmic form, in spite of its similar deviance value. Examination of the figures indicates that the Cauchy distribution is significantly less representative of the data in the regions where the no-leak and leak test data overlap.

A listing of probability of leak results for selected volts is provided in Table 6-3. Up to a bobbin amplitude of 1 volt, predictions based on the log-normal function are less than predictions based on the log-logistic function. For very high voltages the Cauchy distribution forms rise to a probability of leak of one slower than the other distribution functions.

Taken in conjunction with the leak rate versus voltage correlation, the choice of a probability of leak function is relatively moot. The final total leak rate values tend to differ by only a few percent across the spectrum of POL functions.

6.6 SLB Leak Rate Versus Voltage Correlation for 3/4" Tubes

The bobbin coil and leakage data previously reported were used to determine a correlation function between the SLB leak rate and the bobbin amplitude voltage. Since the bobbin amplitude and the leak rate would be expected to be functions of the crack morphology, it is to be expected that a correlation between these variables would exist. Previous plots of the data on linear and logarithmic scales indicated that a linear relationship between the logarithm of the leak rate and the logarithm of the bobbin amplitude would be an appropriate choice for establishing a correlating function via least squares regression analysis. Thus, the functional form of the correlation is

$$\log(Q) = b_3 + b_4 \log(V), \tag{6.19}$$

where Q is the leak rate, V is the bobbin voltage, and b_3 and b_4 are estimates obtained from the data of some coefficients, β_3 and β_4. The final selection of the form of the variable scales, i.e., log-log, was based on performing least squares regression analysis on each possible combination and examining the square of the correlation coefficient for each case. The largest index of determination, 58.2%, was found for the $\log(Q)$ on $\log(V)$ regression. The second largest index, for Q on V, was found to be on the order of 24%, clearly indicating the appropriate choice of scales to be log-log.

A summary of the results of the regression analysis is provided in Table 6-4, and illustrated on Figure 6-6. The number of data points used for the above evaluations was 40 and the number of degrees of freedom (dof) 38. The obtained value of r^2 of 58.2% is significant at a level of >99.99999% based on an F distribution test of the ratio of the mean square of the regression to the mean square of the error. This can also be interpreted as the probability that the log of the leak rate is correlated to the log of the bobbin amplitude. An alternate interpretation is that if the variables are really uncorrelated and the testing was repeated many times, an index of determination equal to or greater than that obtained from the analyzed data would be expected to occur randomly in only <0.000001% of those tests. The conclusion to be drawn from these results is that it is very likely that the variables are correlated.

At the February 8, 1994, meeting between the NRC, EPRI, and NUMARC, information was presented by the NRC that the "use of linear regression is acceptable if shown to be valid at a 5% level with [a] p-value test." The *p-value* is the conditional probability of observing a computed statistic, e.g., the F distribution value reported above, as large or larger than the observed value, under the condition that there is no relationship. In this case, a small p-value is evidence supporting the hypothesis that there is a correlation between $\log(Q)$ and $\log(V)$. The p-values for the estimated parameters of Equation (6.19) are also given in Table 6-4. For the slope of the regression equation, the conditional probability that the slope is zero is <0.000001%. The conditional probability that the intercept is zero is 0.01%. The validity of the regression is judged by the p-value associated with the slope. Since this is significantly less than the 5% value stipulated above the regression is concluded to be valid, and the use of linear regression is acceptable.

The expected, or arithmetic average (AA), leak rate, Q, corresponding to a voltage level, V, was also determined from the above expressions. Since the regression was performed as $\log(Q)$ on $\log(V)$ the regression line represents the mean of $\log(Q)$ as a function of bobbin amplitude. This is not the mean of Q as a function of V. The residuals of $\log(Q)$ are expected to be normally distributed about the regression line. Thus, the median and mode of the $\log(Q)$ residuals are also estimated by the regression line. However, Q is then expected to be distributed about the regression line as a log-normal distribution. The regression line still estimates the median of Q, but the mode and mean are displaced. The corresponding adjustment to the normal distribution to obtain the AA of Q for a log-normal distribution is

$$Q = E\{Q \mid V\} = 10^{b_0 + b_1 \log(V) + \frac{\ln(10)}{2}\sigma^2}, \tag{6.20}$$

for a given V, where σ^2 is the estimated variance of $\log(Q)$ about the regression line. The variance of the expected leak rate about the regression mean is then obtained from

$$\mathrm{Var}(Q) = Q^2\left[e^{\ln(10)\sigma^2} - 1\right]. \tag{6.21}$$

To complete the analysis for the leak rate, the expected leak rate as a function of log(V) was determined by multiplying the AA leak rate by the probability of leak as a function of log(V). The results of this calculation are also depicted on Figure 6-6 for a steam line break differential pressure of 2560 psi.

6.6.1 Analysis of Regression Residuals

As previously noted, the correlation coefficients obtained from the analyses indicate that the log-log regressions at the various SLB ΔPs are significant at a level greater than 99.8%. Additional verification of the appropriateness of the regression was obtained by analyzing the regression residuals, i.e., the actual variable value minus the predicted variable value from the regression equation. A plot of the log(Q) residuals as a function of the predicted log(Q) was found to be nondescript, indicating no apparent correlation between the residuals and the predicted values. A cumulative probability plot of the residuals on normal probability paper approximated a straight line, thus verifying the assumption inherent in the regression analysis that the residuals are normally distributed. Given the results of the residuals scatter plots and the normal probability plots, it is considered that the regression curve and statistics can be used for the prediction of leak rate as a function of bobbin amplitude, and for the establishment of statistical inference bounds.

6.7 SLB Leak Rate Analysis Methodology

The leak rate versus voltage correlation can be simulated in conjunction with the EOC voltage distributions obtained by Monte Carlo methods, or by applying the POL and leak rate correlations to the EOC voltage distribution obtained by Monte Carlo methods as applied for the draft NUREG methodology. This second approach is a hybrid that joins Monte Carlo and deterministic calculations. Parallel analyses verified that the full Monte Carlo leak rates and the direct application of the correlations to the EOC voltage distribution yield essentially the same results. Thus, it is adequate to apply the correlations to the EOC voltage distributions.

The determination of the end of cycle leak rate estimate proceeds as follows. The beginning of cycle voltages are estimated using the methodology provided in draft NUREG-1477. The distribution of indications is binned in 0.1V increments. The number of indications in each bin is divided by 0.6 to account for POD. The resulting number of indications in each bin is reduced by the number of indications plugged in each bin. The final result is the beginning of cycle distribution used for the Monte Carlo simulations. The NDE uncertainty and growth rate distributions are then independently sampled to estimate an end of cycle distribution, also reported in bins of 0.1V increment. Given the EOC voltage distribution the calculational steps to obtain an estimate of the total leak rate are as follows:

(1) For each voltage bin, the leak rate versus bobbin amplitude correlation is used to estimate an expected, or average, leak rate for indications in that bin.

(2) The probability of leakage correlation is then used to estimate the mean probability of leak for the indications in each bin.

(3) The relationships derived in Appendix C of draft NUREG-1477 for the variance of the product of the probability of leak with the leak rate and for the total leak rate are then used to estimate the expected total leakage and variance for the sum of the indications in each bin as a function of the correlation means and estimated variances for the leak rate and probability of leak.

To account for the variances of the coefficients of the regression equation for the leak rate, the σ used in equations (6.20) and (6.21) is that from the predictive distribution for the logarithm of the leak rate as a function of bobbin amplitude, i.e., for each voltage, V_i, an effective standard deviation of the regression error, σ_i, is calculated as

$$\sigma_i = \sigma_e \sqrt{1 + \frac{1}{N} + \frac{\left[\log(V_i) - \overline{\log(V)}\right]^2}{\sum_j \left[\log(V_j) - \overline{\log(V)}\right]^2}}, \qquad (6.22)$$

where N is the number of data pairs in the regression analysis, and σ_e is an unbiased estimate of σ. The expected total leak rate from all of the indications in all of the bins is

$$T = \sum_{i=1}^{N_B} \frac{n_i}{1 + e^{-[b_1 + b_2 \log(V_i)]}} 10^{b_1 + b_2 \log(V_i) + \frac{\ln(10)}{2}\sigma_i^2}, \qquad (6.23)$$

where N_B is the number of bins, and n_i is the number of indications in the bin with bobbin amplitude V_i. Thus, the expected total leakage for the entire distribution is obtained as the sum of the expected leak rates for each bin.

In order to estimate an upper confidence bound for the total leak rate an expression is needed for the variance of the total leak rate. There are two sources of variance to be considered, the variance about the predicted expected value and the variance of the predicted expected value; the estimated total variance about the predicted expected value being the sum of the two. The variance of the total leak rate about the predicted expected value is

$$\mathbf{V}(T) = \sum_{i=1}^{N_B} n_i \left\{ P_i Q_i^2 \left[e^{\ln(10)\sigma_i^2} - 1 \right] + Q_i^2 P_i (1 - P_i) \right\}, \qquad (6.24)$$

where P_i is the probability of leak from equation (6.11). As noted, an additional variance term is added in order to estimate the contribution to the variance from the correlation between the

individual leak rates, i.e., from the covariance, which arises as a consequence of using the regression equations. Thus, the second term accounts for the variances of the positions of the regression equations. A linearized approximation (via Taylor's Theorem) of the variance of the mean of the regression prediction, T_μ, is given by

$$\mathbf{V}(T_\mu) = \sum_{i=1}^{N_s} n_i \left\{ \frac{dT}{d\beta_j} \right\}_i^T \begin{bmatrix} [Cov(\beta_1, \beta_2)] & 0 & 0 \\ 0 & [Cov(\beta_3, \beta_4)] & 0 \\ 0 & 0 & \mathbf{V}(\sigma_i^2) \end{bmatrix} \left\{ \frac{dT}{d\beta_j} \right\}_i , \qquad (6.25)$$

where the derivative of the total leak rate vector contains five elements for j=1,...,5, and the *Covariance Matrix* is a square 5x5 matrix consisting of the estimated variances and covariances of the estimated individual regression coefficients and σ_i. Note that here $[Cov(\beta_1, \beta_2)]$ and $[Cov(\beta_3, \beta_4)]$ are each 2x2 matrices, where the β's are estimated by b_1 through b_4, and recall that σ_i is an estimate of β_5. The variance of the variance is estimated as

$$\mathbf{V}(\sigma_i^2) = \frac{2\sigma_i^4}{n-2} , \qquad (6.26)$$

where n is the number of data pairs used in the leak rate regression analysis. The standard deviation of the total leak rate is then taken as the square root of the variance of the total leak rate. The upper bound 95% confidence limit on the total leak rate is then obtained as the expected total leak rate plus 1.645 times the standard deviation of the total leak rate. The results obtained with this approach have been compared to results obtained from the Monte Carlo simulation without significant differences being observed. For a calculation utilizing only equation (6.24), the total leak rate from SG "D" at the EOC is estimated to be 3.0 GPM. By including the variance from equation (6.25), the estimated total leak rate was estimated to be 3.1 GPM. The value obtained from the Monte Carlo simulation of the total leak rate was 3.2 GPM, as described in Section 6.8.1 below. Thus, for the distribution analyzed, the contribution of terms associated with the covariance, i.e., the uncertainty of the prediction of the mean total expected leak rate, is small (being on the order of 3%) when compared to the variance of the total leak rate about the mean value. The results obtained provide independent verification of the Monte Carlo and hybrid techniques.

6.8 Simulation of Equation Parameter Uncertainties

The estimated, total end of cycle leak rate can also be calculated using Monte Carlo techniques, e.g., the method documented in the EPRI ODSCC report (TR-10047, Rev. 1). In the Monte Carlo analysis the variation in the parameters, i.e., coefficients, and the variation of the dependent variable about the regression line is simulated. A 95% confidence bound on the total leak rate from SG "D" of Braidwood 1 was calculated using a Monte Carlo simulation to

verify the results from the deterministic analysis. The approach used for the simulation is different from that discussed in the EPRI ODSCC report. While both methods simulate the variation of each parameter of the correlation equations, the method discussed herein also simulated the effect of the covariance of the individual indication leak rates. Each of the methods is discussed herein in order to provide clarification regarding their use. In order to simplify the discussion of the Monte Carlo techniques, different nomenclature is used from that of the previous section, i.e., Q_i is used to represent the common logarithm of the leak rate, and V_i is used to represent the common logarithm of the bobbin amplitude. Thus, the following model is used to describe a working relationship between the logarithm of the leak rate and the logarithm of the bobbin amplitude,

$$Q_i = b_3 + b_4 V_i + \varepsilon , \tag{6.27}$$

where ε is the estimated error of the residuals, assumed to be from a population that has a zero mean, and a variance that is not dependent on the magnitude of V_i. The coefficients, b_3 and b_4 are the estimates from the regression analysis of some true coefficients, β_3 and β_4, representing the intercept and slope of the equation, respectively.

6.8.1 Monte Carlo Simulation of the Total Leak Rate for Braidwood 1

The method used by Westinghouse for simulating the total leak rate is the outcome of a series of technical discussions held with the NRC. The method differs from that reported in prior WCAP reports, wherein the predictive distribution was simulated and covariance terms were ignored. It is noted that, although both methods yielded similar results (within ~3%) for Braidwood 1, the method described herein is more statistically accurate. This small difference in the total leak rate results is because the contribution of the covariance terms relative to the variance terms is relatively small for the correlations used herein. In summary, random versions of the POL and leak rate correlations are generated and used to calculate the sum of the leak rates for all of the indications in a SG to obtain a single simulated value of the total leak rate. This process is repeated to obtain a distribution of the total leak rate from 10,000 simulations of the correlation equations. A non-parametric 95% confidence bound on the total leak rate is then estimated from the distribution of total leak rates.

At the start of each SG simulation, i.e., the calculation of a single total leak rate, a random value for the *standard deviation of the errors for the population* is calculated from the χ^2 distribution, the degrees of freedom from the data, and the standard deviation of the regression errors. This is used to calculate random values for the parameters of the regression equation, which remain constant for the entire SG simulation. The variation of the regression predictions are accounted for by randomly estimating the POL from a uniform distribution, and by adding the product of a random normal deviate and the standard deviation of the errors for the population to the predicted logarithm of the leak rate, for each individual indication in the SG

distribution. The total leak rate for the SG simulation is calculated as the sum of the leak rates from all of the indications in the SG. The expression for the total leak rate is

$$T = \sum_{i=1}^{N} R_i(\beta_1, \beta_2)\, Q_i(\beta_3, \beta_4, \beta_5), \tag{6.28}$$

where N = the total number of indications in the SG at EOC,
$R_i(\beta_1, \beta_2)$ = 0 or 1 is the POL from a single indication, i, in a tube,
$Q_i(\beta_3, \beta_4, \beta_5)$ = is the conditional leak rate of indication i, i.e., the leak rate if the indication is leaking,
β_1, β_2 = the coefficients of the POL equation,
β_3, β_4 = the coefficients of the leak rate versus bobbin amplitude equation, and
β_5 = the standard error of the log of the leak rate about the correlation line, also referred to herein as σ.

To simulate the total leak rate from all of the indications in the generator, random coefficients for the probability of leak, POL, and leak rate correlation equations are generated, and then those coefficients are used to simulate the POL and leak rate for each indication. The POL, R_i, for each indication, i, is simulated as,

$$R_i(\beta) = \begin{cases} 1 & \text{if } U_i < logit\left(\beta_1 + \beta_2 \log(V_i)\right) \\ 0 & \text{otherwise} \end{cases}, \tag{6.29}$$

where U_i is an independent draw from a uniform distribution. The step of determining an integer value for the POL accounts for the variation of the distribution of probabilities about the log-logistic regression line. Discussion of the generation of β_1 and β_2 is left until after the discussion of the coefficients for the leak rate equation.

Leak Rate versus Bobbin Amplitude Simulation

To simulate the leak rate from the regression line, random coefficients β_3 and β_4 must be simulated. Each of these has a variance that is dependent on the variance of the error of the log of the leak rate about the regression line. Thus, the first step is to simulate a random error variance by picking a random χ^2 deviate for n-2 degrees of freedom and then calculating a random error variance, σ^2, for the correlation equation from the regression error variance as

$$\sigma^2 = \frac{(n-2)}{\chi^2_{(n-2),\,random}}\,\hat{\sigma}^2 = f_\chi\,\hat{\sigma}^2, \tag{6.30}$$

where n is the number of data pairs used to calculate the regression coefficients, and f_V is defined by equation (6.30). This is now one possible variance for the *population* of log-leak rates about a correlation equation. Thus, it is appropriate to use the normal distribution to obtain random values for the parameters of the correlation equation. The distribution of β_3 and β_4 will be bivariate normal. Since they are correlated, although each is normally distributed marginally, they are not free to vary independently. If a value for the slope is determined first, then the distribution of the intercept values will be conditional on that value of the slope. The degree of correlation is indicated by the off-diagonal entry in the parameter covariance matrix calculated from the regression analysis. The entries of the covariance matrix of the parameters, V_{11}, V_{12}, and V_{22}, for the correlation equation to be used for a SG simulation are obtained from the corresponding estimated matrix obtained from the regression analysis as

$$V_{ij} = f_V \hat{V}_{ij}, \tag{6.31}$$

where the caret, "^", indicates an estimate from the regression data. A bivariate normal intercept for the simulation correlation is then calculated from the regression equation intercept as

$$\beta_3 = b_3 + Z_1 \sqrt{V_{11}}, \tag{6.32}$$

and the bivariate normal slope is calculated from the regression slope as

$$\beta_4 = b_4 + Z_1 \frac{V_{12}}{\sqrt{V_{11}}} + Z_2 \sqrt{V_{22} - \frac{V_{21}^2}{V_{11}}}, \tag{6.33}$$

where Z_1 and Z_2 are random univariate normal deviates, i.e., from a population with a mean of zero and a variance of one. We now have β_3, β_4, and σ for use in simulating all of the leak rates from each of the indications in the SG for one simulation of the total leak rate. For each simulation of an individual indication, i, the leak rate will be

$$Q_i(\beta) = 10^{\beta_3 + \beta_4 \log(V_i) + \beta_5 Z_i}, \tag{6.34}$$

with Z_i representing the i^{th} value from N independent draws from a standard normal distribution. Once the probabilities of leak have been calculated, the total leak rate for one simulation is then calculated using equation (6.28). It is noted that each simulation of T requires the generation of one β vector, N binomial variates R_i, and a maximum of N log-normal variates Q_i. In practice, a value for the leak rate only needs to be generated for each indication that is leaking, i.e., when $R_i = 1$.

Probability of Leak Simulation

The generation of the coefficients of the POL relation to be used in the simulation of the total leak rate proceeds in the same manner as for the coefficients of the leak rate relation. The elements of the covariance matrix are obtained from the GLM regression analysis and used with the estimated coefficients in equations like (6.32) and (6.33) to obtain β_1 and β_2 for a random population POL equation. However, for the simulation of the POL, there is no term of the form $Z_i\sigma$ in the simulation of the total leak rate. This exception is due to the fact that the data are binary. In effect, this additional term is being simulated through the use of the random sampling to determine if R_i is 0 or 1 in equation (6.29).

It is noted that the elements of the covariance matrix obtained from the GLM regression are scaled to a mean square error (mse) of 1. This is because the mse for the binary variables is asymptotically 1. A check of this assumption can be made by calculating an estimate of the square root of the mse from the regression results as

$$\hat{\sigma} = \sqrt{\frac{1}{n-2}\sum_i \frac{(y_i-\mu_i)^2}{\mu_i(1-\mu_i)}}, \qquad (6.35)$$

where the y_i's are the observed probabilities of leak, either zero or one, from the leak and burst testing, and the μ_i's are the calculated probabilities of leak from the *logistic* regression equation. A significant departure from 1 for this quantity could be indicative of an inadequate model. For the simulation of the POL data for 3/4" tubes the root mse was found to be 1.1. This is not significantly different from 1.

A 95% confidence bound on the total leak rate from SG "D" at the end of the fuel cycle was found to be 3.2 GPM. This is in very close agreement with the value found using the deterministic estimate.

6.8.2 EPRI Monte Carlo Simulations

The simulation methodology documented in the EPRI ODSCC report, Reference 6.1, was also used for the estimation of a EOC leak rate for the Braidwood 1 SG "D". The resulting value, 3.1 GPM is provided for information since this analysis was not the reference methodology employed for the evaluation of the Braidwood SG's. Thus, the following discussion of the EPRI model is also for information purposes to clarify how it relates to the methodology employed. Application of the EPRI model involves two major steps. In the first step, an EOC leak rate table as a function of BOC volts is generated from Monte Carlo simulations of NDE uncertainties, plant specific growth rates and uncertainties associated with the correlation analyses. In the second step, the total leak rate is estimated as the sum of the individual EOC leak rates from each indication using the tabulated leak versus BOC volts values.

Using the EPRI methodology, the probe wear and analyst variability are randomly sampled to obtain a random BOC voltage corresponding to a measured BOC voltage. The growth curve is then entered to obtain a random growth for the length of the cycle. This is then added to the BOC voltage to obtain a random EOC voltage. The POL and leak rate versus volts correlations are sampled to obtain a random POL and leak rate for that indication. The expected leak rate from the indication is then taken as the POL times the leak rate. The simulation is repeated several thousand times to obtain an EOC distribution of leak rate at each voltage level, typically in 0.1 volt increments. From the distribution, a non-parametric 95% confidence bound for 95% of the population of the leak rates is determined at each voltage level. These are then used to estimate the EOC leakage from the distribution of BOC indications.

The POL for a specified EOC indication voltage is obtained from the correlation equation as

$$R_i = \frac{1}{1 + e^{-(\beta_1 + \beta_2 \log(V_i) + Z_i \eta_i)}} , \tag{6.36}$$

where β_1 and β_2 are the coefficients from the POL regression analysis, $Z_i \sim N(0,1)$, and η_i is the estimated standard deviation given by

$$\eta_i = \sqrt{V_{11} + [\,2 V_{12} + V_{22} \log(V_i)\,] \log(V_i)} , \tag{6.37}$$

where the V_{ij}'s are the elements of the covariance matrix of the coefficients.

For each indication simulated, the coefficients of the leak rate versus voltage equation are generated. The slope of the regression equation is sampled using a random t-variate, followed by simulation of the intercept. Finally, the regression residual error is sampled with a random t-variate. Random t-variates are used instead of random normal variates because the standard deviation of the population of residuals is estimated, and not known, from the regression analysis. A two-sided $100\cdot(1-\alpha)\%$ confidence band for the true slope, β_4, of the regression equation is given by

$$\beta_4 = b_4 \pm t_{\nu,1-\alpha/2} \sqrt{\frac{\sigma_\varepsilon^2}{\sum (V_j - \bar{V})^2}} , \tag{6.38}$$

where b_4 is the estimated slope from the regression analysis, ν is the number of degrees of freedom used for the determination of σ_ε, the estimated standard deviation of the residuals. Thus, by randomly sampling the t-distribution with ν degrees of freedom, t_ν, random values of

the slope can be generated from equation (6.38), where the sign of the random t-variate governs the sign of the second expression, i.e.,

$$\beta_4 = b_4 + t_\nu \sqrt{\frac{\sigma_\epsilon^2}{\sum_j (V_j - \bar{V})^2}} \qquad (6.39)$$

The coefficients of the regression equation, i.e., equation (6.27), are not statistically independent. Thus, selecting a random value for the intercept must account for the already selected slope. In this case, a joint $100\cdot(1-\alpha)\%$ confidence ellipse for the coefficients is given by

$$(\beta_3 - b_3)^2 + 2\bar{V}(\beta_3 - b_3)(\beta_4 - b_4) + \frac{\sum V_j^2}{n}(\beta_4 - b_4)^2 \le \frac{2\sigma_\epsilon^2 F_{2,\nu}}{n}, \qquad (6.40)$$

where β_3 and β_4 are the true, but unknown, coefficients of the regression equation. Thus, given the random slope from equation (6.39), a random F-distribution value, F, for 2 and ν degrees of freedom, is selected and equation (6.40) is solved (considering the equality) to obtain a random value for β_3. Since there are multiple roots of equation (6.40), i.e.,

$$\beta_3 = b_3 - \bar{V}(\beta_4 - b_4) \pm \sqrt{(\beta_4 - b_4)^2\left[\bar{V}^2 - \frac{\sum V_j^2}{n}\right] + \frac{2\sigma_\epsilon^2 F_{2,\nu}}{n}}, \qquad (6.41)$$

an additional random selection must be made to account for the sign of the radical in equation (6.41). It is also noted that the selection of a random F deviate may result in the radical of (6.41) being imaginary. In this case, it is necessary to sample F until the radical is real. To complete the leak rate versus voltage correlation for the simulation, only the variation about the regression line remains. The standard error, σ_ϵ, from the regression analysis has been shown to be approximately normally distributed with a mean of zero. Since the true variance of the residual population is estimated, the distribution is simulated using a random t-variate and the final leak rate for each simulation case is given by

$$Q_i = 10^{\beta_3 + \beta_4 V_i + t_\nu \sigma_\epsilon}. \qquad (6.42)$$

It is noted that the method described in the EPRI ODSCC report indicates that the effective standard deviation of the residuals, σ_i, from equation (6.22) is to be used instead of the actual standard deviation of the residuals, σ_ϵ, in equation (6.42). This is considered to be an unnecessary conservatism because the variance of the coefficients would enter equation (6.42) twice, i.e., through the simulation of β_3 and β_4 and through σ_i. The net effect would be to

slightly over estimate the leak rate for each individual indication. For the simulation result reported previously herein, equation (6.42) was used.

In summary, the EPRI simulation essentially uses the predictive distribution to simulate the EOC leak rate. This ignores the potential contribution due to the covariance of the individual POL times leak rate values, however, this is likely compensated for by taking each individual EOC leak rate at a 95% confidence level, and the fact that the contribution from the covariance terms is small. Westinghouse has previously reported results, in prior WCAP reports, based on directly simulating the predictive distribution. Results obtained using this method, 3.0 and 3.1 GPM for two independent simulations, were comparable to the result obtained using the methodology described in Section 6.8.1. Thus, the EPRI methodology of Reference 6.1 results in a predicted total leak rate of 3.1 GPM, which is in excellent agreement with the 3.2 GPM result obtained by the Monte Carlo methods of Section 6.8.1, and the 3.1 GPM result from the hybrid method. In conclusion, either of the three methods is adequate for the SLB leak rate analysis.

6.9 References

The references used in this report section are:

6.1 TR-100407, Revision 1 (draft), "PWR Steam Generator Tube Repair Limits - Technical Support Document for Outside Diameter Stress Corrosion Crack at Tube Support Plates," Electric Power Research Institute, August 1993.

6.2 NP-7480-L, Volume 2, "Steam Generator Tubing Outside Diameter Stress Corrosion Cracking at Tube Support Plates - Database for Alternate Repair Limits, Volume 2: 3/4 Inch Diameter Tubing," Electric Power Research Institute, October, 1993.

6.3 EPRI Letter, "Exclusion of Data from Alternate Repair Criteria (ARC) Databases Associated with 7/8 inch Tubing Exhibiting ODSCC," D. A. Steininger (EPRI) to J. Strosnider (USNRC), April 22, 1994 [to become Appendix E of Reference 6.2].

6.4 NUREG-1477 (draft), "Voltage-Based Interim Plugging Criteria for Steam Generator Tubes - Task Group Report," United States Nuclear Regulatory Commission (NRC), June 1, 1993.

6.5 [United States Nuclear Regulatory Commission] Meeting with EPRI, NUMARC, "Resolution of Public Comments on Draft NUREG-1477," United States Nuclear Regulatory Commission, February 8, 1994.

6.6 Regulatory Guide 1.121 (draft), "Bases for Plugging Degraded PWR Steam Generator Tubes," United States Nuclear Regulatory Commission, issued for comment in August, 1976.

6.7 Docket STM-50-456, "Safety Evaluation by the Office of Nuclear Reactor Regulation Related to Amendment No. to Facility Operating License No. NPF-72 Commonwealth Edison Company Braidwood Station, Unit No. 1," United States Nuclear Regulatory Commission, May, 1994.

Table 6-1: Regression Analysis Results - Burst Pressure vs. log(Bobbin Amplitude) 3/4" x 0.050" Alloy 600 MA SG Tubes (Reference σ_f = 75 ksi)			
Parameter	Value	Value	Parameter
b_1	-3.077	7.822	b_0
SE b_1	0.175	0.136	SE b_0
r^2	80.7%	0.955	SE P_B
F	306.1	73	DoF
SS_{reg}	279.03	66.55	SS_{res}
Pr(F)	8.0E-28	29.46	$SS_{log(V)}$
p_1-value	8.0E-28	1.6E-62	p_0-value

Table 6-2: Results of Regression Fits of Logarithmic Forms of POL Distribution Functions to 3/4" OD Tube Data @ 620°F and ΔP = 2560 psi			
Parameter	Log-Logistic Values	Log-Normal Values	Log-Cauchy Values
b_1	-5.5998	-2.7157	-13.8413
b_2	9.1924	4.6317	21.3183
V_{11}	2.1145	0.3664	46.5125
V_{12}	-2.9538	-0.4985	-71.2114
V_{22}	4.5779	0.7993	110.22
Deviance	32.52	33.84	32.43
Results of Regression Fits of Non-Logarithmic Forms of POL Distribution Functions to 3/4" OD Tube Data.			
Parameter	Logistic Values	Normal Values	Cauchy Values
b_1	-5.3890	-2.8544	-10.5327
b_2	1.1945	0.6395	2.3085
V_{11}	1.4958	0.2905	24.4371
V_{12}	-0.3141	-0.0617	-5.3943
V_{22}	0.0787	0.0169	1.2223
Deviance	28.87	28.94	32.47

Table 6-3: Sample Results for Probability of Leak for 3/4" SG Tubes @ 620°F and ΔP = 2560 psi						
Volts	Log-Logistic Function	Log-Normal Function	Log-Cauchy Function	Logistic Function	Normal Function	Cauchy Function
0.1	3.77E-07	1.02E-13	9.05E-03	5.12E-03	2.63E-03	3.08E-02
0.2	5.99E-06	1.32E-09	1.11E-02	5.77E-03	3.20E-03	3.15E-02
0.3	3.02E-05	1.39E-07	1.27E-02	6.49E-03	3.88E-03	3.22E-02
0.4	9.53E-05	2.57E-06	1.42E-02	7.31E-03	4.68E-03	3.30E-02
0.5	2.32E-04	1.98E-05	1.57E-02	8.23E-03	5.63E-03	3.38E-02
0.6	4.81E-04	9.09E-05	1.71E-02	9.26E-03	6.74E-03	3.47E-02
0.7	8.90E-04	2.98E-04	1.85E-02	1.04E-02	8.05E-03	3.55E-02
0.8	1.52E-03	7.77E-04	2.00E-02	1.17E-02	9.57E-03	3.65E-02
0.9	2.42E-03	1.71E-03	2.15E-02	1.32E-02	1.13E-02	3.75E-02
1.0	3.68E-03	3.31E-03	2.30E-02	1.49E-02	1.34E-02	3.85E-02
2.0	5.56E-02	9.32E-02	4.26E-02	4.74E-02	5.76E-02	5.33E-02
5.0	6.95E-01	6.99E-01	7.59E-01	6.42E-01	6.34E-01	7.52E-01
7.0	8.97E-01	8.85E-01	9.25E-01	9.51E-01	9.48E-01	9.44E-01
10.0	9.73E-01	9.72E-01	9.58E-01	9.99E-01	1.00E+00	9.75E-01

Table 6-4: Regression Analysis Results: log(Leak Rate) vs log(Volts) for 3/4" x 0.043" Alloy 600 SG Tubes @ 620°F and ΔP = 2560 psi			
Parameter	Value	Value	Parameter
b_1	3.132	-1.888	b_2
SE b_1	0.431	0.425	SE b_2
r^2	58.2%	0.653	SE log(Q)
F	55.88	38	DoF
SS_{reg}	22.56	16.21	SS_{res}
Pr(F)	<0.000001%	2.300	$SS_{log(Q)}$
p-value	<0.000001%	0.01%	p_0-value

Figure 6-1: Burst Pressure vs Bobbin Amplitude
EPRI Database , @ 650°F, Reference Flow Stress = 75 ksi

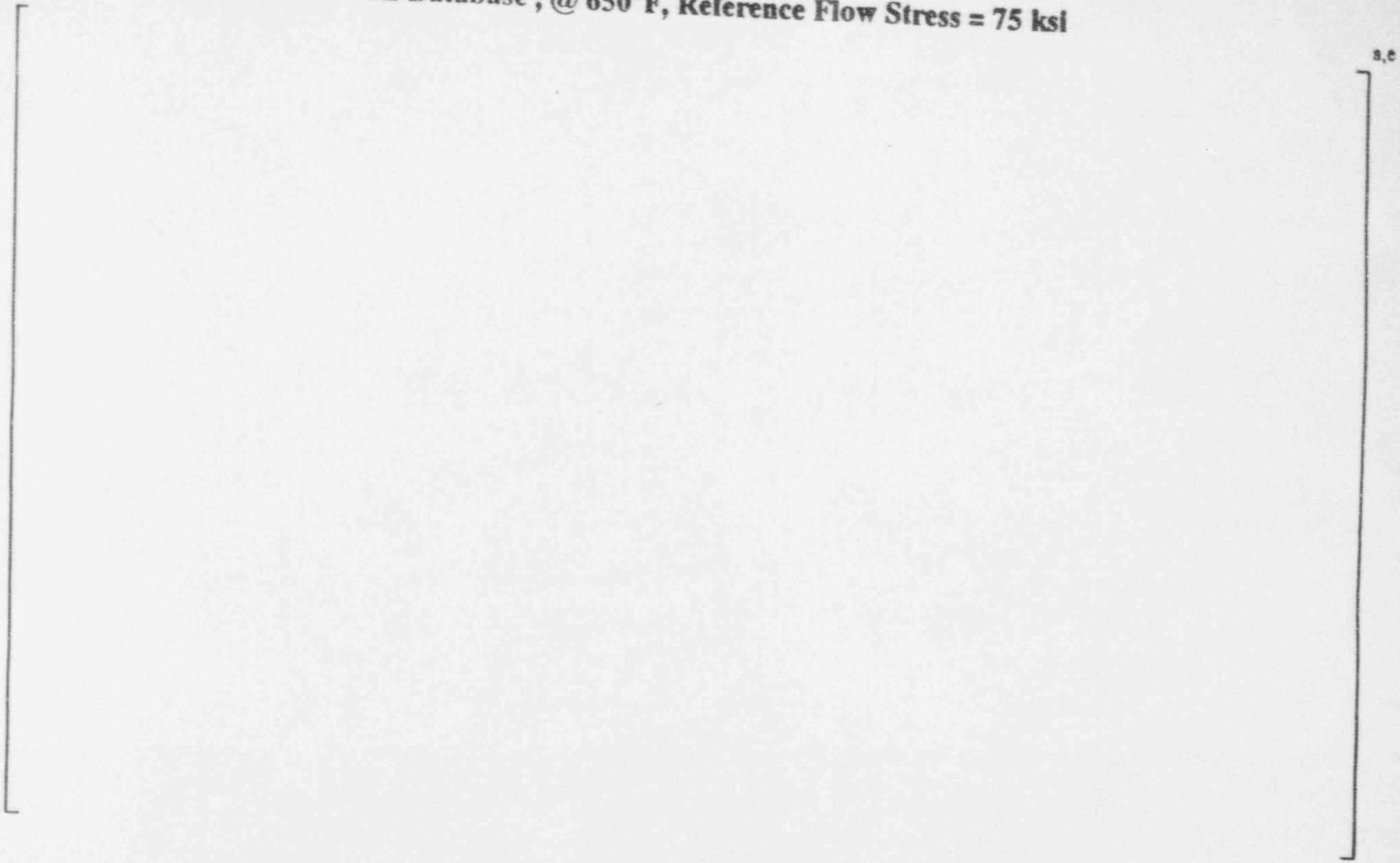

a,c

[34PV_NRC.XLS] EPRI P vs V

RFK 4/15/94, 3:01 PM

Figure 6-2: Burst Pressure vs. Crack Length

0.750" x 0.043", Alloy 600 MA Steam Generator Tubes @ 650°F, Average Flow Stress

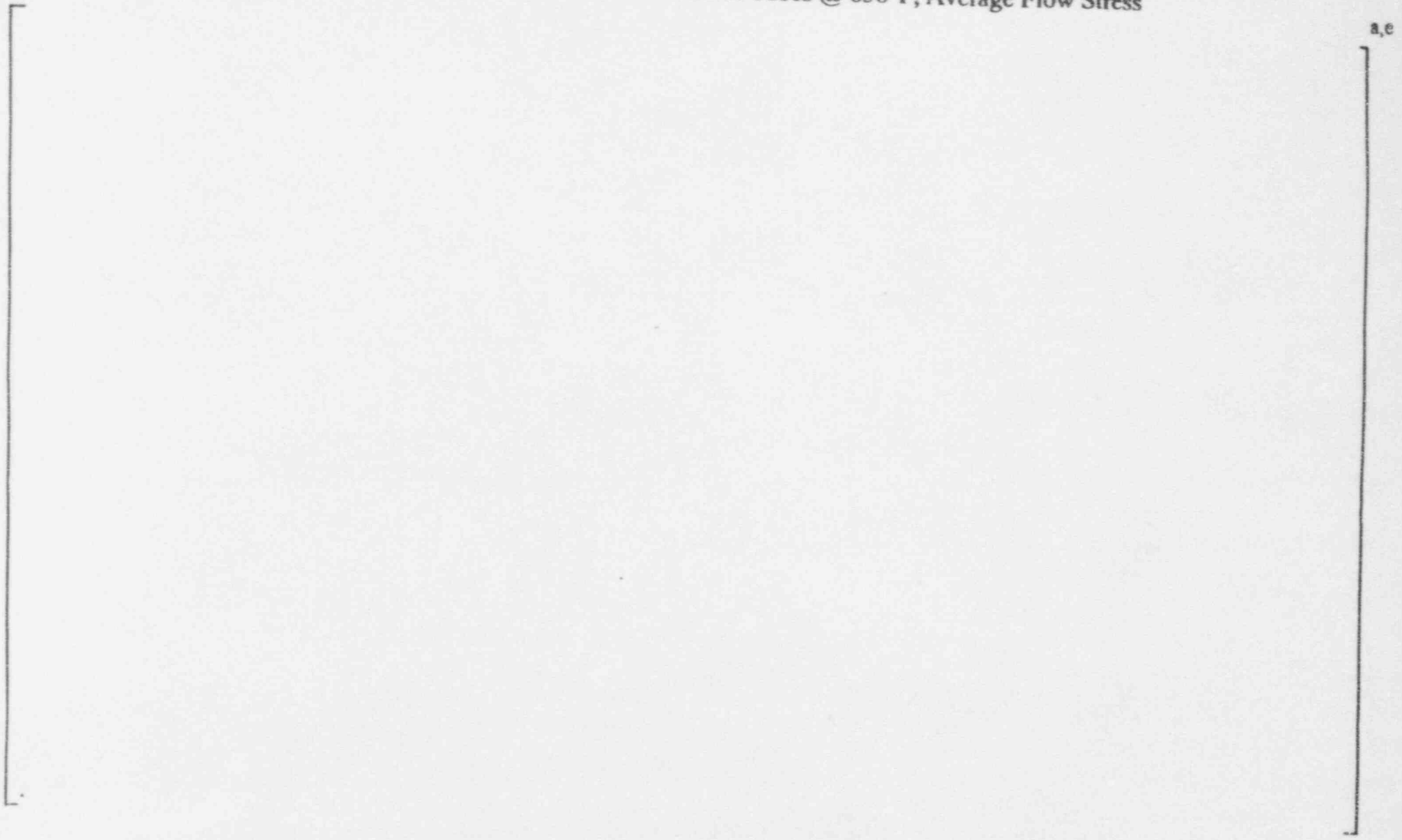

a,c

[TW_BURST.XLS]34 Curve

RFK: 4/16/94, 6:51 PM

Figure 6-3: Probability of Burst vs. Through-Wall Crack Length
3/4" x 0.043" Alloy 600 MA SG Tubes

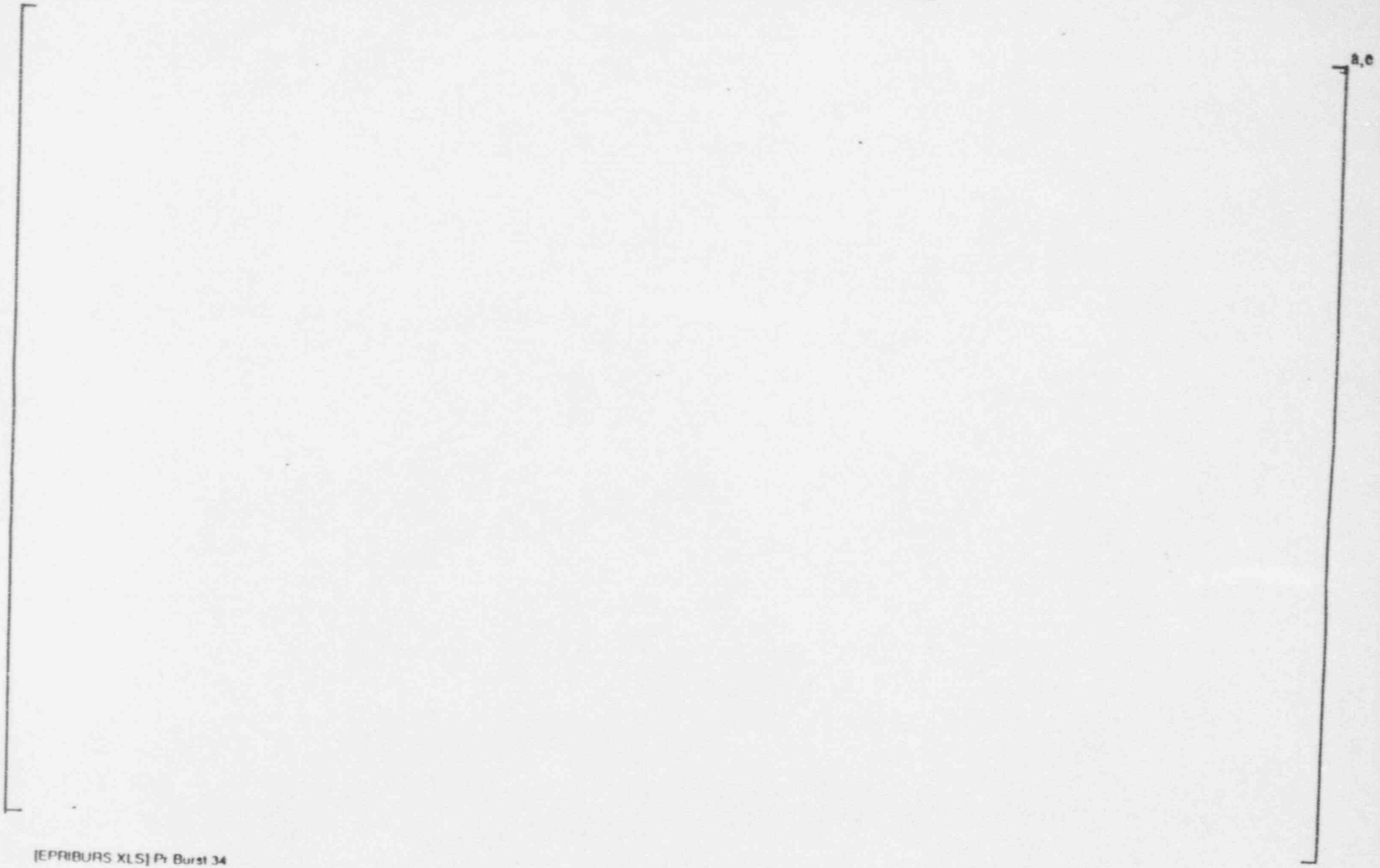

a,c

[EPRIBURS.XLS] Pr Burst 34

RFK: 4/16/94, 6:48 PM

Figure 6-4: Probability of Leak for 3/4" SG Tubes

Comparison of Logarithmic Forms of Logistic, Normal & Cauchy Functions

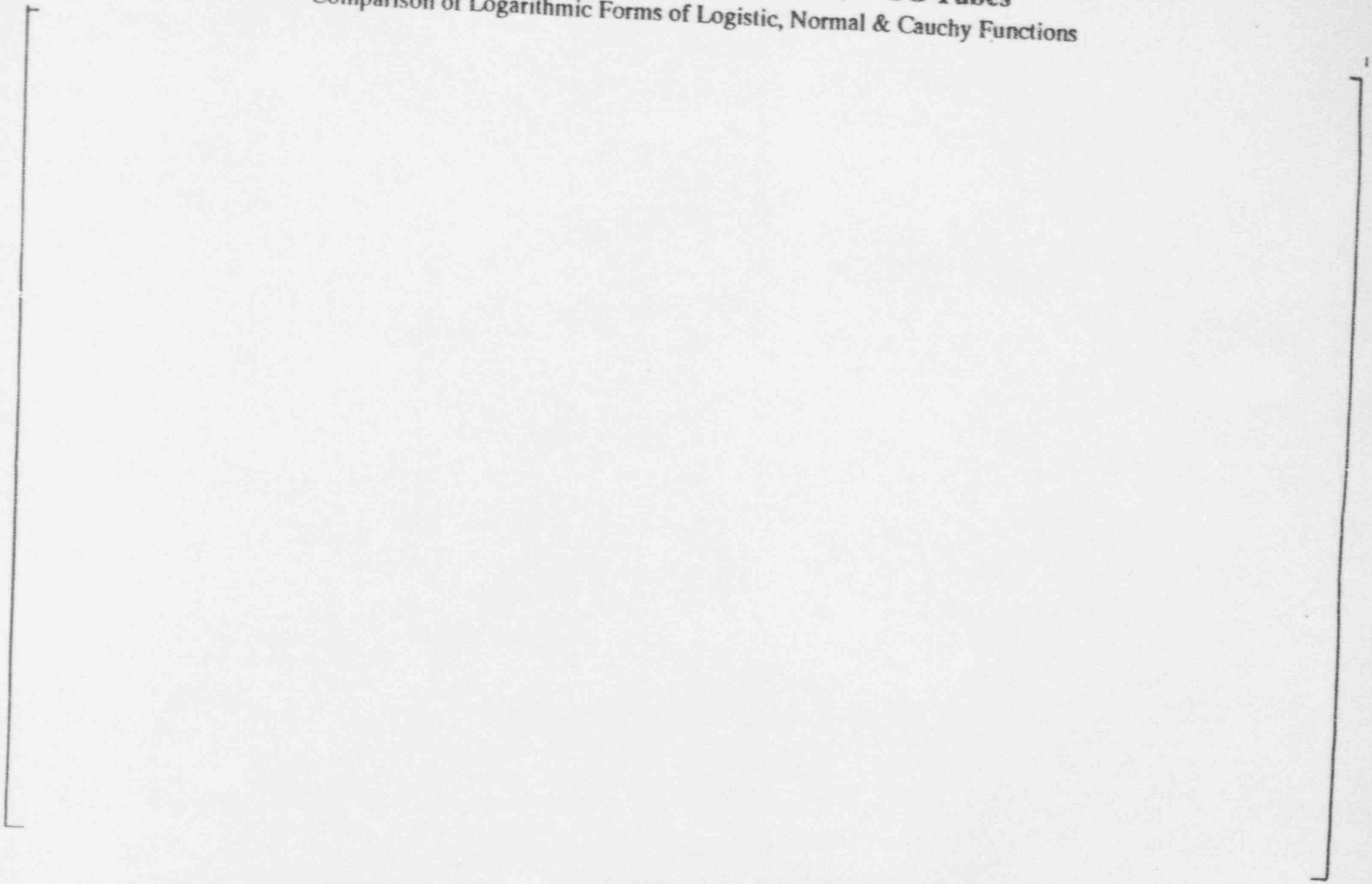

[6CURVE34.XLS] Pol. log(V)

Figure 6-5: Probability of Leak for 3/4" SG Tubes

Comparison of Non-Logarithmic Forms of Logistic, Normal & Cauchy Functions

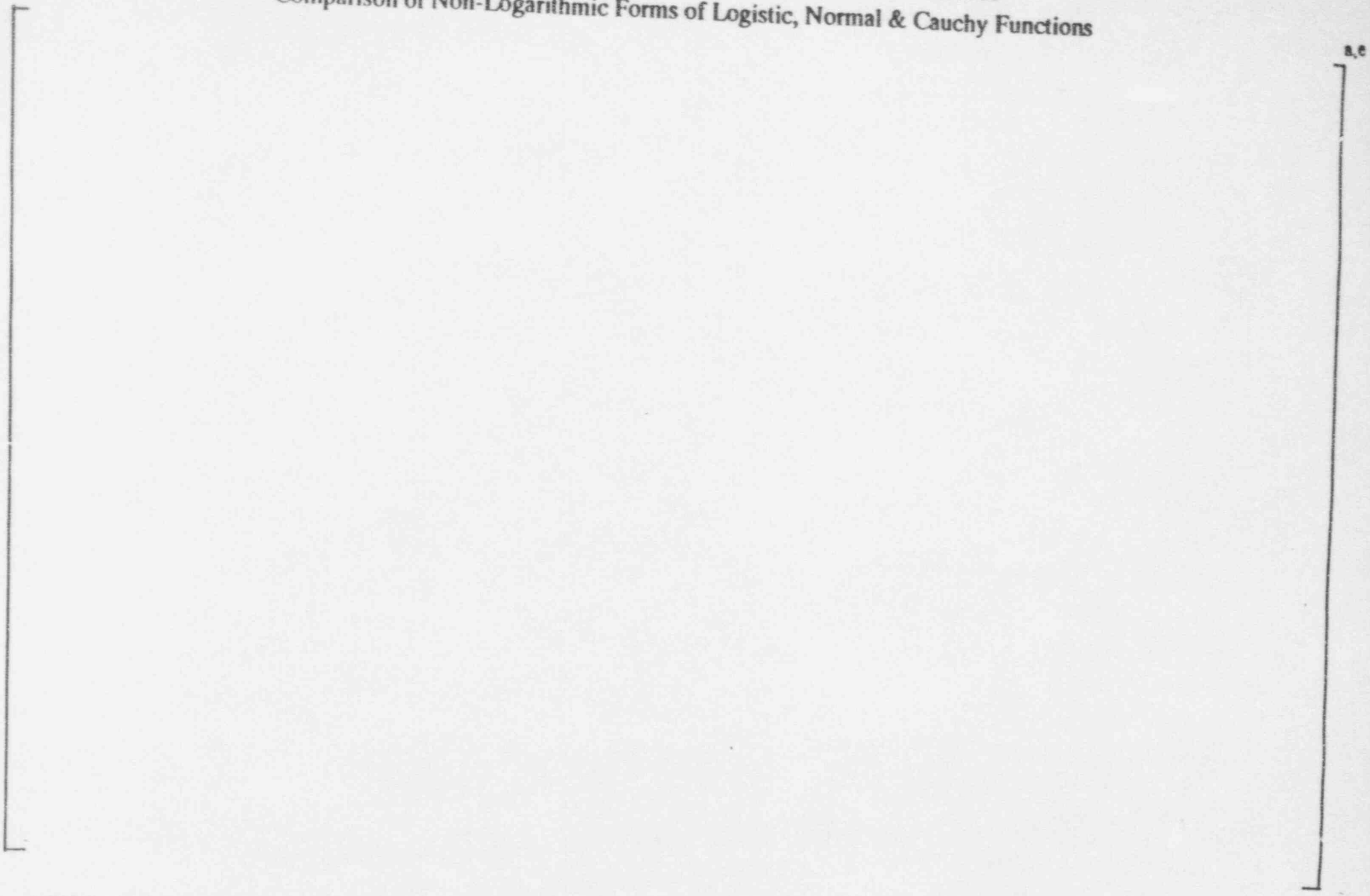

[6CURVE34.XLS] PoL V

RFK: 4/18/94, 6:46 PM

Figure 6-6: 2560 psi SLB Leak Rate vs. Bobbin Amplitude
3/4" x 0.043" Alloy 600 SG Tubes, Model Boiler & Field Data (EPRI)

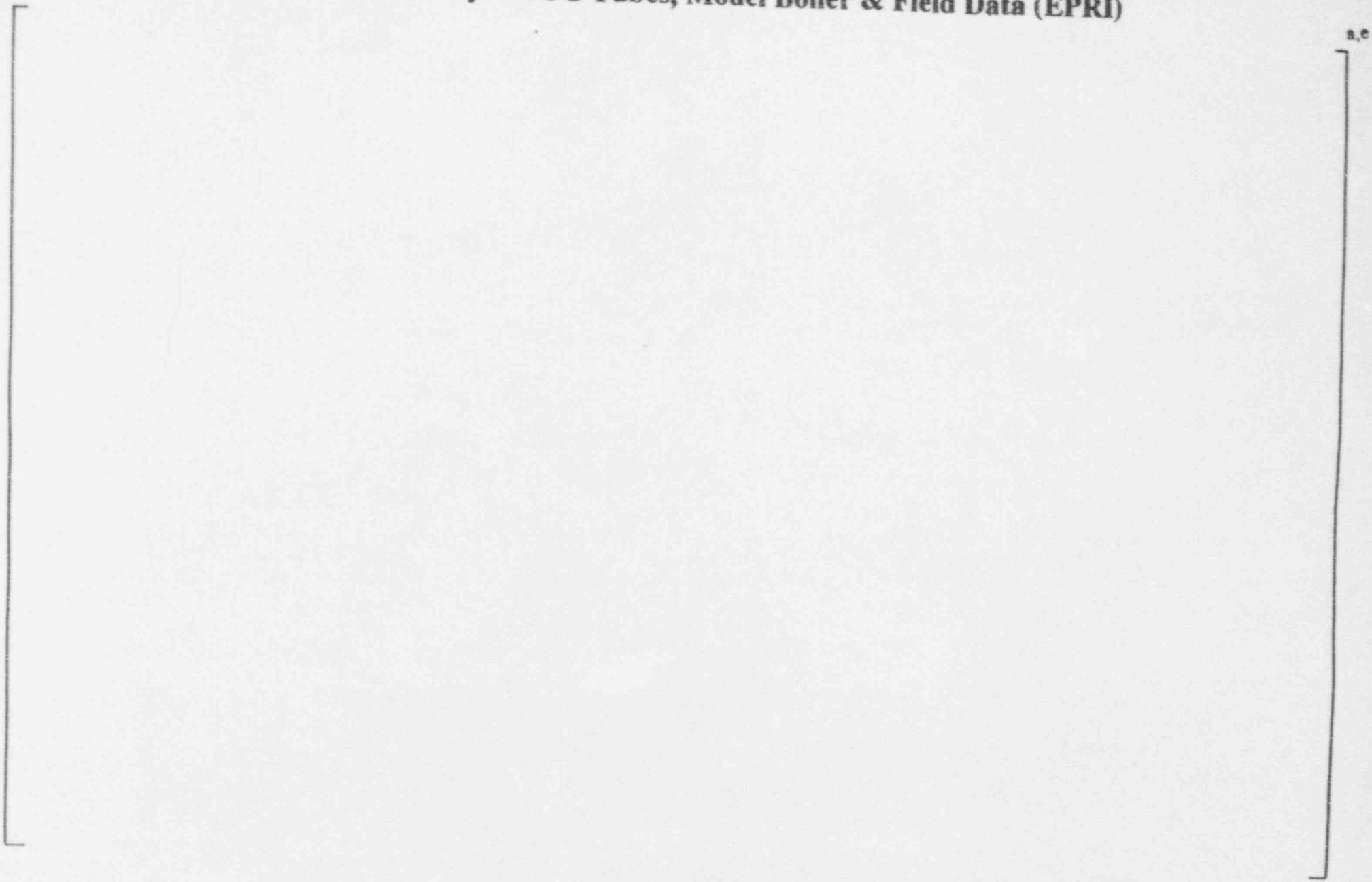

a,c

[34QV_CCE.XLS] Q vs V EPRI

REK 4/16/04 8:58 PM

7.0 BRAIDWOOD-1 EDDY CURRENT INSPECTION RESULTS

7.1 General

The March-April 1994 refueling shutdown was accompanied by 100% full length bobbin probe inspection of all four steam generators. In anticipation of the potential finding of significant ODSCC at support plate intersections, the ASME standards were calibrated to be consistent with IPC guidelines (such as incorporated into Appendix A of WCAP-13854), wear standards were employed to allow tracking of voltage measurement variation, and the eddy current analysts were required to demonstrate their capability to report and to measure indication voltages. TSP indications have been assessed against the prior inspection conditions at the corresponding locations to develop voltage growth rates for the preceding periods of operation.

Previous inspections of the Braidwood-1 steam generator tubes were conducted in November 1993 during an unplanned outage (SG C only), in September 1992 (EOC-3), and in April 1991 (EOC-2); the EOC-1 inspection in September 1989 was not included in the growth rate studies. For each indication reported during the 1994 inspection, both the 1993 (SG C) and the 1992 (all SGs) data were reevaluated to determine, as far as possible, the pre-existing signal amplitude which could be attributed to any detectable precursor condition. Only if a possible flaw indication was observed in the earlier inspection was a growth point calculated for the particular 1994 indication; i.e. no assumptions were made about prior year signal voltages. Because of the unplanned outage during Cycle 4, comparisons in SG C were made to both the 1993 and 1992 inspection results; furthermore, 1992 data for tubes reported in 1993 were compared to obtain an estimate of the partial cycle (4a) growth rate. Cycle 4b growth was determined by comparing the 1993 and 1994 data for SG C only; an overall Cycle 4 growth rate based on comparison of 1994 with 1992 data was also calculated. All the tubes plugged in 1992 were used to develop growth rate data for Cycle 3 by reanalyzing the 1991 data. Table 7-1 presents a summary tabulation of all the growth rates on a per cycle as well as a per Effective Full Power Year (EFPY) basis; also shown for each case are the number of comparisons used, the average BOC voltages, the voltage growth (ΔV), and the length of the operating period in EFPY. For each cycle evaluated, the data was subdivided into indication populations less than 0.75 volt and those equal to or greater than 0.75 volt. This was done to demonstrate the consistency in behavior with prior cases, which have consistently shown higher average percentage growth rates for low voltage indications.

The distribution of the TSP ODSCC indications among the four SGs for the 1994 inspection is shown in Table 7-2, which tabulates the number of indications for each TSP elevation for which indications were observed. For the D4 SGs of Braidwood-1, the 1H level represents the Flow Distribution Baffle (FDB), a plate with oversize tube holes and no flow holes; for this reason the incidence of ODSCC is expected to be low in the absence of unusual

circumstances. In fact, none of the indications reported in Braidwood-1 occur at this elevation. The support levels above are numbered in the cold leg order; i.e., the next hot leg TSP is designated 3H since its height corresponds to the 3rd preheater plate. The remaining TSPs are designated 5H, 7H, 8H, 9H, 10H, and 11H. Thus, though some probability of encountering ODSCC signals at the upper plates exists, it is expected that most of the indications will be observed in TSPs 3H, 5H, and 7H. These levels are in the relatively hotter internal temperature zone of the tubes (maximum in the hot leg tubesheet and decreasing with elevation up to the apexes of the U-bends, thereafter decreasing as the cold leg elevation decreases).

7.2 Inspection Results

7.2.1 March 1994 Inspection

During the scheduled refueling outage (A1R04), all tubes in service were tested full length with bobbin probes. Each distorted support plate indication (DSI) and all TSP indications characterized as a percent (%) call were subjected to confirmatory MRPC testing to assess the consistency of the underlying tube condition with prior cases of TSP ODSCC, and to determine the severity of the indication with respect to the repair criteria. The TSP bobbin indications confirmed by MRPC testing numbered 1567 among the four SGs, 470 in SG A, 76 in SG B, 642 in SG C, and 379 in SG D. The total number of TSP intersections subjected to MRPC testing on the basis of possible ODSCC indications was 2733, distributed among the four SGs; this represents a 57% rate of confirmation of the bobbin calls. It is considered that only those intersections which exhibit detectable ODSCC with pancake coil inspections warrant scrutiny with respect to plugging criteria, whether under Tech. Spec. criteria or under the alternate basis represented by the Interim Plugging Criteria. Two SG C bobbin field calls confirmed as NDD by RPC inspection are not included in the statistics of this report. These indications were more appropriately called permeability variations or residual signals, and inclusion of these two indications would result in misleading growth data.

The axial distribution of TSP ODSCC indications, as expected, exhibits the strong correlation with height above the tubesheet. With the exception of the 1H level (FDB), a strong concentration of the bobbin and MRPC indications are observed at 3H (58%), 5H (28%), and 7H (10%). Figure 7-1 presents the numerical distributions of the TSP ODSCC with respect to elevation in histogram form. The bobbin amplitude distributions associated with the ODSCC indications are presented together with the cumulative distribution curves in Figures 7-2 to 7-6 for the individual SGs and for the composite of all four SGs. Figure 7-7 gives the cumulative RPC confirmation fraction of the bobbin indications as a function of bobbin voltage. As expected, the probability that the RPC probe will detect degradation increases with the bobbin voltage, which increases with the depth and length and number of cracks present. Table 7-3

provides detailed RPC confirmation statistics as a function of bobbin voltage for each of the individual SGs, as well as cumulative confirmation data for the four SG composite results.

An RPC sampling plan was performed to inspect TSP intersections with dent signals greater than 5 volts and artifact/residual signals that could potentially mask bobbin indications of about 1.0 volt. Denting in Braidwood-1 is minor and most of the dents represent mechanical dings rather than corrosion induced denting. The RPC sampling plan was performed on all identified hot leg dents > 5.0 volts in SGs A and B. It included 21 dents (18 in SG A, 3 in SG B) at TSP intersections. There are only 6 dents in SG C (one additional dent was in a tube plugged for other causes) and 2 in SG D left in service above 5 volts that were not RPC inspected. The RPC sample included 40 mix residuals in SG A and 41 in SG B. The mix residuals inspected had greater than a one volt signal and were manually selected to represent the larger residual signals. In addition to this RPC sampling plan, 85 intersections with no bobbin indications were RPC inspected. No RPC flaw indications were found in the RPC sampling plan. In both this RPC sample and the RPC inspection of bobbin flaw indications, no circumferential indications or indications extending outside of the TSP thickness were detected.

Limiting the RPC sampling to only SGs A and B left only 8 dented TSP intersections uninspected in SGs C and D. Reviews of data from previous outages indicate that all 8 of these dent indications were present. The uninspected dent indications lead to a negligible risk of leakage or rupture due to the small number of dents, the fact that no flaw indications were found at the inspected dent locations and the fact that a conservative POD of 0.6, independent of voltage, is applied for the SLB leak rate and tube burst probability estimates. Similarly, uninspected mix residuals in SGs C and D would have negligible concern for leakage or burst considerations.

The two dents in SG D have bobbin voltages of 19.1 and 5.1 volts. The bobbin data for these indications have been reviewed for the 1989, 1991, 1992 and 1994 inspections. There have been no discernable changes in the dent voltages or phase angles. In all inspections, the phase angles are within 3 degrees of the expected 180 degrees for a dent. If a flaw were present, some change to the voltage and phase angle would be expected. Thus, it is judged that the dents are not growing in size and there is a low likelihood of a flaw being present in the dents. SG D is the most limiting SG for tube leakage and burst considerations. Since only two uninspected dents are present, even the assumption of a flaw being present in the dent (a flaw too small to influence the phase angle of the dent) would have negligible influence on leakage or burst. The POD = 0.6 adjustment results in 7.3 indications (actual indications plugged) above 2.7 volts left in service and 2 indications above 5.0 volts left in service. The contributions of these postulated indications to leakage and burst probability would be expected to exceed that of a potential indication in the two dented intersections not RPC inspected. SG C is not a limiting SG for leakage or burst considerations due to the

lower voltages (maximum of 2.74 volts found in the 1994 inspection) and lower growth rates found for this SG compared to SG D. Even if indications were postulated in the six uninspected dents left in service, the additional indications would be very unlikely to cause the leakage or burst probability to approach that for SG D. It can be further noted that the presence of a crack within a dented TSP would result in no or very small leakage due to the constraint provided by the dent, as shown by leak testing in the EPRI database report. If the postulated indication extended more than about 0.2" from the dent, the crack indication would be detectable by bobbin inspection. For these additional reasons, leakage or burst potential would be negligible for uninspected dents.

7.2.2 Prior Inspections: November 1993 and September 1992

The 1993 inspection of SG C was conducted in conjunction with an unplanned outage. This 100% full length inspection with bobbin probes was conducted with 610 mil standard bobbin coils, tubing standards which were subsequently normalized to the laboratory standard which serves as the reference for 3/4" alloy 600 tubing. Using the prevailing industry guidelines for reporting bobbin indications, 116 percent-type indications were reported, along with 300 DSIs. The percent-type indications were removed from service after confirmation with MRPC, and the DSIs were continued in service without MRPC verification. This was considered prudent in light of the A1R04 refueling outage scheduled 4 months later. Since the November 1993 testing was not conducted as a Tech. Spec. inspection, there was no extension of the testing to the other SGs.

The 1993 bobbin indication distributions for number vs. TSP elevation and number vs. amplitude are given in Figure 7-8 and in Table 7-4. Once again, the temperature/elevation dependency of the ODSCC incidence is apparent, and the distribution of amplitudes shows the predominance of low voltage (<1) signals accompanied by a low frequency tail of larger amplitude signals.

During A1R03, the September 1992 inspection, all four SGs were subjected to 100% full length bobbin inspection, again using site-specific bobbin interpretation guidelines consistent with the prevailing industry approach in plants not implementing the IPC. In this inspection, as in A1R04, all bobbin percent (%) and DSI indications reported were subjected to MRPC examination; 166 tubes with bobbin TSP indications confirmed by MRPC testing were removed from service. DSI signals reported on 79 intersections were continued in service after obtaining NDD (no detectable degradation) results from MRPC testing and analysis. The reported distribution of bobbin indications for A1R03 are given in Table 7-5 and Figure 7-9 for the elevation dependency, and the amplitude spectrum of the plugged tube indications is shown in Figure 7-10. It is apparent that the bobbin inspection data for 1992, 1993 and 1994 reflect similar patterns of tube degradation, proceeding for the most part at modest rates in terms of bobbin amplitudes, but progressively involving more tubes.

7.3 TSP Voltage Growth Rates

The progression of ODSCC indications at the TSPs is determined by re-evaluation of prior inspection EC records at the locations identified with indications in the 1994 inspection. In most cases, some element of the precursor is identified as corresponding to the flaw signal reported in 1994. However, it should be noted that rather conservative analysis criteria are invoked to accomplish this task. In this process analysts are required to forego the behavior criteria they may have employed to screen out low signal-to-noise indications, and to report possible flaw-like behavior in the TSP mix residual regardless of clarity. Review of the growth data identifies any anomalous growth data, and these are subjected to further scrutiny to eliminate spurious data.

The evaluation of voltage growth based on reevaluating the prior inspection data for all indications found during the latest inspection is the same approach used for other IPC/APC evaluations. This method of growth evaluation includes the largest growth values (typically repaired at the EOC) for each cycle, and can result in large, conservative average growth values. However, because of tube repair and the occurrence of new indications, there are differences in the population of tubes when comparing growth rates between cycles. This introduces some uncertainty in assessing growth trends between cycles, such as those which may be due to chemistry improvements. A more desirable growth evaluation would track the same population of indications for multiple cycles to more accurately assess growth trends. However, if the last inspection indications are tracked back in time, the larger prior cycle indications which were repaired are not included in the analysis and this method can lead to an underestimate of average prior cycle growth. This method has been applied to SG C over the first and second parts of Cycle 4 as described below. A third option for evaluating growth would be to track the latest inspection results back in time and to add plugged tubes into the population evaluated for prior cycles. This method has not been systematically evaluated. A more systematic evaluation of these three options would be desirable to assess the best option for evaluating both cycle-to-cycle growth trends and the influence of operational chemistry improvements. Such an evaluation has not been performed for Braidwood-1 in this report.

The operational periods for which growth values were determined included Cycle 3 - plugged tubes only, Cycle 4a (9/92-10/93) - SG C only but in three subgroups: all plugged tubes at 10/93, all indications reported at 10/93, and all indications reported at 4/94; Cycle 4b (11/93-4/94) for SG C only for all indications reported in 4/94; and the overall Cycle 4 for all four SGs. For each of these periods, growth data for indications <0.75 volt and those ≥ 0.75 volt were contrasted with the composite growth data for all indications. Table 7-6 shows a summary of the growth rates developed in this fashion for all four SGs. Figure 7-11 illustrates the overall growth/amplitude relationship for all the comparisons obtained in A1R04.

Figure 7-12 presents the same data combined with the elevation (temperature) effect. The dominance of the lower TSP levels in the incidence of the ODSCC indications is also reflected in the growth rates.

The distribution of the growth rate data, expressed as volts difference in the amplitude readings for 2 inspections, are tabulated (Table 7-6) in 0.1 volt bins up to 3 volts, 0.2 volt bins from 3 volts to 5 volts, and in 0.5 volt intervals up to the maximum observed change. For each bin the number of indications is entered along with the corresponding cumulative probability value. Voltage growth distributions are reported on a per EFPY basis. The voltage growth histograms for each of the operational periods evaluated are presented in Figures 7-13 to 7-18 on a composite basis for the prior cycles and on an individual SG basis for the Cycle 4 data. It is seen that for the A1R04 inspection, the average voltage growth rate for the composite of four SGs is 49% per EFPY, or 0.24 volt average growth per EFPY on an average BOC amplitude of 0.48 volt. The maximum growth was observed in SG A, 76% per EFPY, 0.36 volt growth on the average BOC amplitude of 0.47 volt. The largest individual growth observations for Cycle 4 are listed in Table 7-7. For indications with appreciable BOC amplitude readings, i.e., those from 0.75 volt and up, average growth is but a fraction of the composite, 26% in SG A and approximately 16% for the overall population. These estimates are strongly weighted by the SG C results, which exclude the tubes plugged in 11/93 (EOC-4a), for which higher growth rates were observed. The decrease noted in the EOC-4 data and the EOC-4b data correlate with secondary system chemistry changes implemented at Braidwood-1 since the A1R03 outage.

While the voltage growth rates prior to 1993 appear to be larger than those observed in other domestic plants, they fall well below growth rates observed in European plants. Three cases of tube leakage attributable to TSP ODSCC have been reported in Europe, though none has approached even Tech. Spec. leakage limits. None of the domestic plants affected by TSP ODSCC has experienced tube leakage in the absence of denting, notwithstanding indication amplitudes as high as 10.5 volts, and one occurrence of 22 volts.

7.4 Historical Operating Chemistry

Braidwood Unit 1 is currently in its fourth refueling outage. The unit has typically operated in the load follow manner of operation (Figures 7-19 through 7-21). Frequent changes in plant output requirements have resulted in power swings and plant shutdowns on occasion in the past. During periods of operation with chemistry imbalances, more frequent shutdowns with chemistry cleanup prior to restart can result in more limited accumulation of contaminant species in crevice regions subject to superheated conditions. Braidwood Unit 1 has experienced periods of elevated steam generator sodium to chloride molar ratios during prior operating cycles. Operating with these elevated ratios enhances the possibility of developing

caustic crevice conditions conducive to initiation and propagation of Alloy 600 alkaline stress corrosion cracking. Figures 7-19 through 7-27 show the power history, steam generator blowdown sodium to chloride molar ratios, and steam generator blowdown sodium and chloride concentrations during power operation for Braidwood Unit 1 during Cycles 2 through 4. During Cycle 2, SG blowdown sodium to chloride molar ratios (Figure 7-22) were slightly higher than molar equivalency with ratios typically less than 2. These ratio values fluctuated along with variations in plant operating conditions and minor contaminant ingresses - condenser leakage and demineralizer leakage. It should be noted that ratios maintained in this range can lead to development of caustic conditions in steam generator crevice regions. During Cycle 3, SG blowdown sodium to chloride molar ratios (Figure 7-23) were very elevated - both with respect to prior cycles of operation and with respect to good operating chemistry conditions. It is believed that this notable increase is likely to primarily be due to increased attention paid to SG blowdown cation conductivity values and attempts to lower them. As chloride concentration affects cation conductivity, lower chloride concentrations resulted in lower cation conductivity and, consequently, higher sodium to chloride molar ratios. Sodium concentrations were elevated during the first half of Cycle 3 (Figure 7-26). As these concentrations were decreased during the latter part of the fuel cycle, however, chloride concentrations were also decreased. Sodium to chloride molar ratios typically in the range of 2 to 3 and up to 5, as observed during Cycle 3, are strongly indicative of potentially caustic environment development in SG crevice regions as described above. During Cycle 4, a period of operation with higher molar ratios around 2 to 3 was followed by attempts to control molar ratio by modification of blowdown demineralizer operation and, subsequently, ammonium chloride addition (Figure 7-24). Ammonium chloride addition has had the greatest effectiveness at Braidwood Unit 1 in controlling steam generator blowdown sodium to chloride molar ratios in the desired band. The success of this method at controlling crevice chemistry appears to be positive as a result of shutdown hideout return evaluations performed in May and at the end of the cycle.

Hideout return data obtained during Cycle 4 has been evaluated to ascertain the success of the molar ratio control program in modifying the steam generator crevice pH environment. Molar ratios of highly soluble species (sodium, potassium, and chloride) indicate a decreasing trend over the entire cycle (Figure 7-28). In addition, it was reported that the crevice pH calculated by the MULTEQ program indicates an approximate 1.5 pH unit reduction to around 7.5 prior to the end of cycle shutdown. The end of cycle shutdown indicated more acidic conditions and lower molar ratio due to the occurrence of circulating water leakage.

7.5 Relationship Between Operating Chemistry and ODSCC Growth

Corrective actions taken at Braidwood Unit 1 specifically to slow the progression of Alloy 600 tubing ODSCC include molar ratio chemistry control and boric acid addition beginning in

April 1994. Molar ratio chemistry control was initiated during Cycle 4 in December 1992, following nearly two months of plant operation with elevated sodium to chloride molar ratios. Molar ratio control chemistry was begun by varying blowdown demineralizer operations to obtain greater breakthrough of anionic species. These operations have had some success in minimizing sodium leakage from the demineralizers; however, the operational sodium to chloride molar ratio was not able to be fully controlled. When it became apparent that operating in this manner was not achieving the desired degree of control, the decision was made to add ammonium chloride to adjust the sodium to chloride molar ratio in the steam generator blowdown. This method achieved a high degree of control over the operating steam generator blowdown sodium to chloride molar ratio. However, it was not apparent whether the desired result of neutral to slightly acidic hideout return chemistry would be achieved by operating in the identified control band of Na/Cl = 0.3 - 0.6. Following a hideout return evaluation at the end of May 1993, the Na/Cl control band was lowered to 0.2 to 0.4 to further alter the steam generator operating environment. The result of this change is demonstrated in Figure 7-29. Hideout return chemistry data reflect the success of the molar ratio control program in modifying the steam generator environment to the desired degree as indicated by the trends in hideout return chemistry.

Boric acid addition has been identified as the next step to be employed at Braidwood Unit 1 to control Alloy 600 ODSCC progression. Boric acid will be used during the startup for the fifth fuel cycle in April, 1994. Laboratory and operating PWR plant data indicate the usefulness of boric acid as a contributor to the overall corrosion control program. It is anticipated that the use of boric acid will take Braidwood Unit 1 one step further in their goal of minimizing ODSCC growth rates.

Overall, the chemistry review indicates that the high molar ratios of Cycle 3 (4/91-9/92) and the early part of Cycle 4 (up to 1/93) are most likely to be associated with caustic crevice conditions and increased potential for ODSCC initiation and growth. Molar ratios since February 1993 and particularly since the May 1993 reduction in the control band are supportive of reduced potential for ODSCC growth. Since voltage growth rates across the complete Cycle 4 operating period involve both high and low molar ratio operation, the growth rates cannot be readily related to chemistry improvements. However, the SG C growth data of Table 7-1 for Cycle 4a (includes high molar ratio period) and Cycle 4b (low molar ratio period) can provide some insight on the influence of reduced molar ratio on crack growth. SG C had an average growth rate of 39%/EFPY for Cycle 4a and 27%/EFPY for Cycle 4b. This reduction in growth rates for Cycle 4b is supportive of the chemistry improvements in the reduction of growth rates. Cycle 5 experience, which will include boric acid addition, will provide more conclusive data for assessing the influence of chemistry enhancements on growth rates.

7.6 Pulled Tube Eddy Current Data

TSP intersections from 4 tubes were removed from the Braidwood-1 SGs to provide the basis for application of Interim Plugging Criteria and to demonstrate the consistency of the Braidwood-1 experience with other plants in which those criteria have been accepted. From SG A, 2 tubes (R37C43 and R42C44) were pulled, and from SG D, 2 tubes (R37C34 and R16C42). Tube R42C44 was cut above the 7H intersection, permitting the extraction of 4 intersections at the 1H, 3H, 5H and 7H elevations. The three remaining tubes were cut below the 7H TSP level on inlet side, permitting the extraction of 9 additional intersections (total of 13), 3 at each of the 1H, 3H, and 5H elevations. Bobbin and RPC data were collected for each of the removed intersections, which resulted in 6 field bobbin indications with corresponding RPC confirmations and 7 NDD intersections. The bobbin field EC graphics for each of the intersections are given in Figures 7-30 to 7-42. The corresponding RPC field graphics for the tubes reported to have bobbin indications are given in Figures 7-43 to 7-48. Table 7-8 summarizes the field analysis results for each of the intersections. With the exception of the 1.04 volt indication at the 3H level on R37C34 and the 2.09 volt indication at TSP-5H on R42C44, the field calls represent voltages in excess of the full APC limit calculated for the 3/4" tubes in Braidwood-1. The 5H level on R16C42 is considered as representing a possible bobbin indication of 0.61 volt, but field RPC was reported as NDD, suggesting the absence of significant ODSCC; evaluation of the tube metallography for this tube may provide some insight into the relative sensitivities of the bobbin and RPC probes for the less developed areas of ODSCC.

Table 7-1 Average Voltage Growth for Braidwood Unit 1

Cycle 4 9/92 - 3/94 All S/G's	#indications	Average V_{BOC}	Average ΔV	efpy	ΔV/efpy	% Growth % per cycle	% Growth % per efpy
Entire Voltage Range	2654	0.49	0.26	1.147	0.23	53%	48%
V_{BOC} < .75	2289	0.41	0.29		0.25	69%	60%
V_{BOC} ≥ .75	365	0.94	0.13		0.11	14%	16%
S/G A							
Entire Voltage Range	680	0.47	0.41		0.36	86%	75%
V_{BOC} < .75	586	0.39	0.43		0.37	113%	97%
V_{BOC} ≥ .75	94	0.95	0.28		0.24	29%	25%
S/G B							
Entire Voltage Range	261	0.48	0.17		0.15	36%	31%
V_{BOC} < .75	230	0.41	0.16		0.14	39%	34%
V_{BOC} ≥ .75	31	0.94	0.22		0.19	23%	20%
S/G C							
Entire Voltage Range	1030	0.5	0.19		0.17	38%	34%
V_{BOC} < .75	876	0.42	0.24		0.21	57%	50%
V_{BOC} ≥ .75	154	0.95	-0.06		-0.05	-6%	5%
S/G D							
Entire Voltage Range	683	0.49	0.27		0.24	55%	49%
V_{BOC} < .75	597	0.43	0.27		0.24	63%	56%
V_{BOC} ≥ .75	86	0.92	0.29		0.25	31%	27%
Cycle 3 Plugged Tubes 4/91 to 9/92 All S/G's							
Entire Voltage Range	167	0.62	0.62	1.12	0.55	100%	89%
V_{BOC} < .75	145	0.43	0.65		0.58	151%	135%
V_{BOC} ≥ .75	22	0.92	0.42		0.38	46%	41%
Cycle 4a - Plugged Tubes 9/92 to 10/93 S/G C							
Entire Voltage Range	128	0.71	0.67	0.852	0.79	94%	141%
V_{BOC} < .75	71	0.54	0.69		0.81	128%	191%
V_{BOC} ≥ .75	57	0.92	0.65		0.76	71%	105%
Cycle 4a - All Indications 9/92 to 10/93 S/G C							
Entire Voltage Range	428	0.62	0.33	0.852	0.39	53%	79%
V_{BOC} < .75	315	0.51	0.31		0.36	61%	91%
V_{BOC} ≥ .75	113	0.92	0.36		0.42	39%	58%
9/92 to 10/93 to 3/94 - All 1994 Indications Cycle 4a and 4b							
S/G C - Cycle 4a							
Entire Voltage Range	1010	0.5	0.16	0.852	0.19	32%	48%
V_{BOC} < .75	857	0.42	0.19		0.22	45%	68%
V_{BOC} ≥ .75	153	0.95	-0.01		-0.01	-1%	-2%
S/G C - Cycle 4b							
Entire Voltage Range	1069	0.66	0.03	0.295	0.10	5%	16%
V_{BOC} < .75	737	0.5	0.07		0.24	14%	46%
V_{BOC} ≥ .75	332	1.02	-0.04		-0.14	-4%	-13%

Table 7-2. Braidwood #1 TSP ODSCC Indications (A1R04) March, 1994

	Steam Generator A				Steam Generator B				Steam Generator C				Steam Generator D				All Steam Generators			
TSP	#	Volts Max.	Volts Ave.	Growth volts	#	Volts Max.	Volts Ave.	Growth volts	#	Volts Max.	Volts Ave.	Growth volts	#	Volts Max.	Volts Ave.	Growth volts	#	Volts Max.	Volts Ave.	Growth volts
1H	0				0				0				0				0			
3H	344	4.99	0.86	0.37	134	4.25	0.68	0.13	709	2.38	0.72	0.21	403	8.82	0.82	0.3	1590	8.82	0.78	0.27
5H	238	8.33	0.95	0.5	116	2.75	0.59	0.23	235	2.46	0.62	0.16	180	10.44	0.75	0.26	770	10.44	0.75	0.26
7H	91	2.42	0.8	0.35	18	1.37	0.6	0.13	94	2.10	0.64	0.25	77	1.24	0.58	0.17	280	2.74	0.67	0.26
8H	28	3.46	0.83	0.44	3	0.44	0.41	0.06	20	0.92	0.55	0.24	23	1.59	0.57	0.25	74	3.46	0.66	0.31
9H	3	1.02	0.77	0.37	1	0.39	0.39	0.13	1	0.63	0.63	0.1	9	0.53	0.43	0.16	14	1.02	0.51	0.2
10H	2	0.76	0.63	0.22	0				1	0.45	0.45	0.18	1	0.67	0.67	0.43	4	0.76	0.6	0.26
11H	0				0				0				1	0.52	0.52		1	0.52	0.52	

Table 7-3

Braidwood Unit 1 1994 TSP Inspection Summary

	S/G A				S/G B				S/G C				S/G D				Combined Population			
	Bobbin		RPC		Bobbin		RPC		Bobbin		RPC		Bobbin		RPC		Bobbin		RPC	
bin	#ind	cpdf	#obs	%Conf.	#ind	cpdf	#obs	%Conf.	#ind	cpdf	#obs	%Conf.	#ind	cpdf	#obs	%Conf.	#ind	cpdf	#obs	%Conf.
0	0	0.00	0		0	0.00			0	0.00			0	0.00			0	0.00	0	
0.1	1	0.14	0	0.00	0	0.00	0		1	0.09	0	0.00	0	0.00			2	0.07	0	0.00
0.2	6	0.99	0	0.00	5	1.84	0	0.00	7	0.76	1	14.29	3	0.43	0	0.00	21	0.84	1	4.76
0.3	49	7.93	11	22.45	21	9.56	4	19.05	51	5.57	13	25.49	31	4.90	5	16.13	152	6.41	33	21.71
0.4	84	17.00	22	32.81	51	28.31	6	11.76	124	17.28	41	33.06	83	16.86	13	15.86	322	18.20	82	25.47
0.5	92	30.03	46	47.83	43	44.12	9	20.93	156	32.01	68	43.59	111	32.85	39	34.82	402	32.92	162	40.30
0.6	82	43.06	56	58.70	48	61.76	16	33.33	160	47.12	89	55.63	107	46.27	56	52.34	407	47.82	217	53.32
0.7	68	52.69	49	70.59	27	71.69	8	29.63	142	60.53	86	60.56	93	61.67	51	54.84	330	59.90	194	58.79
0.8	45	59.07	26	57.78	25	80.88	6	24.00	117	71.58	86	73.50	68	71.47	41	59.42	255	69.24	159	62.35
0.9	51	66.29	41	80.39	23	89.34	7	30.43	92	80.26	74	80.43	38	76.95	28	73.68	204	76.71	150	73.53
1	44	72.52	38	86.36	3	90.44	1	33.33	64	86.31	57	89.06	34	81.84	29	85.29	145	82.02	125	86.21
1.1	34	77.34	25	73.53	6	92.65	5	83.33	41	90.18	31	75.61	41	87.75	36	87.80	122	86.49	97	79.51
1.2	25	80.88	22	88.00	6	94.85	4	66.67	31	93.11	29	93.55	18	90.35	18	100.00	80	89.42	73	91.25
1.3	25	84.42	25	100.00	2	95.59	0	0.00	18	94.81	17	94.44	14	92.36	13	92.86	59	91.58	55	93.22
1.4	14	86.40	14	100.00	2	96.32	1	50.00	22	96.86	18	81.82	9	93.66	9	100.00	47	93.30	42	89.36
1.5	11	87.96	10	90.91	0	96.32	0		8	97.64	7	87.50	6	94.52	5	83.33	25	94.21	22	88.00
1.6	9	89.24	9	100.00	2	97.06	2	100.00	7	98.30	6	85.71	4	95.10	3	75.00	22	95.02	20	90.91
1.7	13	91.06	13	100.00	0	97.06	0		3	98.58	3	100.00	6	95.97	6	100.00	22	95.83	22	100.00
1.8	8	92.21	8	100.00	2	97.79	2	100.00	3	98.87	3	100.00	3	96.40	2	66.67	16	96.41	15	93.75
1.9	7	93.20	7	100.00	0	97.79	0		3	99.15	3	100.00	4	96.97	4	100.00	14	96.92	14	100.00
2	6	94.05	6	100.00	0	97.79	0		2	99.34	2	100.00	3	97.41	3	100.00	11	97.33	11	100.00
2.1	5	94.76	5	100.00	2	98.53	1	50.00	1	99.43	1	100.00	0	97.41			8	97.62	7	87.50
2.2	8	95.89	8	100.00	0	98.53			3	99.72	3	100.00	4	97.98	4	100.00	15	98.17	15	100.00
2.3	3	96.32	3	100.00	0	98.53			0	99.72	0		1	98.13	1	100.00	4	98.32	4	100.00
2.4	1	96.46	1	100.00	0	98.53			1	99.81	1	100.00	0	98.13			2	98.39	2	100.00
2.5	4	97.03	4	100.00	1	98.90	1	100.00	1	99.91	1	100.00	1	98.27	1	100.00	7	98.65	7	100.00
2.6	2	97.31	2	100.00	0	98.90			0	99.91	0		1	98.41	1	100.00	3	98.76	3	100.00
2.7	1	97.45	1	100.00	0	98.90			0	99.91	0		0	98.41			1	98.79	1	100.00
2.8	0	97.45	0		1	99.26	1	100.00	1	100.00	1	50.00	1	98.56	1	100.00	3	98.90	3	100.00
2.9	0	97.45	0		0	99.26			0	100.00			1	98.70	1	100.00	1	98.94	1	100.00
3	3	97.88	3	100.00	0	99.26			0	100.00			0	98.70			3	99.05	3	100.00
3.2	3	98.30	3	100.00	0	99.26			0	100.00			1	98.85	1	100.00	4	99.19	4	100.00
3.4	2	98.58	2	100.00	0	99.26			0	100.00			1	98.99	1	100.00	3	99.30	3	100.00
3.6	3	99.01	3	100.00	0	99.26			0	100.00			0	98.99			3	99.41	3	100.00
3.8	1	99.15	1	100.00	1	99.63	1	100.00	0	100.00			1	99.14	1	100.00	3	99.52	3	100.00
4	2	99.43	2	100.00	0	99.63			0	100.00			2	99.42	2	100.00	4	99.67	4	100.00
4.2	1	99.58	1	100.00	0	99.63			0	100.00			0	99.42			1	99.71	1	100.00
4.4	0	99.58	0		1	100.00	1	100.00	0	100.00			1	99.57	1	100.00	2	99.78	2	100.00
4.6	0	99.58	0		0	100.00			0	100.00			0	99.57			0	99.78	0	
4.8	0	99.58	0		0	100.00			0	100.00			0	99.57			0	99.78	0	
5	1	99.72	1	100.00	0	100.00			0	100.00			0	99.57			1	99.82	1	100.00
5.5	0	99.72	0		0	100.00			0	100.00			1	99.71	1	100.00	1	99.85	1	100.00
6	1	99.86	1	100.00	0	100.00			0	100.00			0	99.71			1	99.89	1	100.00
6.5	0	99.86	0		0	100.00			0	100.00			0	99.71			0	99.89	0	
7	0	99.86	0		0	100.00			0	100.00			0	99.71			0	99.89	0	
7.5	0	99.86	0		0	100.00			0	100.00			0	99.71			0	99.89	0	
8	0	99.86	0		0	100.00			0	100.00			0	99.71			0	99.89	0	
8.5	1	100.00	1	100.00	0	100.00			0	100.00			0	99.71			1	99.93	1	100.00
9	0	100.00	0		0	100.00			0	100.00			1	99.86	1	100.00	1	99.96	1	100.00
9.5	0	100.00	0		0	100.00			0	100.00			0	99.86			0	99.96	0	
10	0	100.00	0		0	100.00			0	100.00			0	99.86			0	99.96	0	
10.5	0	100.00	0		0	100.00			0	100.00			1	100.00	1	100.00	1	100.00	1	100.00
	706		470		272		76		1059		641		694		379		2731			

Table 7-4. Braidwood Unit 1 10/93 Inspection S/G C Only

Elevation	Number of Indications
1H	0
3H	346
5H	75
7H	23
8H	2
9H	1
10H	1
11H	1
Note: All Bobbin Indications: No RPC Confirmations	

Table 7-5. Braidwood Unit 1 9/92 Inspection
TSP Indication Distribution in Plugged Tubes

Elevation	A	B	C	D	Total
1H	0	0	0	0	0
3H	32	18	94	49	193
5H	14	5	15	15	49
7H	5	3	5	2	15

Table 7-6

Braidwood Unit 1 Cumulative Probability Distributions for Voltage Growth (per EFPY)

	1991 to 1992 All S/G's		1992 to 1993 S/G C		1992 to 1994									
					S/G A		S/G B		S/G C		S/G D		Composite	
Bin	#obs	cpdf	#obs	cpdf	#obs	cpdf	#obs	cpdf	#obs	cpdf	#obs	cpdf	#obs	cpdf
0	8	4.79	60	14.02	161	23.68	75	27.57	268	26.17	198	28.99	702	26.67
0.1	15	13.77	56	27.10	78	34.65	70	53.31	167	42.48	91	42.31	404	40.54
0.2	16	23.35	67	42.76	94	48.68	48	70.98	159	58.01	121	60.03	422	56.19
0.3	21	35.93	64	57.71	63	57.94	40	85.66	157	73.34	86	72.62	346	68.10
0.4	21	48.50	49	69.16	59	66.62	16	91.54	97	82.81	59	81.26	231	77.00
0.5	22	61.68	20	73.83	39	72.35	12	95.96	62	88.87	30	85.65	143	82.94
0.6	12	68.86	26	79.91	32	77.06	2	96.69	36	92.36	28	89.75	98	86.81
0.7	9	74.25	10	82.24	31	81.62	0	96.69	32	95.51	16	92.09	79	89.91
0.8	10	80.24	14	85.51	23	85.00	0	96.69	16	97.07	12	93.85	51	92.25
0.9	6	83.83	14	88.79	21	88.09	1	97.06	6	97.66	9	95.17	37	94.03
1	3	85.63	7	90.42	16	90.44	1	97.43	8	98.44	6	96.05	31	95.14
1.1	6	89.22	5	91.59	17	92.94	1	97.79	5	98.93	6	96.93	29	96.48
1.2	5	92.22	7	93.22	6	93.82	0	97.79	2	99.12	4	97.51	12	97.11
1.3	4	94.61	4	94.16	6	94.71	1	98.16	2	99.32	3	97.95	12	97.59
1.4	1	95.21	5	95.33	4	95.29	1	98.53	3	99.61	0	97.95	8	97.77
1.5	1	95.81	3	96.03	4	95.88	0	98.53	1	99.71	2	98.24	7	98.11
1.6	0	95.81	3	96.73	3	96.32	1	98.90	0	99.71	0	98.24	4	98.33
1.7	0	95.81	1	96.96	3	96.76	0	98.90	1	99.80	1	98.39	5	98.52
1.8	0	95.81	3	97.66	3	97.21	1	99.26	1	99.90	0	98.39	5	98.66
1.9	1	96.41	1	97.90	1	97.35	0	99.26	0	99.90	2	98.68	3	98.81
2	3	98.20	2	98.36	4	97.94	0	99.26	0	99.90	0	98.68	4	98.96
2.1	0	98.20	0	98.36	0	97.94	0	99.26	0	99.90	0	98.68	0	99.00
2.2	0	98.20	1	98.60	2	98.24	0	99.26	1	100.00	0	98.68	3	99.07
2.3	0	98.20	0	98.60	1	98.38	1	99.63	0	100.00	2	98.98	4	99.22
2.4	0	98.20	0	98.60	2	98.63	0	99.63	0	100.00	0	98.98	2	99.30
2.5	1	98.80	0	98.60	1	98.82	0	99.63	0	100.00	0	98.98	1	99.37
2.6	0	98.80	0	98.60	0	98.82	0	99.63	0	100.00	0	98.98	0	99.37
2.7	0	98.80	2	99.07	2	99.12	0	99.63	0	100.00	1	99.12	3	99.48
2.8	0	98.80	0	99.07	0	99.12	0	99.63	0	100.00	0	99.12	0	99.52
2.9	0	98.80	1	99.30	0	99.12	0	99.63	0	100.00	1	99.27	1	99.55
3	0	98.80	0	99.30	2	99.41	0	99.63	0	100.00	0	99.27	2	99.63
3.2	0	98.80	1	99.53	1	99.56	0	99.63	0	100.00	1	99.41	2	99.70
3.4	0	98.80	0	99.53	0	99.56	1	100.00	0	100.00	1	99.56	2	99.78
3.6	0	98.80	1	99.77	0	99.56	0	100.00	0	100.00	0	99.56	0	99.78
3.8	0	98.80	0	99.77	0	99.56	0	100.00	0	100.00	1	99.71	1	99.81
4	1	99.40	0	99.77	0	99.56	0	100.00	0	100.00	0	99.71	0	99.81
4.2	0	99.40	0	99.77	1	99.71	0	100.00	0	100.00	0	99.71	1	99.85
4.4	0	99.40	1	100.00	1	99.85	0	100.00	0	100.00	0	99.71	1	99.89
4.6	1	100.00	0	100.00	0	99.85	0	100.00	0	100.00	0	99.71	0	99.89
4.8	0	100.00	0	100.00	0	99.85	0	100.00	0	100.00	0	99.71	0	99.89
5	0	100.00	0	100.00	0	99.85	0	100.00	0	100.00	0	99.71	0	99.89
5.5	0	100.00	0	100.00	0	99.85	0	100.00	0	100.00	0	99.71	0	99.89
6	0	100.00	0	100.00	1	100.00	0	100.00	0	100.00	0	99.71	1	99.93
6.5	0	100.00	0	100.00	0	100.00	0	100.00	0	100.00	0	99.71	0	99.93
7	0	100.00	0	100.00	0	100.00	0	100.00	0	100.00	0	99.71	0	99.93
7.5	0	100.00	0	100.00	0	100.00	0	100.00	0	100.00	1	99.85	1	99.96
8	0	100.00	0	100.00	0	100.00	0	100.00	0	100.00	0	99.85	0	99.96
8.5	0	100.00	0	100.00	0	100.00	0	100.00	0	100.00	0	99.85	0	99.96
9	0	100.00	0	100.00	0	100.00	0	100.00	0	100.00	1	100.00	1	100.00
9.5	0	100.00	0	100.00	0	100.00	0	100.00	0	100.00	0	100.00	0	100.00
10	0	100.00	0	100.00	0	100.00	0	100.00	0	100.00	0	100.00	0	100.00
10.5	0	100.00	0	100.00	0	100.00	0	100.00	0	100.00	0	100.00	0	100.00

Table 7-7. Braidwood Unit 1 Summary of Largest Bobbin Voltage Growth Rates for Cycle 4

S/G	Tube		Elevation	EOC 4 Signal Size		Boc 4	Growth	New Ind.
	Row	Col		Bobbin	RPC	Bobbin		
D	37	34	5H	10.44	8.62	0.68	9.76	Yes
D	23	12	3H	8.82	8.78	0.76	8.06	Yes
A	45	41	5H	8.33	8.25	1.66	6.67	Yes
A	18	23	5H	5.54	6.72	0.50	5.04	Yes
A	27	43	3H	4.99	4.82	0.32	4.67	Yes
D	12	9	3H	5.02	4.01	0.76	4.26	Yes
D	11	9	3H	4.28	5.16	0.39	3.89	Yes
B	7	9	3H	4.25	4.13	0.55	3.70	Yes
D	19	7	3H	3.95	3.79	0.29	3.66	Yes
A	6	91	5H	4.18	2.01	0.68	3.50	DSI 0.52V No RPC Conf.
A	8	60	3H	3.91	3.29	0.47	3.44	Yes
A	29	88	3H	3.91	1.55	0.49	3.42	Yes
D	35	29	3H	3.62	1.21	0.32	3.30	Yes
A	6	19	8H	3.46	3.05	0.41	3.05	Yes
A	43	35	5H	3.52	3.53	0.49	3.03	Yes
D	33	20	3H	3.83	3.68	0.80	3.03	DSI 0.73V No RPC Conf.
A	3	13	5H	3.30	0.9	0.49	2.81	Yes
A	37	88	3H	2.99	3.35	0.27	2.72	Yes
A	30	24	5H	2.93	2.02	0.28	2.65	Yes
B	15	88	3H	3.62	5.64	1.00	2.62	Yes
A	42	44	3H	3.73	3.11	1.13	2.60	Yes
D	11	12	3H	3.21	3.41	0.63	2.58	Yes
D	16	42	3H	3.12	3.43	0.54	2.58	Yes
A	45	55	3H	3.02	2.79	0.59	2.43	Yes
A	33	75	3H	3.04	3.08	0.63	2.41	Yes
A	32	85	3H	2.46	1.62	0.21	2.25	Yes
A	42	54	5H	2.56	2.31	0.34	2.22	Yes
A	47	75	5H	3.44	0.4	1.23	2.21	Yes
A	35	42	3H	2.96	3.07	0.76	2.2	Yes
D	2	105	3H	2.84	2.32	0.67	2.17	Yes
D	32	27	5H	2.48	2.52	0.36	2.12	Yes
A	45	26	7H	2.42	2.32	0.34	2.08	Yes
A	4	12	5H	3.06	3.19	1.01	2.05	Yes
A	4	16	3H	3.23	2.08	1.18	2.05	Yes
A	10	67	5H	2.48	1.56	0.43	2.05	Yes
C	20	24	3H	2.38	1.56	0.35	2.03	Yes

Table 7-8					
Braidwood Unit 1 A1RO4 Pulled Tube EC Results					
Tube	I.D.	Bobbin Voltage	Bobbin Call	RPC Call	RPC Voltage
SG A					
R27C43	1H	-	NDD	NDD	-
	3H	4.88	85%	SAI	5.28
	5H	-	NDD	NDD	-
R42C44	1H	-	NDD	NDD	-
	3H	3.73	68%	MAI	3.24 max.
	5H	2.09	49%	SAI	1.62
	7H	-	NDD	NDD	-
SG D					
R37C34	1H	-	NDD	NDD	-
	3H	1.04	92%	SAI	0.31
	5H	10.44	82%	SAI	8.77
R16C42	1H	-	NDD	NDD	-
	3H	3.12	70%	MAI	1.70 max.
	5H	0.61 *	NDD	NDD	-

* Indication not reported in field inspection

Figure 7-1 Braidwood Unit 1 Number of Indications as Function of Elevation

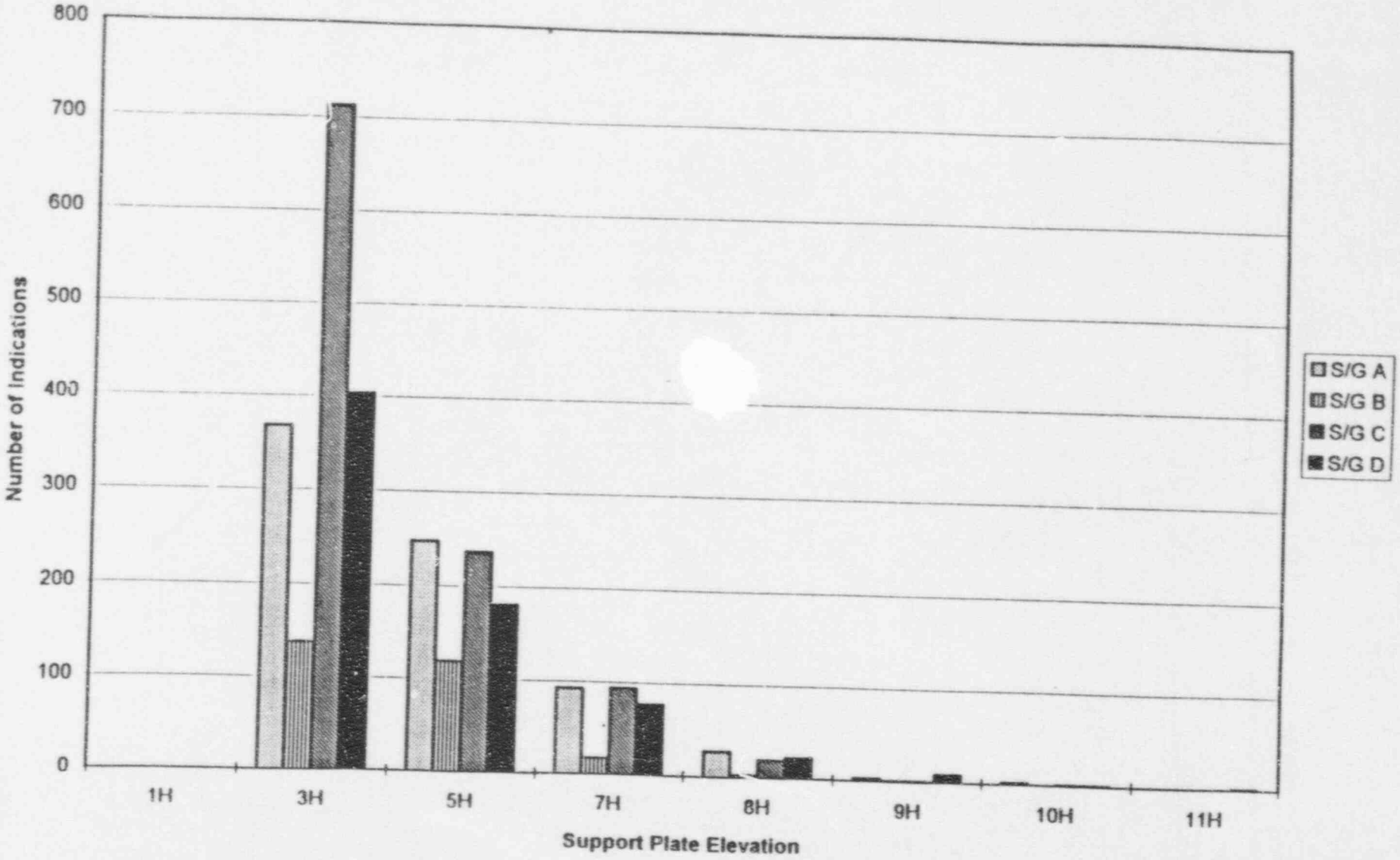

Figure 7-2 Braidwood Unit 1 S/G A Bobbin Statistics 4/94 Inspection

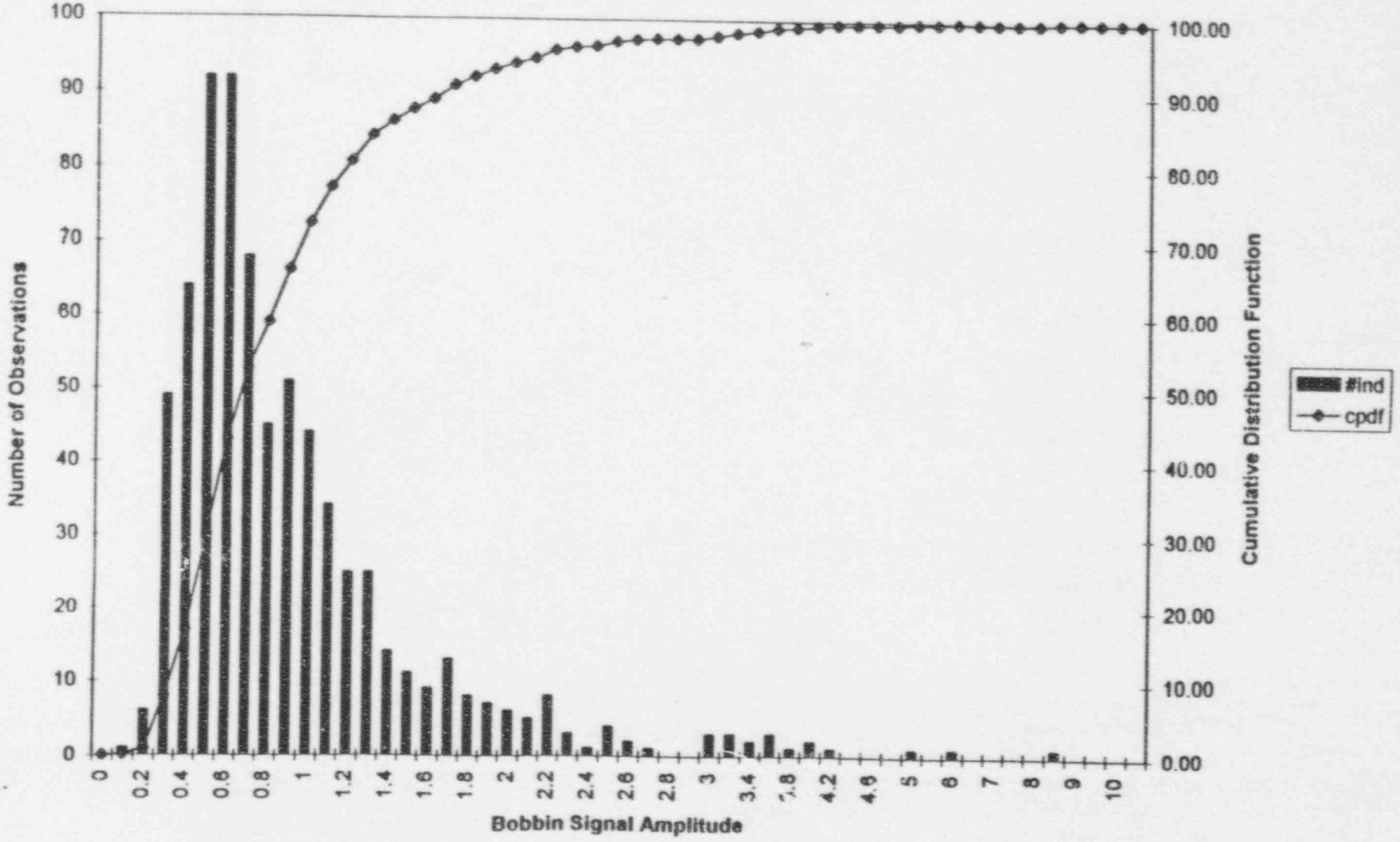

Figure 7-3 Braidwood Unit 1 S/G B Bobbin Statistics 4/94 Inspection

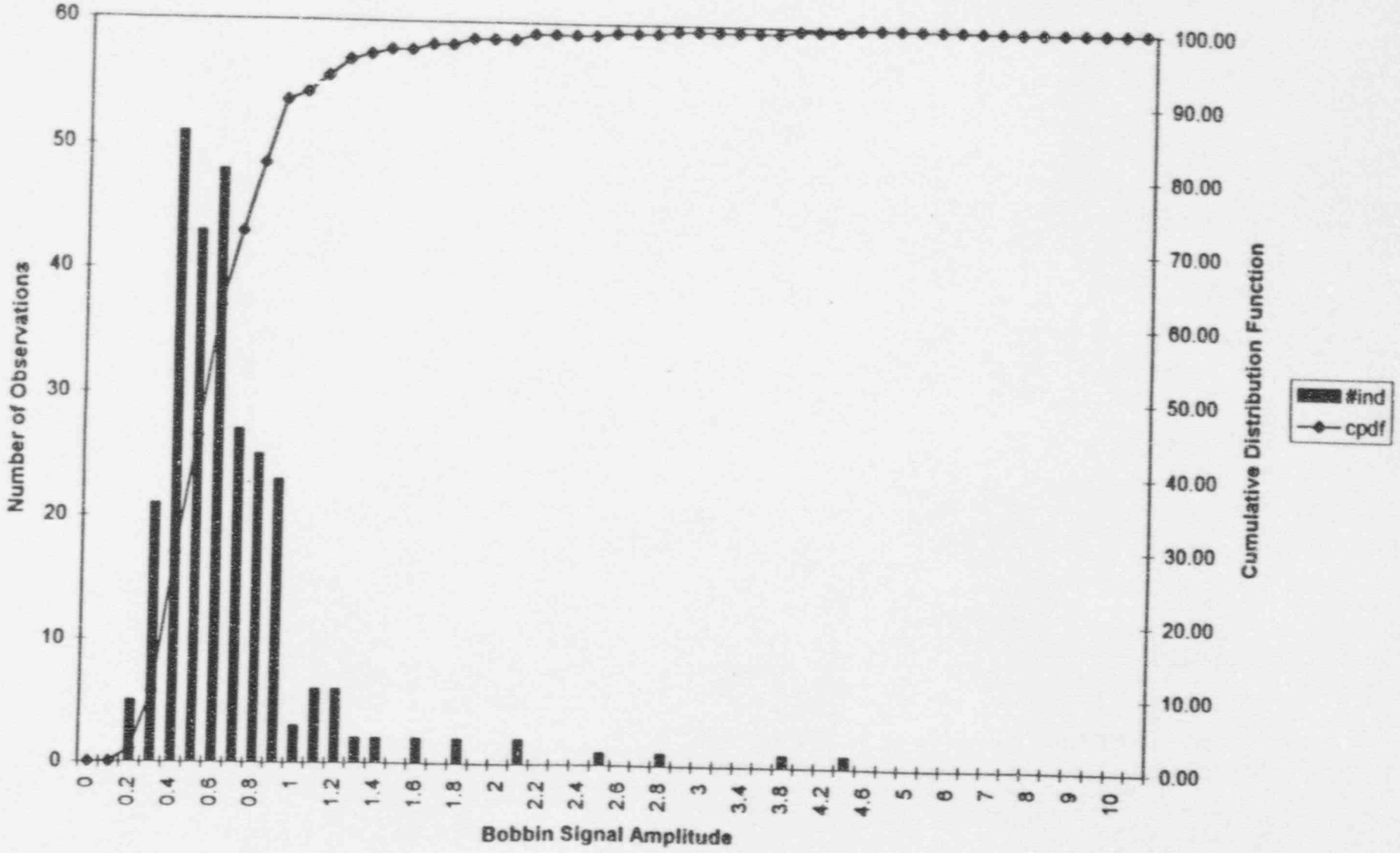

Figure 7-4 Braidwood Unit 1 S/G C Bobbin Statistics 4/94 Inspection

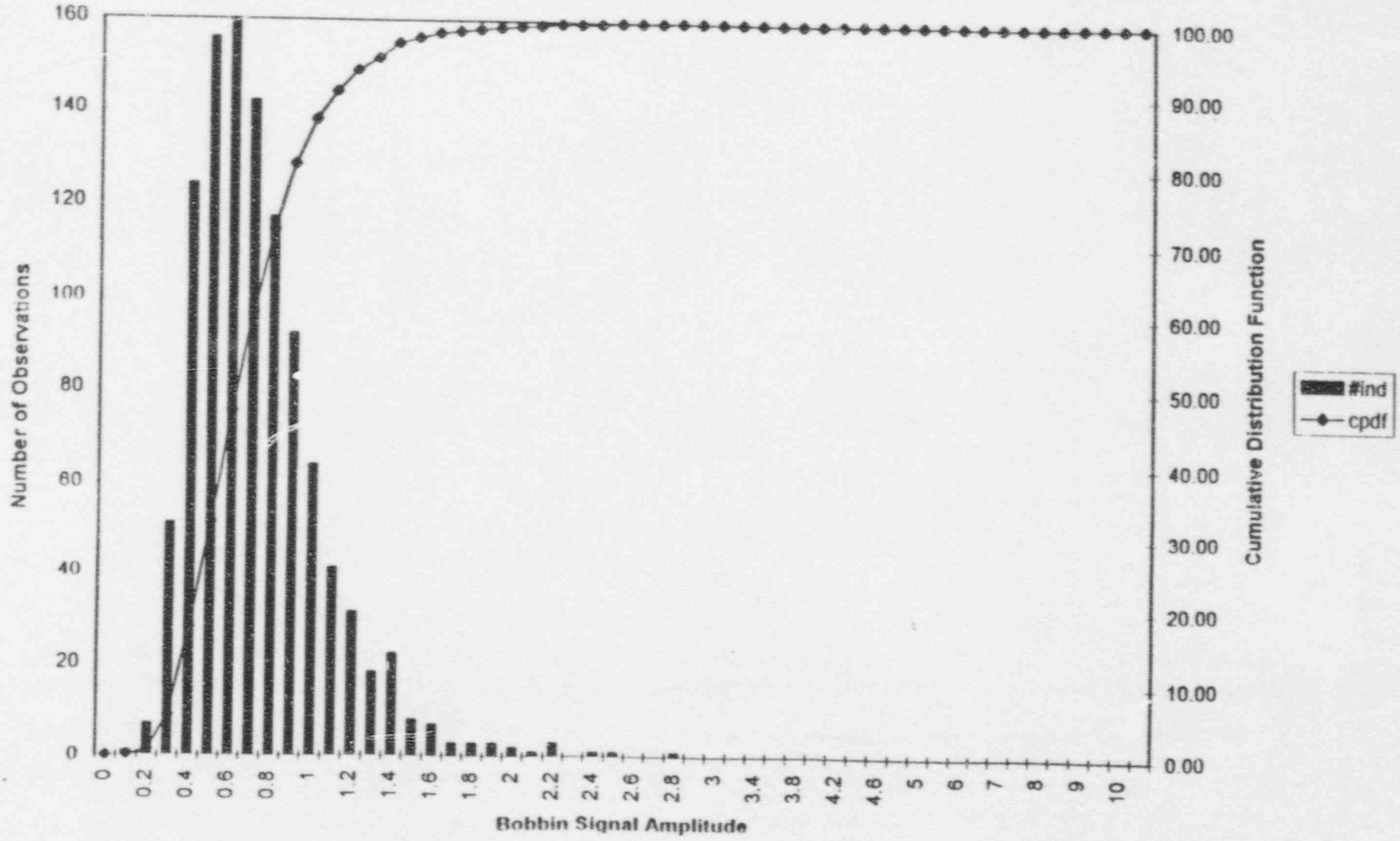

Figure 7-5 Braidwood Unit 1 S/G D Bobbin Statistics 4/94 Inspection

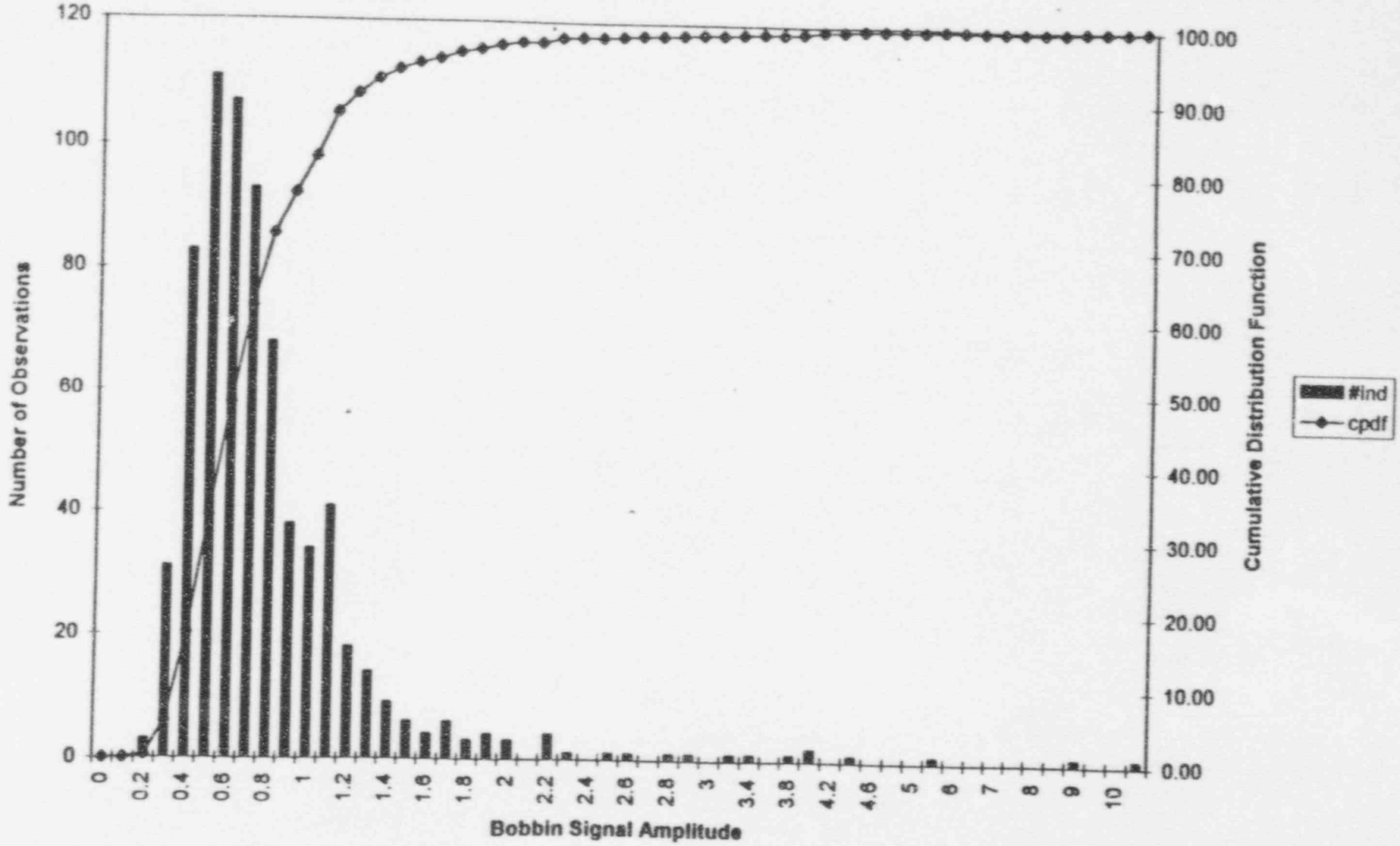

Figure 7-6 Braidwood Unit 1 All S/G's - Bobbin Statistics 4/94 Inspection

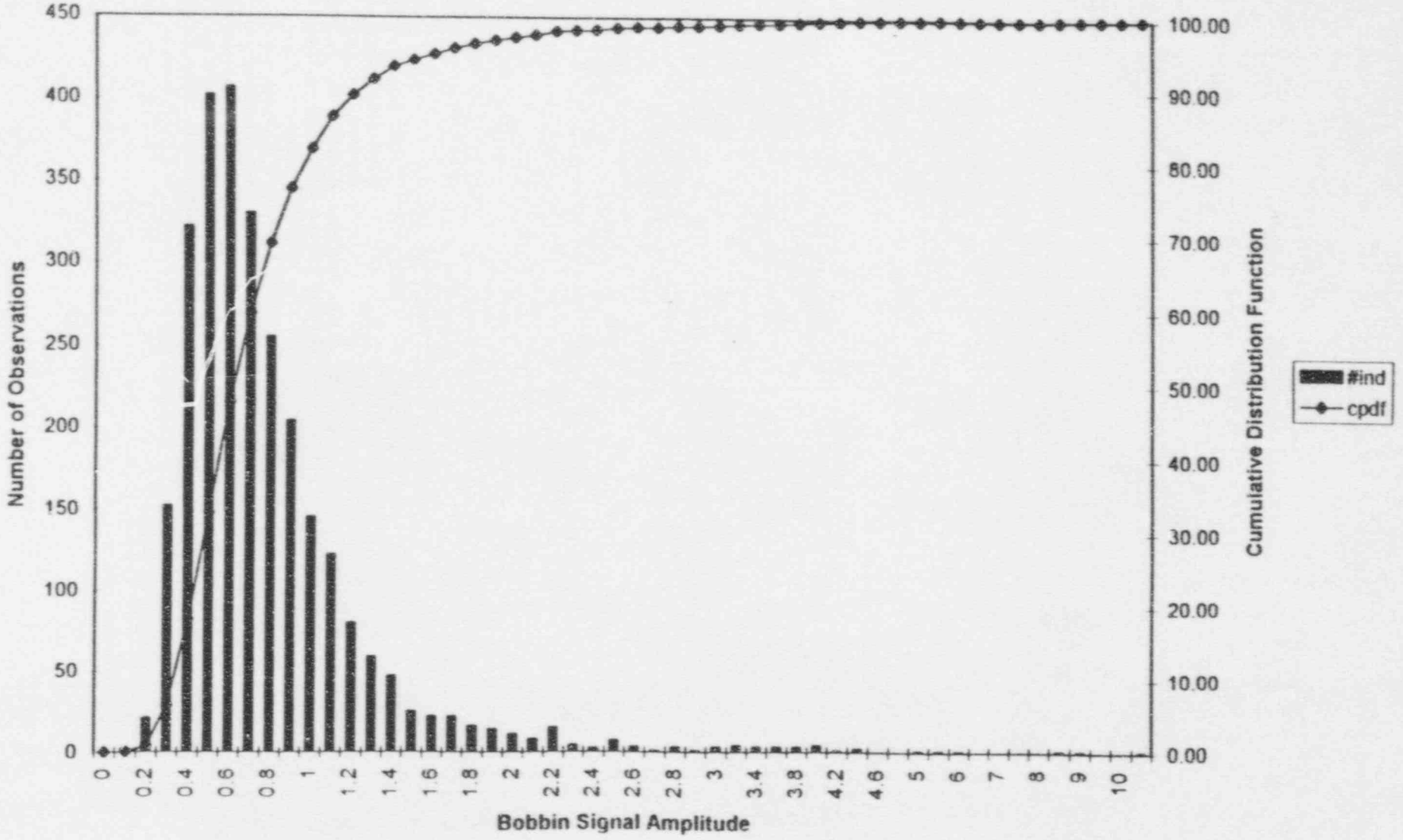

Figure 7-7 Braidwood Unit 1 All S/G's RPC Statistics 4/94 Inspection

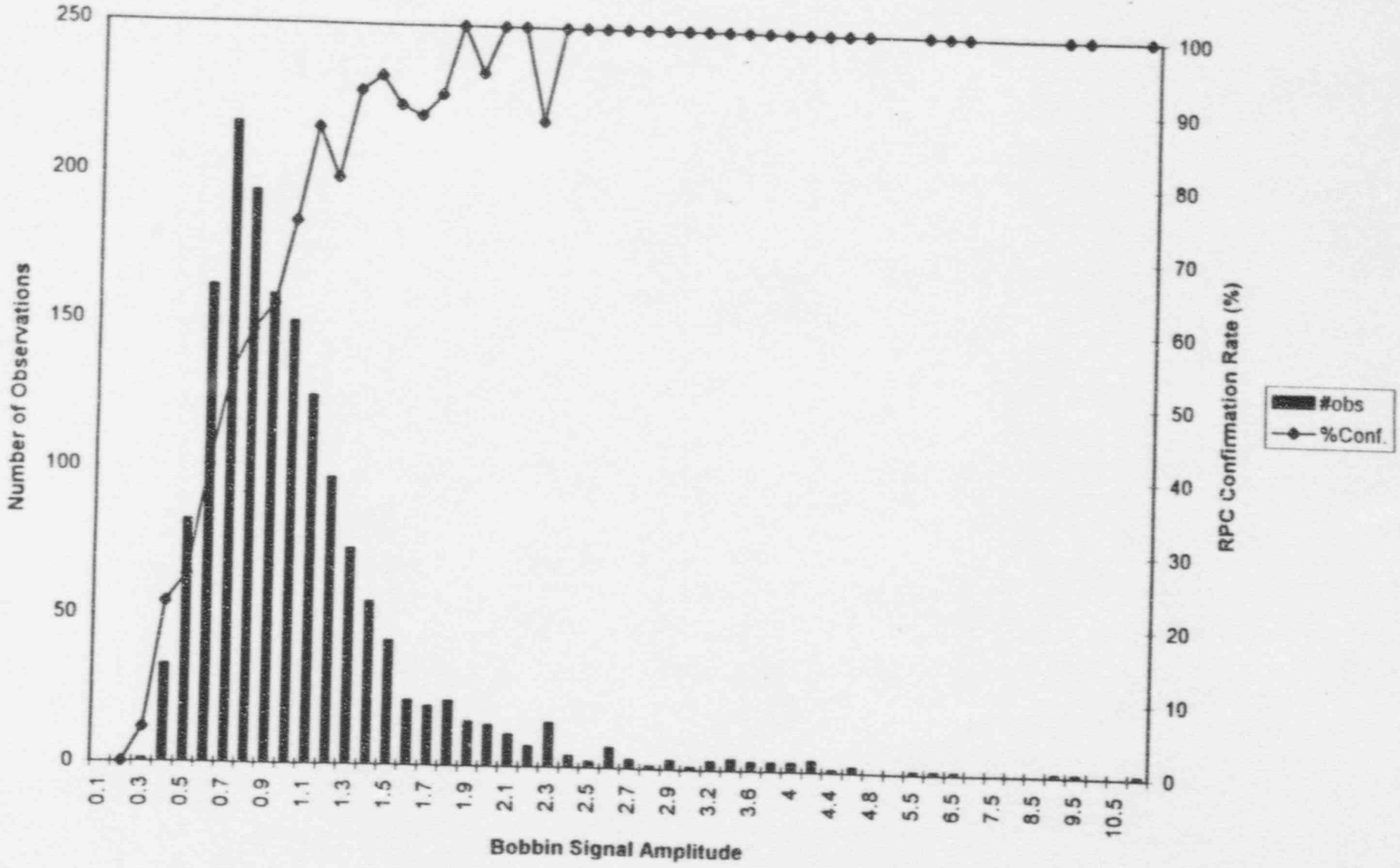

Figure 7-8. Braidwood Unit 1 SG C TSP Amplitude Distribution

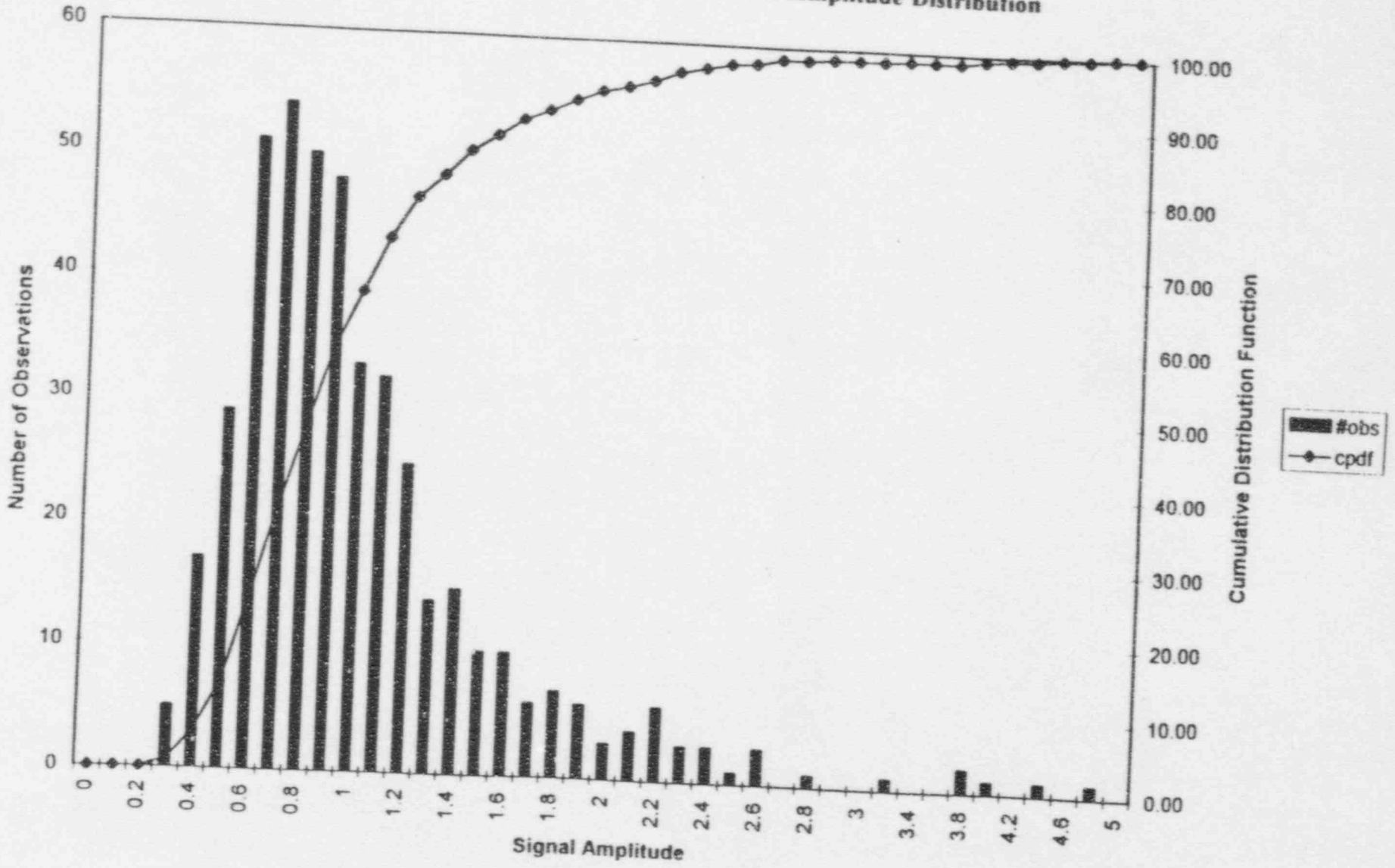

Figure 7-9. Braidwood Unit 1 9/92 TSP Indication Distribution

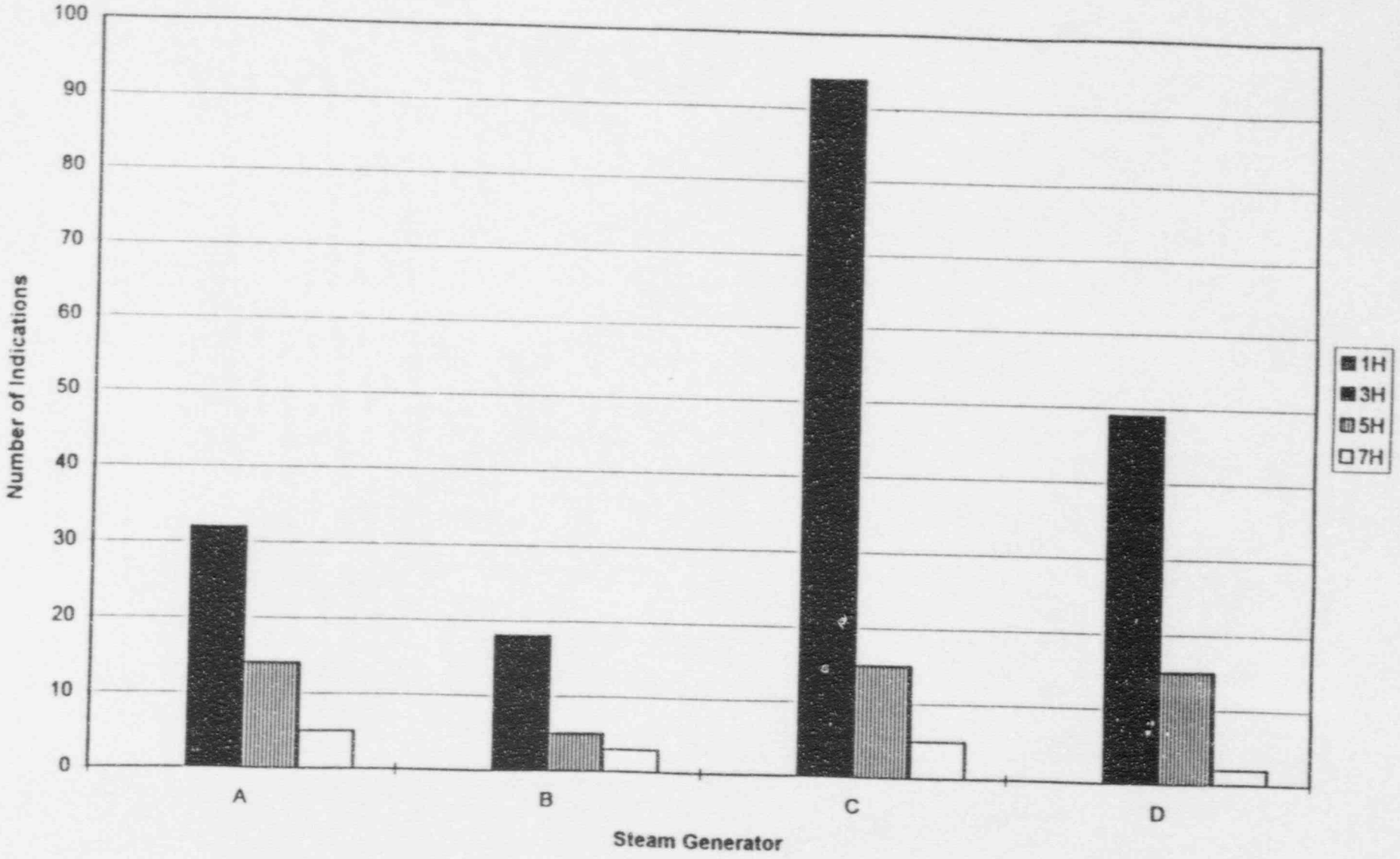

CCEMISC XLS

Figure 7-10. Braidwood Unit 1 9/92 Inspection Amplitude Distribution of Confirmed Bobbin Indications

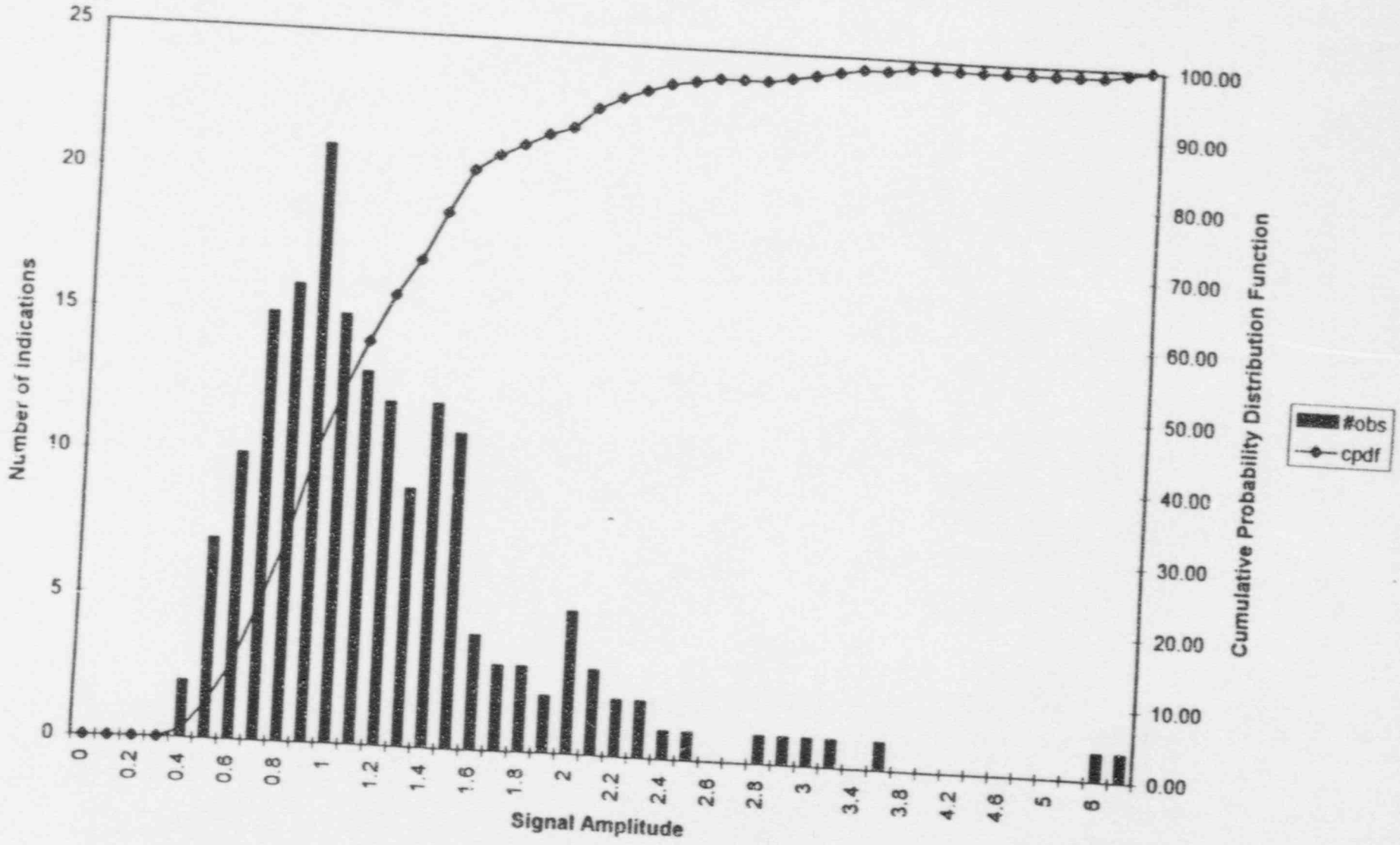

CCEMISC XLS

Figure 7-11. Braidwood Unit 1 1994 Inspection, Support Plate ODSCC Signal Progression

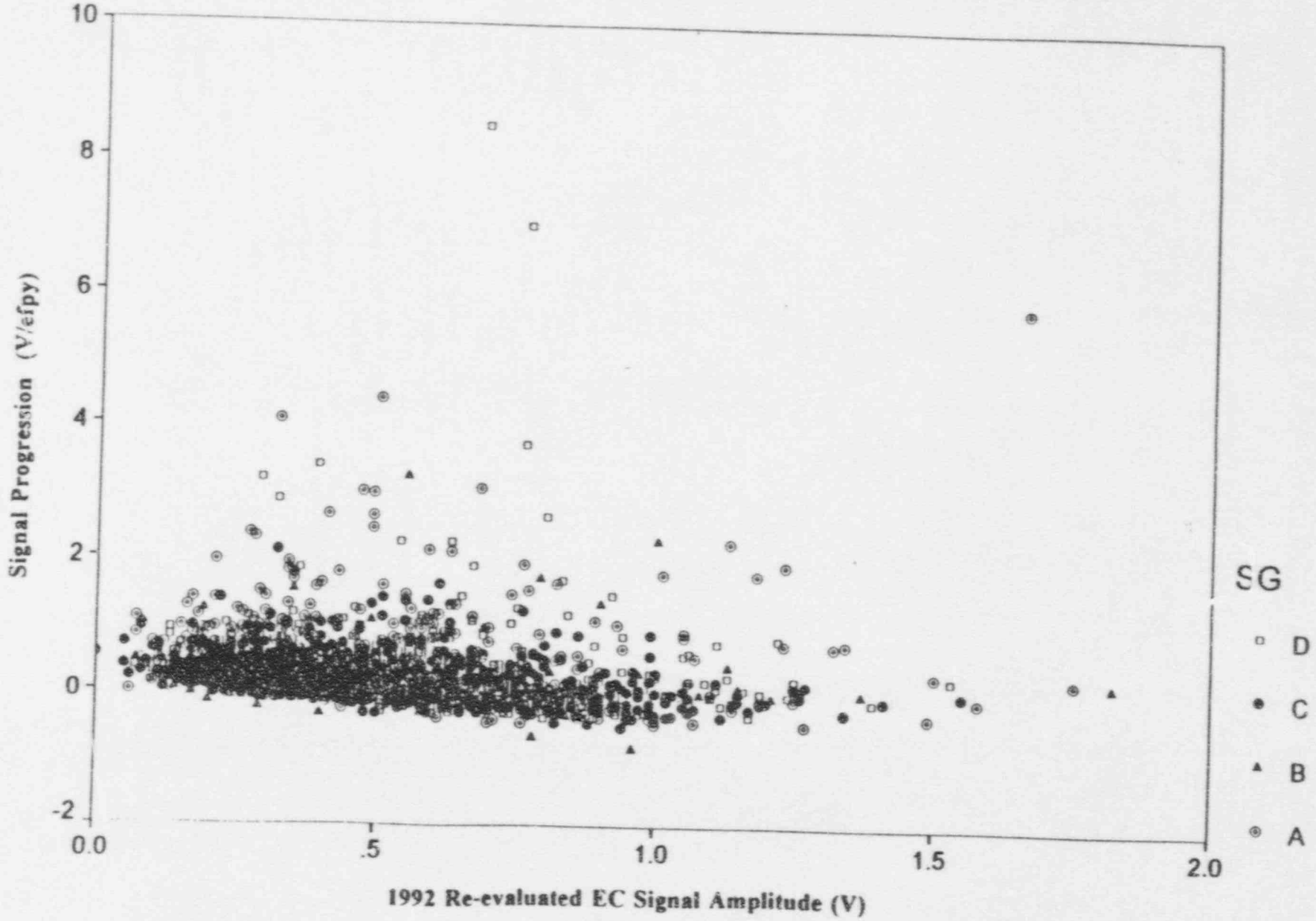

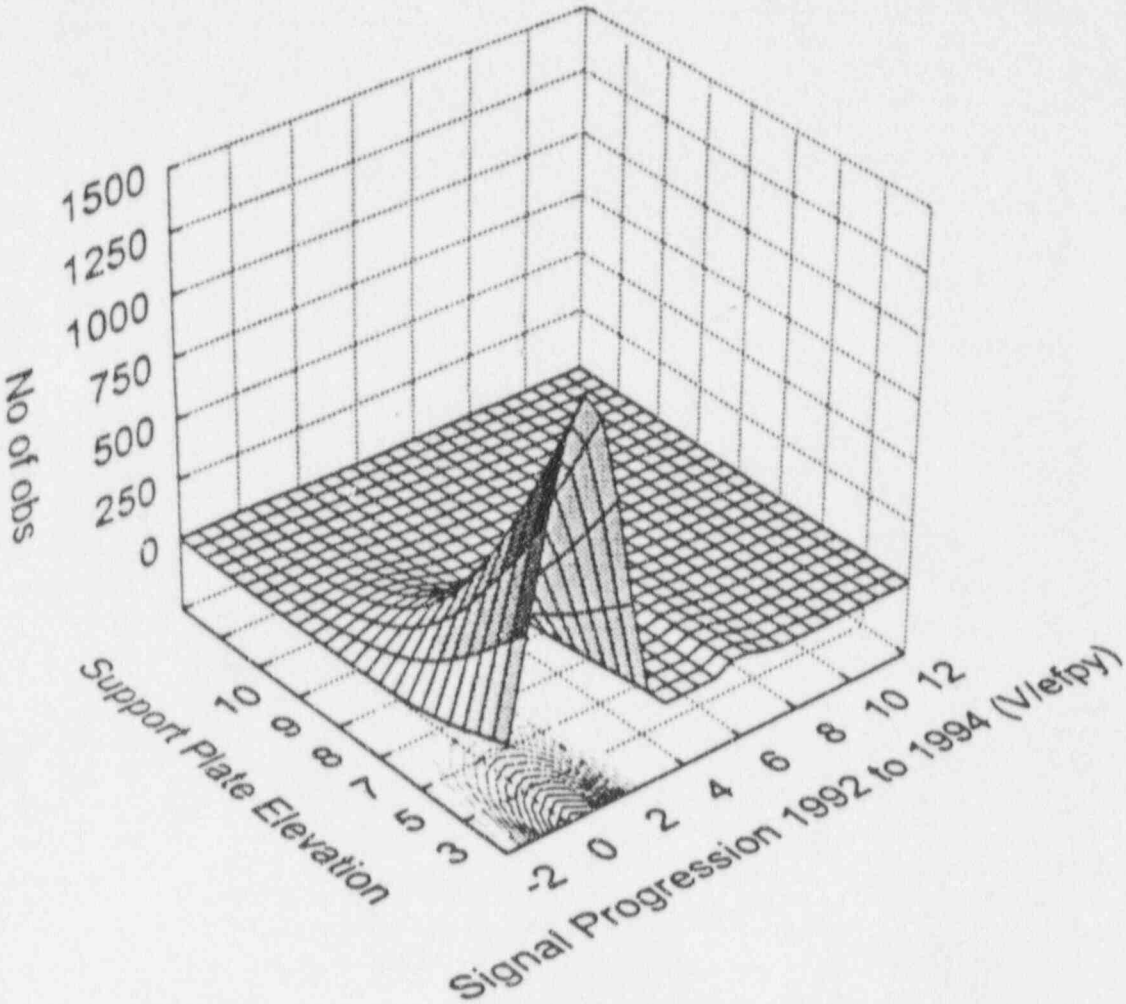

Figure 7-12. Braidwood Unit 1 1994 Inspection Results, Support Plate ODSCC EC Signal Progression

Figure 7-13. Braidwood Unit 1 TSP Bobbin Signal Progression
1991 - 1992, All SGs

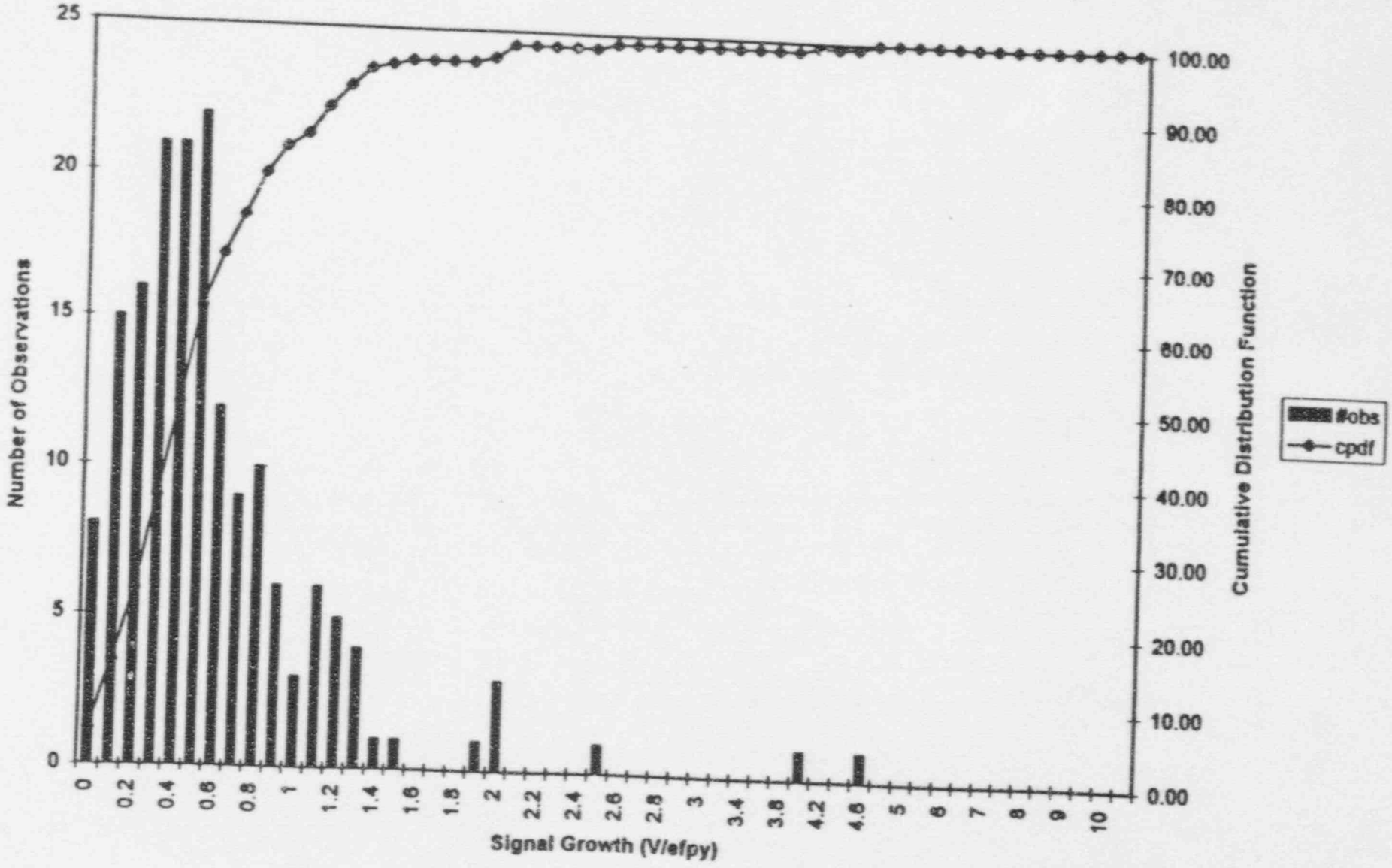

Figure 7-14. Braidwood Unit 1 TSP Bobbin Signal Progression
1992 - 1993, SG C

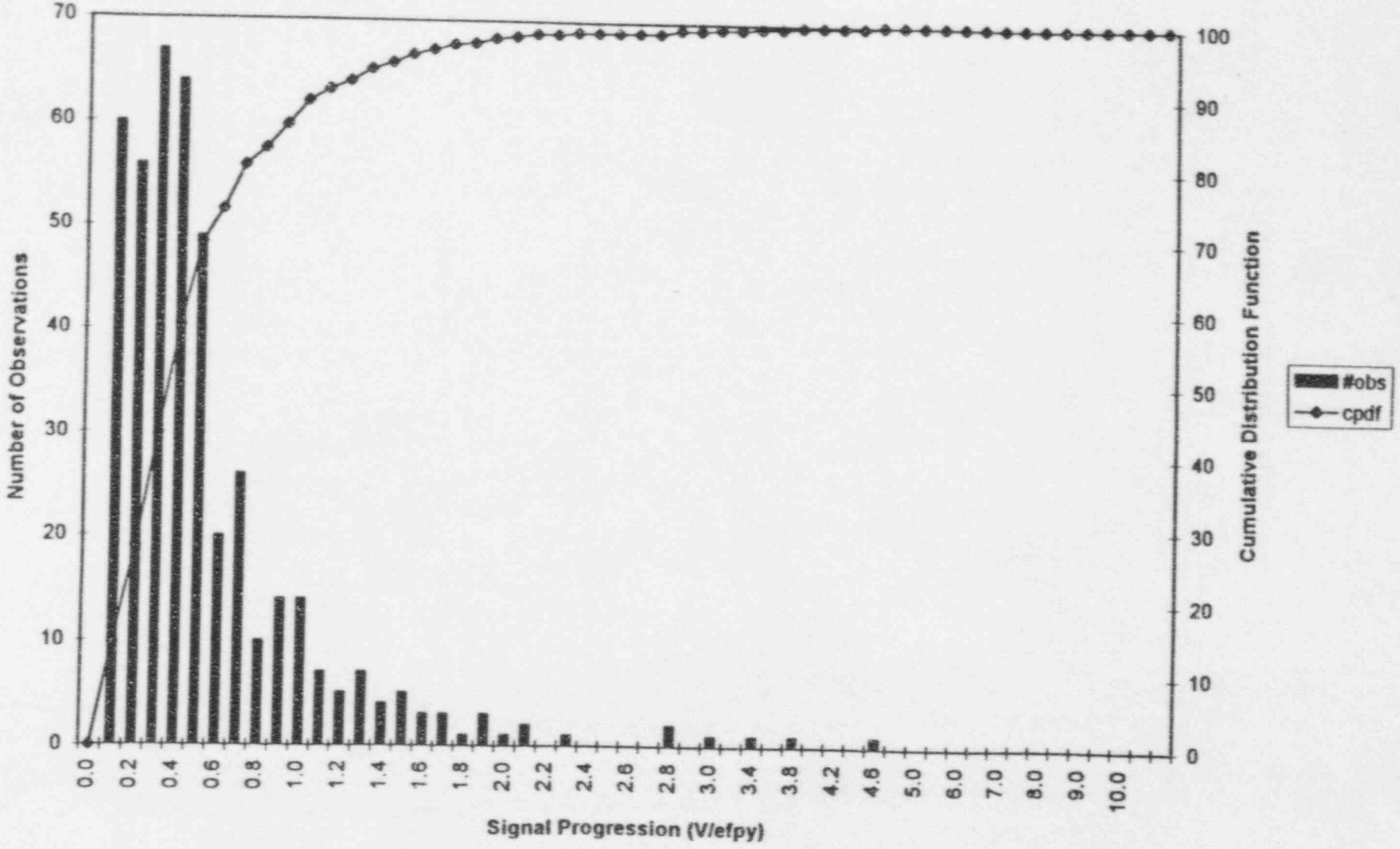

Figure 7-15 Braidwood Unit 1 S/G A TSP Bobbin Progression 92-94

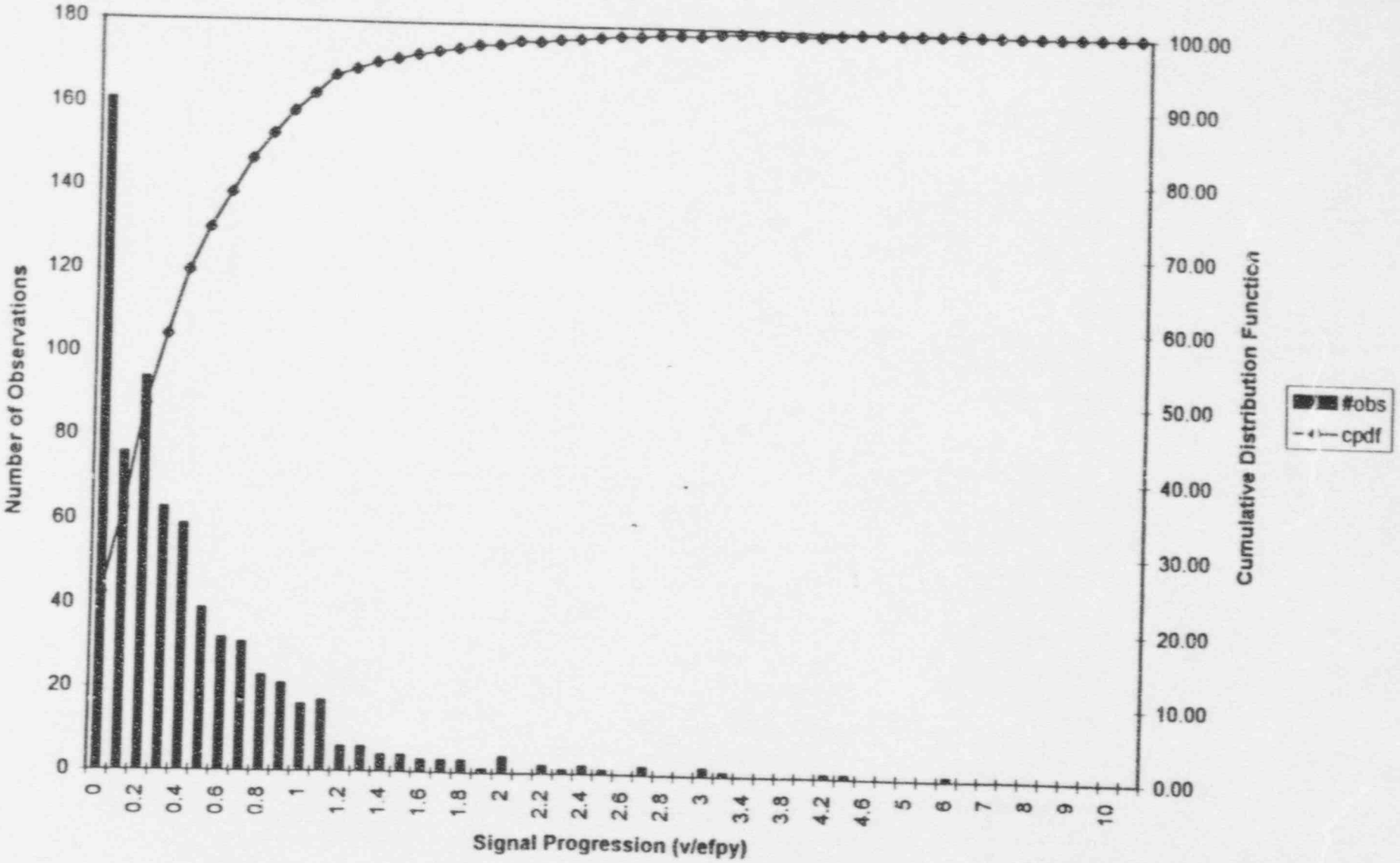

Figure 7-16 Braidwood Unit 1 S/G B TSP Bobbin Progression 92-94

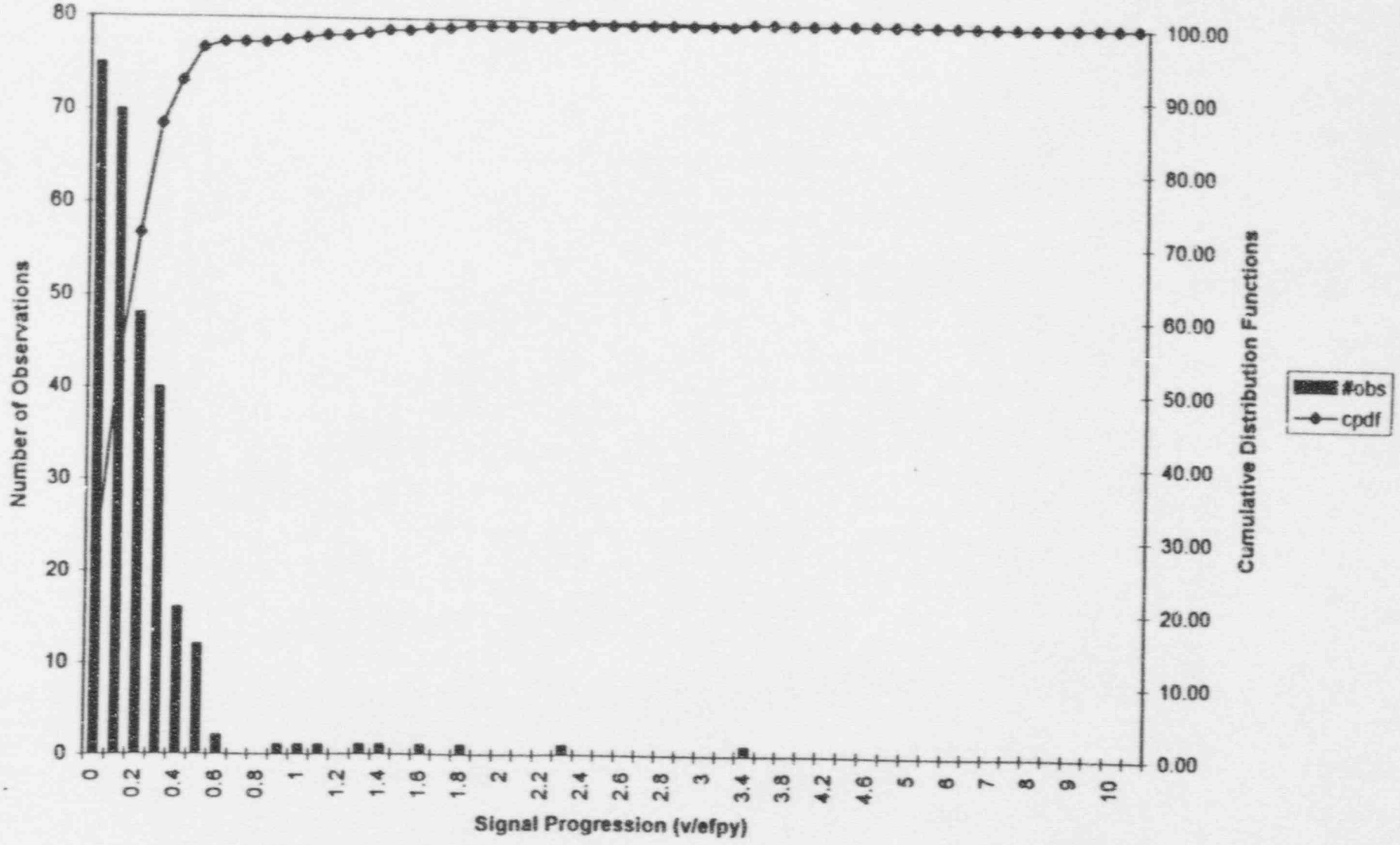

Figure 7-17 Braidwood Unit 1 S/G C TSP Bobbin Progression 92-94

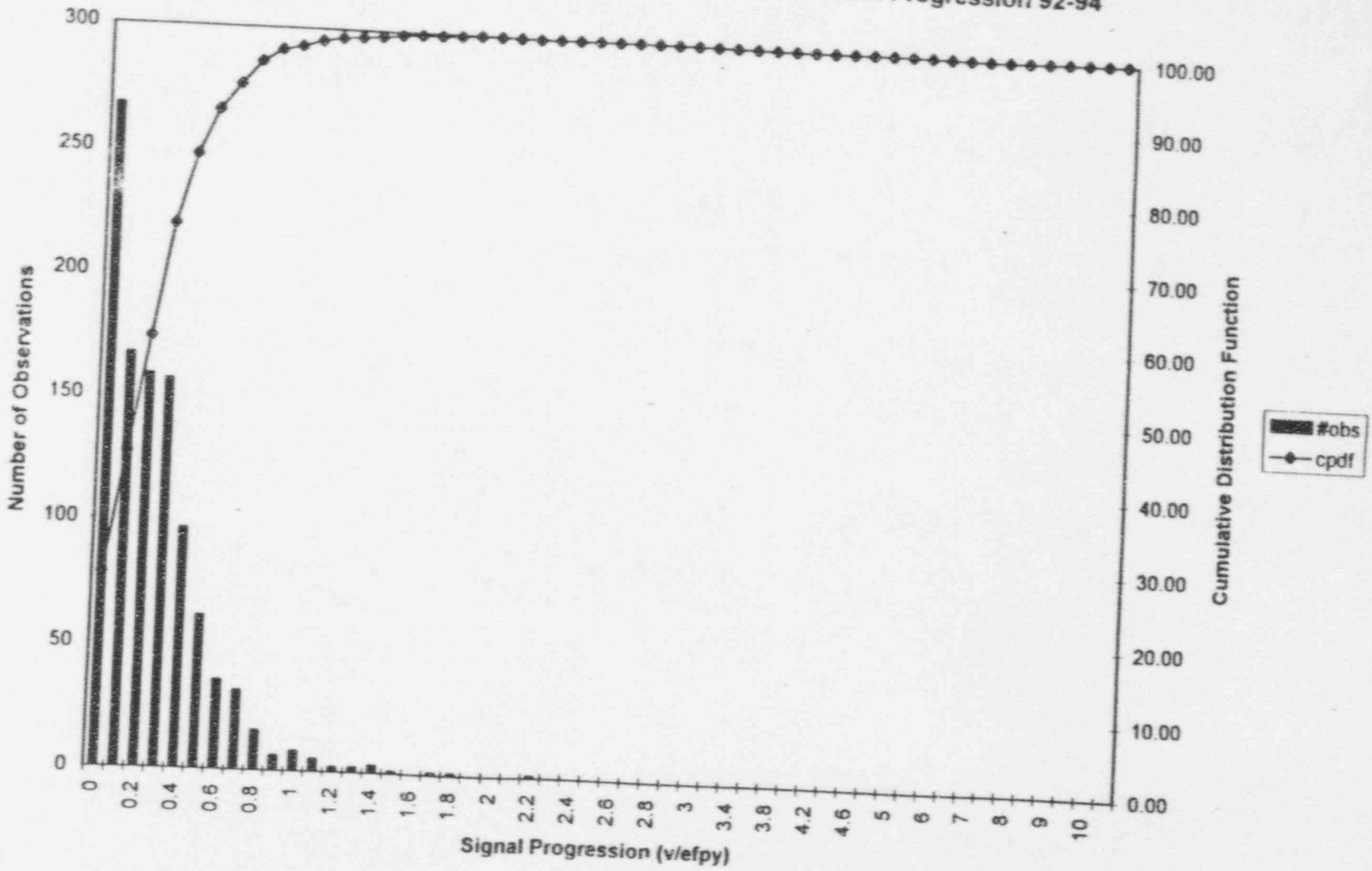

Figure 7-18 Braidwood Unit 1 S/G D TSP Bobbin Progression 92-94

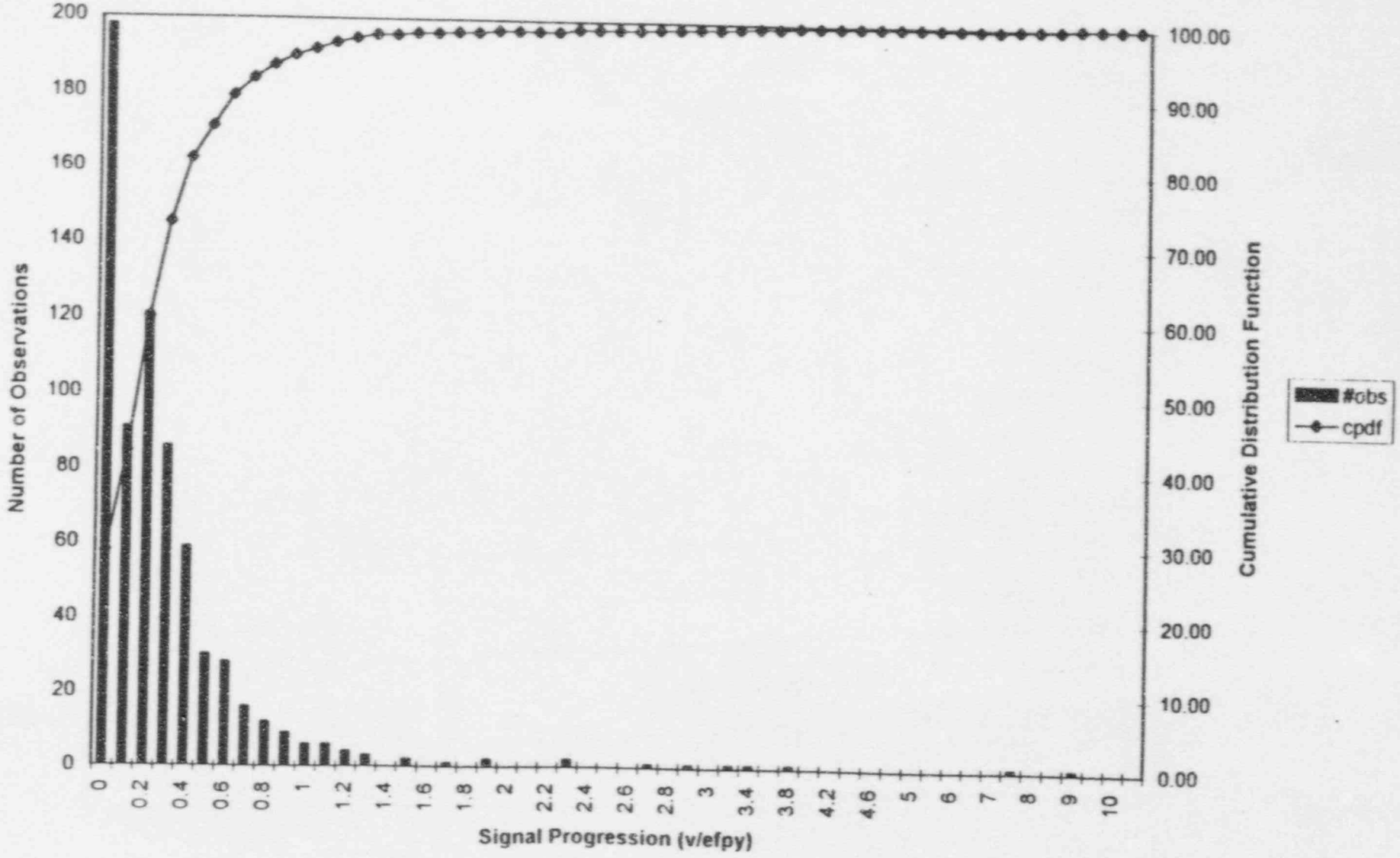

Figure 7-19

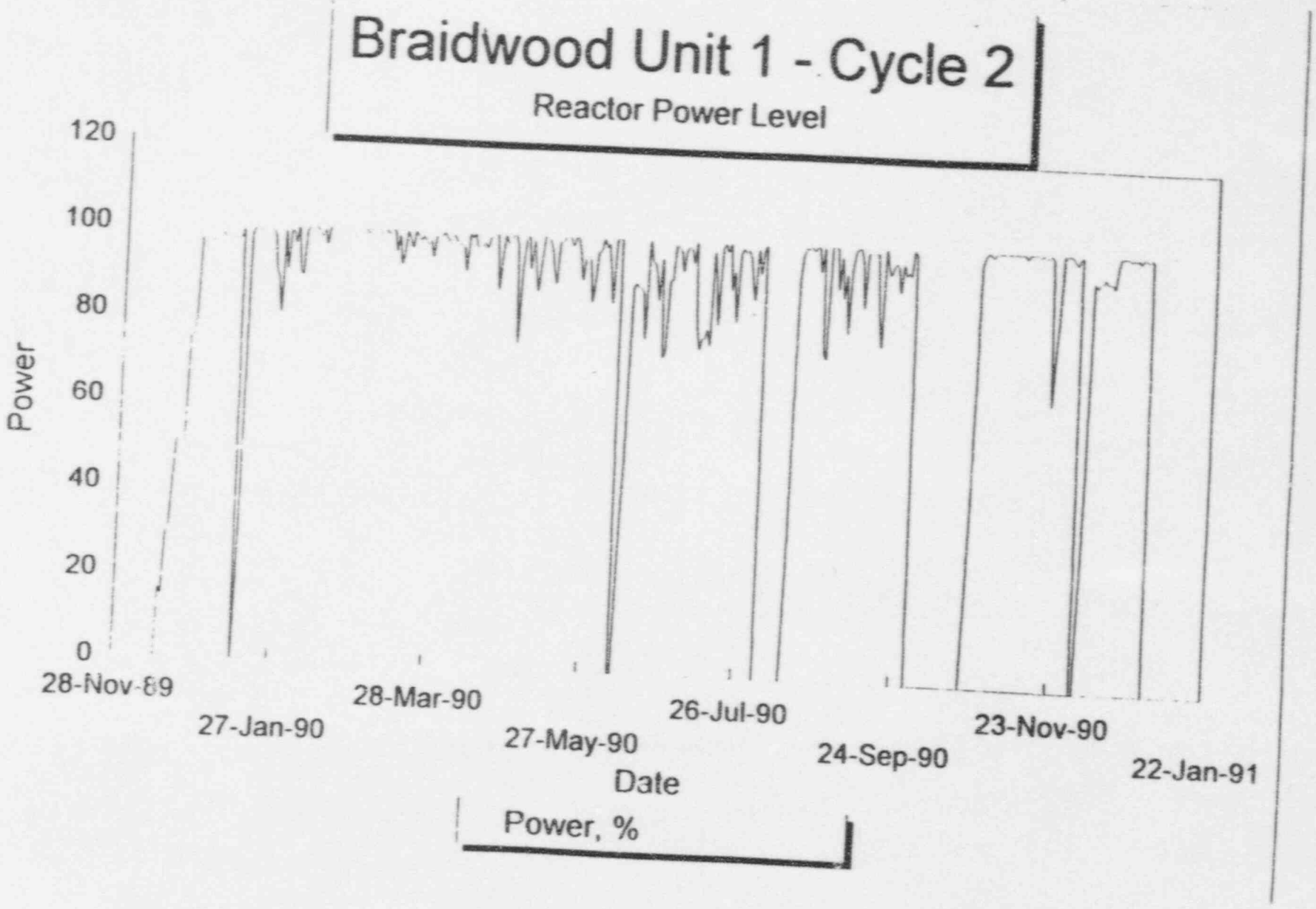
Braidwood Unit 1 - Cycle 2
Reactor Power Level
120
100
80
60
40
20
0
Power
28-Nov-89
27-Jan-90
28-Mar-90
27-May-90
26-Jul-90
24-Sep-90
23-Nov-90
22-Jan-91
Date
Power, %

Figure 7-20

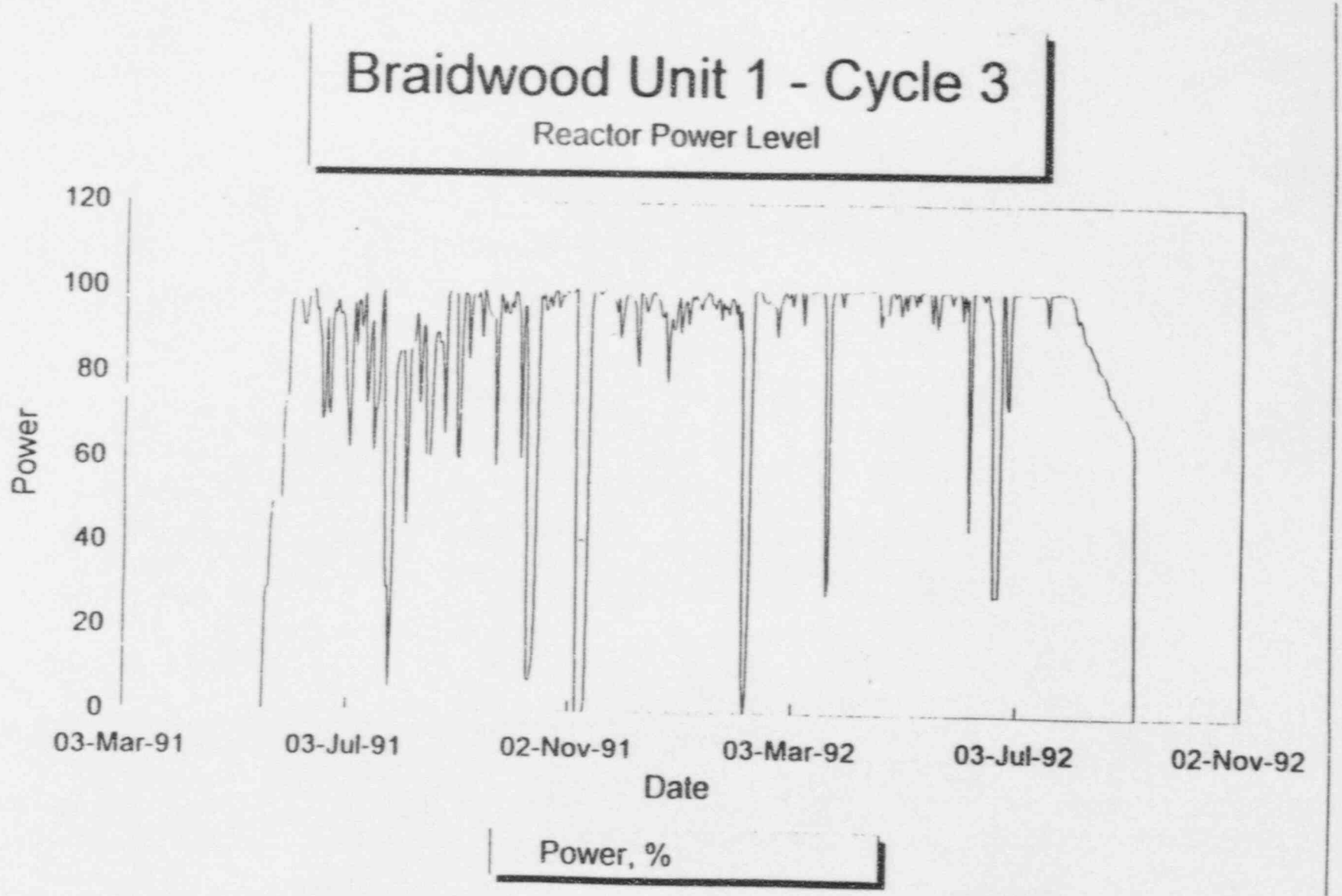
Braidwood Unit 1 - Cycle 3
Reactor Power Level
120
100
80
60
40
20
0
Power
03-Mar-91
03-Jul-91
02-Nov-91
03-Mar-92
03-Jul-92
02-Nov-92
Date
Power, %

Figure 7-21

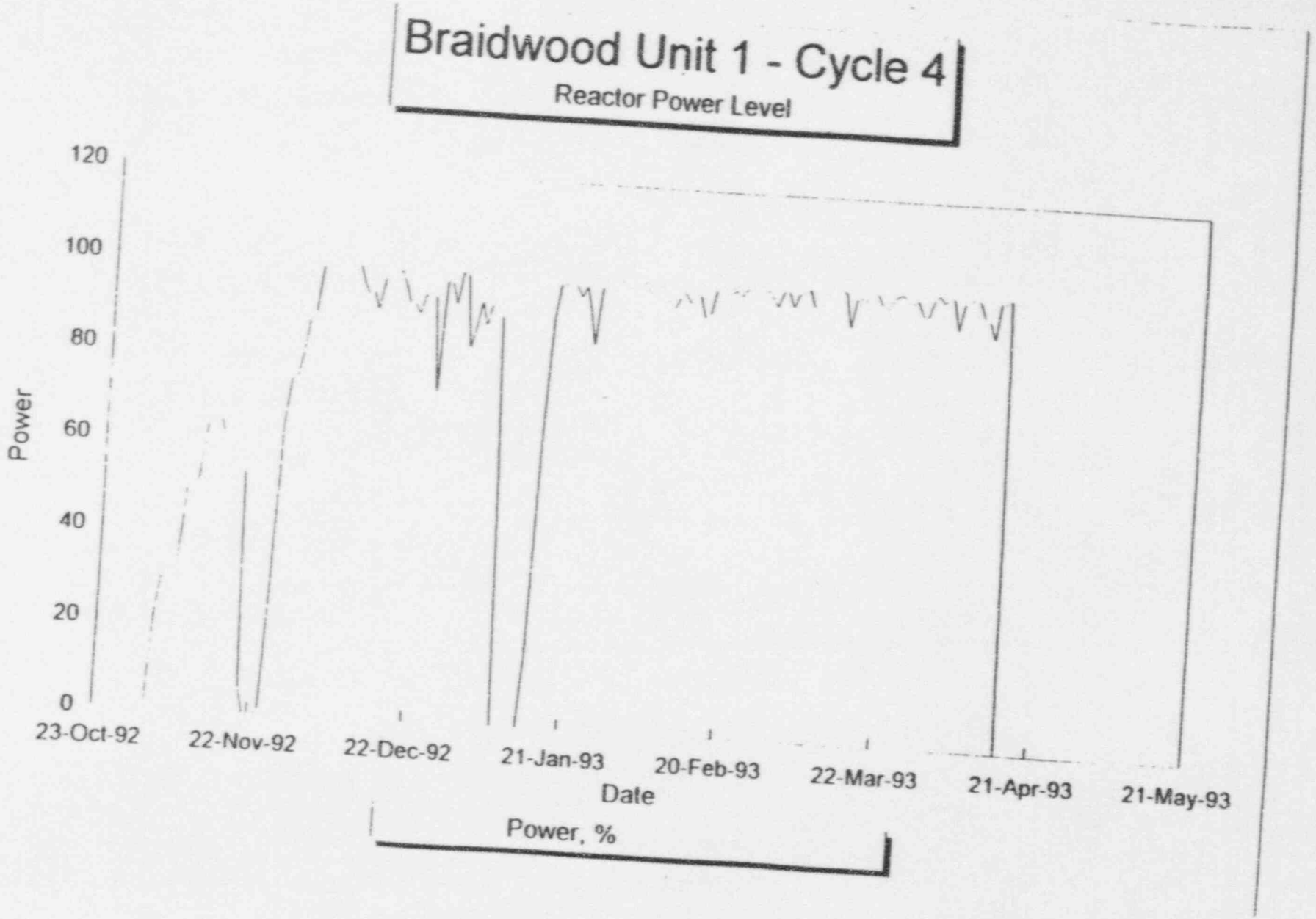
Braidwood Unit 1 - Cycle 4
Reactor Power Level
120
100
80
60
40
20
0
Power
23-Oct-92
22-Nov-92
22-Dec-92
21-Jan-93
20-Feb-93
22-Mar-93
21-Apr-93
21-May-93
Date
Power, %

Figure 7-22

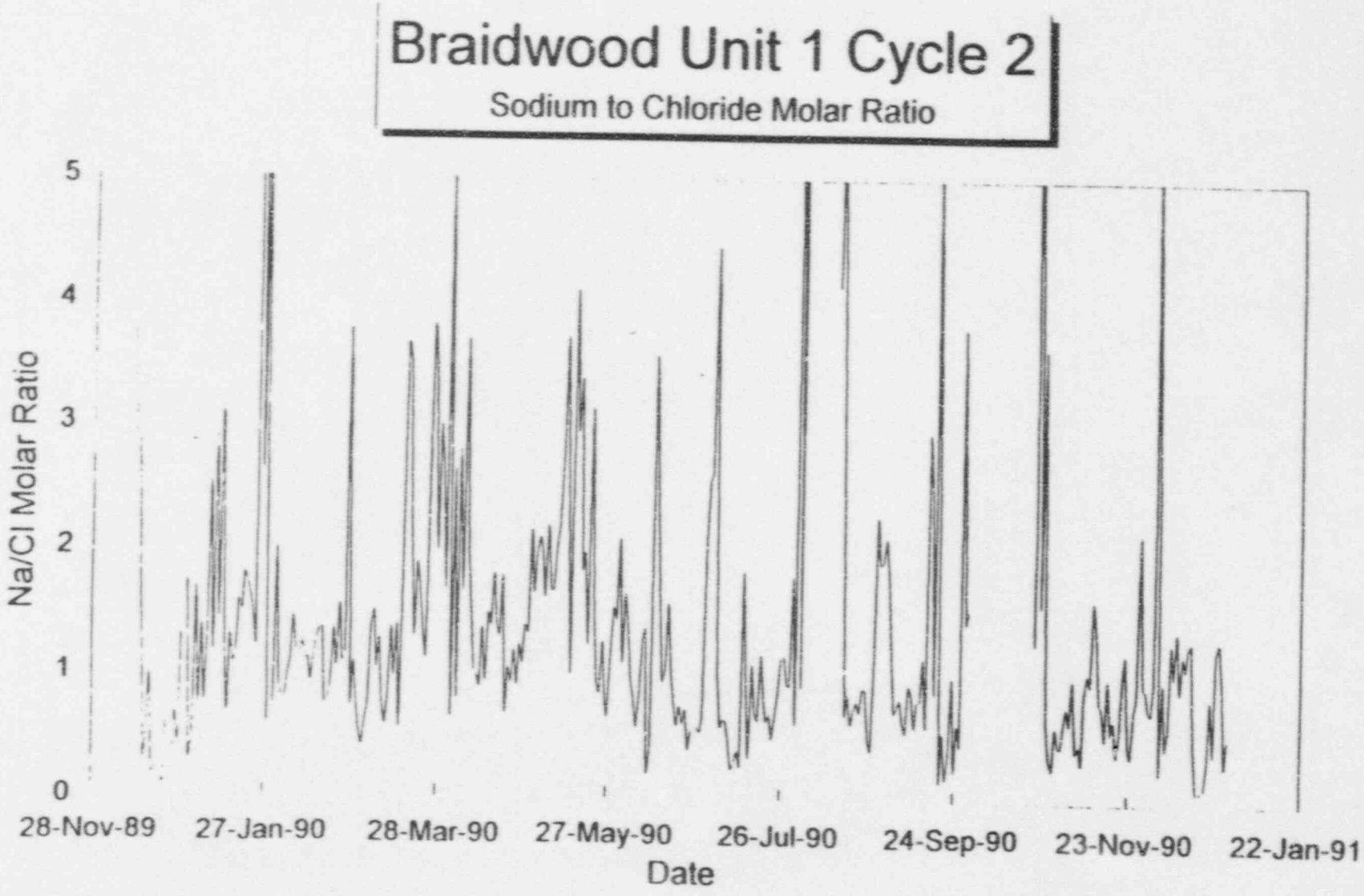
Braidwood Unit 1 Cycle 2
Sodium to Chloride Molar Ratio
Na/Cl Molar Ratio
0
1
2
3
4
5
28-Nov-89
27-Jan-90
28-Mar-90
27-May-90
26-Jul-90
24-Sep-90
23-Nov-90
22-Jan-91
Date

Figure 7-23

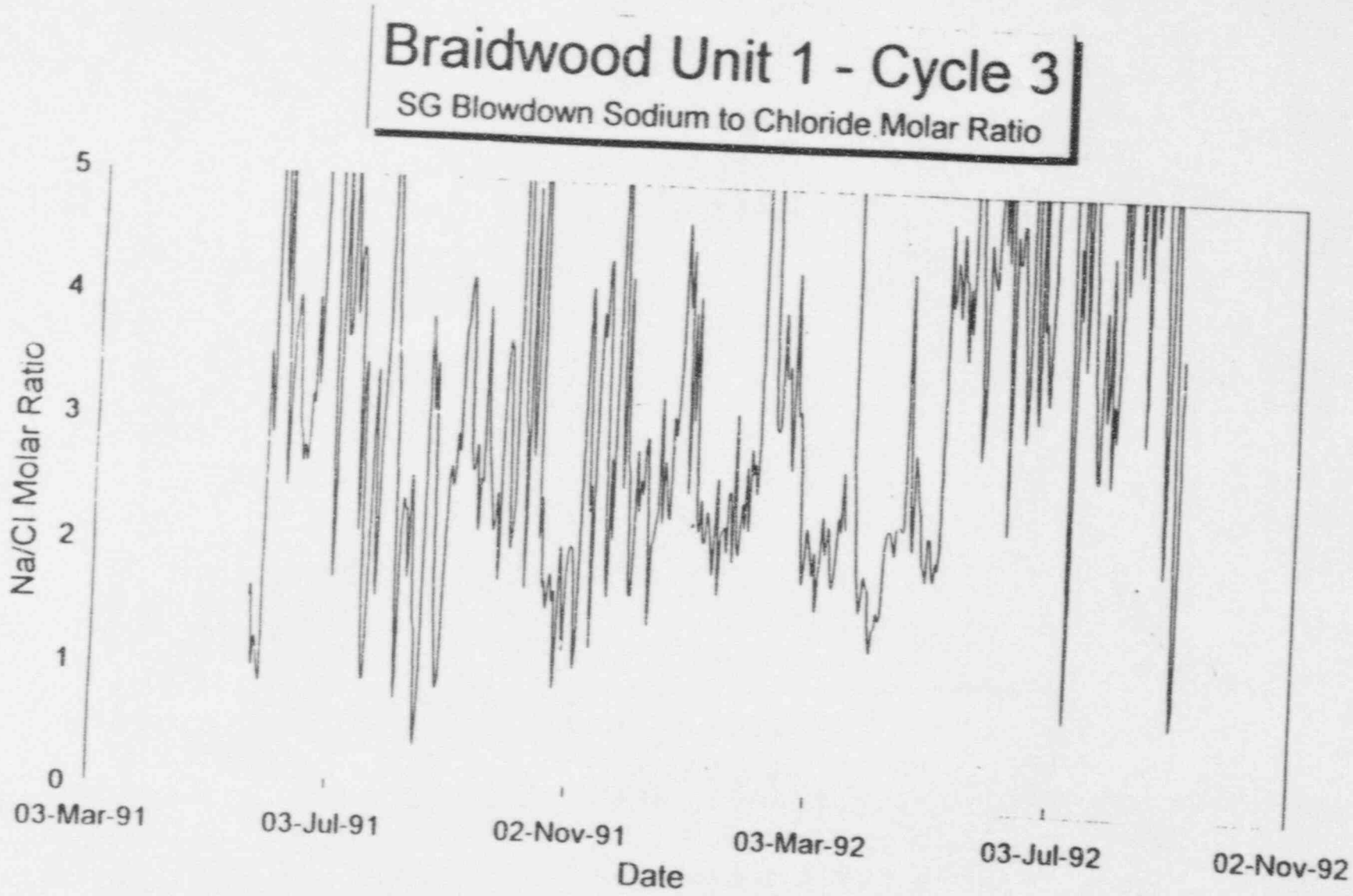
Braidwood Unit 1 - Cycle 3
SG Blowdown Sodium to Chloride Molar Ratio
Na/Cl Molar Ratio
5
4
3
2
1
0
03-Mar-91
03-Jul-91
02-Nov-91
03-Mar-92
03-Jul-92
02-Nov-92
Date

Figure 7-24

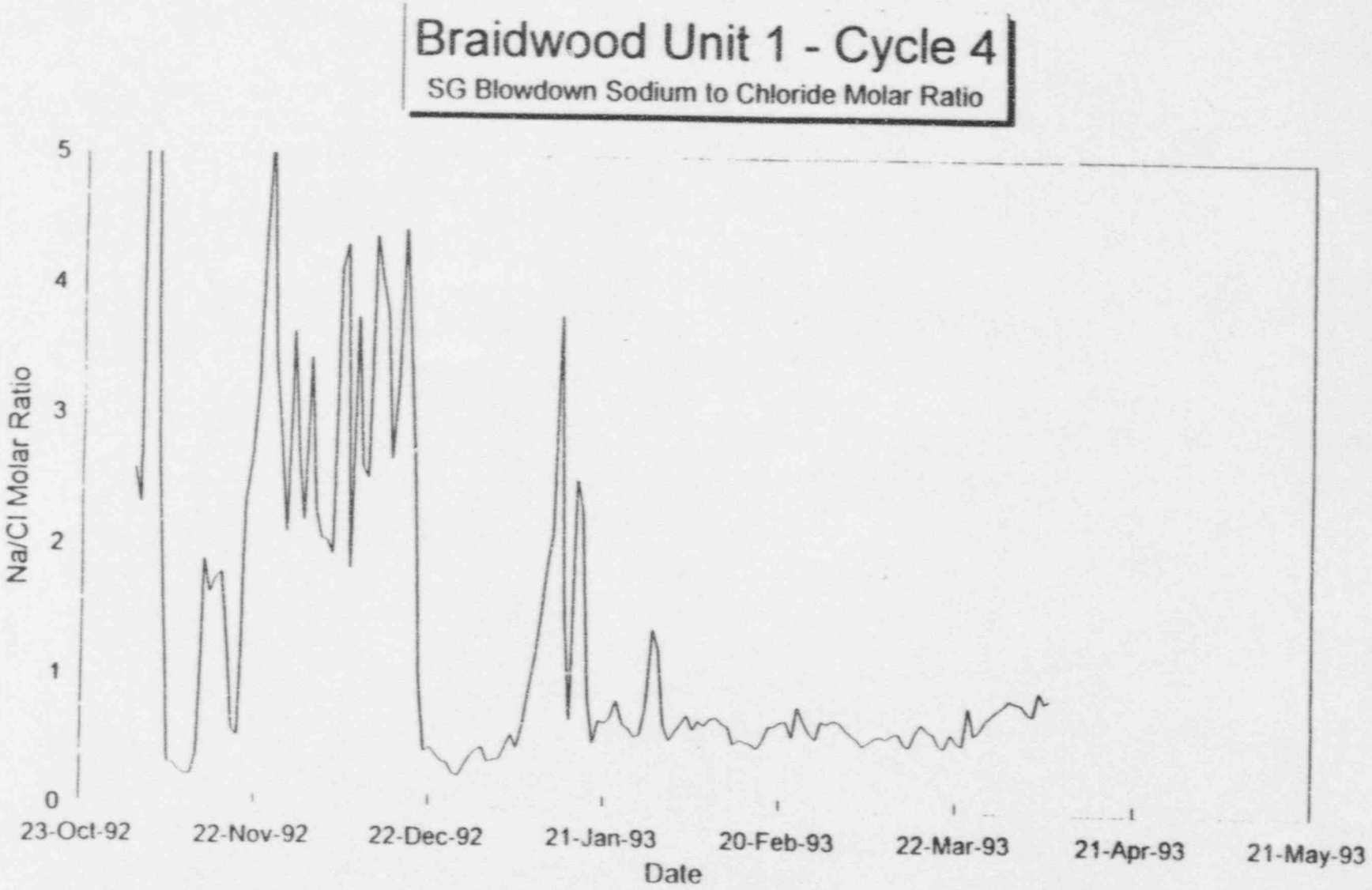
Braidwood Unit 1 - Cycle 4
SG Blowdown Sodium to Chloride Molar Ratio
Na/Cl Molar Ratio
0
1
2
3
4
5
23-Oct-92
22-Nov-92
22-Dec-92
21-Jan-93
20-Feb-93
22-Mar-93
21-Apr-93
21-May-93
Date

Figure 7-25

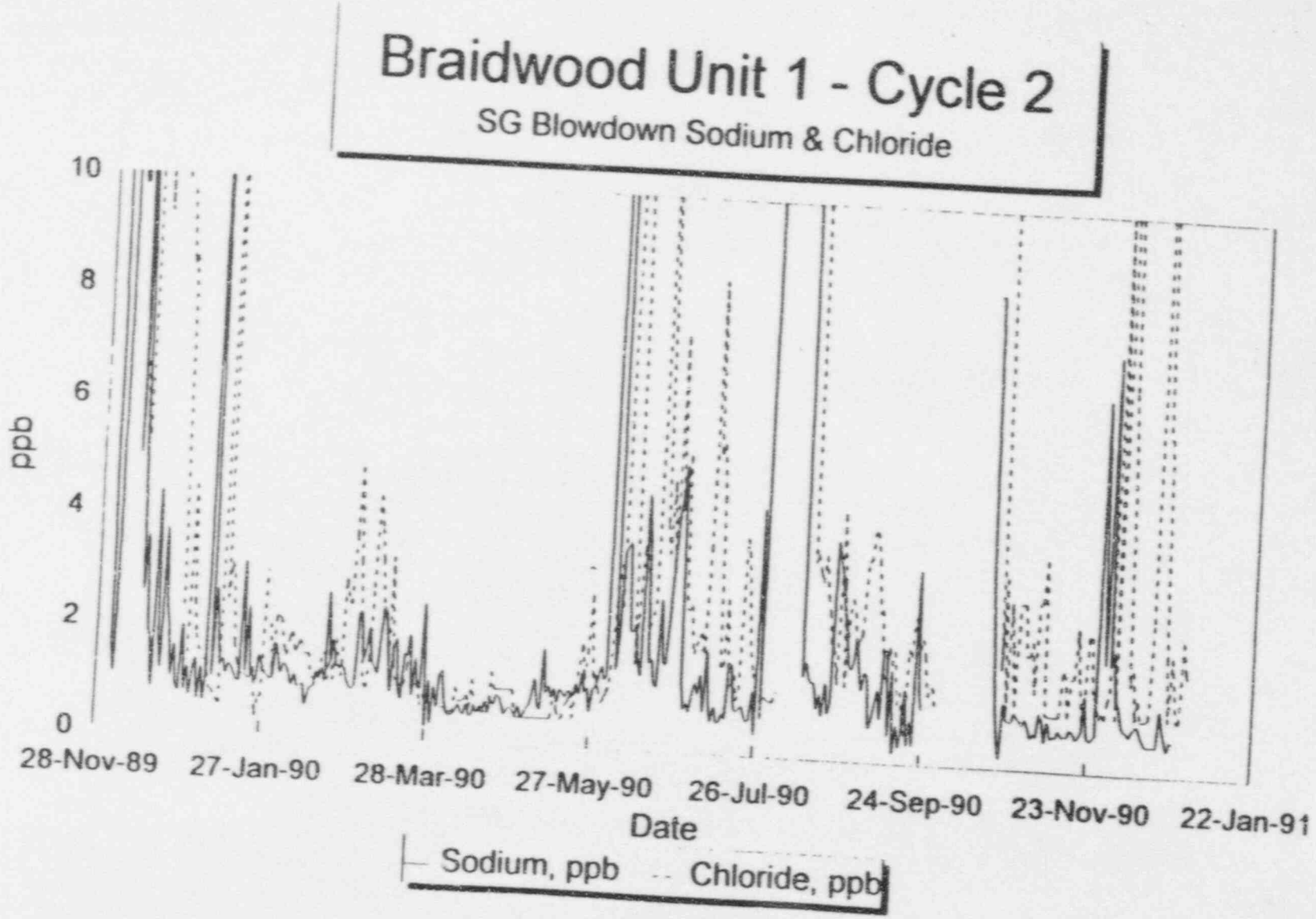
Braidwood Unit 1 - Cycle 2
SG Blowdown Sodium & Chloride
ppb
10
8
6
4
2
0
28-Nov-89
27-Jan-90
28-Mar-90
27-May-90
26-Jul-90
24-Sep-90
23-Nov-90
22-Jan-91
Date
Sodium, ppb
Chloride, ppb

Figure 7-26

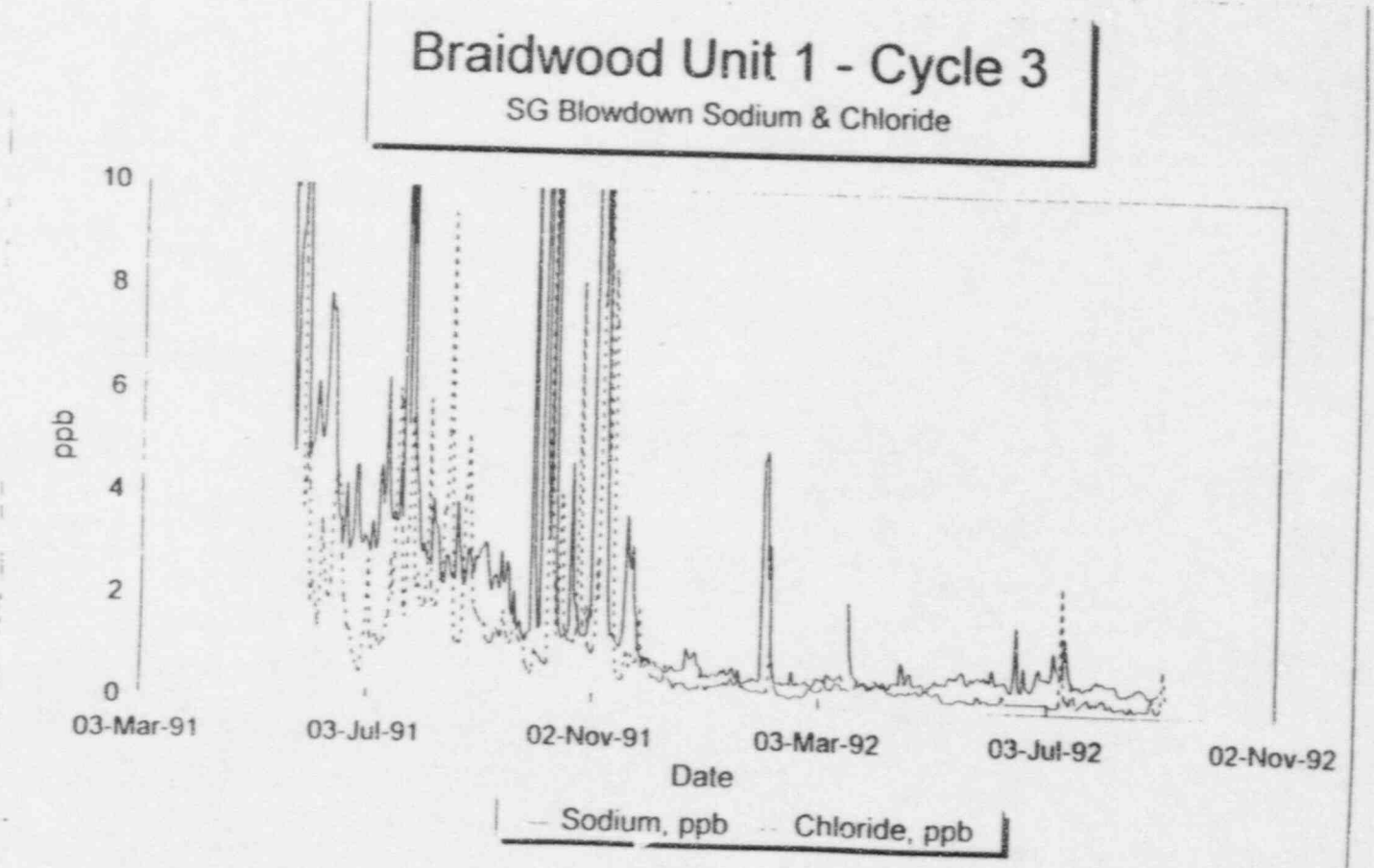
Braidwood Unit 1 - Cycle 3
SG Blowdown Sodium & Chloride
10
8
6
4
2
0
ppb
03-Mar-91
03-Jul-91
02-Nov-91
03-Mar-92
03-Jul-92
02-Nov-92
Date
Sodium, ppb
Chloride, ppb

Figure 7-27

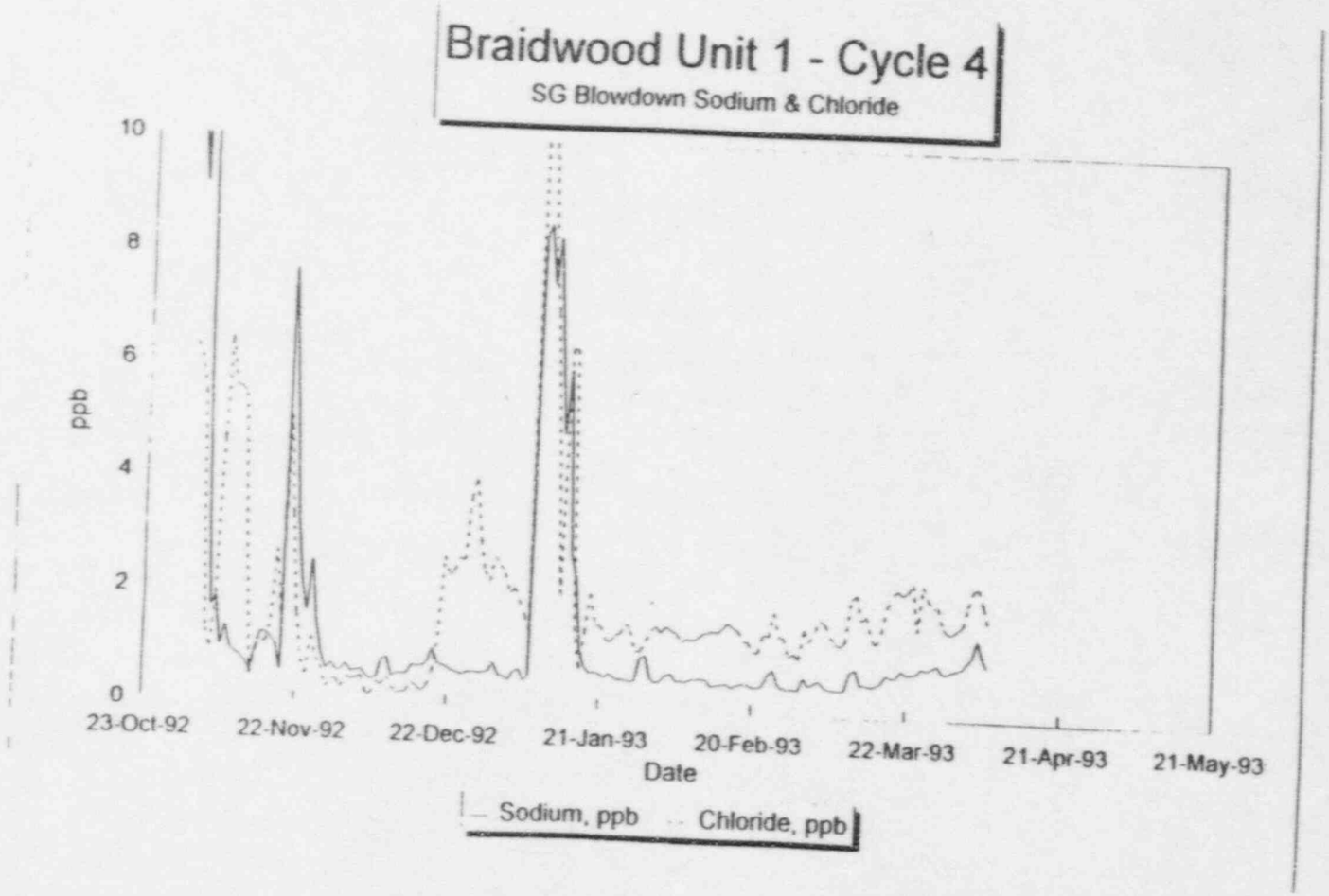
Braidwood Unit 1 - Cycle 4
SG Blowdown Sodium & Chloride
10
8
6
4
2
0
ppb
23-Oct-92
22-Nov-92
22-Dec-92
21-Jan-93
20-Feb-93
22-Mar-93
21-Apr-93
21-May-93
Date
Sodium, ppb
Chloride, ppb

Figure 7-28

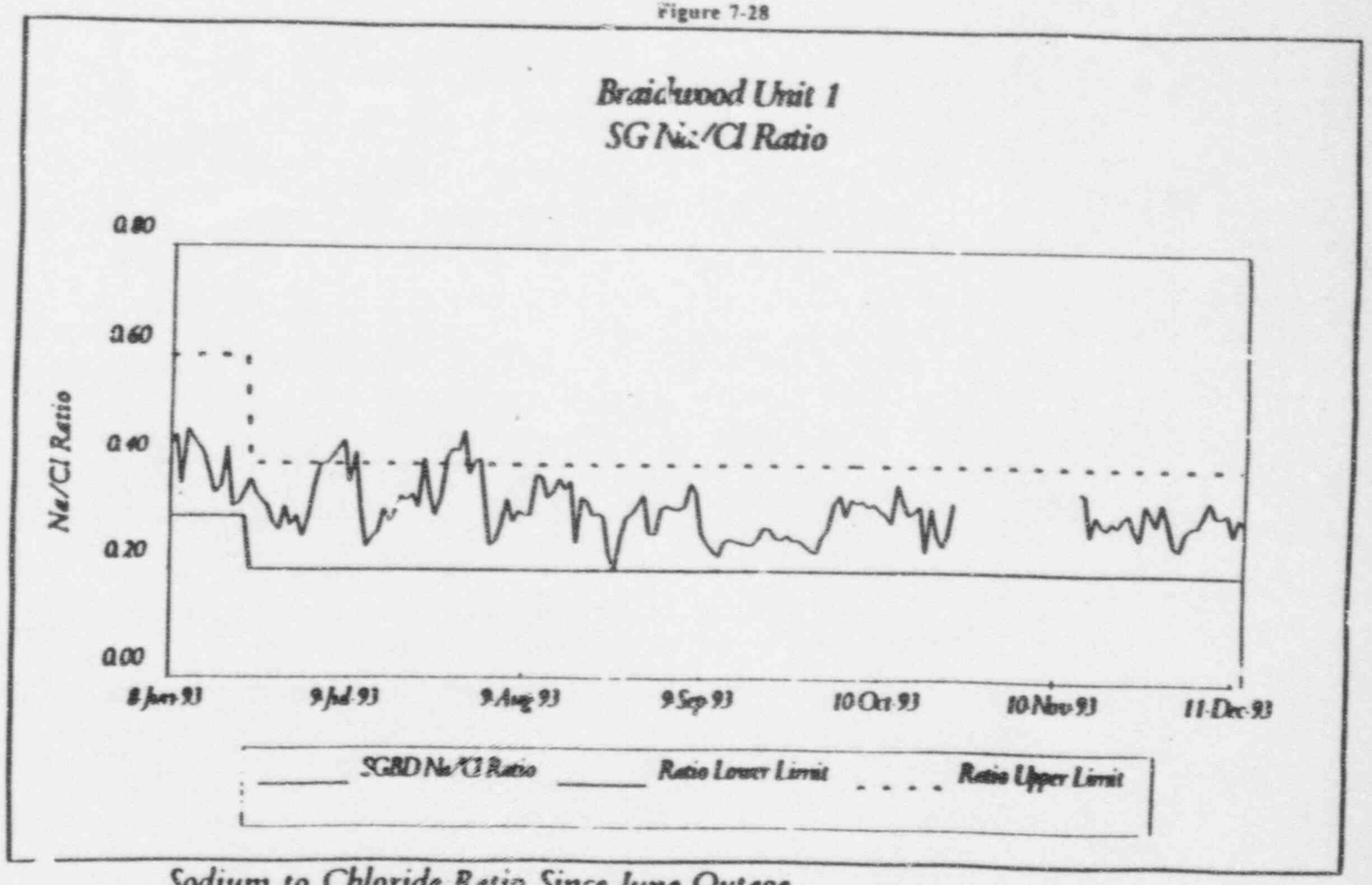

Sodium to Chloride Ratio Since June Outage

Figure 7-29. Braidwood Unit 1 Hideout Return Molar Ratios

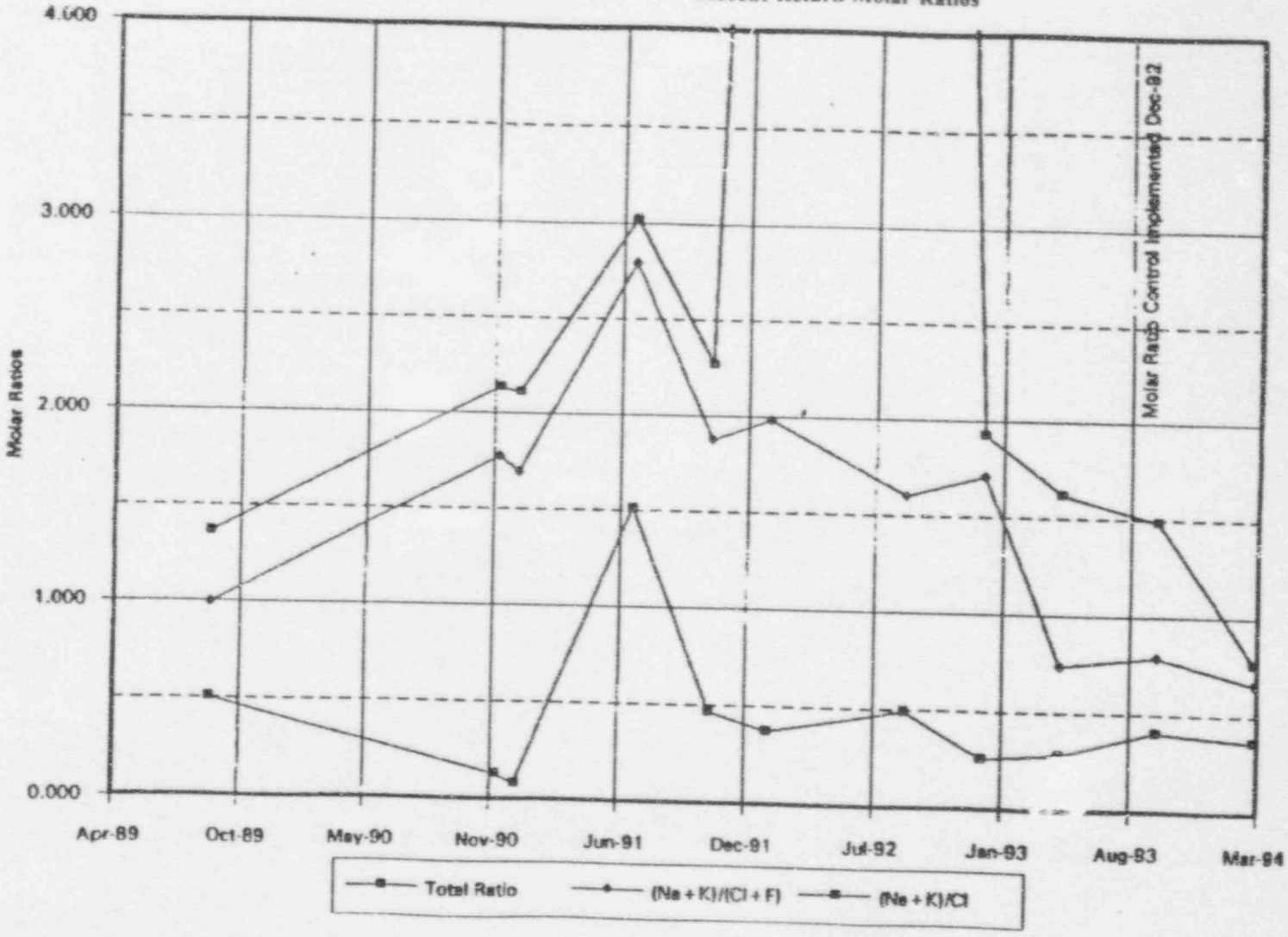

Figure 7-30

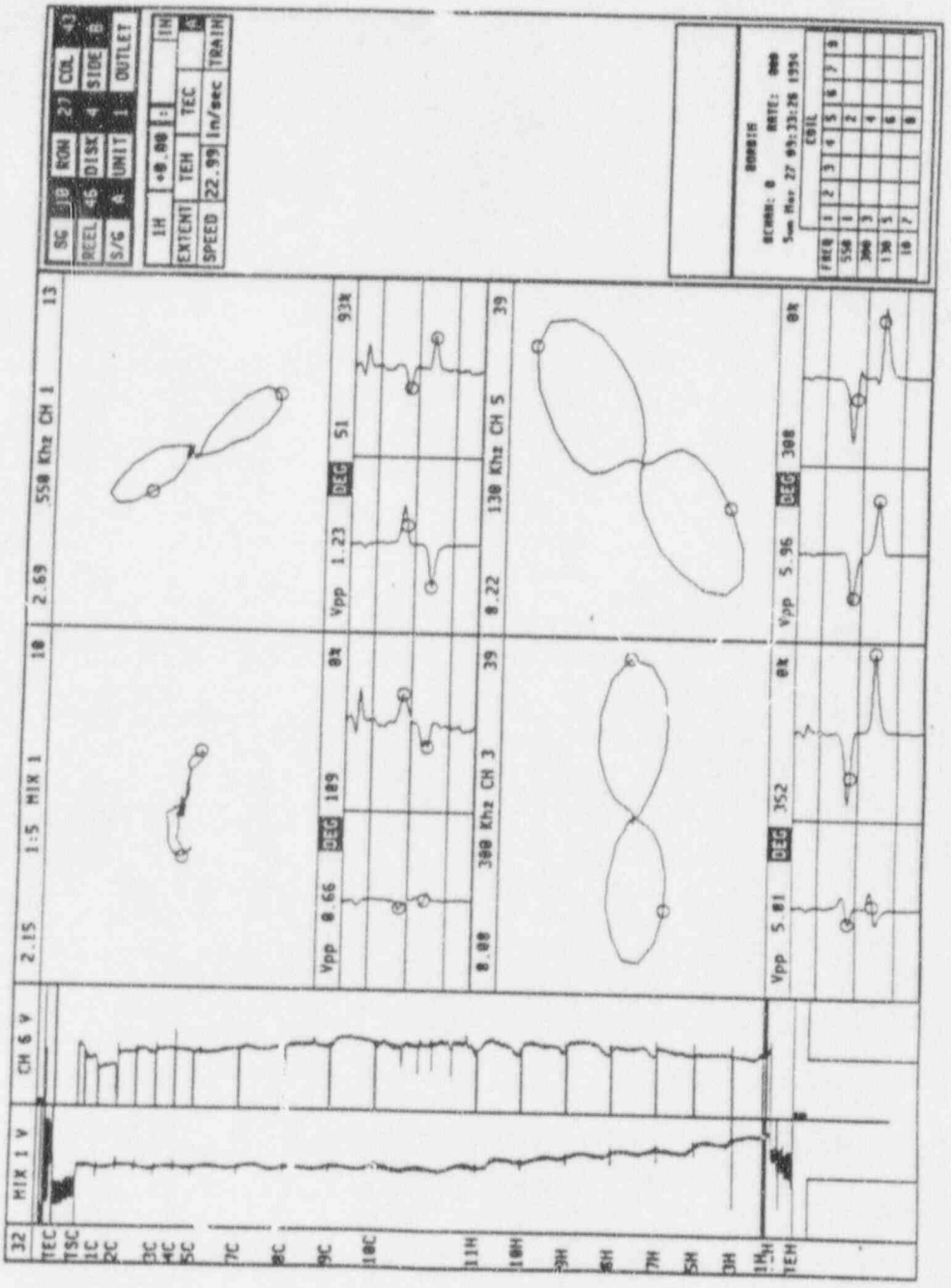
SG 10 ROW 27 COL 40
REEL 46 DISK 4 SIDE B
S/G A UNIT 1 OUTLET
1H +0.00 1H
EXTENT TEM TEC
SPEED 22.99 in/sec TRAIN
2.69 550 Khz CH 1 13
Vpp 1.23 DEG 51 93%
2.15 1:5 MIX 1 10
Vpp 0.66 DEG 189 0%
0.22 130 Khz CH 5 39
0.00 300 Khz CH 3 39
Vpp 5.96 DEG 308 0%
Vpp 5.01 DEG 352 0%
MIX 1 V
CH 6 V
32
TEC
TSC
1C
2C
3C
4C
5C
7C
8C
9C
10C
11H
10H
9H
8H
7H
6H
5H
4H
3H
2H
1H
1M
TEM

Figure 7-31

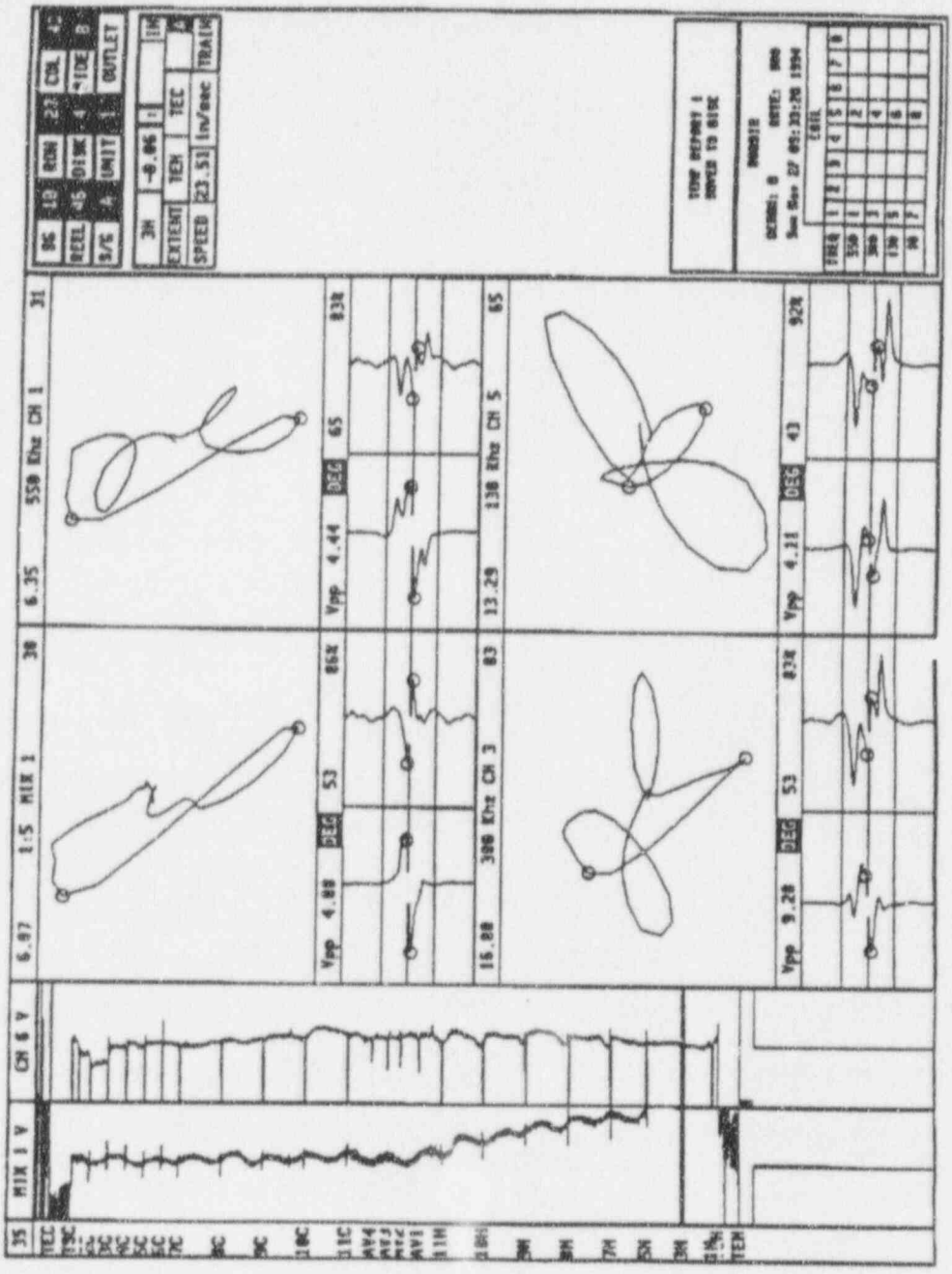

Figure 7-32

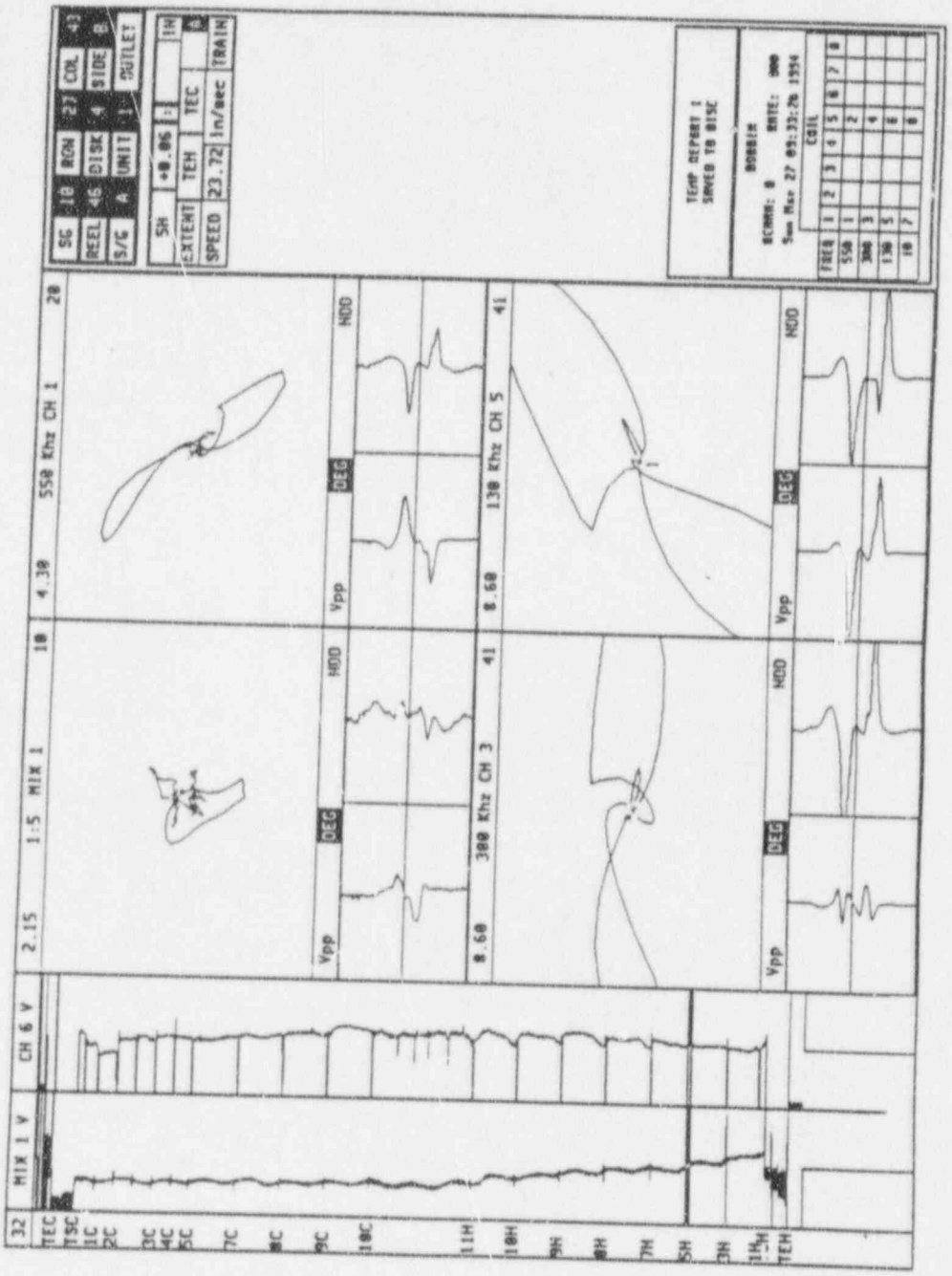
SC 10
REEL 46
S/G A
RGN 27
DISK 4
UNIT 1
COIL 43
SIDE B
OUTLET
SH +0.06
EXTENT TEH TEC
SPEED 23.72 in/sec
TRAIN
TEMP DEPART I
SAVED TO DISC
DOBBIE
SCHAN: 0 DATE: 000
Sun Mar 27 09:33:26 1994
COIL
FREQ 1 2 3 4 5 6 7 8
550 1 2
300 3 4
130 5 6
10 7 8
2.15 1:5 MIX 1 10 4.39 550 Khz CH 1 20
8.60 300 Khz CH 3 41
8.60 130 Khz CH 5 41
MIX 1 V
CH 6 V
32
TEC TSC 1C 2C 3C 4C 5C 7C 8C 9C 10C 11H 10H 9H 8H 7H 5H 3H 1H TEH

Figure 7-33

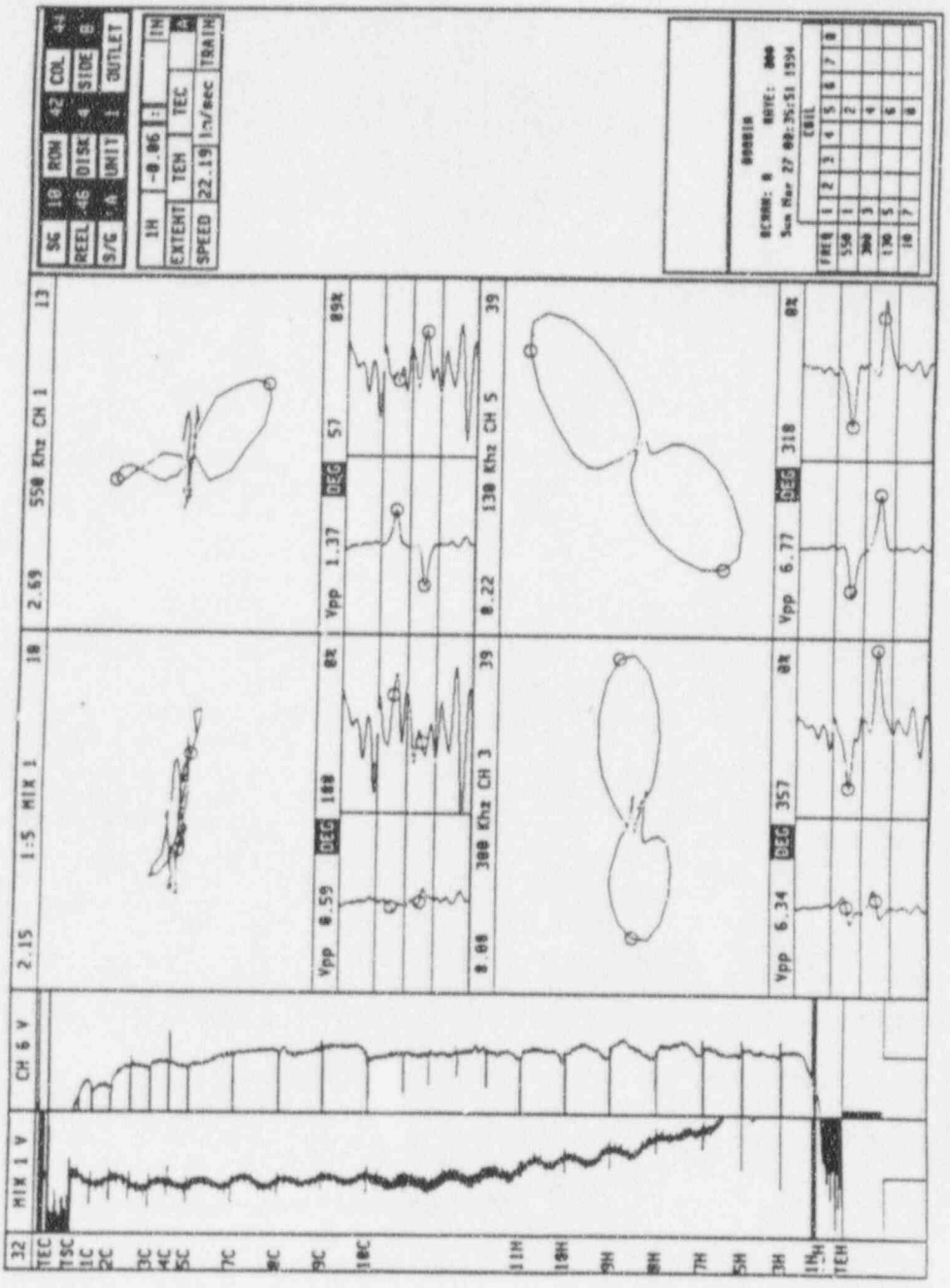
SG 10 ROW 42 COL 44
REEL 46 DISK 4 SIDE B
S/G A UNIT 1 OUTLET
1H -0.06 1H
EXTENT TEM TEC
SPEED 22.19 in/sec TRAIN
RECNO: 0 RATE: 000
Sun Mar 27 00:35:51 1994
FREQ 1 2 3 4 5 6 7 8
550 1 2
300 3 4
130 5 6
10 7 8
2.69 550 Khz CH 1 13
Vpp 1.37 DEG 57 89%
8.22 130 Khz CH 5 39
2.15 1:5 MIX 1 18
Vpp 0.59 DEG 188 0%
8.08 300 Khz CH 3 39
Vpp 6.77 DEG 318 0%
Vpp 6.34 DEG 357 0%
MIX 1 V
CH 6 V
32
TEC
TSC
1C
2C
3C
4C
5C
7C
8C
9C
10C
11H
10H
9H
8H
7H
5H
3H
1H
TEH

Figure 7-34

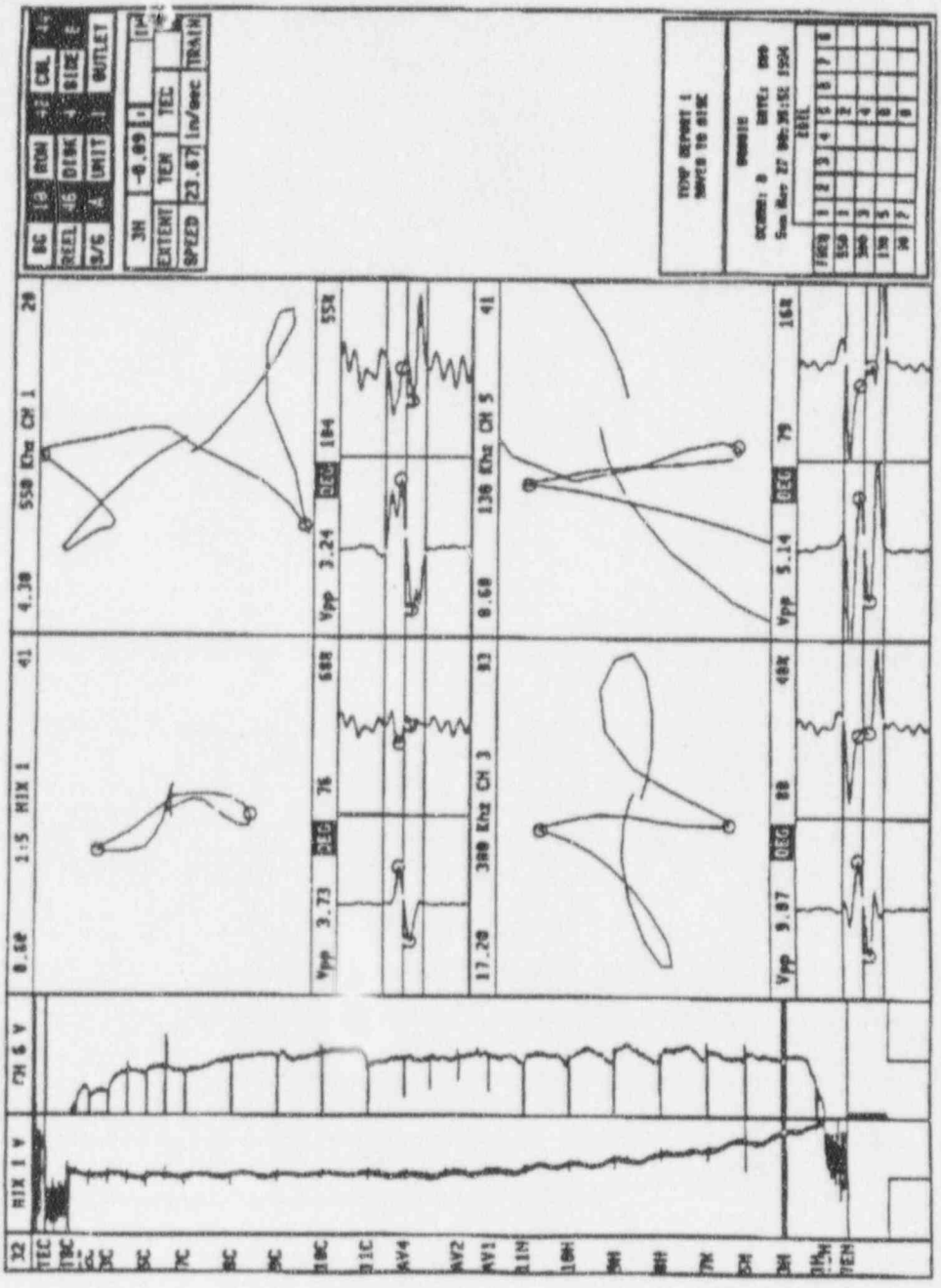

Figure 7-35

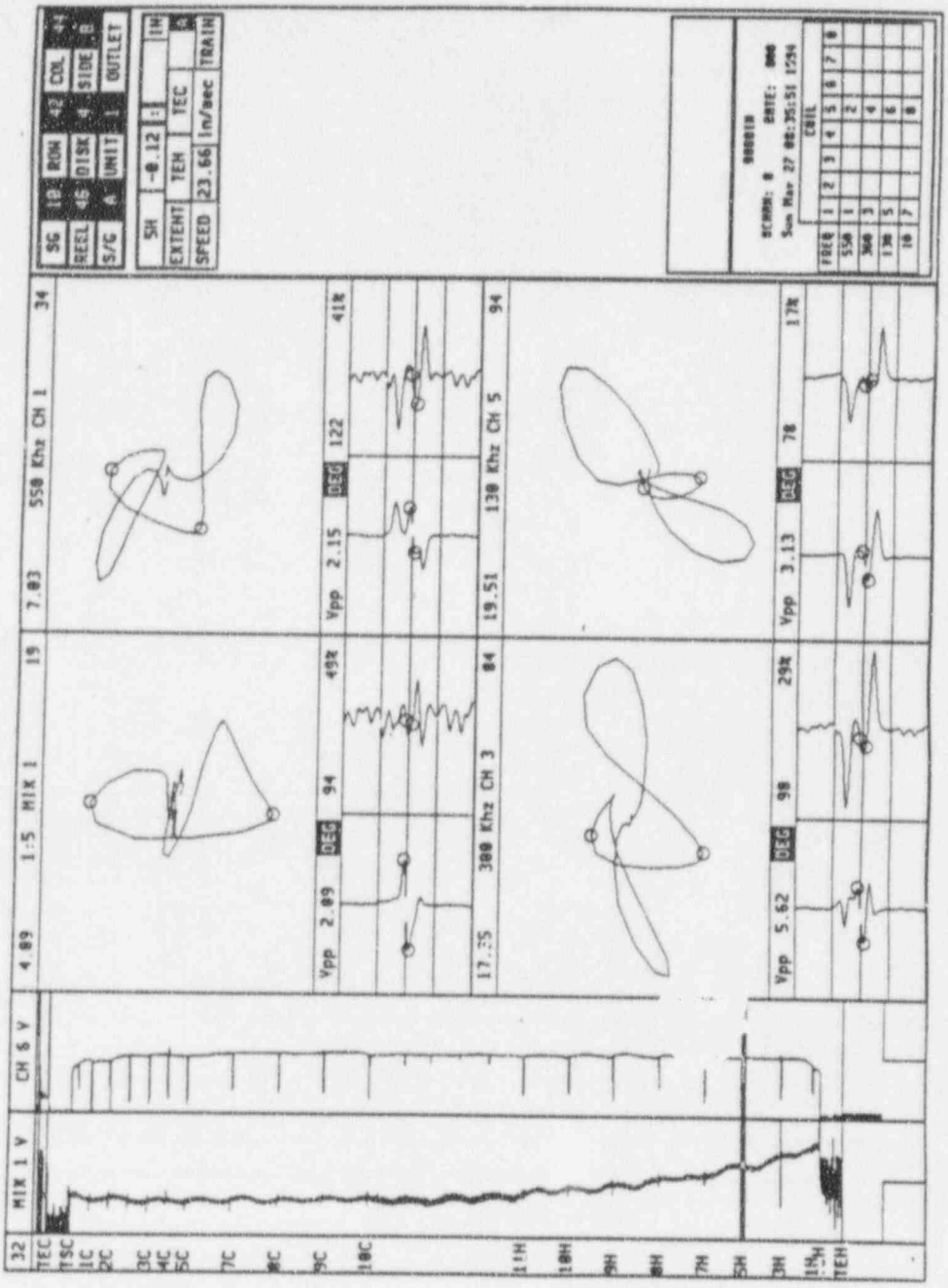
SG 10 RUN 42 COL 44
REEL 46 DISK 4 SIDE B
S/G A UNIT 1 OUTLET
SH -0.12 IN
EXTENT TEM TEC
SPEED 23.66 in/sec TRAIN
DEMON: 0 DATE: 000
Sun Mar 27 00:35:51 1994
COIL
FREQ 1 2 3 4 5 6 7 8
550 1
300 3 4
130 5 6
10 7 8
32 MIX 1 V CH 6 V
4.89 1:5 MIX 1 19
7.83 550 Khz CH 1 34
Vpp 2.89 DEG 94 49%
17.35 300 Khz CH 3 84
Vpp 2.15 DEG 122 41%
19.51 130 Khz CH 5 94
Vpp 5.62 DEG 98 29%
Vpp 3.13 DEG 78 17%
TEC TSC 1C 2C 3C 4C 5C 6C 7C 8C 9C 10C 11H 12H 9H 8H 7H 5H 3H 1H TEH

Figure 7-36

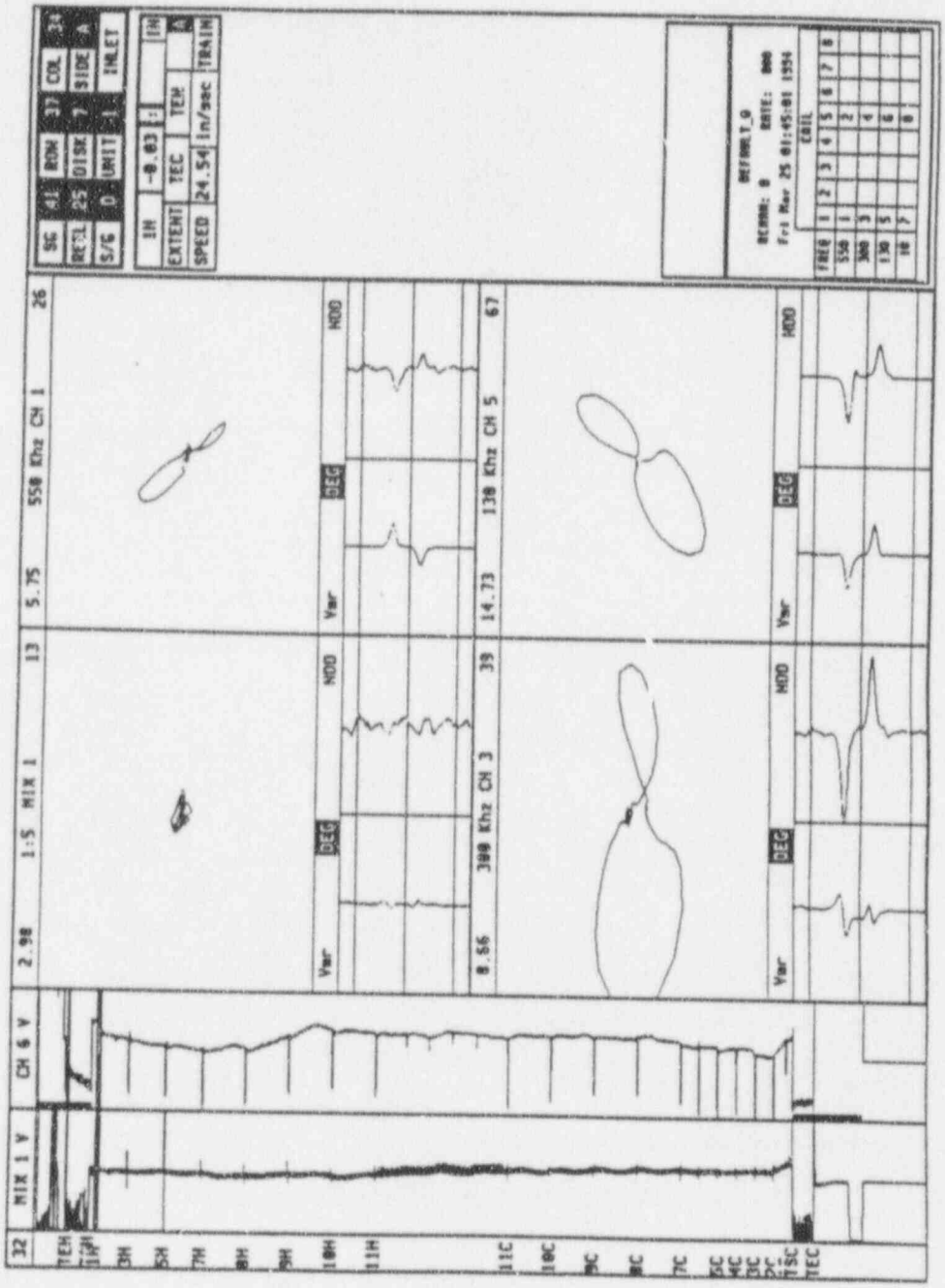
SG 41 ROW 37 COL 34
RETL 25 DISK 7 SIDE A
S/G 0 UNIT 1 INLET
IN -0.03
EXTENT TEC TEM
SPEED 24.54 in/sec TRAIN
DEFAULT_9
RECNO: 0 DATE: 000
Fri Mar 25 01:45:01 1994
FREQ 1 2 3 4 5 6 7 8
550 1
300 3
130 5
2.98 1:5 MIX 1 13
5.75 550 Khz CH 1 26
8.66 300 Khz CH 3 39
14.73 130 Khz CH 5 67
MIX 1 V
CH 6 V
NOD
DEG
Var

Figure 7-37

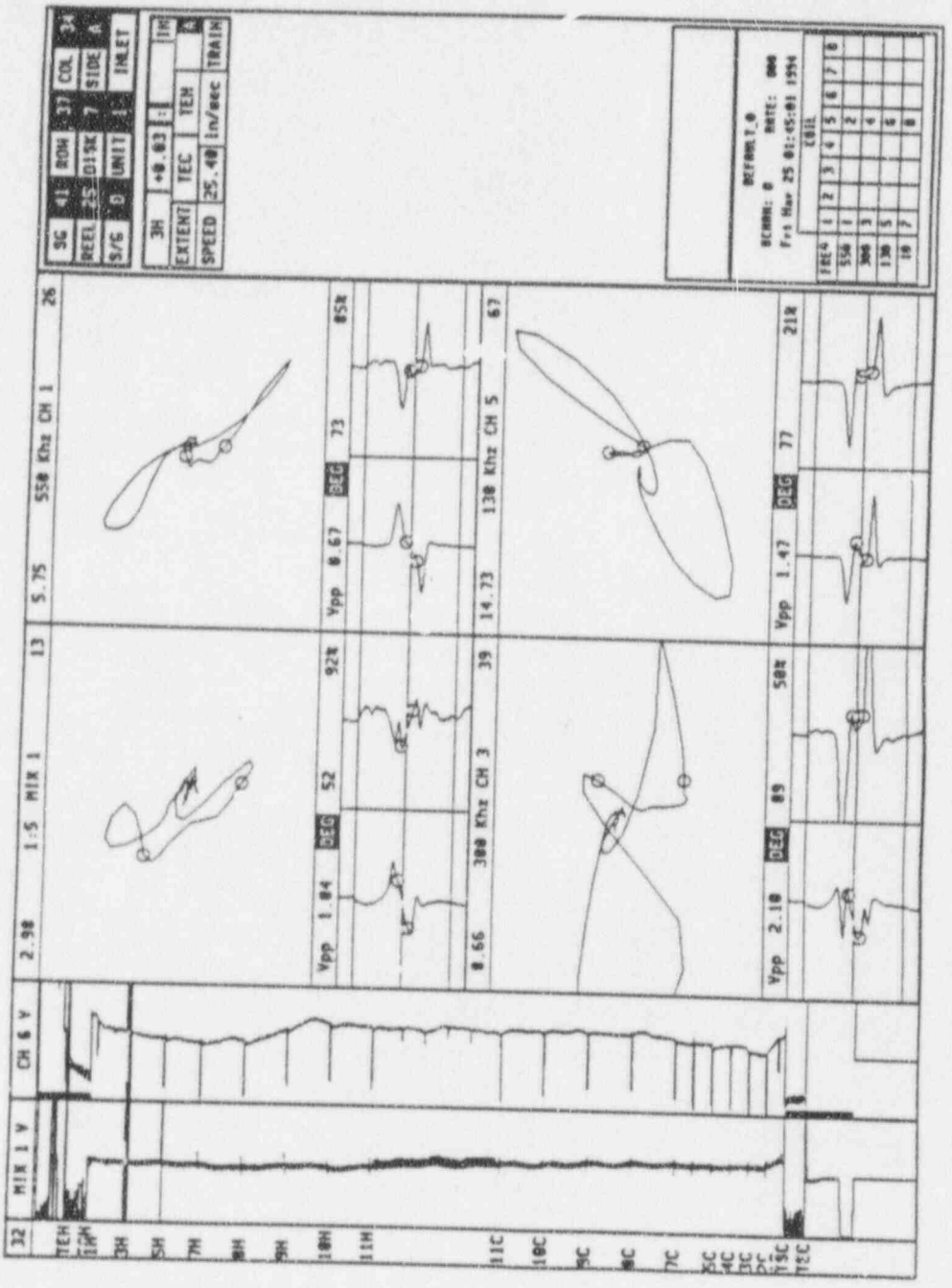
SG 41 ROW 37 COL 34
REEL 25 DISK 7 SIDE A
S/G 0 UNIT 1 INLET
3H +0.63 IM
EXTENT TEC TEM A
SPEED 25.40 in/sec TRAIN
DEFAULT.0
SCANN: 0 DATE: 000
Fri Mar 25 01:45:01 1994
FREQ 1 2 3 4 5 6 7 8
550 1
300 3
130 5
10 7
2 4 6
CH 6 V
MIX 1 V
2.98 1.5 MIX 1 13
5.75 550 Khz CH 1 26
Vpp 1.84 DEG 52 92R
Vpp 0.67 DEG 73 85R
0.66 300 Khz CH 3 39
14.73 130 Khz CH 5 67
Vpp 2.10 DEG 89 50R
Vpp 1.47 DEG 77 21R
32
TEH
TEM
3H
5H
7H
9H
10H
11H
11C
10C
9C
8C
7C
5C
4C
3C
2C
1SC
12C

Figure 7-38

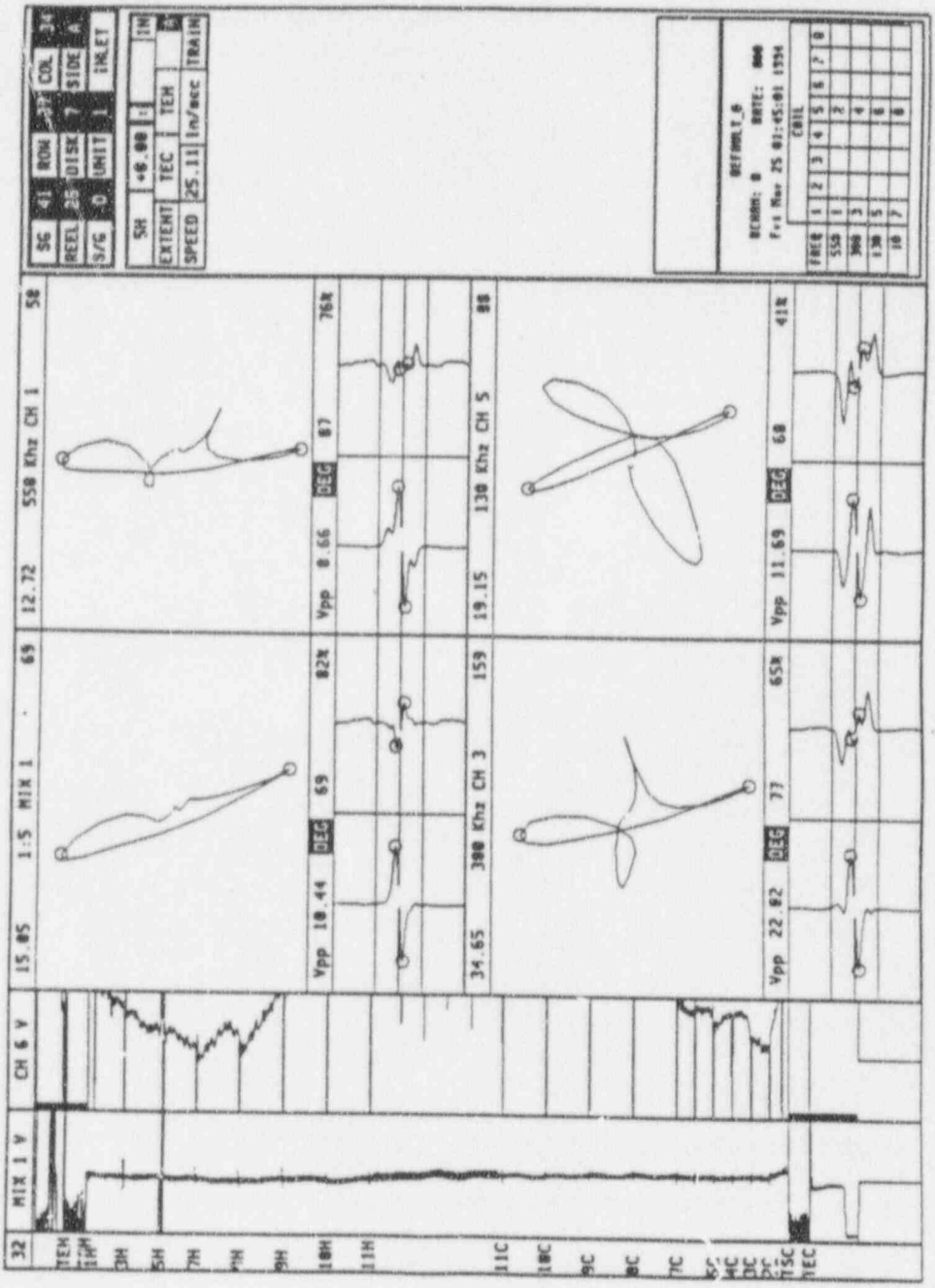
SG
REEL
S/G
ROW
COL
DISK
SIDE
UNIT
INLET
SH
EXTENT
SPEED
+6.00
TEC
TEM
25.11
in/sec
TRAIN
DEFAULT_0
RECORD: 0
DATE: 000
Fri Mar 25 01:45:01 1994
CHAN
FREQ
550 Khz CH 1
380 Khz CH 3
130 Khz CH S
MIX 1
CH 6 V
MIX 1 V
Vpp 8.66
Vpp 10.44
Vpp 11.69
Vpp 22.82
DEG
12.72
15.85
19.15
34.65
76%
82%
41%
65%
TEM
TEC

Figure 7-39

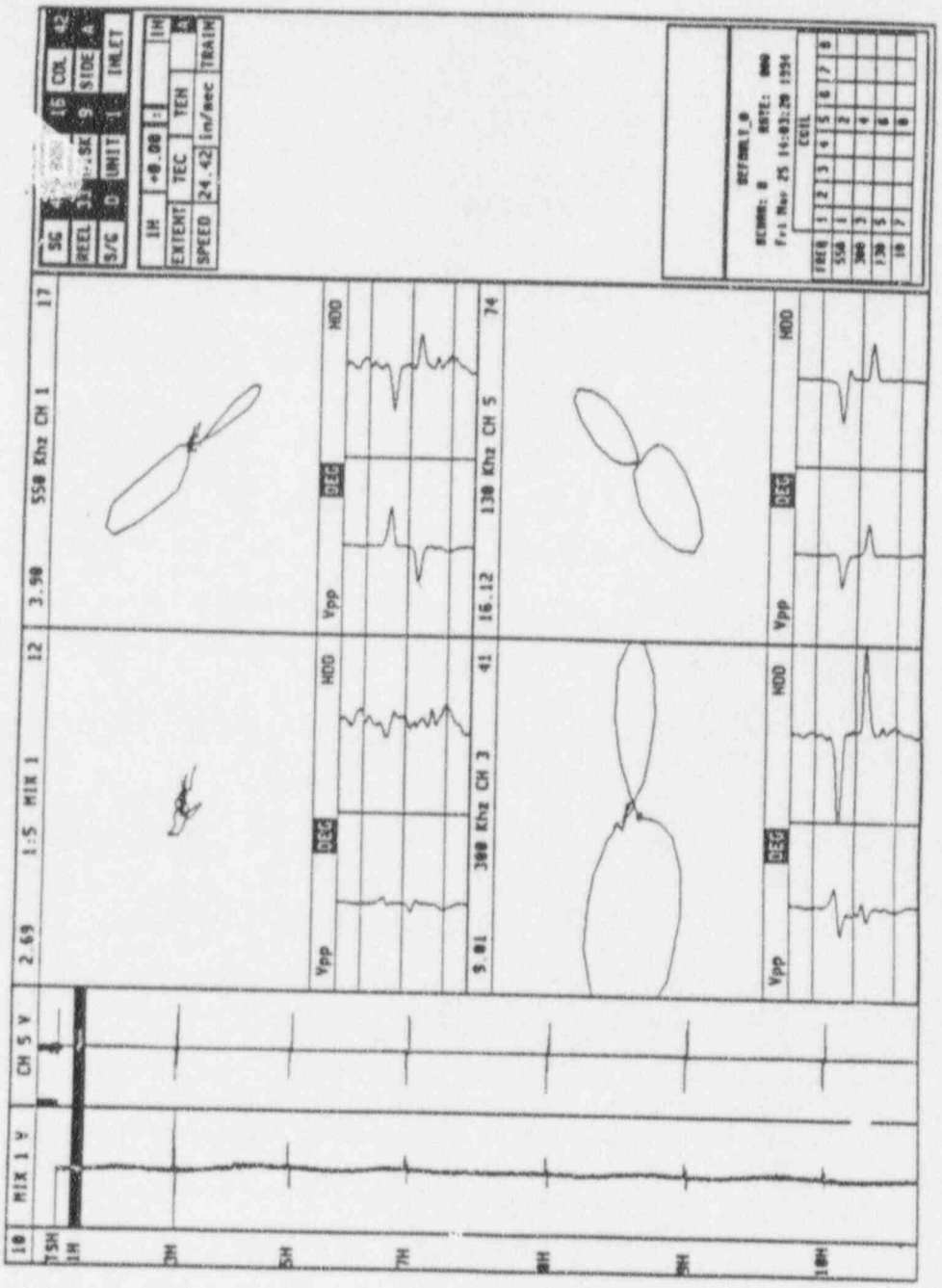
SG
REEL
S/C
UNIT
INLET
SIDE
COL
TRAIN
SPEED
EXTENT
TEC
TEN
in/sec
550 Khz CH 1
300 Khz CH 3
130 Khz CH 5
MIX 1
CH 5
Vpp
DEG
MOD

Figure 7-40

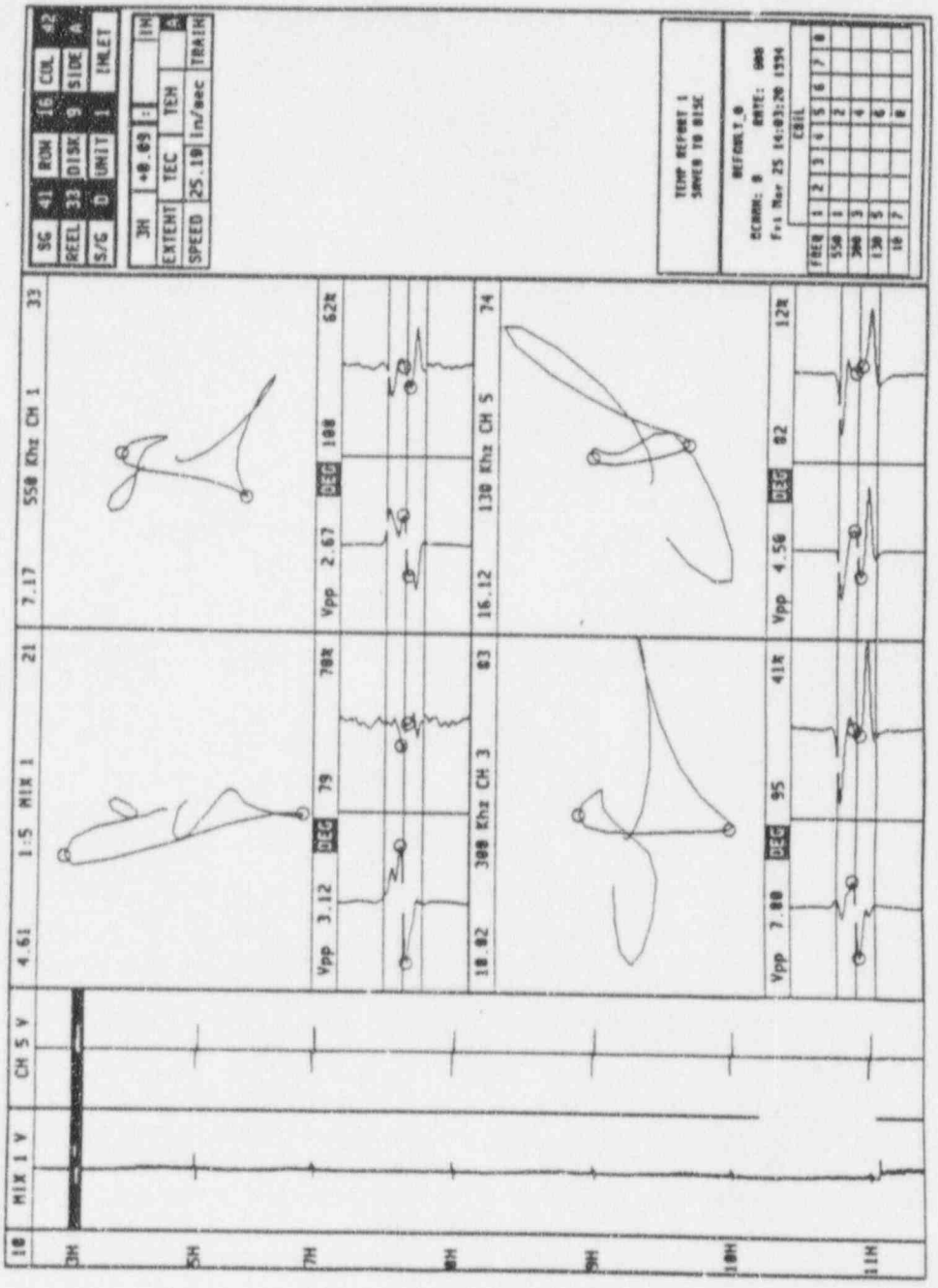
SG 41 ROW 16 COL 42
REEL 33 DISK 9 SIDE A
S/G 0 UNIT 1 INLET
JH +0.69 IN
EXTENT TEC TEH
SPEED 25.10 in/sec TRAIN
TEMP REPORT 1
SAVED TO DISK
RECORD1_0
RECNUM: 0 DATE: 000
Fri Mar 25 14:03:20 1994
COIL
FREQ 1 2 3 4 5 6 7 8
550 1 2
300 3 4
130 5 6
10 7 8
4.61 1:5 MIX 1 21
7.17 550 Khz CH 1 33
Vpp 3.12 DEG 79 78%
Vpp 2.67 DEG 108 62%
18.02 300 Khz CH 3 63
16.12 130 Khz CH 5 74
Vpp 7.80 DEG 95 41%
Vpp 4.56 DEG 82 12%
MIX 1 V
CH 5 V
0H
5H
7H
9H
10H
11H

Figure 7-41

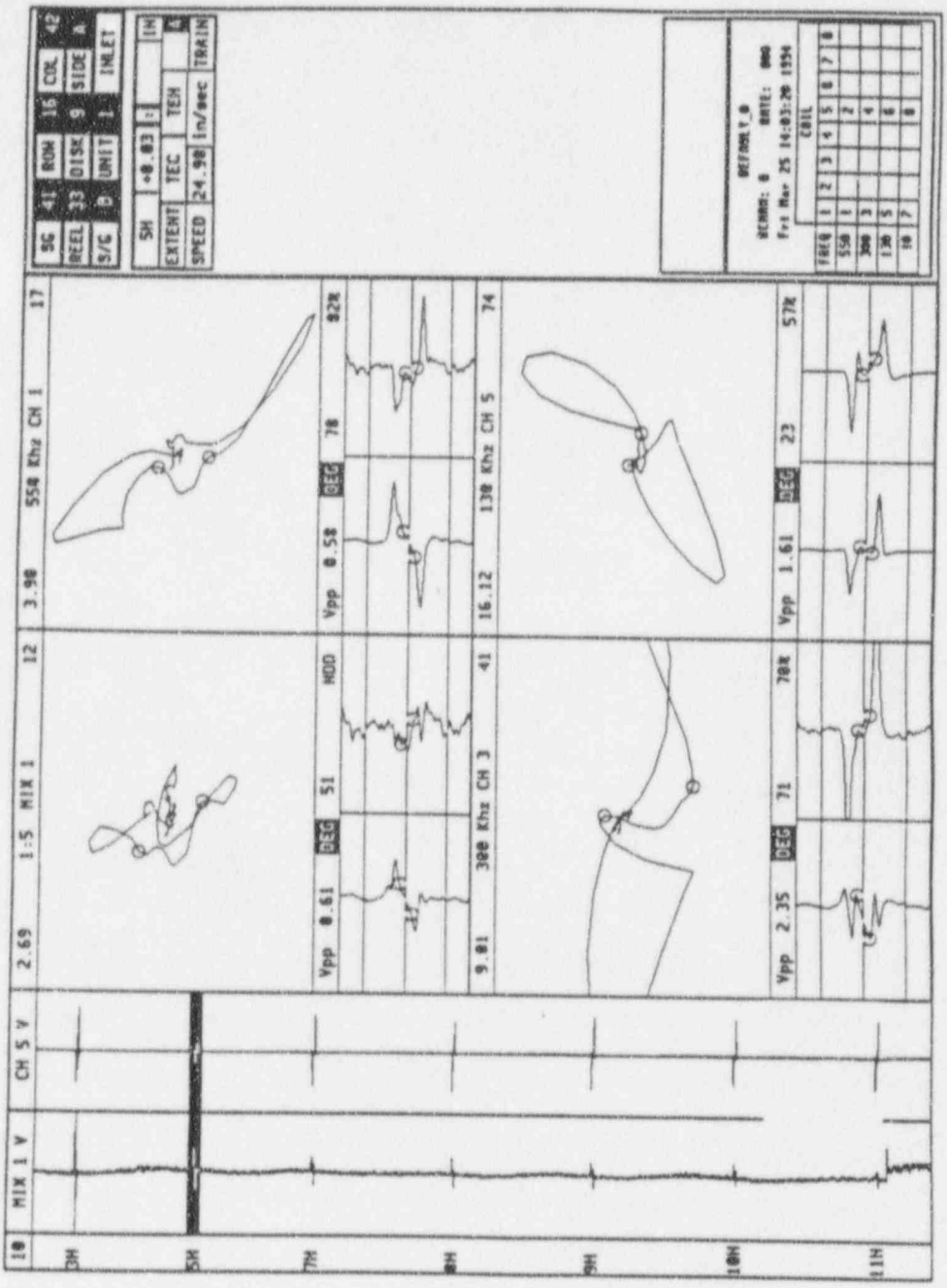
SG 41 ROW 16 COL 42
REEL 33 DISK 9 SIDE A
S/G B UNIT 1 INLET
SM +0.03 IN
EXTENT TEC TEM
SPEED 24.98 in/sec TRAIN
2.69 1:5 MIX 1 12
3.90 554 Khz CH 1 17
Vpp 0.61 DEG 51 MOD
9.01 300 Khz CH 3 41
Vpp 0.58 DEG 78 82%
16.12 130 Khz CH 5 74
Vpp 2.35 DEG 71 78%
Vpp 1.61 DEG 23 57%
COIL
FREQ 1 2 3 4 5 6 7 8
554 1
300 3
130 5
MIX 1 V
CH 5 V
5M
7M
8M
9M
10M
11M

Figure 7-42

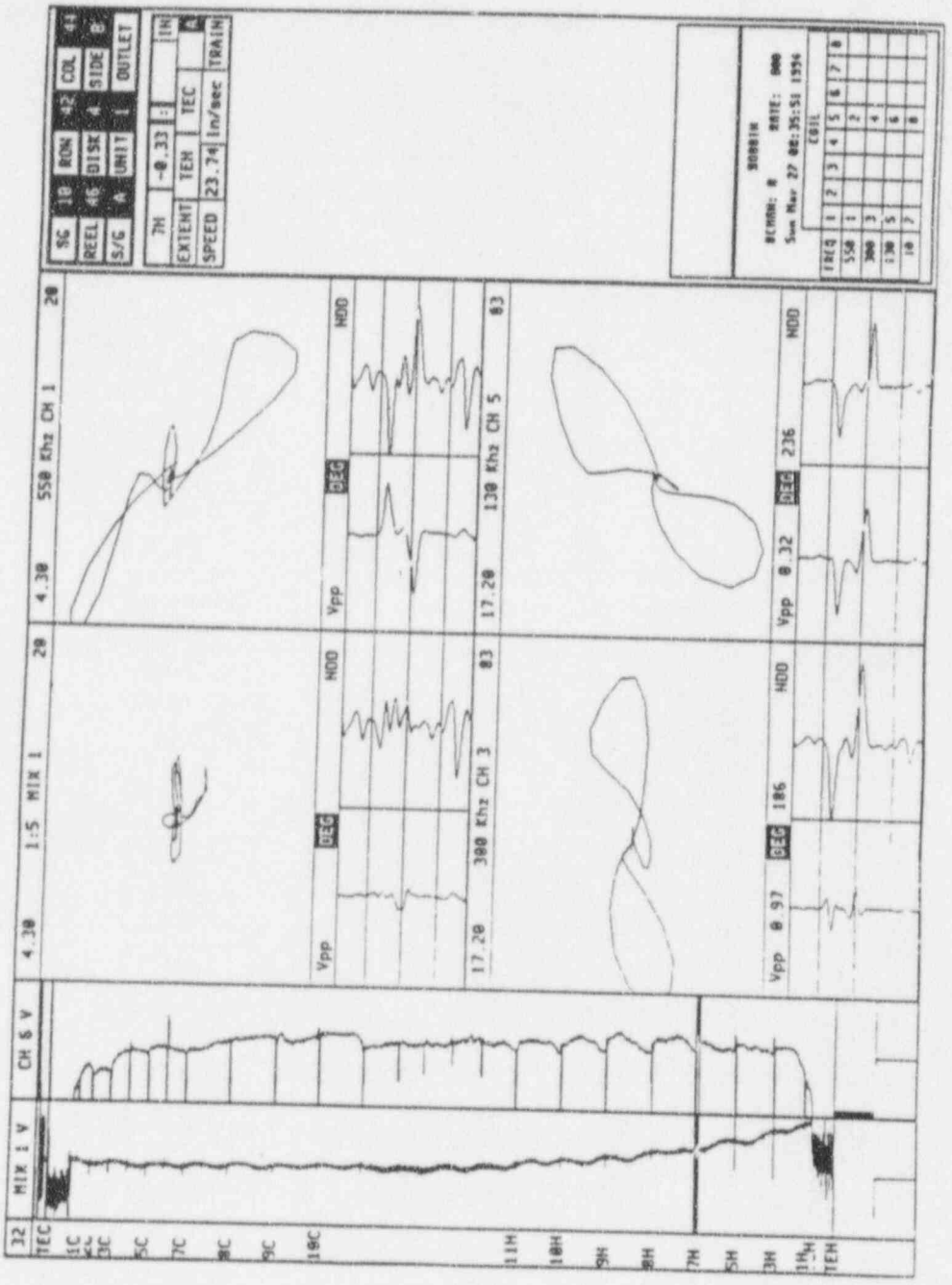
SG 10 RON 42 COL 44
REEL 46 DISK 4 SIDE B
S/G A UNIT 1 OUTLET
ZM -0.33 IN
EXTENT TEM TEC A
SPEED 23.74 in/sec TRAIN
SOBBIN
RECORD: 0 TAPE: 000
Sun Mar 27 02:35:51 1994
COIL
FREQ 1 2 3 4 5 6 7 8
550 1
300 3
130 5
10 7
4.30 550 Khz CH 1 20
4.30 1:5 MIX 1 20
17.20 130 Khz CH 5 83
17.20 300 Khz CH 3 83
Vpp 0.32 DEG 236 NOD
Vpp 0.97 DEG 186 NOD
MIX 1 V
CH 6 V
22
TEC
11H
10H
9H
8H
7H
6H
5H
4H
3H
2H
1H
TEH

Figure 7-43

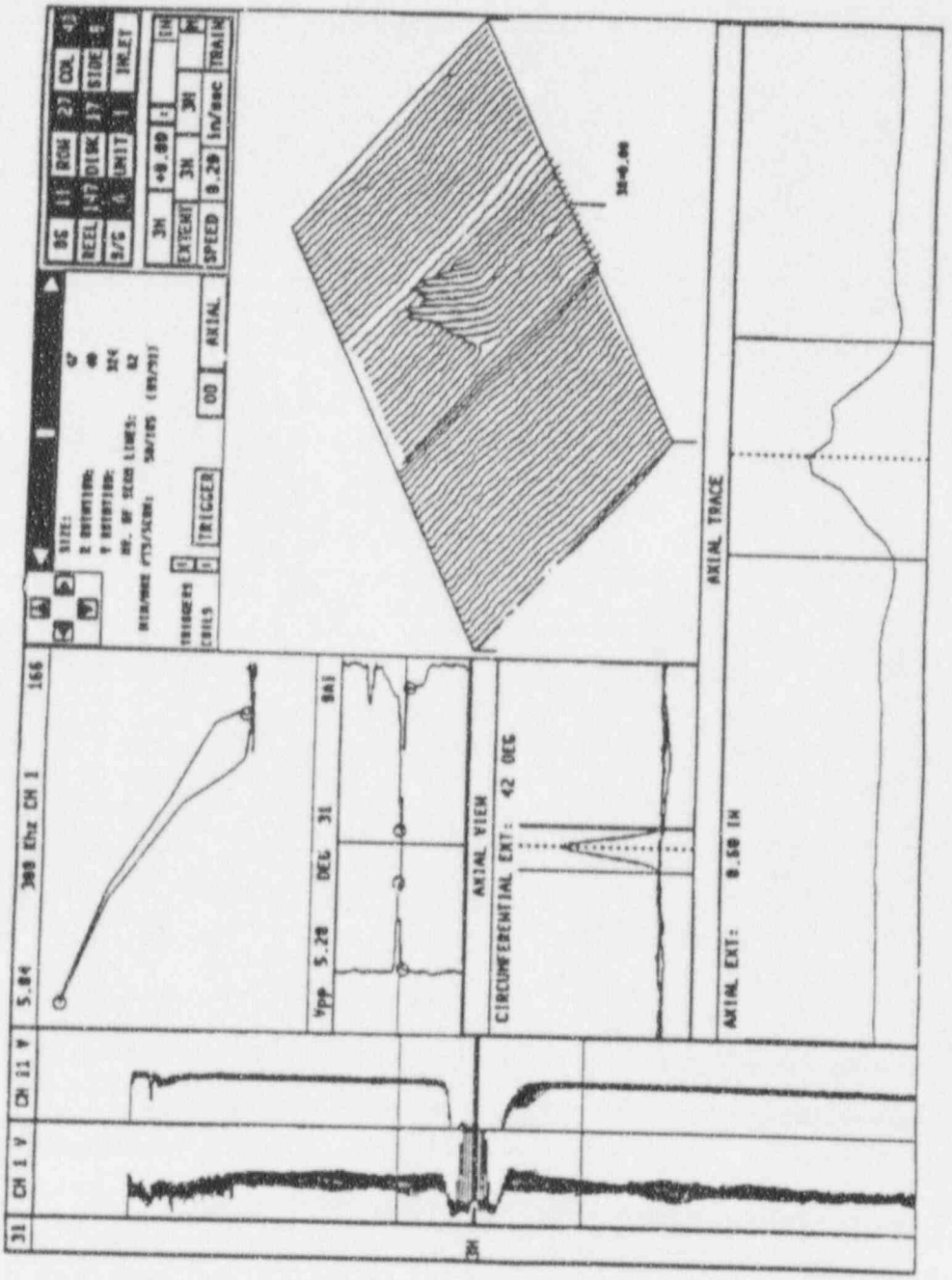
AXIAL VIEW
CIRCUMFERENTIAL EXT: 42 DEG
AXIAL TRACE
AXIAL EXT: 0.60 IN
CH 1 V
CH 11 V
TRIGGER
AXIAL
TRAIN
INLET
SIDE B
COL
ROW
DISK
UNIT
REEL
SPEED
EXTENT
TRIGGERS
COILS

Figure 7-44

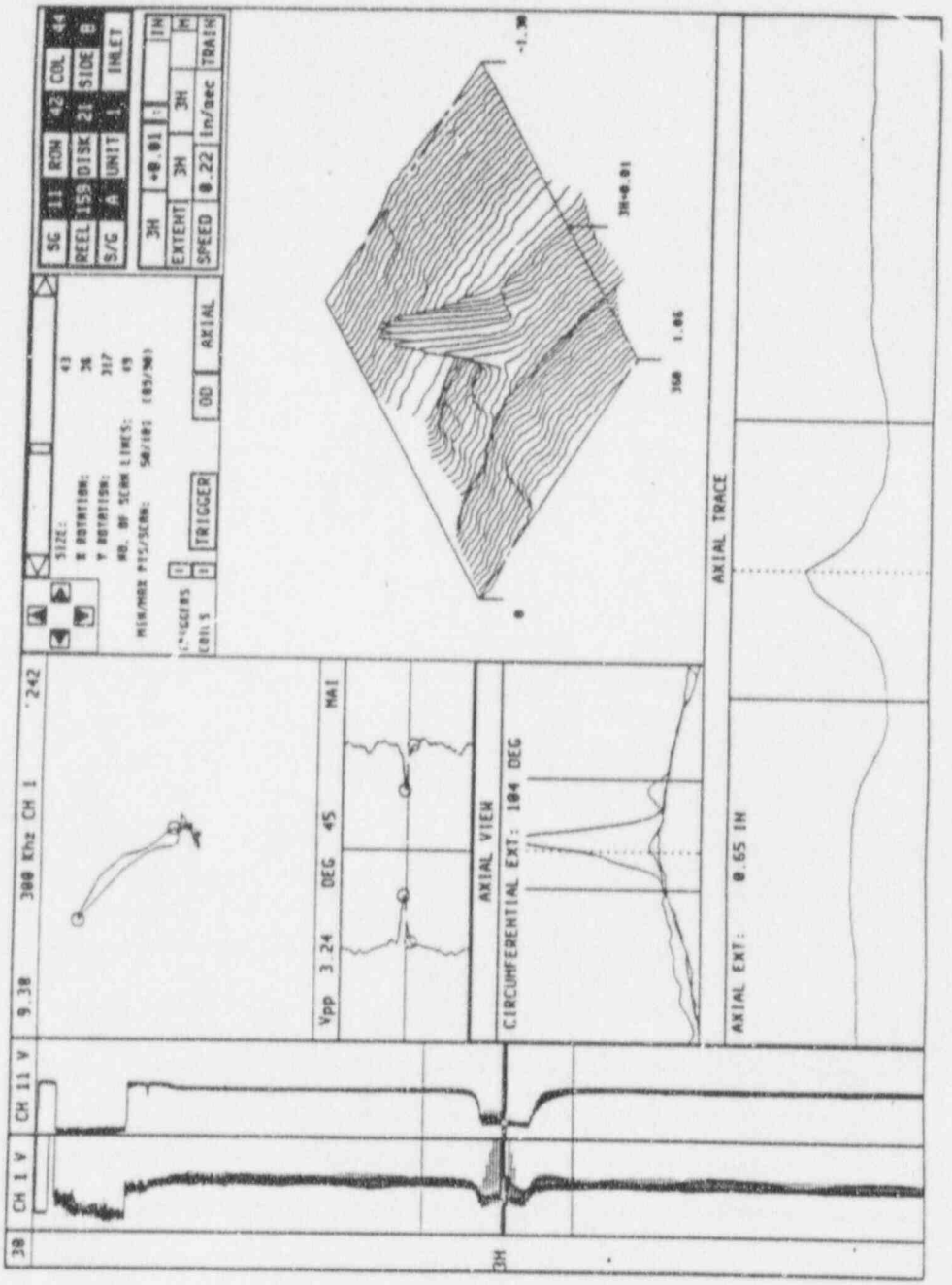
AXIAL TRACE
AXIAL VIEW
CIRCUMFERENTIAL EXT: 104 DEG
AXIAL EXT: 0.65 IN
Vpp 3.24 DEG 45
300 Khz CH 1
CH 1 V
CH 11 V
INLET
SIDE B
COL 44
ROW 42
DISK 21
UNIT 1
REEL 159
S/G A
AXIAL
TRIGGER
OD
SPEED 0.22 in/sec
EXTENT
TRAIN

Figure 7-45

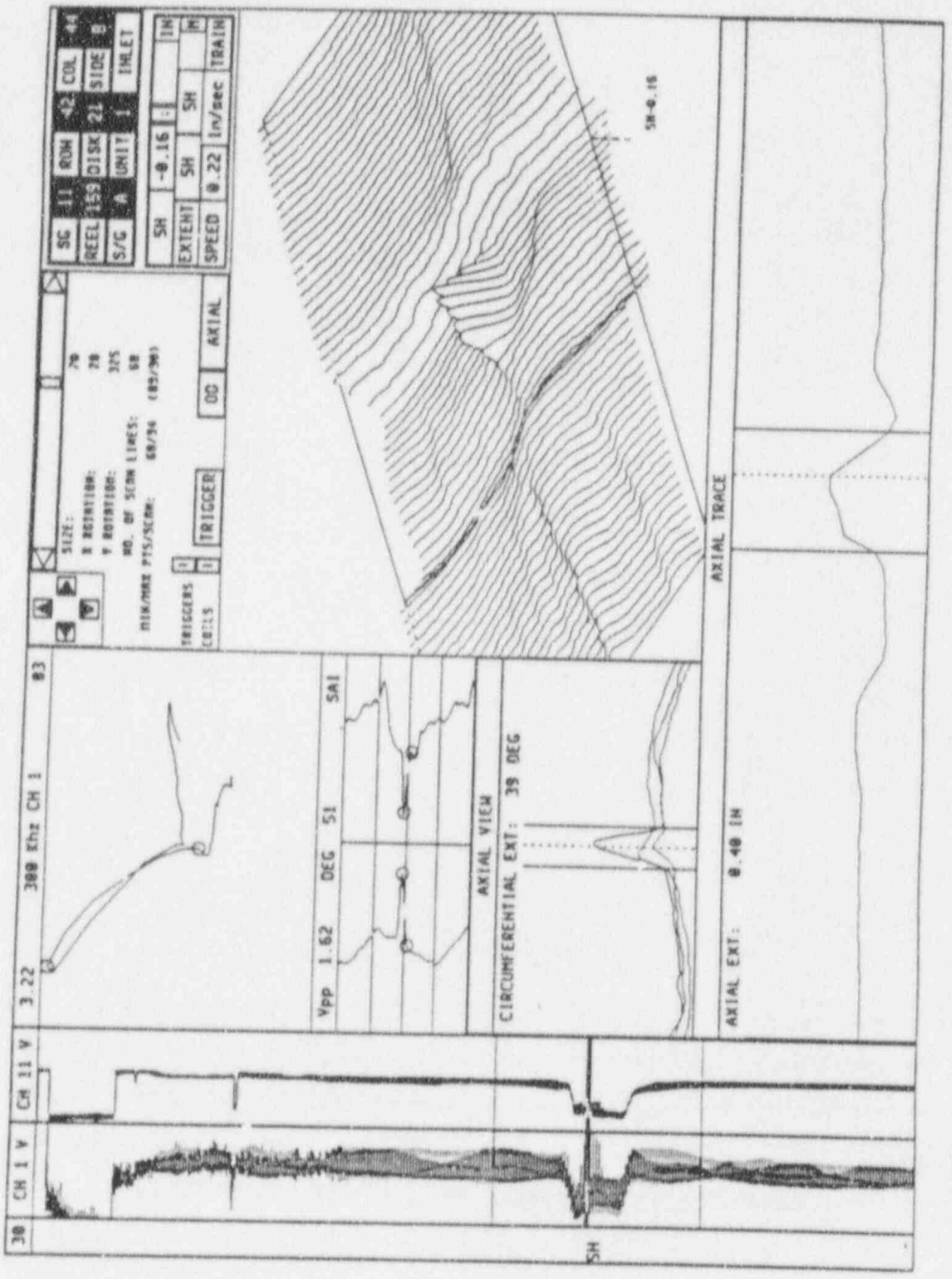
SG
REEL
S/G
ROW
DISK
UNIT
COL
SIDE
INLET
SH
EXTENT
SPEED
TRIGGER
AXIAL
CH 1 V
CH 11 V
300 Khz CH 1
AXIAL VIEW
CIRCUMFERENTIAL EXT: 39 DEG
AXIAL TRACE
AXIAL EXT: 0.40 IN

Figure 7-46

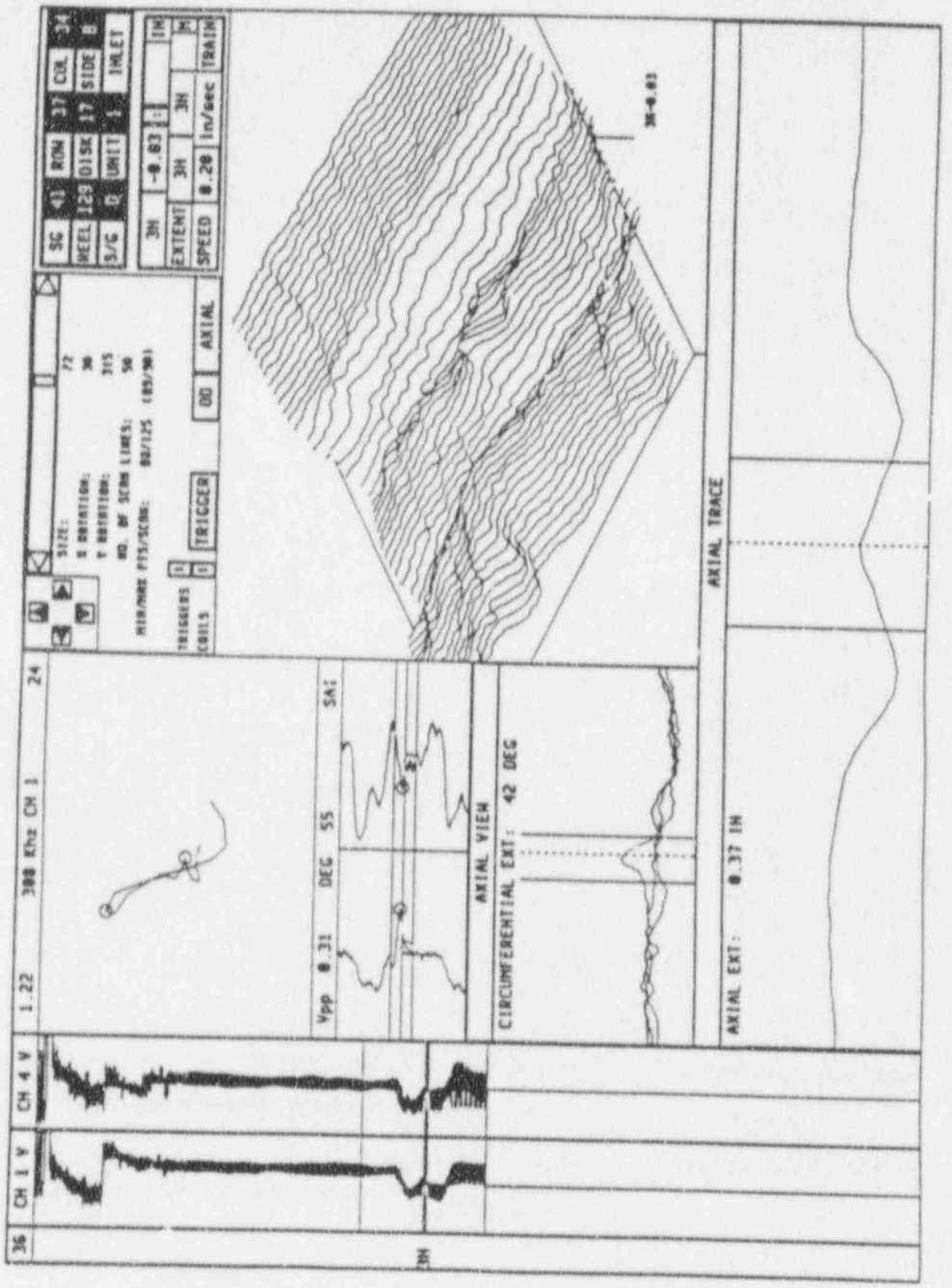
CH 1 V
CH 4 V
1.22
300 Khz CH 1
24
SC 41 RON 37 COL 34
REEL 129 DISK 17 SIDE B
S/G 0 UNIT 1 INLET
EXTENT 3N -0.63 IN
SPEED 0.20 in/sec TRAIN
TRIGGER OD AXIAL
Vpp 0.31 DEG 55
AXIAL VIEW
CIRCUMFERENTIAL EXT: 42 DEG
AXIAL TRACE
AXIAL EXT: 0.37 IN
3N-0.63
3N

Figure 7-47

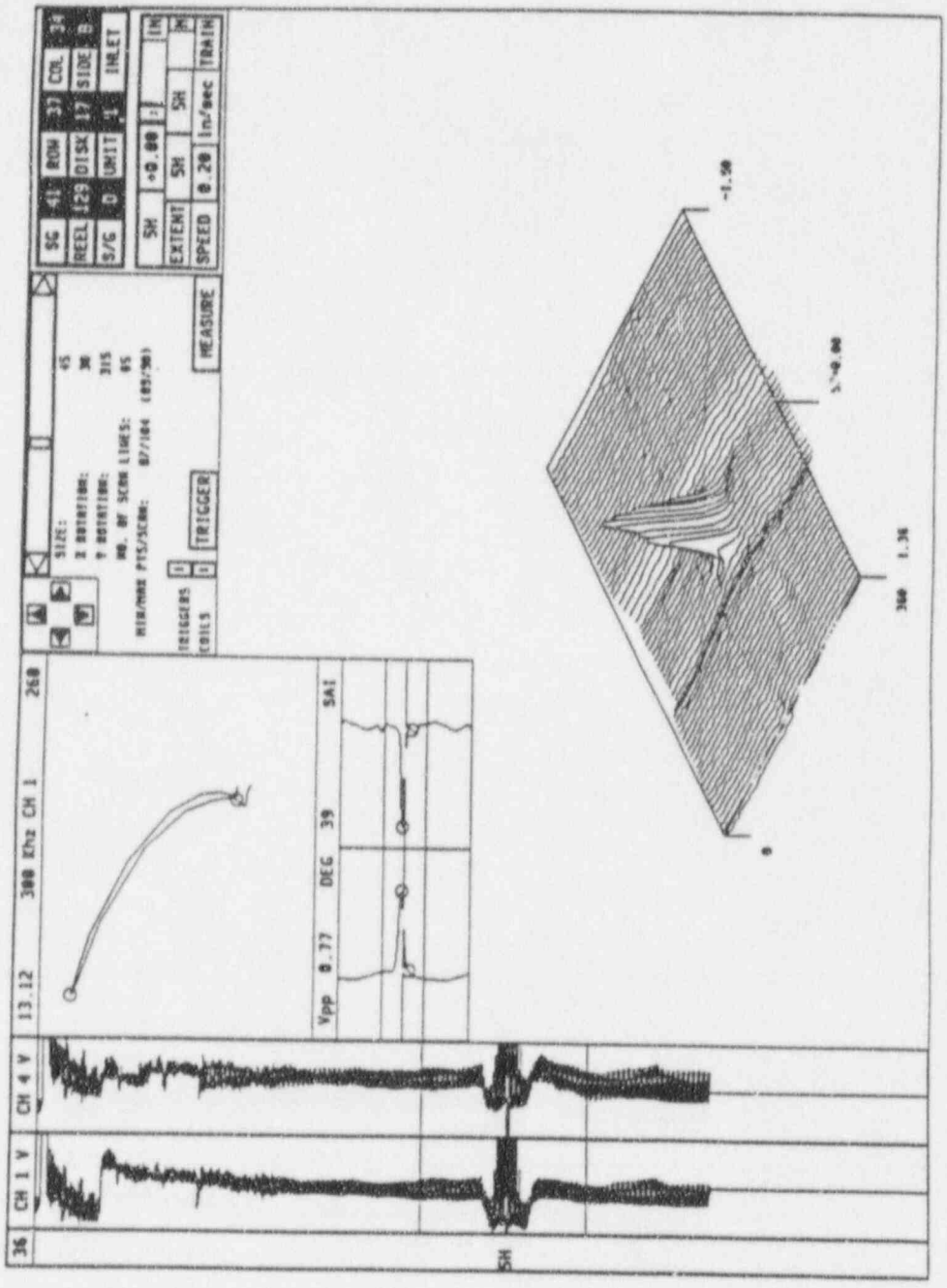

Figure 7-48

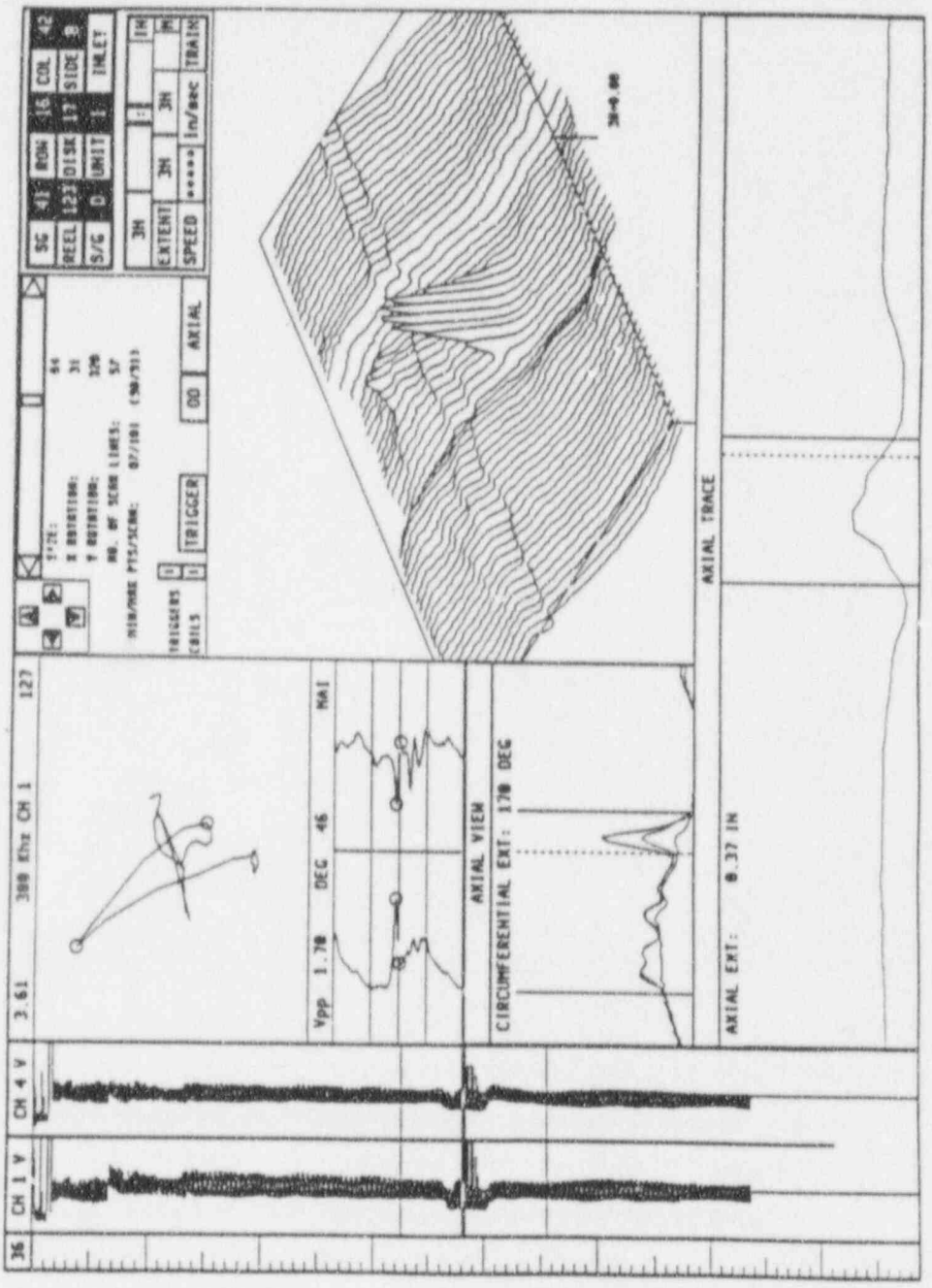
CH 1 V
CH 4 V
3.61
300 Khz CH 1
127
TRIGGER
OD
AXIAL
AXIAL VIEW
CIRCUMFERENTIAL EXT: 170 DEG
AXIAL TRACE
AXIAL EXT: 0.37 IN
Vpp 1.70
DEG
45
MAI
SG
REEL
S/G
BOM
DISK
UNIT
COL
SIDE
INLET
EXTENT
SPEED
in/sec
TRAIN

8.0 BRAIDWOOD-1 IPC CRITERIA AND EVALUATION

This section summarizes the 1.0 volt IPC implemented for Cycle 5 at Braidwood-1 and the supporting evaluations. The supporting evaluations include projected EOC-5 voltage distributions, SLB leak rates and tube burst assessments. Both deterministic and probabilistic tube burst assessments are given in this section.

8.1 General Approach to the IPC Assessment

The tube integrity assessment approach applied to support the Braidwood-1 IPC is based on demonstrating limited TSP displacement in a SLB event to reduce the likelihood of a tube burst to negligible levels and to conservatively calculate SLB leakage as free span leakage even though the limited TSP displacement would reduce leakage compared to free span tube conditions. The structural analyses of Section 4 for obtaining TSP displacements in a SLB event are applied to a conservative assumption that the TSP displacements expose a throughwall crack length equal to the TSP displacement. By applying the burst pressure versus throughwall crack length correlation of Section 6.2, both deterministic and probabilistic burst assessments are made for the assumed exposed throughwall crack length. That is, the burst capability is a function of the exposed throughwall crack length. This analysis is equivalent to assuming that the indication at the TSP has a throughwall crack length approximately equal to the TSP thickness. This is an extremely conservative assumption since the bobbin voltages associated with such long throughwall cracks would be in the many tens of volts and much higher than that found at Braidwood-1 which are bounded by a maximum indication of 10.4 volts at EOC-4. Consequently, the conservatism of the burst assessment bounds any realistic growth rate for Braidwood-1 and the burst margins obtained at EOC-5 based on limited SLB TSP displacements are essentially independent of growth rates.

The limited SLB TSP displacement would result in most of the crack length for indications at TSPs covered by the TSPs and associated crevice deposits. This effect would tend to reduce leakage below that of free span indications which is the basis for data developed to support the EPRI SLB leak rate correlations of Section 6.5 which are used for the leakage analyses of this report. EdF has performed system leak rate measurements on French S/Gs at pressure differentials exceeding SLB conditions. Bobbin voltage levels in the French units at the time of these tests exceeded that found at Braidwood-1. In addition, the French units included axial free span cracks in the roll transition at the top of the tubesheet which are left in service per repair criteria implemented by EdF. The total system leakage at pressure differentials typical of SLB conditions from these tests was on the order of a few gpm. This leak rate is much lower than would be predicted by the EPRI leak rate correlations considering only the indications at TSPs and ignoring the roll transition indications. Thus the EdF tests

demonstrate the conservatism of the EPRI correlations particularly when the indications are within the packed crevice of the TSP.

The BOC-5 bobbin voltage distributions are developed by applying a probability of detection (POD) of 0.6 to all indications found at EOC-4 per the guidance of draft NUREG-1477. This methodology divides the EOC-4 voltage distribution by 0.6 and then subtracts the repaired indications to define the BOC-5 distribution. When voltage indications above a few volts are found in the inspection, for which the POD would be expected to be > 0.6, this methodology becomes very conservative for the BOC distribution as it leaves 0.7 indication in service for each indication found in the inspection, independent of the voltage level.

8.2 IPC Repair Criteria Implemented at Braidwood-1

This section describes the IPC implemented at the Cycle 4 refuel outage (EOC-4) and the inspection/analysis performed to support the IPC.

Braidwood-1 Interim Plugging Criteria

The implementation of the IPC at Braidwood-1 for ODSCC at TSPs can be summarized as follows:

- Tube Plugging Criteria
  Tubes with bobbin flaw indications exceeding the 1.0 volt IPC voltage repair limit and ≤2.7 volts are plugged or repaired if confirmed as flaw indications by RPC inspection. Bobbin flaw indications >2.7 volts attributable to ODSCC are repaired or plugged independent of RPC confirmation.

- Operating Leakage Limits
  Plant shutdown will be implemented if normal operating leakage exceeds 150 gpd per SG.

- SLB Leakage Criterion
  Predicted end of cycle SLB leak rates from tubes left in service, including a POD = 0.6 adjustment and allowances for NDE uncertainties and ODSCC growth rates, must be less than 9.1 gpm for the S/G in the faulted loop.

- Exclusions from Tube Plugging Criteria
  Certain tube locations, as identified in Section 4 of this report, are excluded from application of the IPC repair limits. The analyses indicate that these tubes may potentially deform or collapse following a postulated LOCA + SSE event.

Braidwood-1 EOC-4 Inspection

- Eddy current analysis guidelines and voltage normalization consistent with the EPRI ISI guidelines and with prior IPC applications (typical of Appendix A for prior Westinghouse IPC WCAPs such as WCAP-13854).

- Eddy current analysts were trained specifically to voltage sizing per the analysis guidelines and 52% of the analysts were qualified to the industry standard Qualified Data Analysis program.

- Use of ASME calibration standards cross-calibrated to the reference laboratory standard and use of a probe wear standard requiring probe replacement at a voltage change of 15% from that found for the new probe.

- 100% bobbin coil, full length inspection of all active tubes with a 0.610 inch diameter bobbin probe for all straight length tubing.

- RPC inspection of all bobbin indications greater than the 1.0 volt repair limit (actual implemented was all bobbin indications). RPC inspections were performed with a 0.620 inch diameter, 3 coil motorized RPC probe.

- RPC sample inspection of more than 100 TSP intersections with dents (at Braidwood-1, these are typically mechanically induced "dings") or artifact/residual signals that could potentially mask a 1.0 volt bobbin signal. Any RPC flaw indications in this sample will be plugged or repaired.

- The NRC will be informed, prior to plant restart from the refueling outage, of any unexpected inspection findings relative to the assumed characteristics of the flaws at the TSP intersections. This includes any detectable circumferential indications or detectable indications extending outside the thickness of the TSP.

The IPC evaluations given in this report are based on the inspection results implementing the above guidelines and the 1.0 volt IPC repair limit.

8.3 Operating Leakage Limit

Regulatory Guide 1.121 acceptance criteria for establishing operating leakage limits are based on leak-before-break (LBB) considerations such that plant shutdown is initiated if the leakage associated with the longest permissible crack is exceeded. The longest permissible crack length is the length that provides a factor of safety of 1.43 against burst at SLB conditions

since a factor of 3 against bursting at normal operating pressure differential is satisfied by the TSP constraint at normal operation. As noted previously, a voltage amplitude of 4.54 volts for typical ODSCC cracks corresponds to meeting this tube burst requirement at the lower 95% prediction interval on the burst correlation. Alternate crack morphologies could correspond to 4.54 volts so that a unique crack length is not defined by the burst pressure-to-voltage correlation. Consequently, typical burst pressure versus throughwall crack length correlations are used below to define the "longest permissible crack" for evaluating operating leakage limits.

The CRACKFLO leakage model has been developed for single axial cracks and compared with leak rate test results from pulled tube and laboratory specimens. Fatigue crack and SCC leakage data have been used to compare predicted and measured leak rates. Generally good agreement is obtained between calculation and measurement with the spread of the data being somewhat greater for SCC cracks than for fatigue cracks. Figure 8-1 shows normal operation leak rates including uncertainties as a function of crack length.

The throughwall crack lengths resulting in tube burst at 1.43 times SLB pressure differentials (3657 psi) and SLB conditions (2560 psi) are about 0.51 and 0.75 inch, respectively, as shown in Figure 6-2. Nominal leakage at normal operating conditions for these crack lengths would range from about 0.24 to ~5 gpm while ~95% confidence level leak rates would range from about 0.04 to 0.5 gpm. Leak rate limits at the lower range near 0.04 gpm would cause undue restrictions on plant operation and result in unnecessary plant outages, radiation exposure and cost of repair. In addition, it is not feasible to satisfy LBB for all tubes by reducing the leak rate limit. Crevice deposits, the presence of small ligaments and irregular fracture faces can, in some cases, reduce leak rates such that LBB cannot be satisfied for all tubes by lowering leak rate limits.

An operating leak rate of 150 gpd (~0.1 gpm) is implemented in conjunction with application of the tube plugging criteria. As shown in Figure 8-1 this leakage limit provides for detection of 0.4 inch cracks at nominal leak rates and 0.6 inch cracks at the ~95% confidence level leak rates. Thus, the 150 gpd limit provides for plant shutdown prior to reaching critical crack lengths for SLB conditions (2560 psi) at leak rates less than a ~95% confidence level and for 1.43 times SLB pressure differentials at less than nominal leak rates.

The tube plugging limits coupled with 100% inspection at affected TSP locations provide the principal protection against tube rupture. Consistent with a defense-in-depth approach, the 150 gpd leakage limit provides further protection against tube rupture. In addition the 150 gpd limit provides the capability for detecting a crack that might grow at greater than expected rates and thus provides additional margin against exceeding SLB leakage limits.

8.4 Projected EOC-5 Voltage Distributions

The BOC-5 voltage distributions are obtained by applying the draft NUREG-1477 POD = 0.6 adjustment to all indications found in the EOC-4 inspection and subtracting the repaired indications. Data to develop the BOC-5 bobbin voltage distributions are given in Table 7.3. Monte Carlo analyses are then applied to develop the EOC-5 voltage distributions from the BOC distributions. The BOC voltages are increased by allowances for NDE uncertainties (Section 5.3) and voltage growth (Section 7.3) to obtain the EOC values. In the Monte Carlo analyses, each voltage bin of the BOC distributions (Figure 8-2 for S/G D, for example) is increased by a random sample of the NDE uncertainty and growth distributions to obtain a EOC voltage sample. Each sample is weighted by the number of indications in the voltage bin. The sampling process is repeated 100,000 times for each BOC voltage bin and then repeated for each voltage bin of the voltage distribution. Since the Monte Carlo analyses yield a cumulative probability distribution of EOC voltages, a method must be defined to obtain a discrete maximum EOC voltage value. The method adopted in this report is to integrate the tail of the Monte Carlo distribution over the largest 1/3 of an indication to define a discrete value with an occurrence of 0.33 indication. For N indications in the distribution, this is equivalent to evaluating the cumulative probability of voltages at a probability of (N-0.33)/N. The largest voltages for all distributions developed by Monte Carlo in this report have been obtained with this definition for the maximum EOC discrete voltage. The next largest discrete EOC voltage indication is obtained by integrating the tail of the Monte Carlo distribution to one indication and assigning the occurrence of 0.67 indication. This process for developing the largest EOC voltage indications provides appropriate emphasis to the high voltage tail of the distribution and permits discrete EOC voltages for deterministic tube integrity analyses.

As described in Section 8.5 below, S/G D is the most limiting S/G for SLB leakage analyses and has been evaluated using final Braidwood-1 inspection results and tube plugging data. The Cycle 4 voltage growth distribution of Table 7.6 for S/G D has been used to obtain the EOC voltages by Monte Carlo analyses as described above. The resulting BOC-5 and EOC-5 bobbin voltage distributions are shown in Figure 8-2. Based on applying the POD adjustment, the largest BOC voltage indication left in service is 0.7 indication at 10.4 volts. At EOC-5, the largest voltage indication is projected to be 11.2 volts. The EOC-5 distribution of Figure 8-1 is used for the S/G D SLB leakage analyses in Section 8.5.

As shown in Table 7.3, the number of indications found at EOC-4 in S/G B was 277 compared to 741 in S/G A, 1062 in S/G C and 696 in S/G D. It is clear that S/G B is not limiting for tube integrity considerations and this S/G was not analyzed to obtain EOC distributions or leak rates. S/Gs A and C were analyzed using preliminary inspection results and growth rate data which have not had large changes in the final data. The voltage growth distribution for S/G A was applied in the Monte Carlo analyses for both S/Gs A and C. The

S/G C Cycle 4 growth distribution may have been influenced by tube repairs made in the October, 1993 unplanned outage and thus could be an underestimate of the growth distribution. It is conservative to apply the S/G A growth distribution for S/G C since it has the largest Cycle 4 growth rates. Figures 8-3 and 8-4 show the BOC and EOC-5 voltage distributions obtained from the preliminary data. For S/G A, the largest POD adjusted BOC voltage is 8.33 volts and the largest projected EOC-5 voltage is 9.0 volts. For S/G C, the largest POD adjusted BOC voltage is 2.73 volts and the largest projected EOC-5 voltage is 7.2 volts.

8.5 SLB Leakage Analyses

This section summarizes the results of the projected EOC-5 SLB leak rate analyses applying the EPRI correlations for probability of leakage (POL) and the SLB leak rate versus voltage correlation. The EPRI methodology applies the log logistic form for the POL correlation and the leak rate results are given in Section 8.5.1 as the reference SLB leak rate. The NRC has requested leak rate results to be provided also for the log normal, log Cauchy, logistic, normal and Cauchy POL distributions and the results are also given in Section 8.5.2. The POL and leak rate correlations used for these analyses are described in Sections 6.4 and 6.5, respectively. The SLB leak rate analysis methodology for applying the probability of leakage and leak rate versus voltage correlations is described in Sections 6.6 to 6.8. SLB leak rates are provided at the upper, one-sided confidence of 95% based on the NRC guidance of the February 8, 1994 NRC/industry meeting on resolution of draft NUREG-1477 comments. The EOC-5 voltage distributions have been described above.

SLB leak rate analyses were performed for S/Gs A, C and D using preliminary voltage indication, voltage growth and tube plugging distributions. As noted above, S/G B has fewer indications than the other S/Gs and is not a candidate for the limiting S/G for leakage considerations. The preliminary leak rate analyses showed that S/G D had the highest projected EOC-5 SLB leak rate. The leak rate for S/G A was about half of that for S/G D and S/G C was only about one-third of the S/G D leak rate. Thus S/G D is the limiting S/G for SLB leakage analyses and the results for this generator are given in Section 8.5.1 for the reference EPRI methodology and in Section 8.5.2 for sensitivity to the alternate POL correlations.

8.5.1 Reference SLB Leakage Analyses (Log Logistic POL)

The projected EOC-5 SLB leak rate for the limiting S/G D, as obtained with the reference EPRI correlations of Section 6, is 3.1 gpm. This leak rate is less than the allowable SLB leak of 9.1 gpm developed in Section 4.8 and thus is acceptable for the Braidwood-1 IPC application. Table 8-1 provides details of the leak rate calculation. The column titled N.i

provides the projected EOC-5 voltage distribution including the POD = 0.6 adjustment. The P.i and Q.i columns represent the POL and expected leak rate for each voltage bin. The remaining columns provide data for the upper bound confidence of 95% applied to the leak rate.

Application of the POD adjustment to the EOC-4 voltage distribution leads to large voltage indications postulated to have been missed in the inspection and left in service at BOC-5. With the 1.0 volt repair limit and only RPC NDD indications above 1.0 volt left in service, the expected SLB leakage at BOC-5 would be about zero. The influence of the POD adjustment on predicted leakage values can be estimated by calculating the leak rate for the BOC-5 voltage distribution. The resulting SLB leak rate for S/G D at BOC-5 is 1.7 gpm compared to the expected near zero value. The leak rate thus increases only from 1.7 gpm at BOC to 3.1 gpm at EOC. Thus growth to the EOC only increases the SLB leak rate by about 1.4 gpm which would be near the projected leak rate assuming a POD of about 1.0.

8.5.2 SLB Leak Rate Sensitivity to POL Correlations

The NRC has requested that the projected EOC-5 SLB leak rate be provided for all six POL correlations discussed in draft NUREG-1477. These results provide sensitivity estimates to the form of the POL correlation. As discussed in Section 6.4, the linear and log Cauchy distributions are not consistent with the pulled tube database for low voltage (< 2.0 volt) probability of leakage and are not recommended for consideration as acceptable POL correlations. The estimated BOC-5 and EOC-5 SLB leak rates for all six POL correlations are given in Table 8-2. The results for the reference log logistic POL correlation have been described above and are repeated in Table 8-2.

It is seen from Table 8-2 that the SLB leak rates are essentially independent of the POL correlation applied to obtain the leak rates. The low leak rates for indications below 1 to 2 volts tend to offset the effects of the differences in POL correlations. As seen in Table 8-1 for the column titled N.i*P.i*Q.i, which gives the expected leak rate, the SLB leak rates are dominated by EOC indications above about 3 volts even though only a small fraction of the EOC indications are in this voltage range.

8.6 Assessments of SLB Burst Margins and Probability of Burst

8.6.1 Deterministic Burst Margin Assessments

Although the technical support for the Braidwood-1 IPC is based on tube burst for limited TSP displacement, significant margins exist for free span burst considerations for voltage growth in excess of 95% cumulative probability. Limited TSP displacement considerations

are necessary to accommodate only the largest few growth rates. A deterministic assessment of margins against assumed free span burst is given in Table 8-3. For the largest RPC confirmed indications of 1.0 volt left in service, the projected EOC-5 voltage at 95% growth is 2.8 volts compared to the 4.54 volts structural limit for free span burst at 1.43 x ΔP_{SLB}. As shown in Table 8-3, a burst margin in excess of one volt exists even for the largest unconfirmed bobbin indication left in service. Even at 99% cumulative probability, the voltage growth is bounded by 2.7 volts (S/Gs A, D - Table 7.6) and the structural limit is satisfied for the 1.0 volt RPC confirmed indications left in service. Thus the evaluation for tube burst with limited TSP displacement is applied to accommodate only the largest 1% of the voltage growth distribution.

As shown in Section 4, Table 4.5.1, TSP displacements for an SLB at normal operating conditions are small for most plates and bounded by a maximum TSP displacement of 0.45 inch. Only about 40 TSP intersections at the tubelane corners of the 7th TSP are subject to TSP displacements exceeding 0.35". As shown in Section 6, Figure 6-2, a throughwall crack length of about 0.51 inch (lower tolerance limit material properties - LTL) corresponds to a burst capability of 1.43 x ΔP_{SLB} = 3660 psi. Thus, for an SLB at normal operating conditions, the maximum exposed potential throughwall crack length of 0.45 inch is less than the R.G. 1.121 structural limit of 0.51 inch. It is shown in Section 8.6.4 that this corresponds to an extremely low probability of burst. It can also be noted from Figure 6-2, that the free span throughwall crack length for burst at SLB conditions of 2560 psi is about 0.75 inch. Thus a free span throughwall crack the length of the TSP thickness is required for burst at SLB conditions.

The exposed crack lengths associated with the maximum TSP displacements exceed the R.G. 1.121 structural limit of 0.51 inch only for a small number of TSP intersections for the conservative SLB at hot standby conditions. The remainder of this section emphasizes the probability of a SLB tube burst at hot standby conditions resulting from a potentially large indication at the TSP intersections where displacements are large.

8.6.2 Method of Analysis for SLB Tube Burst Probability

Assessment of the tube burst probability at SLB conditions for limited TSP displacement requires an estimate of the probability of a large indication occuring at the corners of the TSP where the TSP displacements are significant. Only plates 3 and 7 have significant TSP displacements such that a burst assessment is appropriate. Although the flow distribution baffle (FDB, plate 1) has a few TSP intersections with significant displacements, no bobbin indications have been found at the FDB. The FDB in the Model D4 S/Gs has large tube to FDB gaps (nominally 100 mils diametral clearance toward the center of the plate and 88 mils with radialized holes for the outer region). Thus there is a significantly lower likelihood of

packed crevices with associated tube corrosion at the FDB intersections. Since no Braidwood-1 indications at the FDB have been found, the FDB is not included in the tube burst assessment.

The projected EOC-5 voltage distributions of Section 8.4 above are total indications independent of TSP elevation and tube location. The EOC-4 inspection results can be used to develop the distribution of indications between TSP elevations and the fraction of indications occuring at tube locations where the TSP displacements are significant. TSP displacements as a function of tube location were developed from the analyses described in Section 4 and the number of tube locations as a function of displacement are summarized in Table 4.5.3. Table 8-4 provides the inspection results for S/Gs A, C and D as a function of TSP elevation and TSP displacement. S/G B is not included due to the smaller number of indications found in this S/G. The table includes the fraction, F_D, of indications found as a function of displacement. Also given in the table are the number and fractions of indications for a uniform distribution of all tube intersections. Only 9 indications on plate 7 have been found in all S/Gs at tube locations having displacements large enough (greater than about 0.6 inch) to significantly influence the tube burst probability. The largest bobbin voltage for any of these 9 indications was 1.24 volts and the largest indication found anywhere on plate 7 was 2.74 volts. These indications would have a high burst pressure even as free span indications. Thus, the inspection results indicate a low frequency of indications and low voltages at tube locations subject to significant SLB TSP displacements.

The data of Table 8-4 can be used to define bounding distributions for indications as a function of TSP elevation and displacement. The highest fraction of indications at TSPs 3 and 7 were 67% at TSP 3 in S/G C and 13% at TSP 7 in S/G A. These values are used for the fraction of total indications at these TSP elevations. The bounding distribution for the fraction of indications on the TSP as a function of TSP displacement is obtained as the larger found by inspection or the uniform distribution. The resulting bounding distributions for plates 3 and 7 are given in Table 8-4. Also given is the weighted sum for the fraction of TSP indications as a function of displacement. This is obtained as the sum of the individual plate fractions multiplied by the fraction of indications for the TSP elevation. This weighted sum of the bounding distributions is applied in the tube burst probability analyses as described below.

The number of indications as a function of TSP displacement can be obtained as the product of the total number of indications times the bounding fractional distribution of Table 8-4. This product can be obtained as a function of bobbin voltage by applying the number of indications in each voltage bin. The voltage bins and the number of EOC-5 indications in each voltage bin are shown in Figure 8-2 and Table 8-1 for S/G D, the most limiting S/G. Conservatively assuming that the TSP displacements expose throughwall cracks, the

probability of tube burst as a function of exposed crack length is given by the upper curve in Figure 6-3. The probability of tube burst (PRB) can then be obtained as:

$$PRB = \sum_i PRB_i = \sum_i NV_i \left(0.67 \sum_j F_{D_j}^3 PRB_{D_j} + 0.13 \sum_j F_{D_j}^7 PRB_{D_j} \right) \quad (8.1)$$

$$PRB = \sum_i NV_i \sum_j \left(0.67\, F_{D_j}^3 + 0.13 F_{D_j}^7 \right) PRB_{D_j} \quad (8.2)$$

where

i = i^{th} voltage bin

j = j^{th} TSP displacement bin

NV_i = Number of indications in the i^{th} voltage bin

$F_{D_j}^3, F_{D_j}^7$ = Fraction of indications at plates 3 and 7 having TSP displacement in bin j

PRB_{D_j} = The smaller burst probability of either:

- $PRB(V_i)$ = Probability of burst for a free span indication of voltage V_i
- $PRB(D_j)$ = Prob. of burst for throughwall crack length equal to TSP disp. D_j

PRB_i = Probability of burst for the i^{th} voltage bin

The term in parentheses in Equation 2 is the weighted sum for the bounding distribution given in Table 8-4. Equation 2 is applied in Section 8.6.5 to estimate the burst probability at EOC-5.

8.6.3 SLB Burst Probability for S/G D at EOC-4

The burst probability for S/G D at EOC-4 with limited TSP displacement can be obtained directly from the indications found and the TSP displacement at each specific indication. This application demonstrates the general methodology for the limited TSP displacement, burst probabilities without the need for distributing the indications as described in Section 8.6.2 above. Table 8-5 identifies the indications found in the inspection for the larger voltage indications and for indications at locations having the largest TSP displacements in the hot standby SLB event. The bobbin voltage and free span burst probability at the given voltage level are provided for each indication. Also given in the table are the local TSP displacement and the burst probability for a throughwall crack length equal to the TSP displacement (conservatively assumed exposed throughwall crack length). The applicable SLB burst probability column shows the lower of the free span or throughwall burst probability for each indication. The lower of the two burst probabilities is the appropriate value since the limited TSP displacement can reduce the free span burst probability but the free span probability cannot be exceeded. The throughwall burst probability can exceed the free span value only because it is conservatively calculated for a throughwall crack while the free span value, based on bobbin voltage, is more realistically based on the actual crack morphology as reflected in the voltage amplitude.

For the S/G D indications given in Table 8-5, the total burst probability calculated assuming free span (very large SLB TSP displacements) conditions is 3.7×10^{-2}. Accounting for the limited SLB TSP displacements at the locations of the indications, the total burst probability is 1.7×10^{-5}. Thus the limited TSP displacements reduce the burst probability by three orders of magnitude. It can be noted that none of the high voltage indications occurred at locations of high TSP displacement and the TSP constraint reduces the burst probability for these high voltage indications to approximately zero. Only the small voltage indications found at the corners of plate 7, where SLB displacements are significant, contribute to the burst probability.

The results of Table 8-5 show the effectiveness of limited TSP displacements in reducing the tube burst probability to small values and also show that Braidwood-1 had an acceptably low burst probability at EOC-4.

8.6.4 Conservative Burst Probability for SLB at Normal Operating Conditions

For a SLB at normal operating conditions, it is shown in Section 4, Table 4.5.1 that TSP displacements are small and significantly less than that for an SLB at hot standby conditions. The maximum TSP displacement occurs for plate J and is limited to 0.438 inch. The maximum displacements for all other plates are < 0.2 inch. An extremely conservative or bounding burst probability for this event can be obtained by assuming that the SLB

displacements expose a throughwall crack equal to the displacements at every TSP intersection on all seven hot leg TSPs above the FDB. The FDB is excluded from the analysis as no indications have been found at this plate and the larger tube to TSP gap at the FDB would require supplemental burst tests to determine the influence of the FDB constraint on the burst pressure. The throughwall crack assumption is approximately equivalent to assuming that a throughwall crack equal to the TSP thickness is present at every hot leg TSP intersection.

Table 8-6 summarizes the bounding analysis for the burst probability resulting from an SLB at normal operating conditions. The maximum TSP displacement column represents the maximum displacement at any location on the plate except for plate 7 which is divided into three displacement magnitudes to permit separation of the number of TSP intersections subject to the larger TSP displacements. The number and maximum voltages for EOC-4 indications found at each plate are given in the table for general information. The number of tubes column represents the number of TSP intersections with the maximum displacement of column 2. The exposed length burst probability is that associated with a throughwall crack length equal to the maximum TSP displacement. The last column provides the burst probability obtained by multiplying the exposed length probability by the number of tubes.

The total S/G burst probability for this conservative assumption of throughwall indications at each hot leg TSP intersection is $< 5 \times 10^{-3}$. This very low probability bounds all realistic potential indications at the TSP intersections and demonstrates the effectiveness of modest TSP displacements under the SLB at normal operating conditions. As noted in Section 8.6 below, normal operating conditions dominate the operating time and the highest frequency for an SLB event occurs at power conditions where the SLB loads on the TSPs and associated displacements are lower than for a SLB at hot standby conditions.

8.6.5 Burst Probability for a SLB at Hot Standby Conditions

For Cycle 5 SLB leakage and burst considerations, S/G D is the most limiting and the projected EOC-5 voltage distribution is given in Figure 8-2. The tube burst probability for S/G D at EOC-5, assuming an SLB at hot standby conditions, is evaluated in this section. The methodology of Equation 8.2 given in Section 8.6.2 is applied for this assessment. The total EOC-5 voltage distribution of Figure 8-2 is distributed as a function of TSP displacement using the weighted sum of the bounding distribution of Table 8-4. Free span burst probabilities as a function of voltage are developed from the burst pressure versus bobbin voltage correlation of Section 6.1 and burst probabilities for exposed throughwall cracks are given in Figure 6-3.

The results of the burst probability analysis are summarized in Table 8-7. For each voltage bin of the projected EOC-5 voltage distribution (including POD = 0.6 adjustment), the number

of indications, free span burst probability, the distribution of indications and throughwall burst probability as a function of the SLB TSP displacement are given in Table 8-7. By applying Equation 2, the net probability of burst for each voltage level is obtained as given in the last column of the table. The total limited TSP displacement burst probability is obtained as 8×10^{-4}. The influence of the limited TSP displacement can be seen by comparison with the estimated free span burst probability (column 3) of 9×10^{-2}. The latter free span result is dominated by the large projected EOC-5 voltage indications up to 11.2 volts which are traceable to applying the POD adjustment to all indications found in the last inspection prior to reducing the population for tubes repaired at EOC-4.

The estimated SLB tube burst probability of 8×10^{-4} is significantly less than the acceptance guideline for IPC applications of 2.5×10^{-2}, which was found acceptable in NUREG-0844. The normal operating and hot standby burst probabilities can be combined by weighting the separate burst probabilities by the fraction of operating time in each operating condition. Applying the Section 4.6 Braidwood 1 fractions of 0.962 for normal operation and 0.038 for hot standby, the combined burst probability is 3.1×10^{-5}.

8.6.6 Braidwood-1 Frequency of SLB Event with a Tube Rupture

In Section 4.6, Braidwood-1 frequencies of occurrence were developed for an SLB at both normal operating and hot standby (Mode 3) conditions. The frequencies are summarized in Figure 8-5. The frequency for an SLB event at hot standby conditions is a factor of 25 lower than at operating conditions and is only about 6.8×10^{-5} per year. Figure 8-5 includes the conditional probability of a tube rupture at normal operating and hot standby conditions as developed in Sections 8.6.4 and 8.6.5, respectively. The SLB event frequencies and conditional tube rupture probabilities are combined in Figure 8-5 to obtain a frequency of about 5.5×10^{-4} per year for a Braidwood-1 SLB event with a subsequent tube rupture. This very low frequency has negligible influence on the core damage frequency and supports full cycle operation at Braidwood-1 following implementation of the IPC for Cycle 5.

8.7 Summary of Results

An IPC with a 1.0 bobbin voltage repair limit has been implemented for Braidwood-1 Cycle 5 operation. Inspection requirements typical of IPC practice, such as the guidelines of the Catawba-1 NRC SER, were applied at the Cycle 4 refueling outage to support implementation of the IPC. An operating leakage limit of 150 gpd is being applied for Cycle 5 operation. The results of the Braidwood-1 IPC assessment can be summarized as follows:

- The projected EOC-5 SLB leakage is 3.1 gpm which is less than the allowable limit of 9.1 gpm for Braidwood-1. The SLB leak rate was evaluated for the six alternate formulations of the probability of leak versus voltage correlation identified in draft NUREG-1477 and

found to be essentially independent of the correlation applied in the analysis. The SLB leak rates were obtained by applying the leak rate versus voltage correlation based on the EPRI database and outlier evaluation consistent with the NRC guidance of the February 8, 1994 NRC/industry meeting on resolution of draft NUREG-1477 comments.

- The tube burst probabilities estimated at EOC-5 are 5×10^{-7} for a SLB at normal operating conditions and 8×10^{-4} for a SLB at hot standby conditions. The combined probability of burst during a postulated SLB is then 3.1×10^{-5}. These burst probabilities are significantly lower than the IPC acceptance guideline of 2.5×10^{-2}. When combined with the corresponding SLB event frequencies, the frequency of a postulated SLB event with a subsequent tube rupture is very low at 5.5×10^{-8} per year. The tube burst analyses are developed based on limited TSP displacements predicted during an SLB event for the Braidwood-1 S/Gs even when applying very conservative load conditions for the hot standby SLB.

- Deterministic tube burst analyses show that the projected EOC voltage, with voltage growth rates up to 99% cumulative probability on the Cycle 4 measured growth distribution, is less than the R.G. 1.121 structural limit of 4.54 volts for a $1.43 \times \Delta P_{SLB}$ burst margin.

- The modest EOC-5 SLB leakage and low tube burst probabilities strongly support full cycle operation for Cycle 5 at Braidwood-1 following implementation of the 1.0 volt IPC.

Table 8-1: Braidwood 1, SG "D", PoD = 0.6, EOC 5 Volts								Cauchy
EOC Volts	Cum Prob	Tubes with >= Volts	N.i	P.i	Expected Q.i @2560 psi	Variance Q.i	N.i*P.i*Q.i	Variance P.i * Q.i
0.2	0.000964	1016.00	1.0	3.11E-02	5.17E-04	6.15E-05	1.61E-05	1.92E-06
0.3	0.010827	1015.33	10.0	3.19E-02	1.78E-03	3.49E-04	5.67E-04	1.12E-05
0.4	0.049213	1005.09	39.0	3.26E-02	4.12E-03	1.22E-03	5.24E-03	4.02E-05
0.5	0.123031	966.28	75.0	3.34E-02	7.83E-03	3.26E-03	1.96E-02	1.11E-04
0.6	0.222441	891.35	101.0	3.42E-02	1.32E-02	7.40E-03	4.55E-02	2.59E-04
0.7	0.334646	790.25	114.0	3.51E-02	2.04E-02	1.50E-02	8.17E-02	5.40E-04
0.8	0.447835	675.79	115.0	3.60E-02	2.99E-02	2.78E-02	1.24E-01	1.03E-03
0.9	0.550197	561.22	104.0	3.70E-02	4.18E-02	4.84E-02	1.61E-01	1.85E-03
1.0	0.639764	456.55	91.0	3.80E-02	5.64E-02	8.00E-02	1.95E-01	3.16E-03
1.1	0.712596	366.30	74.0	3.91E-02	7.41E-02	1.27E-01	2.14E-01	5.16E-03
1.2	0.771654	291.82	60.0	4.02E-02	9.51E-02	1.94E-01	2.29E-01	8.13E-03
1.3	0.817913	231.92	47.0	4.14E-02	1.20E-01	2.87E-01	2.33E-01	1.25E-02
1.4	0.853346	184.96	36.0	4.27E-02	1.48E-01	4.15E-01	2.27E-01	1.86E-02
1.5	0.880906	148.63	28.0	4.40E-02	1.81E-01	5.86E-01	2.23E-01	2.72E-02
1.6	0.902559	120.69	22.0	4.55E-02	2.18E-01	8.12E-01	2.18E-01	3.90E-02
1.7	0.919291	99.09	17.0	4.70E-02	2.60E-01	1.11E+00	2.07E-01	5.50E-02
1.8	0.932087	82.01	13.0	4.86E-02	3.06E-01	1.46E+00	1.94E-01	7.65E-02
1.9	0.942913	69.04	11.0	5.04E-02	3.59E-01	1.96E+00	1.99E-01	1.05E-01
2.0	0.950787	58.50	8.0	5.23E-02	4.16E-01	2.56E+00	1.74E-01	1.42E-01
2.1	0.956693	50.34	6.0	5.43E-02	4.80E-01	3.30E+00	1.57E-01	1.91E-01
2.2	0.961614	43.86	5.0	5.66E-02	5.50E-01	4.22E+00	1.56E-01	2.55E-01
2.3	0.965551	38.83	4.0	5.89E-02	6.27E-01	5.34E+00	1.48E-01	3.36E-01
2.4	0.968504	34.97	3.0	6.15E-02	7.11E-01	6.69E+00	1.31E-01	4.41E-01
2.5	0.971457	31.96	3.0	6.44E-02	8.01E-01	8.33E+00	1.55E-01	5.75E-01
2.6	0.973425	29.39	2.0	6.75E-02	9.00E-01	1.03E+01	1.21E-01	7.45E-01
2.7	0.975394	27.19	2.0	7.09E-02	1.01E+00	1.26E+01	1.43E-01	9.60E-01
2.8	0.976378	25.24	1.0	7.47E-02	1.12E+00	1.54E+01	8.36E-02	1.23E+00
2.9	0.978346	23.55	2.0	7.89E-02	1.24E+00	1.86E+01	1.96E-01	1.58E+00
3.0	0.979331	21.99	1.0	8.35E-02	1.37E+00	2.24E+01	1.15E-01	2.01E+00
3.1	0.981299	20.58	2.0	8.86E-02	1.52E+00	2.68E+01	2.69E-01	2.57E+00
3.2	0.982283	19.34	1.0	9.47E-02	1.67E+00	3.19E+01	1.58E-01	3.26E+00
3.3	0.983268	18.25	1.0	1.01E-01	1.83E+00	3.79E+01	1.85E-01	4.15E+00
3.4	0.984252	17.35	1.0	1.09E-01	2.00E+00	4.47E+01	2.18E-01	5.27E+00
3.6	0.985236	15.74	1.0	1.29E-01	2.37E+00	6.15E+01	3.05E-01	8.55E+00
3.7	0.986220	15.01	1.0	1.41E-01	2.57E+00	7.18E+01	3.63E-01	1.09E+01
3.9	0.987205	13.56	1.0	1.74E-01	3.01E+00	9.67E+01	5.24E-01	1.81E+01
4.0	0.988189	12.83	1.0	1.96E-01	3.25E+00	1.12E+02	6.37E-01	2.35E+01
4.1	0.989173	12.08	1.0	2.23E-01	3.50E+00	1.28E+02	7.83E-01	3.08E+01
4.3	0.990157	10.55	1.0	3.01E-01	4.05E+00	1.69E+02	1.22E+00	5.42E+01
4.4	0.991142	9.71	1.0	3.55E-01	4.34E+00	1.93E+02	1.54E+00	7.26E+01
4.5	0.992126	8.94	1.0	4.19E-01	4.64E+00	2.19E+02	1.95E+00	9.71E+01
4.7	0.993110	7.51	1.0	5.63E-01	5.30E+00	2.82E+02	2.99E+00	1.66E+02
4.8	0.994094	6.90	1.0	6.30E-01	5.65E+00	3.19E+02	3.56E+00	2.06E+02
5.1	0.995079	5.62	1.0	7.69E-01	6.80E+00	4.54E+02	5.22E+00	3.57E+02
5.7	0.996063	4.60	1.0	8.79E-01	9.55E+00	8.75E+02	8.40E+00	7.50E+02
7.4	0.997047	3.52	1.0	9.51E-01	2.14E+01	4.24E+03	2.04E+01	4.05E+03
8.9	0.998031	2.52	1.0	9.68E-01	3.81E+01	1.33E+04	3.69E+01	1.29E+04
9.7	0.999016	1.58	1.0	9.73E-01	5.00E+01	2.29E+04	4.87E+01	2.24E+04
10.5	0.999705	0.65	0.7	9.77E-01	6.43E+01	3.80E+04	4.20E+01	3.72E+04
11.2	1.000000	0.33	0.3	9.79E-01	7.89E+01	5.76E+04	2.32E+01	5.65E+04
							Regression Equations Analysis	
							Sum[Ni * E(Qi) * Pi] =	205.592
							Sum[Var + Cov] =	9.17E+04
							Effective Standard Deviation =	3.03E+02
							Confidence =	95.0%
							Z - Deviate =	1.645
							Q.total (LPH) =	703.6
							Q.total (GPM) =	3.098

Table 8-2. Summary of Cycle 5 SLB Leak Rate Analyses for S/G D		
Method of Analysis	BOC	EOC
EPRI SLB Leak Rate versus Voltage Correlation		
• POD = 0.6 • Leak rates based on EPRI voltage correlation • POL Correlation		
Reference SLB Leak Rate		
- Log logistic POL	1.71	3.1
SLB Leak Rate Sensitivity to POL Correlation		
- Log normal POL	1.71	3.1
- Log Cauchy POL	1.69	3.1
- Logistic POL	1.73	3.1
- Normal POL	1.73	3.2
- Cauchy POL	1.70	3.1

Table 8-3. Summary of Deterministic Margins Against Burst at SLB Conditions (95% Confidence)				
Parameter	S/G A	S/G B	S/G C	S/G D
RPC Confirmed Indications Left in Service				
Largest bobbin voltage	1.00	1.00	1.00	1.00
NDE uncertainty at 95% confidence • 20% of bobbin voltage	0.20	0.20	0.20	0.20
Voltage growth at 95% cumulative probability	1.40	0.50	1.40[1]	1.00
Projected EOC-5 Voltage	2.60	1.7	2.60	2.20
Allowable EOC Voltage at $1.43 \times \Delta P_{SLB}$	4.54 volt			
Largest Bobbin Voltage, RPC NDD Left in Service				
Largest bobbin voltage	1.48	2.03	1.55	1.8
NDE uncertainty at 95% confidence • 20% of bobbin voltage	0.30	0.41	0.31	0.36
Voltage growth at 95% cumulative probability	1.40	0.50	1.40[1]	1.00
Projected EOC-5 Voltage	3.18	2.49	3.26	3.16
Allowable EOC Voltage at $1.43 \times \Delta P_{SLB}$	4.54			
Notes 1. Growth rate for S/G A conservatively applied to S/G C				

Table 8-4

Distribution of Indications as a Function of Hot Standby TSP Displacement and Elevation

SG	TSP	Cycle 4 Indications		Number and Fraction of Indications as a Function of TSP Displacement															
				< 0.45"		0.45" - 0.50"		0.50" - 0.55"		0.55" - 0.60"		0.60" - 0.65"		0.65" - 0.70"		0.70" - 0.75"		> 0.75"	
		No.	%	No.	F_D	No.	F_D	No.	F_D	No.	F_D	No.	F_D	No.	F_D	No.	F_D	No.	F_D
A	3	368	50%	368	1.0	0		0		0		0							
	5	248	33%	248	1.0														
	7	93	13%	86	0.924	2	0.0215	0		2	0.0215	1	0.0108	1	0.0108	1	0.0108	0	
	≥8	33	4%	33	1.0														
C	3	713	67%	712	0.999	1	0.0014	0		0		0							
	5	237	22%	237	1.0														
	7	94	9%	88	0.936	2	0.0213	3	0.0319	0		0		0		1	0.0106	0	
	≥8	22	2%	22	1.0														
D	3	404	58%	403	0.998	0		1	0.0025	0		0							
	5	181	26%	181	1.0														
	7	77	11%	66	0.857	3	0.0390	3	0.0390	0		1	0.0130	2	0.0260	1	0.0130	1	0.0130
	≥8	34	5%	34	1.0														
Uniform TSP Dist. (4578 tubes)	3			4548	0.993	18	0.0039	10	0.0022	2	0.00044	0							
	7			4366	0.954	48	0.0105	42	0.0092	34	0.0074	30	0.0066	22	0.0048	14	0.0031	22	0.0048
Bounding Distribution	3		67%		0.993		0.0039		0.0025		0.0004		0						
	7		13%		0.834		0.0390		0.0390		0.0215		0.0130		0.0260		0.0130		0.0130
• Weighted Sum	3+7				0.774		0.0077		0.0067		0.0031		0.0017		0.0034		0.0017		0.0017

Table 8-5
Braidwood-1, SG D - Estimated Hot Standby SLB Burst Probability at EOC-4

Tube/Location			Free Span Burst		Limited TSP Disp. Burst (1)		Applicable SLB Burst Prob. (2)
Row	Col.	TSP	Volts	Burst Prob.	Local TSP Disp.	TW Burst Prob.	
37	34	5	10.44	2.0E-02	< 0.12	< 1.0E-12	~ 0.0
23	12	3	8.82	1.1E-02	< 0.35	< 1.0E-11	~ 0.0
12	9	3	5.02	1.5E-03	< 0.35	< 1.0E-11	~ 0.0
11	9	3	4.28	8.0E-04	< 0.35	< 1.0E-11	~ 0.0
19	7	3	3.95	5.7E-04	< 0.35	< 1.0E-11	~ 0.0
33	20	3	3.83	5.0E-04	< 0.35	< 1.0E-11	~ 0.0
35	29	3	3.62	3.9E-04	< 0.35	< 1.0E-11	~ 0.0
11	12	3	3.21	2.3E-04	< 0.35	< 1.0E-11	~ 0.0
16	42	3	3.12	2.0E-04	< 0.35	< 1.0E-11	~ 0.0
2	105	3	2.84	1.3E-04	< 0.35	< 1.0E-11	~ 0.0
8	20	3	2.77	1.2E-04	< 0.35	< 1.0E-11	~ 0.0
43	56	3	2.60	8.8E-05	< 0.35	< 1.0E-11	~ 0.0
32	27	5	2.48	7.1E-05	< 0.12	< 1.0E-12	~ 0.0
45	53	3	2.30	4.9E-05	< 0.35	< 1.0E-11	~ 0.0
31	20	3	2.20	4.0E-05	< 0.35	< 1.0E-11	~ 0.0
27	35	3	2.18	3.8E-05	< 0.35	< 1.0E-11	~ 0.0
41	55	3	2.16	3.7E-05	< 0.35	< 1.0E-11	~ 0.0
43	53	3	2.11	3.3E-05	< 0.35	< 1.0E-11	~ 0.0
2	113	3	0.59	2.2E-07	0.514	1.9E-05	2.2E-07
3	110	3	0.58	2.1E-07	0.406	3.5E-09	3.5E-09
2	113	7	0.56	1.9E-07	0.804	4.5E-01	1.9E-07
2	108	7	1.10	3.5E-06	0.631	9.0E-03	3.5E-06
2	105	7	0.64	3.5E-07	0.530	5.3E-05	3.5E-07
2	11	7	0.72	5.6E-07	0.498	4.9E-06	5.6E-07
4	106	7	0.52	1.4E-07	0.532	6.3E-05	1.4E-07
4	112	7	1.24	6.0E-06	0.718	1.2E-01	6.0E-06
5	112	7	1.24	6.0E-06	0.692	6.4E-02	6.0E-06

(continued on next page)

Table 8-5
Braidwood-1, SG D - Estimated Hot Standby SLB Burst Probability at EOC-4

Tube/Location			Free Span Burst		Limited TSP Disp. Burst (1)		Applicable SLB Burst Prob. (2)
Row	Col.	TSP	Volts	Burst Prob.	Local TSP Disp.	TW Burst Prob.	
7	105	7	0.59	2.2E-07	0.456	2.7E-07	2.2E-07
13	110	7	0.88	1.3E-06	0.417	8.0E-09	8.0E-09
Total Burst Probability				3.7E-02			1.7E-05

Notes:
1. Analysis conservatively assumes the TSP displacement exposes a throughwall crack length equal to the displacement.
2. The applicable burst probability is the lower of the free span or TW burst probabilities.

Table 8-6. Bounding SLB Burst Probability at Normal Operating Conditions

TSP	Maximum TSP Displacement (inch)	EOC-4 Indications		Bounding SLB Burst Probability		
		Max. No. Ind at TSP	Max. Volts at TSP	Number Tubes	Exposed Length Burst Prob.[2]	Burst Prob. for Ind. at All H.L. Int.[3]
1/A						
3/C						
5/F						
7/J						
8/L						
9/M						
10/N						
11/P						
				Total Burst Probability		$<5 \times 10^{-7}$

Notes:
1. Maximum number of indications in any S/G at the noted TSP.
2. Burst probability for a throughwall crack length equal to the maximum TSP displacement of column 2.
3. Burst probability assuming all hot leg TSP intersections have a throughwall crack length at maximum TSP displacement.

Table 8-7
Braidwood-1 SG D: EOC-5 Burst Probability for Hot Standby SLB with Limited TSP Displacement

Voltage Bin	EOC-5 No. of Ind. NV_i	Free Span Burst Prob. $PRB(V_i)$	Plate 3 and 7 Contribution: F_D and PRB_D as a Function of TSP Displacement												Net Prob. of Burst PRB_i
			< 0.45"		0.45" - 0.50"		0.50" - 0.55"		0.55" - 0.60"		0.60" - 0.65"		≥ 0.65" (2)		
			F_D	PRB_D	F_D	PRB_D	F_D	PRB_D (1)	F_D	PRB_D (1)	F_D	PRB_D (1)	F_D	PRB_D (1)	
1.0			0.774	1.1E-8	0.0077	7.9E-7	0.0067	3.0E-5	0.0031	6.1E-4	0.0017	6.5E-3	0.0068	≤3.8E-2	
1.1	74.0	3.5E-6	0.774	1.1E-8	0.0077	7.9E-7	0.0067	3.5E-6	0.0031	3.5E-6	0.0017	3.5E-3	0.0068	≤3.5E-2	5.8E-6
1.2	60.0	5.1E-6	8.5E-9 (Note 3)		6.1E-9 (Note 3)		0.0067	5.1E-6	0.0031	5.1E-6	0.0017	5.1E-6	0.0068	5.1E-6	6.5E-6
1.3	47.0	7.3E-6	8.5E-9		6.1E-9		0.0067	7.3E-6	0.0031	7.3E-6	0.0017	7.3E-6	0.0068	7.3E-6	7.0E-6
1.4	36.0	1.0E-5	8.5E-9		6.1E-9		0.0067	1.0E-5	0.0031	1.0E-5	0.0017	1.0E-5	0.0068	1.0E-5	7.1E-6
1.5	28.0	1.4E-5	8.5E-9		6.1E-9		0.0067	1.4E-5	0.0031	1.4E-5	0.0017	1.4E-5	0.0068	1.4E-5	7.6E-6
1.6	22.0	1.8E-5	8.5E-9		6.1E-9		0.0067	1.8E-5	0.0031	1.8E-5	0.0017	1.8E-5	0.0068	1.8E-5	7.6E-6
1.7	17.0	2.3E-5	8.5E-9		6.1E-9		0.0067	2.3E-5	0.0031	2.3E-5	0.0017	2.3E-5	0.0068	2.3E-5	7.4E-6
1.8	13.0	3.0E-5	8.5E-9		6.1E-9		0.0067	3.0E-5	0.0031	3.0E-5	0.0017	3.0E-5	0.0068	3.0E-5	7.3E-6
1.9	11.0	3.8E-5	8.5E-9		6.1E-9		2.0E-7 (Note 3)		0.0031	3.8E-5	0.0017	3.8E-5	0.0068	3.8E-5	7.2E-6
2.0	8.0	4.7E-5	8.5E-9		6.1E-9		2.0E-7		0.0031	4.7E-5	0.0017	4.7E-5	0.0068	4.7E-5	6.1E-6
2.1	6.0	5.8E-5	8.5E-9		6.1E-9		2.0E-7		0.0031	5.8E-5	0.0017	5.8E-5	0.0068	5.8E-5	5.2E-6
2.2	5.0	7.1E-5	8.5E-9		6.1E-9		2.0E-7		0.0031	7.1E-5	0.0017	7.1E-5	0.0068	7.1E-5	5.2E-6
2.3	4.0	8.5E-5	8.5E-9		6.1E-9		2.0E-7		0.0031	8.5E-5	0.0017	8.5E-5	0.0068	8.5E-5	4.8E-6
2.4	3.0	1.0E-4	8.5E-9		6.1E-9		2.0E-7		0.0031	1.0E-4	0.0017	1.0E-4	0.0068	1.0E-4	4.1E-6
2.5	3.0	1.2E-4	8.5E-9		6.1E-9		2.0E-7		0.0031	1.2E-4	0.0017	1.2E-4	0.0068	1.2E-4	4.8E-6
2.6	2.0	1.4E-4	8.5E-9		6.1E-9		2.0E-7		0.0031	1.4E-4	0.0017	1.4E-4	0.0068	1.4E-4	3.7E-6

Table 8-7
Braidwood-1 SG D: EOC-5 Burst Probability for Hot Standby SLB with Limited TSP Displacement

Voltage Bin	EOC-5 No. of Ind. NV_i	Free Span Burst Prob. $PRB(V_i)$	Plate 3 and 7 Contribution: F_D and PRB_D as a Function of TSP Displacement												Net Prob. of Burst PRB_s
			< 0.45"		0.45" - 0.50"		0.50" - 0.55"		0.55" - 0.60"		0.60" - 0.65"		≥ 0.65" (2)		
			F_D	PRB_D	F_D	PRB_D	F_D	PRB_D (1)	F_D	PRB_D (1)	F_D	PRB_D (1)	F_D	PRB_D (1)	
2.7	2.0	1.7E-4	8.5E-9 (Note 3)		6.1E-9 (Note 3)		2.0E-7 (Note 3)		0.0031	1.7E-4	0.0017	1.7E-4	0.0068	1.7E-4	4.4E-6
2.8	1.0	2.0E-4	8.5E-9		6.1E-9		2.0E-7		0.0031	2.0E-4	0.0017	2.0E-4	0.0068	2.0E-4	2.5E-6
2.9	2.0	2.3E-4	8.5E-9		6.1E-9		2.0E-7		0.0031	2.3E-4	0.0017	2.3E-4	0.0068	2.3E-4	5.8E-6
3.0	1.0	2.6E-4	8.5E-9		6.1E-9		2.0E-7		0.0031	2.6E-4	0.0017	2.6E-4	0.0068	2.6E-4	3.2E-6
3.1	2.0	3.0E-4	8.5E-9		6.1E-9		2.0E-7		0.0031	3.0E-4	0.0017	3.0E-4	0.0068	3.0E-4	7.4E-6
3.2	1.0	3.4E-4	8.5E-9		6.1E-9		2.0E-7		0.0031	3.4E-4	0.0017	3.4E-4	0.0068	3.4E-4	4.2E-6
3.3	1.0	3.8E-4	8.5E-9		6.1E-9		2.0E-7		0.0031	3.8E-4	0.0017	3.8E-4	0.0068	3.8E-4	4.4E-6
3.4	1.0	4.3E-4	8.5E-9		6.1E-9		2.0E-7		0.0031	4.3E-4	0.0017	4.3E-4	0.0068	4.3E-4	5.2E-6
3.6	1.0	5.4E-4	8.5E-9		6.1E-9		2.0E-7		0.0031	5.4E-4	0.0017	5.4E-4	0.0068	5.4E-4	6.5E-6
3.7	1.0	6.0E-4	8.5E-9		6.1E-9		2.0E-7		0.0031	6.0E-4	0.0017	6.0E-4	0.0068	6.0E-4	7.2E-6
3.9	1.0	7.4E-4	8.5E-9		6.1E-9		2.0E-7		0.0031	6.1E-4	0.0017	7.4E-4	0.0068	7.4E-4	8.4E-6
4.0	1.0	8.2E-4	8.5E-9		6.1E-9		2.0E-7		1.9E-6 (Note 3)		0.0017	8.2E-4	0.0068	8.2E-4	9.1E-6
4.1	1.0	9.0E-4	8.5E-9		6.1E-9		2.0E-7		1.9E-6		0.0017	9.0E-4	0.0068	9.0E-4	9.8E-6
4.3	1.0	1.1E-3	8.5E-9		6.1E-9		2.0E-7		1.9E-6		0.0017	1.1E-3	0.0068	1.1E-3	1.1E-5
4.4 -	1.0	1.2E-3	8.5E-9		6.1E-9		2.0E-7		1.9E-6		0.0017	1.2E-3	0.0068	1.2E-3	1.2E-5
4.5	1.0	1.3E-3	8.5E-9		6.1E-9		2.0E-7		1.9E-6		0.0017	1.3E-3	0.0068	1.3E-3	1.3E-5
4.7	1.0	1.5E-3	8.5E-9		6.1E-9		2.0E-7		1.9E-6		0.0017	1.5E-3	0.0068	1.5E-3	1.5E-5

Table 8-7
Braidwood-1 SG D: EOC-5 Burst Probability for Hot Standby SLB with Limited TSP Displacement

Voltage Bin	EOC-5 No. of Ind. NV_i	Free Span Burst Prob. $PRB(V_i)$	Plate 3 and 7 Contribution: F_D and PRB_D as a Function of TSP Displacement												Net Prob. of Burst PRB_i
			< 0.45"		0.45" - 0.50"		0.50" - 0.55"		0.55" - 0.60"		0.60" - 0.65"		≥ 0.65" (2)		
			F_D	PRB_D	F_D	PRB_D	F_D	PRB_D (1)	F_D	PRB_D (1)	F_D	PRB_D (1)	F_D	PRB_D (1)	
4.8	1.0	1.7E-3	8.5E-9 (Note 3)		6.1E-9 (Note 3)		2.0E-7 (Note 3)		1.9E-6 (Note 3)		0.0017	1.7E-3	0.0068	1.7E-3	1.7E-5
5.1	1.0	2.1E-3	8.5E-9		6.1E-9		2.0E-7		1.9E-6		0.0017	2.1E-3	0.0068	2.1E-3	2.0E-5
5.7	1.0	3.1E-3	8.5E-9		6.1E-9		2.0E-7		1.9E-6		0.0017	3.1E-3	0.0068	3.1E-3	2.8E-5
7.4	1.0	7.8E-3	8.5E-9		6.1E-9		2.0E-7		1.9E-6		0.0017	6.5E-3	0.0068	7.8E-3	6.6E-5
8.9	1.0	1.4E-2	8.5E-9		6.1E-9		2.0E-7		1.9E-6		1.1E-5 (Note 3)		0.0068	1.4E-2	1.1E-4
9.7	1.0	1.9E-2	8.5E-9		6.1E-9		2.0E-7		1.9E-6		1.1E-5		0.0068	1.9E-2	1.4E-4
10.5	0.7	2.4E-2	8.5E-9		6.1E-9		2.0E-7		1.9E-6		1.1E-5		0.0068	2.4E-2	1.2E-4
11.2	0.3	2.9E-2	8.5E-9		6.1E-9		2.0E-7		1.9E-6		1.1E-5		0.0068	2.9E-2	6.3E-5
Net Free Span Burst Probability $\Sigma NV_i*PRB(V_i)$		$9x10^{-3}$											Net Limited TSP Displacement Burst Probability, ΣPRB_i		$8x10^{-4}$

Notes:
1) Initial column entry shows the burst probability for an exposed throughwall crack equal to the TSP displacement. The remaining column entries show the lower burst probability for either free span based on the bobbin voltage or a throughwall crack at the length exposed by the TSP displacement.

2) For TSP displacements >0.65 inch, the free span burst probability for the EOC-5 voltages are always lower than for an assumed throughwall crack greater than the 0.65 inch TSP displacement.

3) Numerical value represents F_D*PRB_D for the TSP displacement bin. Below this entry, the burst probability for an assumed throughwall crack at the given TSP displacement is always less than that for free span based on the voltage level.

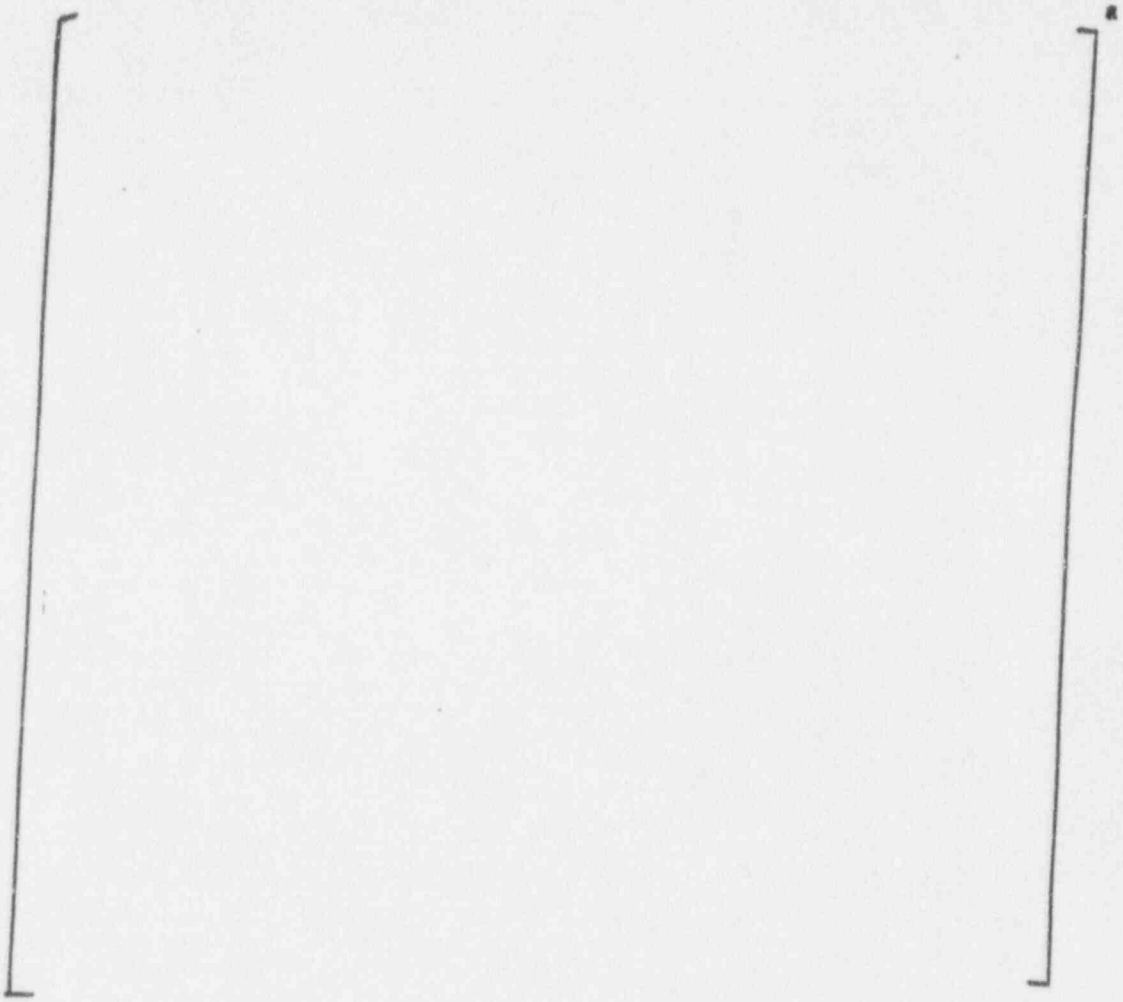

Figure 8-1. Leak Rate Under Normal Operating Conditions
versus Crack Length for 3/4 Inch Tubing

Figure 8-2: Braidwood 1, SG "D" BOC & EOC 5 Indications
BOC Indications Adjusted for PoD = 0.6

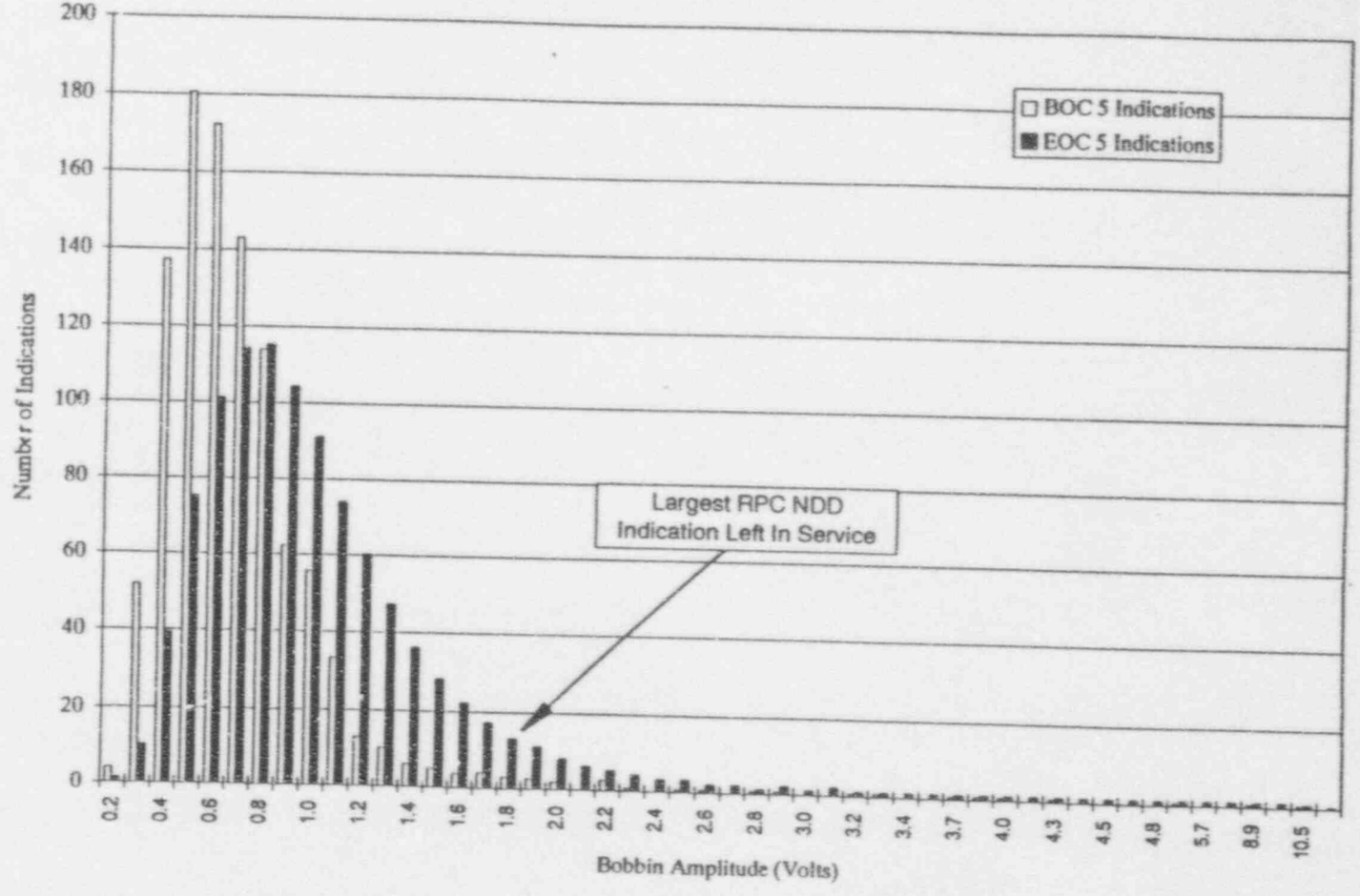

[CCE5SIMD.XLS] BOC EOC 5

RFK: 4/20/94, 7:01 PM

Figure 8-3: Braidwood 1, SG "A" BOC & EOC 5 Indications

BOC Indications (Preliminary) Adjusted for PoD = 0.6

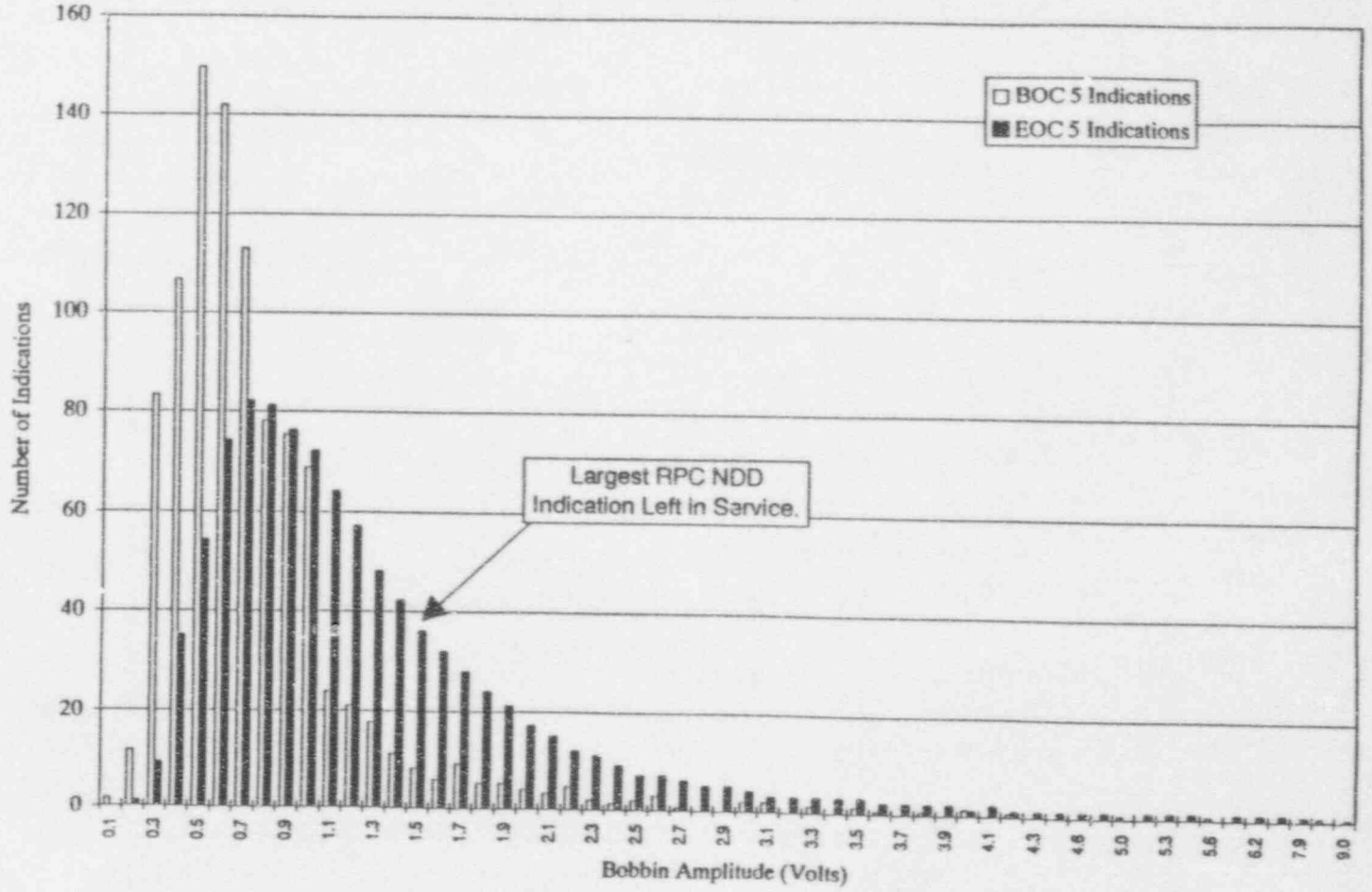

[CCE5S3MA.XLS] BOC EOC 5

RFK: 4/20/94, 7:10 PM

Figure 8-4: Braidwood 1, SG "C" BOC & EOC 5 Indications

BOC Indications (Preliminary) Adjusted for PoD = 0.6

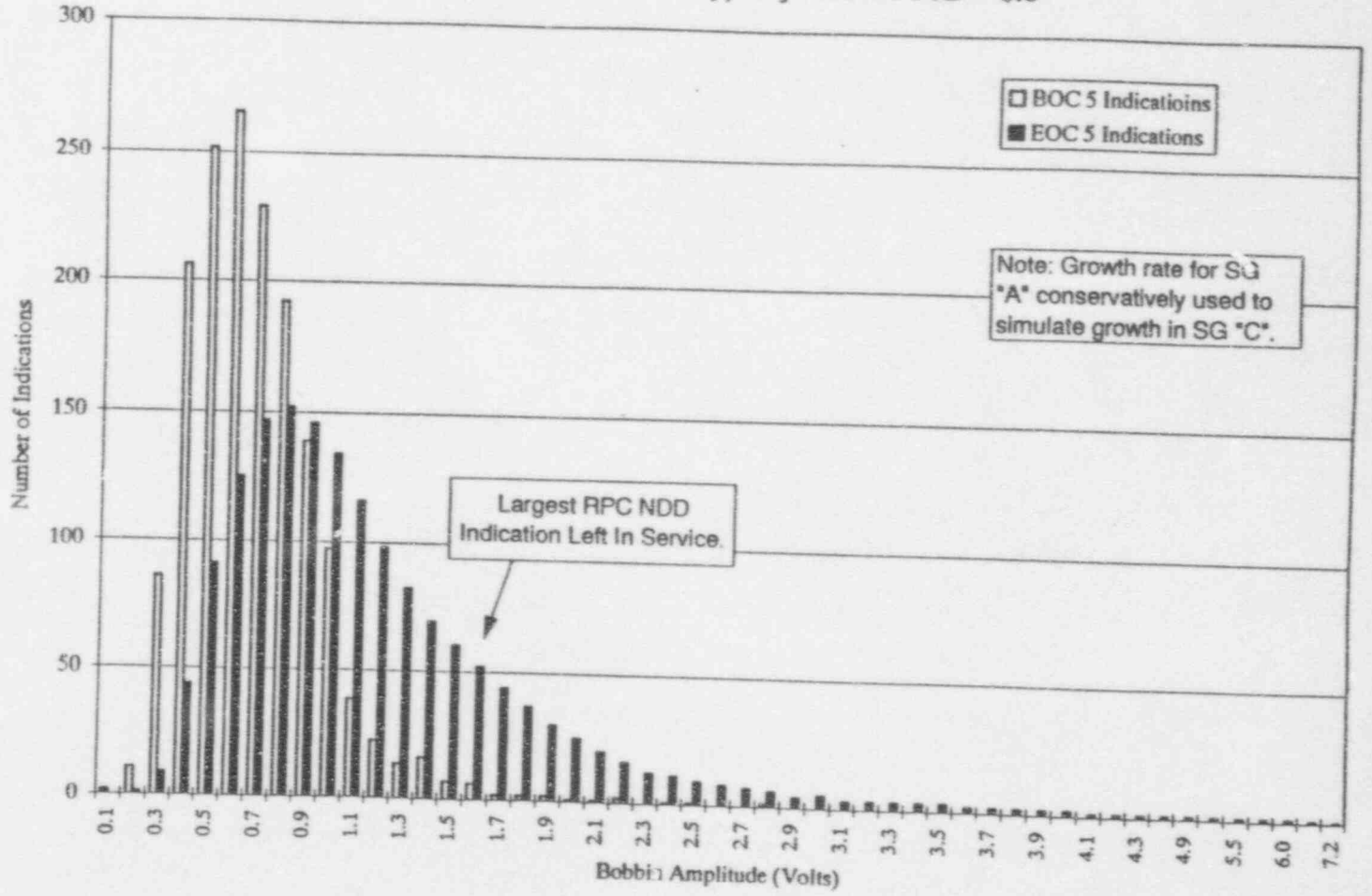

[CCESSIMC.XLS] BOC EOC 5

RFK: 4/20/04 7:07 PM

Figure 8-5. Estimated Braidwood-1 EOC-5 Frequency of SLB Event with a Tube Repair

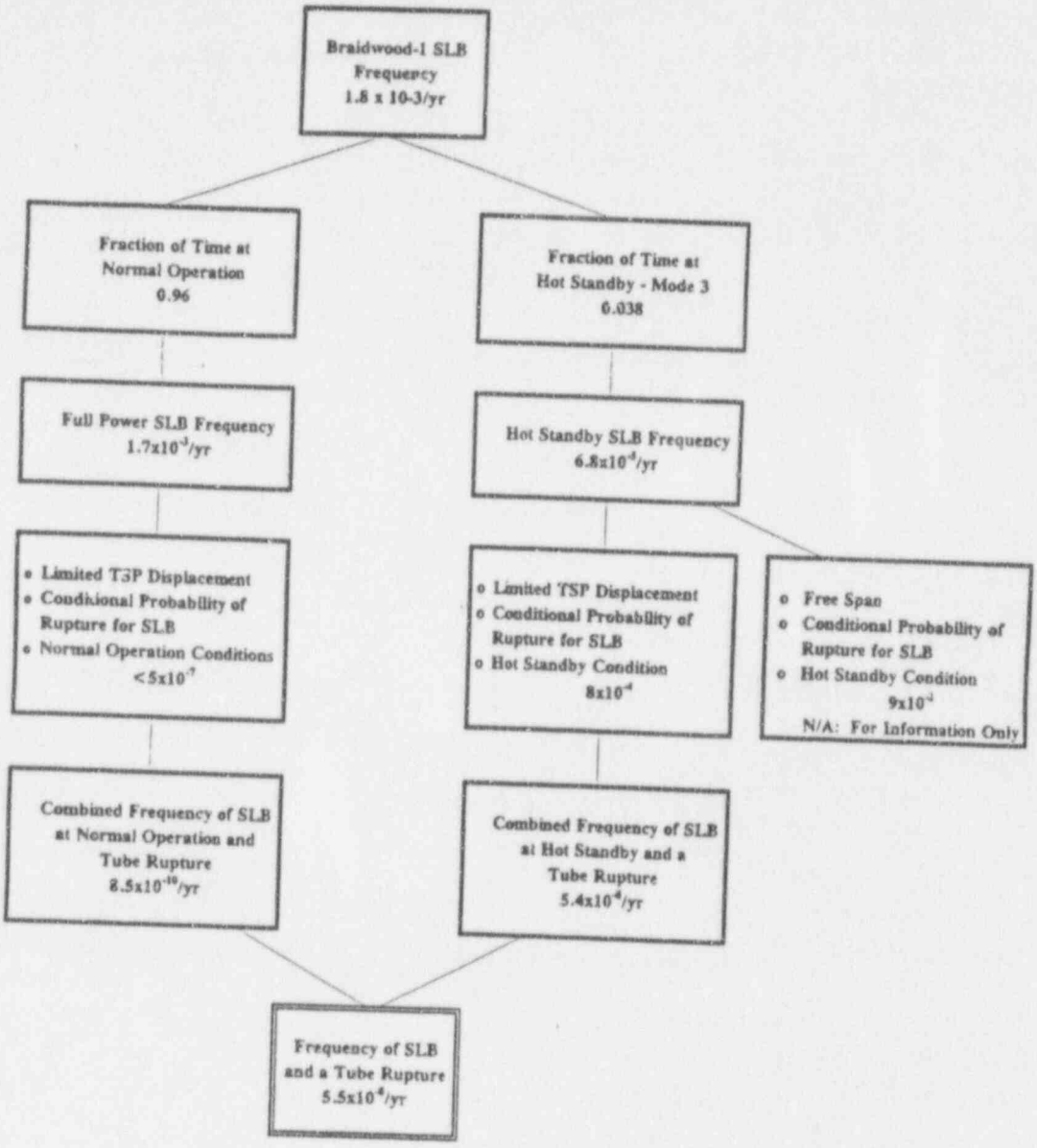

ATTACHMENT I

Byron/Braidwood Eddy Current Inspection Guidelines
July 1994